Photo, Electro, Sono and Fenton based Advanced Oxidation Processes and their hybrids for the decontamination of water from multiple chemical pollutants

Thesis submitted to

Cochin University of Science and Technology

in partial fulfillment of the requirements

for the award of the degree of

Doctor of Philosophy

Under the Faculty of Environmental Studies

By

Veena Vijayan
(Reg. No. 4405)

SCHOOL OF ENVIRONMENTAL STUDIES
COCHIN UNIVERSITY OF SCIENCE AND TECHNOLOGY
KOCHI 682 022

November **2019**

Photo, Electro, Sono and Fenton based Advanced Oxidation Processes and their hybrids for the decontamination of water from multiple chemical pollutants

Ph.D. Thesis under the Faculty of Environmental Studies

Author

Veena Vijayan
Research Scholar
School of Environmental Studies
Cochin University of Science and Technology
Kochi 682 022
Kerala, India

Supervising Guide

Dr. Suguna Yesodharan
Professor (Emeritus)
School of Environmental Studies
Cochin University of Science and Technology
Kochi 682 022
Kerala, India

School of Environmental Studies
Cochin University of Science and Technology
Kochi, Kerala, India 682 022

November 2019

SCHOOL OF ENVIRONMENTAL STUDIES
COCHIN UNIVERSITY OF SCIENCE AND TECHNOLOGY
KOCHI 682 022

Dr. SugunaYesodharan
Professor (Emeritus)

Certificate

This is to certify that this thesis entitled **"Photo, Electro, Sono and Fenton based Advanced Oxidation Processes and their hybrids for the decontamination of water from multiple chemical pollutants"** is an authentic record of the research work carried out by **Smt. Veena Vijayan**, Full-Time Research Scholar (Reg. No. 4405) under my guidance at the School of Environmental Studies, Cochin University of Science and Technology in partial fulfillment of the requirements for the award of the degree of Doctor of Philosophy and no part of this work has previously formed the basis for the award of any other degree, diploma, associateship, fellowship or any other similar title or recognition. All the relevant corrections and modifications suggested by the audience during the pre-synopsis seminar and recommended by the Doctoral Committee have been incorporated in the thesis.

Kochi 22
-11-2019

Dr. Suguna Yesodharan
(Supervising Guide)

Declaration

I do hereby declare that the work presented in the thesis entitled **"Photo, Electro, Sono and Fenton based Advanced Oxidation Processes and their hybrids for the decontamination of water from multiple chemical pollutants"** is based on the authentic record of the original work done by me, for my Doctoral Degree under the guidance of **Dr. Suguna Yesodharan**, Professor (Emeritus), School of Environmental Studies, Cochin University of Science and Technology in partial fulfillment of the requirements for the award of the degree of Doctor of Philosophy and no part of this work has previously formed the basis for the award of any other degree, diploma, associateship, fellowship or any other similar title or recognition.

Kochi 22 -11-2019

Veena Vijayan

Acknowledgements

It gives me immense pleasure to acknowledge all those people who have helped me in one way or other in accomplishing this piece of work successfully. I humbly dedicate this work to all those who have helped me in exploring the expanses of knowledge.

I wish to express my deep, sincere and heartfelt gratitude to my supervising guide, Dr. Suguna Yesodharan, Professor (Emeritus), School of Environmental Studies (SES), Cochin University of Science and Technology (CUSAT) for her inspiring guidance, encouragement and motherly affection throughout this research work.

I find no words to express my intense admiration, gratitude and respect to Dr. E. P. Yesodharan, Professor (Emeritus), SES, CUSAT who was my motivation to venture into the world of Advanced Oxidation Processes. His in-depth knowledge, positive attitude, dedication and constant encouragement helped me a lot in accomplishing this work. His understanding, encouragement and personal guidance have provided me with a good base for the present thesis. I feel myself honoured and fortunate to enjoy a wonderful research atmosphere in his presence. I am really short of words to express my sincere appreciation for his patience and tolerance to me throughout this period.

I offer my gratitude to Dr. Sivanandan Achari, present Director of SES as well as to previous Directors Dr. S. Rajathy, Dr. Suguna Yesodharan, Dr. Ammini Joseph and Dr. Harindranathan Nair for providing me the facilities of the School for the smooth conduct of the study. I also wish to place on record my thanks to Dr. M. Anand, Dr. Preethi Chandran and Dr. C.S. Ratheesh Kumar, faculty members of the school for all their suggestions, help, support and encouragement throughout the period of this research. I also thank the non-teaching staff of the school for their assistance and co-operation. My heartfelt gratitude also goes to

Dr. Valsamma John Koshy, Prof. (Dr.) C.T Aravinda Kumar and Dr. Usha K Aravind of the School of Environmental Sciences / Inter University Instrumentation Center (SES/IUIC), Mahatma Gandhi University, Kottayam, Kerala for providing necessary facilities, support and encouragement during my stay there. The help by the students/Technical staff of the SES/IUIC is also gratefully acknowledged.

I would like to express my sincere and heartfelt gratitude to all the research scholars of our laboratory, Dr. Anju, Dr. Jyothi, Ms. Sindhu, Dr. Phonsy, Dr. Vidya, Dr. Gayathri, Dr. Rajeev, Dr. Shibin, Ms. Deepthi, and Mr. Hariprasad Narayanan, for their timely advice, help and affection, which made my stay in the laboratory a pleasant one. I thank all the research scholars and other friends at CUSAT for their support throughout the program.

I would like to extend my sincere gratitude to the UGC for awarding me the Research Fellowship and to the authorities of CUSAT for providing me with the facility to conduct the research work.

Finally I thank my parents, my brother, my in-laws, other family members and above all my loving husband Renjith and my sweet little heart Namasiva for providing me continuous support and inspiration to carry on with my research.

Above all, this piece of work is accomplished with the blessings and powers that work within me and also of the people in my life. I bow before GOD for all with a sense of humility and gratitude.....

Veena Vijayan

Preface

Advanced Oxidation Process (AOP) is one of the most effective emerging methods for the treatment of wastewater containing chemical and bacterial pollutants. The method involves the formation and interaction of highly reactive hydroxyl radicals under suitable activation conditions. The sources of activation include UV/VIS light, ultrasound, microwave, electricity, gamma radiation, Fenton process etc and their possible combinations.

The current study involves investigations on the potential application of UV/Vis light, ultrasound (US), electrical energy, Fenton process and their combinations for the irreversible removal of various chemical pollutants in water with special focus on the recalcitrant dye pollutant Indigo Carmine (IC).

Solar photocatalysis mediated by ZnO is an efficient AOP for the mineralization of IC in water and the process is facilitated in the presence of H_2O_2 oxidant. The process follows pseudo first order kinetics and Langmuir-Hinshelwood mechanism. Salts/anions naturally present in water influence the rate of degradation in different ways depending on their relative concentration in the system. Both dissolved and adsorbed oxygen get photochemically transformed into reactive radicals which interact with the pollutant resulting in ultimate mineralization. Sonolysis by using ultrasound as the source of activation also leads to the degradation of IC in water, though at much slower rate compared to photolysis or photocatalysis.

In the electrolytic method, various electrode-electrolyte combinations were tested for its efficacy in wastewater treatment. An important observation is that all systems which are efficient for the decolorization/ degradation of the dye need not necessarily be equally efficient for the

mineralization. After testing a number of systems, BiO_2-TiO_2/Ti – SS – NaCl and BiO_2-TiO_2/Ti - graphite - Na_2SO_4 are identified as the most efficient for the decolorization and mineralization respectively. The slow mineralization in NaCl electrolyte is due to the formation of recalcitrant chloro intermediates.

Extensive investigations on the classic Fenton as well as solar, sono and electroFenton processes showed that solar photocatalyticFenton is the most efficient process for the mineralization of a variety of chemical pollutants. The efficacy and viability of this technique is further illustrated using natural river water with all its contaminants as the matrix. Comparative efficiency of various process tested here is summarized as follows;

Decolorization: Solar photoFenton > Solar photocatalyticFenton ≈ SonoFenton ≈ ElectroFenton > Photocatalysis ≈ Sonocatalysis > Sonolysis > Fenton ≈ Electrolysis > SonocatalyticFenton.

Mineralization: Solar photocatalyticFenton > Solar photoFenton ≈ SonoFenton ≈ ElectroFenton > Photocatalysis > Sonocatalysis > Sonolysis > Fenton > Electrolysis > Sonocatalytic Fenton.

The current study demonstrates that Solar photocatalyticFenton process using relatively harmless chemicals Fe^{2+} and H_2O_2 as reactants, sunlight as the source of energy and ZnO as catalyst is a potentially viable "green technology" for the decontamination of water from a wide variety of chemical pollutants.

Certain chemical reactions, equations and other salient points which are crucial in explaining the results convincingly are repeated in different Chapters as deemed appropriate. In such cases of repetition, the equations/reactions are given new serial numbers for ease of reference.

The Thesis is presented in 8 Chapters and related Annexures as follows:

Chapter 1: Introduction

Chapter 2: Objectives of the study, Materials used, General procedures Plan of the thesis

Chapter 3: Solar photocatalysis mediated by ZnO for the decontamination of water from Indigo Carmine dye pollutant.

Chapter 4: Electrochemical AOPs for the decontamination of water from Indigo Carmine dye pollutant.

Chapter 5: Ultrasound as a source of activation in AOPs for the decontamination of water from Indigo Carmine dye pollutant.

Chapter 6: Fenton and Fenton based hybrid AOPs for the decontamination of water from Indigo Carmine dye pollutant.

Chapter 7: Solar photocatalyticFenton process as a highly efficient AOP for the mineralization of multiple chemical pollutants in water.

Chapter 8: Summary and Conclusion

Annexures:

Annexure I List of Abbreviations

Annexure II List of Publications

Annexure III Reprints of Papers Published

Annexure IV Copy of the certificate awarded for "Best Poster Presentation" at the ISAC National Conference 2019

Contents

List of Tables

List of Figures

.....ꕥ.....

Chapter

1

INTRODUCTION

Contents

1.1 General

Water is essential for the existence of life on earth. More than 70% of the earth is covered with water. Water flows everywhere on the earth and is like the blood flowing in the human body. Most part of the human body is filled with water and it can be termed the elixir of life. The sustainability of every form of life on earth depends upon the availability of fresh water.

Pure water has no smell, taste, or color. There is plenty of water everywhere on the earth but there is scarcity of water in some cities and dry lands. Human beings can survive a few months without food but they can survive only for a day or two without water. Few desert animals can get enough water from their food, but all others must drink water for their survival. Therefore the presence of pure water is inevitable for our life. Water is known as the 'universal solvent' because it can dissolve something of everything. Therefore there is high chance for the water to get polluted from anywhere and everywhere.

Water pollution is the contamination of water and water bodies including lakes, rivers, oceans and ground water. Water pollution occurs when pollutants are present in water due to natural means or by human activities. These polluting compounds are dangerous to plants and organisms living in these water bodies. Sometimes the toxicity affects individual species and populations while in other cases it affects the entire biodiversity. Contaminating materials such as chemical compounds including aromatics, halo aromatics, aliphatics, dyes, dioxin and other polluting materials are present in the waste effluent from petrochemical, pharmaceutical, textile, agricultural, food and other industries. Most of these compounds are highly toxic and the waste effluent must be treated properly prior to discharge into the water bodies.

1.2 Dyes and their intermediates as water pollutants

Colors and colored materials have become unavoidable ingredients of modern life. The colors in the form of dyes are used in textiles, food and many other industries. Excessive use of various types of dyes in the textile industry has resulted in severe surface water contamination through toxic and colored effluents. These are resistant to biological destruction. The textile industry alone uses 10,000 different dyes and colored compounds. The total quantity of dyes used in different segments of industry will be of the order of millions of metric tons. Many of these dyes are toxic and hazardous.

Textile dyes and dye intermediates with high aromaticity and low biodegradability have emerged as major environmental pollutants [1, 2]. Considerable amount of water is used for dyeing and finishing of fabrics

in the textile industry. Nearly 10-15% of the dye is lost in the dyeing process and is released through the wastewater which is an important cause of environmental contamination.

The wastewater from textile mills causes serious impact on natural water bodies and land in the surrounding area. High values of COD and BOD, presence of particulate matter and sediments, inherently colored dyes leading to turbidity etc. in water, cause depletion of dissolved oxygen which has an adverse effect on the aqueous ecological system. Dyes are highly persistent in natural environments because they are chemically and photolytically stable. Improper handling of hazardous chemicals in textile water also has some serious impact on the health and safety of human beings. Some of the adverse health effects include chemical burns, irritation, ulcers etc. and respiratory problems.

Major difficulty in treating wastewater containing dyes is the ineffectiveness of biological processes. Physical processes such as adsorption and coagulation transfer the pollutants from one medium to another which causes secondary pollution. Traditional waste treatment systems involve the use of techniques such as coagulation, chorination or ozonation which utilize potentially hazardous or polluting materials. Chlorination presents a particular problem since it will often generate trihalomethanes as by-proucts when used to treat water contaminated with organic compounds. Many of the conventional methods used for the treatment of wastewater containing wide variety of toxic contaminants are inadequate and unacceptable. Hence, an effective treatment system which can degrade the polluting materials prior to discharge of the effluent is

required. Some of the recently developed treatment techniques such as Advanced Oxidation Processes (AOPs) are promising in this respect.

1.3 Advanced Oxidation Processes (AOPs)

Advanced Oxidation Processes are chemical treatment processes which can destroy organic and inorganic contaminants present in water and wastewater through oxidation using insitu formed highly reactive hydroxyl radicals ($^{\bullet}OH$). These reactive species are the strongest oxidants that can be applied in water and can oxidize almost any compound present in the water matrix. The $^{\bullet}OH$ reacts nonselectively with organic contaminants and fragments them quickly and efficiently into small inorganic molecules. Schematic presentation of typical AOP is shown in figure 1.1.

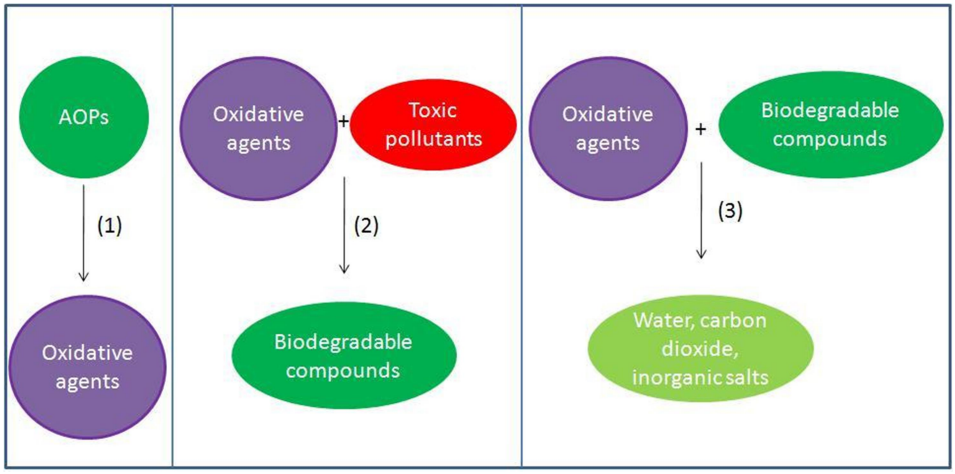

Fig. 1.1: Schematic representation of Advanced Oxidation Processes

Hydroxyl radicals are produced with the help of one or more primary oxidants (e.g. ozone, hydrogen peroxide, oxygen) or energy sources (e.g. ultraviolet light, ultrasound etc.) and catalysts (e.g. titanium

dioxide, zinc oxide). Precise, pre-programmed dosages, sequences and combinations of these reagents are applied in order to obtain maximum $^{\bullet}OH$ yield. The characteristics of hydroxyl radicals are shown in figure 1.2.

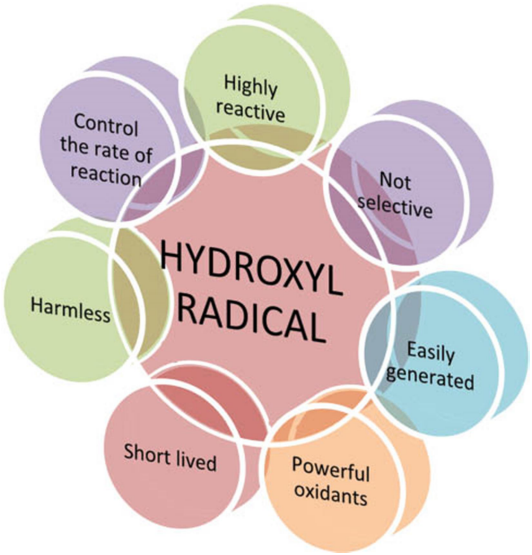

Fig. 1.2: Diagrammatic representation of the characteristics of hydroxyl radical

It is clear that when applied in a well organized manner, AOPs can alleviate the concentration of pollutants from a bulk amount to nanoscale and thus bring down the TOC and COD values. The AOP technique can be used for cleaning biologically hazardous or non-degradable materials such as aromatics, petroleum constituents and volatile organic compounds present in wastewater [3,5]. Due to these reasons, AOPs earned the compliment as "water treatment processes of the 21st century" [6].

In addition, AOPs have the extra benefit that they can be used for tertiary treatment. Tertiary treatment is the one which is used to treat

effluent of secondary treated wastewater. The pollutant materials present in wastewater in traces after secondary treatment are transformed into stable inorganic compounds including water, carbon dioxide and salts. This process is termed as mineralization. The benefit of using AOP techniques for wastewater treatment is that it can be used for the total destruction of chemical compounds and the toxicity can be eliminated to a great extent. The treated wastewater can be discharged into the receiving water bodies or it can be reused for irrigation, cleaning etc. AOPs still have not been put into use on a large scale (especially in developing countries) even today mostly because of the relatively high costs. Nevertheless, its high oxidative capability and efficiency make AOP a popular technique in tertiary treatment in which the most recalcitrant organic and inorganic contaminants are to be eliminated. The increasing interest in water reuse and more stringent regulations regarding water pollution are currently accelerating the implementation of AOPs in full-scale.

The chemistry of AOPs could be essentially divided into three parts: [7]

1) Formation of $^{\bullet}OH$;
2) Initial attacks on target molecules by $^{\bullet}OH$ and their breakdown to fragments;
3) Subsequent attacks by $^{\bullet}OH$ until ultimate mineralization.

Advanced oxidation process can be generally classified into heterogeneous and homogeneous depending on the physical composition

of the reaction system. These may be further classified based on the reaction conditions. The classification is shown in figure 1.3.

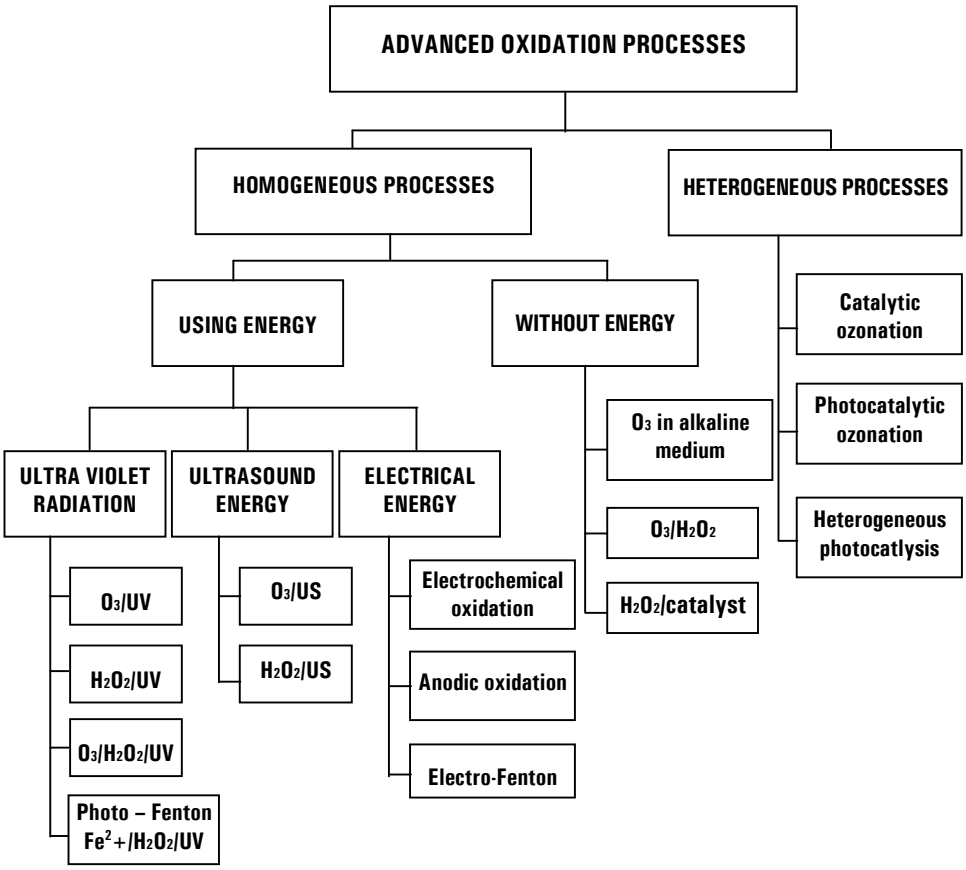

Fig. 1.3: Different types of AOPs [8]

1.3.1 Homogeneous AOP

Homogeneous AOPs using ultraviolet (UV) radiation are generally employed for the degradation of compounds that absorb UV radiation. Processes based on this include UV/Photolysis, UV/H_2O_2, O_3/UV, Photo Fenton, etc. Other sources of radiation such as ultrasound (US), electrical

energy, microwave (MW), etc. are also being investigated. Instances of 'no irradiation' with H_2O_2, O_3, homogeneous catalysts, etc. as the initiator have also been reported.

1.3.2 Heterogeneous AOP

Heterogeneous AOPs generally use catalysts to enhance the degradation of compounds. The term heterogeneous refers to the fact that the contaminants are present in the aqueous phase, while the catalyst is in the solid phase. The catalyst accelerates the chemical reaction through a process involving the formation of electron-hole pairs on irradiation with an appropriate energy source. The AOP-generated holes and electrons lead to oxidation and reduction processes respectively.

1.3.3 General mechanism of AOP

Oxidation is a process by which one or more electrons from an electron donor (reductant) is transferred to an electron acceptor (oxidant), which has a higher affinity for electron. As a result of this, chemical transformation takes place in both the oxidant and reductant.

In some cases, odd electron species known as radicals are produced during this process which are unstable and highly reactive. Oxidation reactions that produce radicals tend to be followed by additional oxidation reactions between the radical oxidants and other reactants (both organic and inorganic) until thermodynamically stable oxidation products are formed. The ability of the oxidant to initiate chemical reactions is measured in terms of its oxidation potential. The oxidation potentials of some of the common oxidizer species are given in table 1.1.

General mechanism of AOP involves generation of highly reactive free radicals viz. hydroxyl radicals ($^{\bullet}OH$), which are very effective in destroying organic chemicals. They are reactive electrophiles (electron preferring) that react rapidly and non-selectively with nearly all electron-rich organic compounds. They have an oxidation potential of 2.8 eV and exhibit faster rates of oxidation reactions compared to conventional oxidants such as H_2O_2 and $KMnO_4$. Once generated, the hydroxyl radicals can attack organic chemicals by radical addition, hydrogen abstraction and electron transfer.

Table 1.1: Oxidation potential of common oxidizers

Sl. No.	Oxidation species	Oxidation potential (eV)
1	Fluorine	3.06
2	Hydroxyl radical	2.80
3	Sulphate radical	2.60
4	Atomic oxygen	2.42
5	Nascent oxygen	2.42
6	Ozone	2.07
7	Persulphate	2.01
8	Hydrogen peroxide	1.77
9	Perhydroxyl radical	1.70
10	Permanganate	1.68
11	Hypobromous acid	1.59
12	Hypochlorous acid	1.49
13	Hypochlorite	1.49
14	Hypoiodous acid	1.45
15	Chlorine	1.36
16	Chlorine dioxide	1.27
17	Oxygen (molecular)	1.23
18	Bromine	1.09
19	Iodine	0.54

In the following reactions, R represents the reacting organic compound.

$$R + {}^{\bullet}OH \rightarrow ROH \quad : \text{Addition} \quad .....(1.1)$$

$$R + {}^{\bullet}OH \rightarrow R^{\bullet} + H_2O \quad : \text{Abstraction} \quad .....(1.2)$$

$$R + {}^{\bullet}OH \rightarrow R^{+} + OH^{-} \quad : \text{Electron transfer} \quad .....(1.3)$$

In view of the importance of the role played by ${}^{\bullet}OH$ radicals in AOP, the process is classified as photochemical and non-photochemical, depending on the mode of generation of the radical. Some of the common photochemical and nonphotochemical AOPs are listed in table 1.2.

Table 1.2: Photochemical and Non-photochemical AOPs.

Photochemical	**Non-photochemical**
H_2O_2/UV (Ultraviolet)	$O_3/{}^{\bullet}OH$
O_3/UV	O_3/H_2O_2
O_3/ H_2O_2/UV	O_3/ Ultrasound (US)
Fe^{2+}/ H_2O_2/UV (Photo Fenton)	O_3 /GAC*
TiO_2/UV, ZnO/UV	Fe^{2+}/H_2O_2(Fenton system)
H_2O_2/TiO_2/UV	Electro-Fenton
O_2/ TiO_2/UV	Electron beam irradiation
UV/US	US
	H_2O_2/US

*GAC- Granulated Activated Carbon

1.3.4 Advantages of AOP

Some of the major advantages of AOP are listed below;

1) AOPs do not create any sludge as in the case of physicochemical and biological processes. Hence they will not cause any secondary pollution

2) They have the potential to reduce toxicity and possibly to complete mineralization of the organics treated

3) Faster reaction rate
4) Small footprint.

1.3.5 Disadvantages of AOP

Major disadvantages of AOPs are:

1) High treatment cost
2) Must be tailored to suit specific application
3) For some applications, quenching is needed because of the use of very reactive chemicals.

1.3.6 Photocatalysis as an AOP

Photocatalysisis is considered as a prominent Advanced Oxidation Process (AOP) because of its capacity to generate the powerful oxidizing agent, hydroxyl radicals ($^{\bullet}OH$) when irradiated by suitable light sources. The degradation efficiency of photochemical AOPs is greatly enhanced using either homogeneous or heterogeneous photocatalysis [9]. Heterogeneous processes employ semiconductor slurries (e.g. TiO_2/UV, ZnO/UV) for catalysis, whereas homogeneous photochemistry (e.g. H_2O_2/UV, Fe^{3+}/UV) is used in a single-phase system.

1.3.7 Heterogeneous Photocatalysis

The field of heterogeneous photocatalysis has expanded rapidly in the last four decades, having undergone various developments especially in relation to energy and the environment. It can be defined as the acceleration of photoreaction in the presence of a catalyst. The two most significant applications of photocatalysis have been in solar water splitting

and the purification of air and water containing low concentrations of pollutants. The multidisciplinary nature of the field has also expanded significantly and includes semiconductor physics, surface sciences, photo and physical chemistry, materials science and chemical engineering [10].

Heterogeneous photocatalysis can be described as the acceleration of photoreaction in the presence of a catalyst. A photocatalyst is defined as a substance which is activated by absorbing a photon and is capable of accelerating a reaction without being consumed [11,12]. Semiconducting oxides as photocatalysts have been increasingly focused in recent years due to their potential applications in solar energy conversion and environmental purification. Semiconductor heterogeneous photocatalysis has enormous potential to treat organic contaminants in water and air. In the past two decades numerous studies have been carried out on the application of heterogeneous photocatalytic oxidation process for the decomposition and mineralization of recalcitrant organic compounds. Several semiconductors (TiO_2, ZnO, Fe_2O_3, CdS, ZnS) can act as photocatalysts. The photocatalytic generation of various reactive species using semiconductor oxide catalyst is shown in figure 1.4.

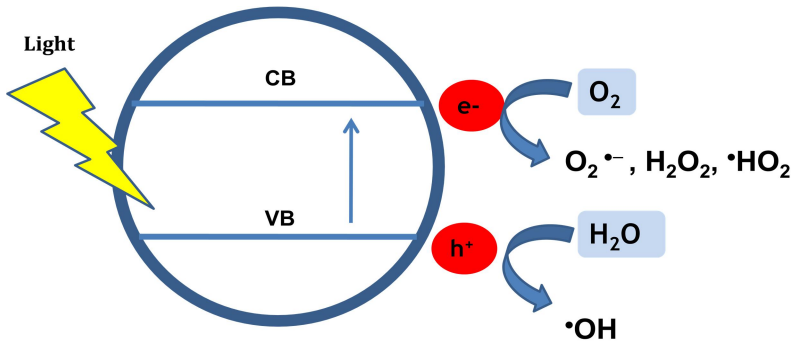

Fig. 1.4: Photocatalytic generation of various reactive species

1.3.8 Mechanism of Semiconductor mediated Photocatalysis

A photocatalyst harnesses light (UV/visible radiation from sunlight or artificial light) and uses the energy to break down different substances including organic materials, organic acids, estrogens, pesticides, dyes, crude oil, microbes (including viruses) and chlorine resistant organisms, inorganic molecules such as nitrous oxides (NO_x) etc. In combination with precipitation or filtration, the technique can also remove metals such as mercury [13,14,15]. Due to this universal applicability, photocatalysis with nanoparticles as catalysts is used to reduce air pollution and for water purification. Titanium dioxide (TiO_2) is the most common photocatalyst. Zinc oxide (ZnO), could be used as a viable alternative for some applications. To avoid free nanoparticles in water, TiO_2 nanoparticles are usually immobilized on a substrate or integrated into thin-films and other materials. For the activation of TiO_2, UV irradiation from sunlight or artificial light is needed, with UVB being more efficient than UVA. To allow activation by visible light, TiO_2 can be modified with a second semiconductor, dyes, nitrogen, carbon or sulphur. For example, TiO_2 doped with nitrogen had superior photocatalytic activities compared to commonly used unmodified TiO_2 nanoparticles for both chemical and bactericidal decontamination of water [16].

Semiconductor (SC) mediated photocatalytic reactions are initiated by the absorption of light with energy equal to or greater than the band gap of the semiconductor. This produces electron-hole (e^-/h^+) pairs as in equation (1.4),

$$SC + hv \rightarrow e^{-}_{cb}\,(SC) + h^{+}_{vb}\,(SC) \qquad .....(1.4)$$

where cb is the conduction band and vb is the valence band. Thus, as a result of irradiation, the SC particle can behave either as an electron donor or electron acceptor for molecules in contact with it. The electron and hole can recombine, releasing the absorbed light energy as heat, with no chemical reaction taking place. On the other hand, they can participate in redox reactions with adsorbed species as the valence band hole is strongly oxidizing while the conduction band electron is strongly reducing. On the semiconductor surface, the excited electron and the hole can participate in redox reactions with water, hydroxide ion (OH^{-}), organic compounds or oxygen leading to degradation and eventual mineralization of the pollutant [16]. Schematic presentation of a typical heterogeneous photocatalytic process is shown in figure 1.5.

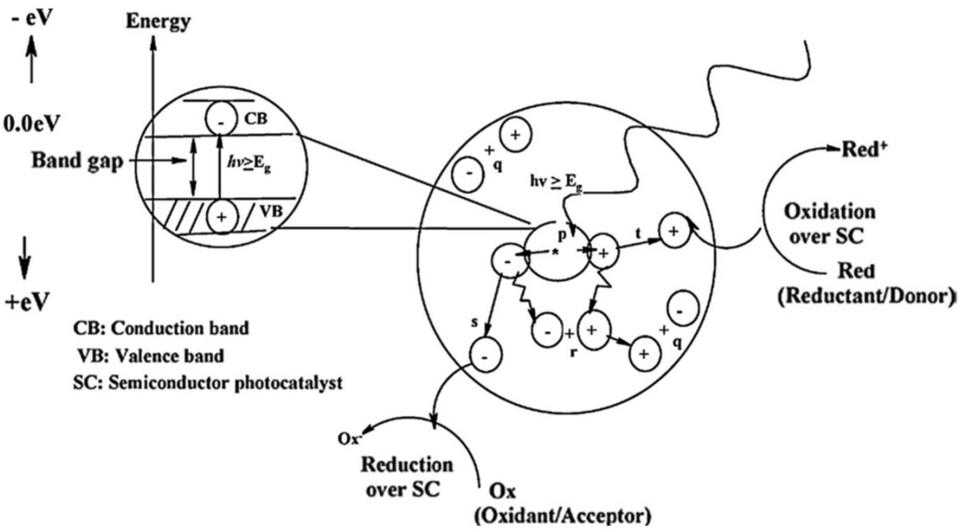

Fig. 1.5: Schematic diagram of semiconductor photocatalytic process [17]

It has been shown that the charges can react directly with adsorbed pollutants, but reactions with water are predominant since the water molecules are more abundant than contaminant molecules. Consequently, oxidation of water or OH^- by the hole produces the hydroxyl radical ($^{\bullet}OH$), a powerful oxidant. The oxidation potential of hydroxyl radical ($^{\bullet}OH$) is 2.8 V relative to the normal hydrogen electrode. Apart from electrons and holes, other substances that may be used for water disinfection include O_3 (2.07 V), H_2O_2 (1.78 V), HOCl (1.49 V) and Cl_2 (1.36V). Hydroxyl ($^{\bullet}OH$) radicals are able to rapidly attack pollutants on the semiconductor surface and, as such, are the most important radicals formed in TiO_2 photocatalysis. An important reaction of the conduction band electron is reduction of adsorbed oxygen to oxygen radicals and this prevents the electron from recombining with the hole. This leads to accumulation of oxygen radicals that can also participate in degrading contaminants in solution.

Heterogeneous photocatalytic process with semiconductor oxide catalysts involves at least five separate reaction steps taking place on the surface of the catalyst, i.e., (i) diffusion of reactants to the surface, (ii) adsorption of reactants, (iii) reaction on the surface, (iv) desorption of products from the surface and (v) diffusion of products from the surface.

1.3.9 Zinc oxide as a semiconductor Photocatalyst

The most investigated semiconductor oxide photocatalyst is TiO_2. ZnO has been often considered as an alternative to TiO_2 as photocatalyst because of its good optoelectronic, catalytic and photochemical properties [18-21]. ZnO has high catalytic efficiency, low cost, large bandgap (3.37 eV), and nontoxic nature. In fact, it has been shown to be more effective than

TiO_2 as photocatalysts in different studies [22]. Upon illumination by light, ZnO generates holes that are strong enough to oxidize organic pollutants into less harmful materials [23-27]. Various ZnO nanostructures have been used to degrade the harmful dyes into less harmful components by photocatalytic reaction under UV and visible light illumination.

1.3.9.1 Mechanism of photosensitization of ZnO by dyes

The mechanism of photocatalysis by ZnO and TiO_2 is similar and is as explained earlier in Section 1.3.8. The photocatalytic efficiency of these two semiconductor oxides also is comparable since they have identical band gaps (3.3 eV). However, depending on the surface characteristics of the catalyst, the chemistry of the substrate and reaction conditions, especially pH and the wavelength range of light, the efficiency can differ. For e.g., in the case of dye substrate, ZnO is often more photoactive, especially in the visible region of light.

Dyes can act as sensitizers to the catalyst by the absorption of visible light. Transfer of photogenerated electrons from the dye molecule to the semiconductor has been reported to be very effective leading to the generation of reactive free radicals with less energy consumption. Various steps involved in this case are:

$$\text{Dye} + h\nu \rightarrow \text{Dye}^* \quad .....(1.5)$$

$$\text{Dye}^* \rightarrow \text{Dye}^+ + e^- \quad .....(1.6)$$

$$ZnO + e^- \rightarrow ZnO^{\bullet -} \quad .....(1.7)$$

$$ZnO^{\bullet -} + O_2 \rightarrow ZnO + O_2^{\bullet -} \quad .....(1.8)$$

$$2O_2^{\bullet -} + 2H^+ + e^- \rightarrow 2HO_2^{\bullet} \rightarrow H_2O_2 + O_2 \quad .....(1.9)$$

$$H_2O_2 + e^- \rightarrow {}^{\bullet}OH + OH^- \quad ....(1.10)$$

Eq. (1.5) depicts the absorption of light by the dye molecule (Dye). This excited dye (Dye*) injects an electron to the conduction band of ZnO in Eq. (1.7), where it is scavenged by O_2 to form active oxygen molecule as shown in Eq. (1.8). Further, the active oxygen molecule formed in Eq. (1.8) subsequently reacts with H_2O to generate $OH^{\bullet}$ radicals (Eq. 1.9, 1.10). These active radicals drive the photodegradation or mineralization of the dye molecule as follows;

$$\mathrm{Dye}^{\bullet +} + {}^{\bullet}\mathrm{OH} \rightarrow \text{hydroxyl or peroxo intermediate}$$
$$\downarrow$$
$$\text{Degraded or mineralized products} \qquad ....(1.11)$$

1.3.9.2 Selected relevant earlier reports on the photocatalytic degradation of dyes

Sakthivel et al. [28] reported the sunlight induced degradation of a complex diazo dye, Acid brown 14 in presence of both ZnO and TiO_2 catalysts. Complete mineralization was attained with the formation of carbon dioxide, water, nitrate, ammonia, sulphate and chloride. Acid brown 14 was converted completely into colourless intermediates within 120 and 300 min by ZnO and TiO_2, respectively. Complete mineralization was observed within 360 min with ZnO and 420 min with TiO_2. Comparison of photocatalytic activity of different semiconducting materials has clearly indicated that ZnO is the most active photocatalyst in the degradation of acid brown 14 using sunlight as the energy source. The main reason for the greater activity of ZnO is that it absorbs large fraction of the solar spectrum. UV-Vis absorption spectrum of ZnO shows that it absorbs more quantum of light. Hence it is evident that

considerable amount of visible light could be utilized when ZnO is used as catalyst. Thus it is concluded that for solar applications, ZnO will be a better catalyst compared to TiO_2 for the pollutants degradation. The amphoteric behaviour of both ZnO and TiO_2 is an important parameter in reactions taking place on semiconductor particle surfaces. The experimental results indicate that photocatalytic oxidation rate is pH dependent. Furthermore, the rate of degradation of Acid brown 14 linearly depends on the illumination by solar light at different periods of time with different light intensity.

Pare et al. [29] made a detailed investigation of the photocatalytic degradation of the dye, Acridine orange, in aqueous heterogeneous medium containing ZnO as photocatalyst in a batch reactor. Visible light in the absence of ZnO has negligible effect on degradation. The disappearance of the dye follows approximately pseudo-first order kinetics according to the Langmuir–Hinshelwood model. The total degradation/mineralization of dye was tested using the chemical oxygen demand (COD) method. The addition of an optimal amount of hydrogen peroxide (H_2O_2) and potassium persulphate ($K_2S_2O_8$) increases the degradation rate while salts like NaCl and Na_2CO_3 decreases the rate. The effect of addition of cationic and anionic surfactants has also been investigated. Bubbling of nitrogen in the reaction solution decreases the reaction rate. The study has shown that ZnO is a highly efficient photocatalyst for the degradation of Acridine orange dye. This also points to the potential of ZnO photocatalysis in the treatment of organic pollutants such as dyes.

Daneshvar et al. [30] reported that the degradation of Acid red 14 (AR14), commonly used as a textile dye, can be photocatalysed by ZnO. The degradation follows first order kinetics. The effects of parameters such as pH, amount of photocatalyst, added H_2O_2 and ethanol etc. were also examined. Appropriate amounts of H_2O_2 improved the decolorization, while excess of H_2O_2 quenched the formation of hydroxyl radicals ($^{\bullet}OH$) and inhibited the degradation.

Investigations on the crystal structure, morphology, optical properties, rate of electronic-hole recombination and photodegradation performance of {001}TiO_2 for methylene blue demonstrated that rutile TiO_2 is a much more active photocatalyst compared to normal TiO_2 [31]. Treatment of normal TiO_2 with NaOH under appropriate conditions can change the morphology (of TiO_2) which in turn can modify the specific surface area and the optical electronic-hole recombination rate. Radical scavenging tests showed that hydroxyl radicals and holes are very important in photocatalysis.

Semiconductor nanocomposites of SnS_2-SiO_2@α-Fe_2O_3 were investigated as photocatalysts for the degradation of methylene blue (MB) [32]. The results show an effective enhancement in the photocatalytic activity for the degradation of MB by compositing, especially for the 15 wt % SiO_2@α-Fe_2O_3 nanocomposites on SnS_2 flowers.

In a comprehensive review of photocatalysis, Chiu et al. [33] discusses the kinetics and mechanisms of the photodegradation reactions of various dyes. The operational factors affecting the photodegradation of both cationic and anionic dye molecules, as well as the charge-carrier properties

of the photocatalyst, are critically examined. The review provides helpful guidelines that can be applied to foster the development of efficient photodegradation systems.

Optimization of a bench-scale UV-C photocatalytic process using a TiO_2 catalyst suspension for degradation of two textile dyes, Acid Blue 113 (AB 113) and Acid Red 88 (AR 88) is reported [34]. Using techniques such as Response surface methodology (RSM), Analysis of variance (ANOVA), Least-squares cubic regression models etc. it was demonstrated that solution pH and initial dye concentration had the strongest effects on degradation rates of AB 113 and AR 88, respectively. Under optimum treatment conditions, removal efficiencies reached 98.7% for AB 113 and 99.6% for AR 88. Kinetic studies showed that a first-order kinetic model could describe degradation data for both dyes.

Large number of reports on the application of photocatalysis in water treatment have been appearing in recent years. Semiconductor mediated photocatalysis as a means of degrading dye pollutants in water is demonstrated in these reports. Only those reports relevant in the context of the present study are presented here.

1.3.10 Sonolysis/ Sonochemical reaction as an AOP

Sonochemistry refers to the chemical effects of ultrasound. Generally, the sound whose frequency is pitched above human hearing (i.e., above 20 kHz) is referred as ultrasound. The chemical effects of ultrasound are due to a phenomenon called “acoustic cavitation”. Acoustic cavitation in liquid results in the formation, growth, and

implosive collapse of bubbles. This cavitational implosion produces radicals from many solvents. In the case of water, $^{\bullet}H$ and $^{\bullet}OH$ are the main resultant free radicals. These radicals can further combine or react with other substances. This results in secondary oxidation and reduction reactions [35].

The ultrasound can be classified based on the frequency range. The conventional power ultrasound (also called low-frequency high-power ultrasound) ranges between 20–100 kHz. The high-frequency medium power ultrasound (ranges 20–1000 kHz) is mainly used for the chemical applications. The therapeutic ultrasound (also called high-frequency low power ultrasound) ranges between 1 MHz and 10 MHz and has a lot of applications in the medical field [36-38].

In contrast with electromagnetic radiation, acoustic waves do not change the electronic, vibrational or rotational molecular energy level. The chemical effect of ultrasound arises due to cavitation phenomenon. Ultrasound exerts positive and negative pressure in a liquid medium during the compression and rarefaction cycle of the ultrasonic wave. This will result in an increase or decrease in the total pressure of the medium. However, at a certain time, they may experience the additive effect of the two pressures such as P_a (due to the acoustic wave) and P_h (due to the hydrostatic pressure) [32].

The total pressure (P_t) is given by the equation 1.12

$$P_t = P_h + P_a \qquad ....(1.12)$$

If the rarefaction cycle is powerful, it can break the van der waals forces which hold the liquid molecules together. This sets off the formation of gas-filled microbubbles. These bubbles expand during the rarefaction stage and compress during the compression stage as shown in Figure 1.6.

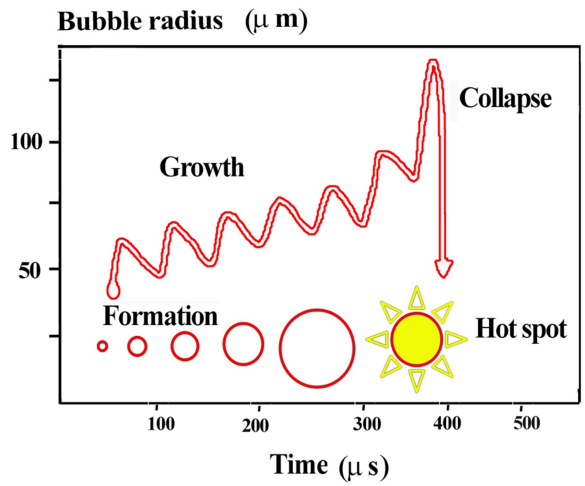

Fig. 1.6: Illustration of the cavitating bubble formation and collapse

But the rate of compression of the bubble is low compared to the expansion stage. Therefore the size of the bubble increases at each consecutive cycle. When it reaches an unstable state it undergoes extreme violent collapses to create an unusual environment for a chemical reaction in terms of enormous local temperatures and pressure (temperature and pressure to about 5000 K and 1700 bar, respectively). Water vapor is pyrolytically cleaved under this condition to produce $^{\bullet}OH$ and $^{\bullet}H$ [39,40] and it can be represented as,

$$H_2O \;)))\rightarrow\; ^{\bullet}OH + ^{\bullet}H \qquad ....(1.13)$$

These generated radicals can undergo either of the following reactions in the subsequent steps.

$$^{\bullet}OH + ^{\bullet}H \rightarrow H_2O \quad ....(1.14)$$

$$2\,^{\bullet}OH \rightarrow H_2O_2 \quad ....(1.15)$$

$$2^{\bullet}H \rightarrow H_2 \quad ....(1.16)$$

$$^{\bullet}H + O_2 \rightarrow HO_2^{\bullet} \quad ....(1.17)$$

The cavitation may either be stable or transient which is related to resonant size, lifetime of the cavity and/or bubble collapse. The bubble size and the lifetime are very small in the case of transient cavitation and the energy released during the collapse is high. However in the case of stable cavitation, bubble expansion and compression take place very slowly and therefore the size of the cavity can reach moderately higher size.

The most accepted theory for explaining the cavitational phenomenon is the hot spot theory, although there exists two other theories too, ie, electrical theory and plasma discharge theory. According to the hot spot theory, the cavitational collapse may lead to the rise in the temperature and pressure to about 5000 K and 1700 bar, respectively. Moreover, this remains only for about 100 ns with high cooling rate (greater than 1010 Ks^{-1}) [41]. This is a nearly adiabatic process. Sufficient energy release results in the generation of the reactive species followed by its stabilization by thermal quenching. The cavitational technique is utilized by many researchers in various fields such as material science,

organic synthesis, biology and the removal of hazardous wastes from water [35].

The use of ultrasound has been reported for the wastewater treatment containing various pollutants such as aromatic compounds, chlorinated aliphatic compounds, explosives, herbicides and pesticides, organic dyes, organic and inorganic gaseous pollutants, organic sulfur compounds, oxygenates and alcohols, pharmaceuticals, personal care products, pathogens and bacteria in water. But till now, no industrial installation of this technology has been reported due to its high cost and inefficient conversion of energy in producing ultrasonic cavitation. However, the coupling of ultrasound with other AOP technologies like ozone, hydrogen peroxide, Fenton's reagent, photocatalysts and enzymes might help to reduce the cost of wastewater treatment.

1.3.10.1 The reaction sites in sonolysis

Sonochemical reaction is distinct from other AOPs. The energy of ultrasonic sound wave affects sonochemical reactions, providing huge amount of heat and producing reactive free radicals. Ultrasound increases the mass transfer rate in aqueous solutions via turbulence [42]. Three main reaction zones are reported in a cavitating bubble [35]. They are

- Cavity interior
- Gas-liquid interface
- Bulk liquid.

The zones are schematically presented in figure 1.7.

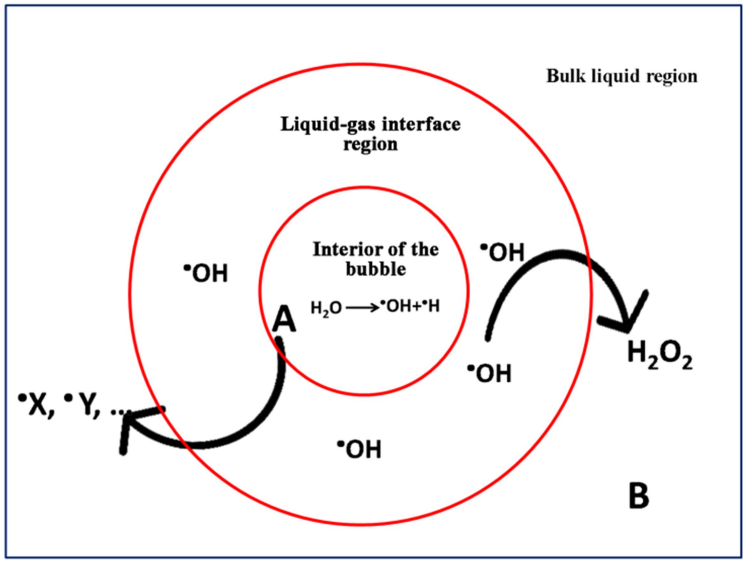

A: Volatile compound

B: Non volatile compound

Fig. 1.7: Various reaction zones in a cavitating bubble

The most reactive zone in the bubble is the interior of the bubble. The water molecules undergo pyrolysis inside the cavity to produce $^{\bullet}OH$ and $^{\bullet}H$ [42-44]. The target pollutants either undergo pyrolysis or reacts with the free radicals. Mostly, the volatile and hydrophobic compounds degrade in the interior of the cavitating bubble. For example, a highly volatile compound like CCl_4 is reported to be removed completely within a short period of time by sonolysis compared to the other AOPs [45-47]. The gas-liquid interface region of the cavitating bubble is also a high-temperature region. This region is hydrophobic and the chance of binding hydrophobic substance in this region is probably high. Thus, the hydrophobic substances can undergo easy degradation. Some stable

compounds are reported to undergo hydrolysis here due to the high temperature [48]. The recombination of $^{\bullet}OH$ takes place in this region to produce H_2O_2 and get released into the liquid region. Finally, only a small portion of the so formed $^{\bullet}OH$ is released into the liquid region. The reactions in the bulk phase are basically between substrates and $^{\bullet}OH$ or H_2O_2. The hydrophilic substances are found in the bulk phase and therefore only the radical reaction is feasible [49]. The possible reaction in a cavitating bubble is given in figure 1.7. The speciation of the target compound to these regions may occur with reference to their physicochemical properties. The major physicochemical parameters that might influence the degradation in sonolysis are partition coefficient, solubility, vapor pressure and Henry's law constant [50-52]. The target compound might move from the interior of the bubble to the liquid region with decrease in its volatility leading to variation in the reaction rates.

The intensity of cavitation is usually enhanced when solvents with low vapor pressure, high viscosity and high surface tension are used. At the same time, the bubbles are easily generated with solvents of opposite properties [52]. Thus any factor which affects these properties would also change the cavitation phenomena. Various operational parameters such as ultrasonic frequency, ultrasonic power, reaction temperature, nature of dissolved gas etc. influence the process significantly.

1.3.10.2 Selected relevant works reported on the sonochemical degradation of dyes

Merouani et al. [53] investigated the sonolytic degradation of cationic dye, Rhodamine B (RhB), in water with special reference to the

influence of bicarbonate and carbonate ions. As a consequence of ultrasonic cavitation that generates $^{\bullet}OH$ radicals, carbonate radicals were formed as secondary products, when the solution/suspension contains dissolved bicarbonate or carbonate ions. The results clearly demonstrated the significant intensification of sonolytic destruction of RhB in the presence of bicarbonate and carbonate, especially at lower dye concentrations. Degradation intensification occurs because sonochemically formed carbonate radicals undergo radical–radical recombination at a lesser extent than hydroxyl radicals. The generated carbonate radicals are likely to migrate far from the cavitation bubbles towards the solution bulk and are suitable for degradation of an organic dye such as RhB. Therefore, at low dye concentrations, carbonate radical presents a more selective reactivity towards RhB molecules than hydroxyl radical. The degradation rate reached a maximum at 3 g L^{-1} of bicarbonate, but subsequent addition retards the destruction process. In RhB solutions containing carbonate, the oxidation rate gradually increased with increasing carbonate concentration up to 10 g L^{-1} and slightly decreased afterwards. Sonochemically generated carbonate radicals are suitable for total removal of the COD of sonicated RhB solutions.

The sonochemical degradation of aqueous solutions of azobenzene and related azo dyes (methyl orange, *o*-methyl red, and *p*-methyl red) was performed at 500 kHz and 50 W, under air, O_2, or Ar saturation at 288 K [54]. Reaction products and intermediates were identified by HPLC-ES-MS. Total organic carbon (TOC) was also determined as a function of reaction time. Addition of OH radicals to the azo double bond is considered to be the first step of the sequence of oxidative bond

cleavages. This leads to the production of carboxylic acids, quinones, carbon dioxide, and nitrate ions as the main degradation products. The effects of the structure of the dye structures and of the dissolved gas on the sonochemical bleaching rates were also investigated. The reaction rates for *o*-methyl red were approximately 30-40% faster than those for the other compounds. This appears to be due to strong influence by a carboxylic group ortho to the azo group. Saturating with Ar instead of air or O_2 increased the pseudo first-order rate constants for the degradation by 10%. The acceleration of the sonochemical bleaching and the mineralization process upon addition of Fe (II) was also investigated in Ar saturated methyl orange solutions. A 3-fold increase in the reaction rate was observed at optimal Fe(II) concentrations. This kinetic effect is quantitatively accounted for by a simple model based on the reaction of Fe(II) with sonochemically produced H_2O_2 (Fenton's reaction). This Fenton (Fenton-like) process is proven to be a simple way of achieving a substantial improvement in the efficiency of sonochemical degradation reactions.

Titanium dioxide coated activated carbon (TiO_2/AC) synthesized using sol gel method is tested for the removal of Rhodamine B (RhB) dye under sonolysis [55]. The effect of operational parameters such as pH, temperature, ultrasonic frequency etc in the presence and absence of the catalyst on the sono degradation was studied in detail. The degradation efficiency of RhB in aqueous solution is 82 % in the presence of TiO_2/AC in 60 minutes at the optimum conditions ie, at pH 6, temperature 50°C and ultrasonic frequency of 30 kHz.

The degradation of oxalic acid with/without Pt/TiO_2 catalyst under sonication at 20 and 360 kHz was studied in the presence of Ar/O_2 (20 vol% O_2) and pure O_2 [56]. Oxidation rate of oxalic acid increased under Ar/O_2 atmosphere in presence of Pt/TiO_2 catalyst due to strong dispersion effect of both low and high ultrasonic frequency and formation of chemically active species by sonolysis. High frequency ultrasonic irradiation under Ar/O_2 atmosphere gives the highest kinetic increase compared to silent conditions with oxalic acid degradation rate around 13 mol min^{-1} at 40°C with 2 g L^{-1} of 3 wt% Pt on P25 TiO_2 catalyst.

Ghows and Entezari [57] studied the sonocatalytic degradation of Reactive Black 5 (RB5) in presence of nanocrystals of $CdS-TiO_2$ and the kinetic models were analysed. Two kinetic models were proposed and fitted properly to the data. In the first one, the heterogeneous reaction was considered similar to the Langmuir–Hinshelwood (L–H) mechanism and the kinetic rate parameters were determined. In this model, short time of sonication at different initial concentration of the substrate has been applied and the contribution of the reaction intermediates has been neglected. Hence, this model may not be valid for longer reaction times where the reaction intermediate effects prevail. In the second model, two first-order reactions in series provided the most convincing rate form for the sonodegradation of dyes adsorbed on the catalyst. In these series reactions, the first step is the conversion of the colored dye to colored intermediate, and the second step is the conversion to colorless product(s). The results were in good agreement with the proposed kinetic models. The rate constants of degradation of catalyzed reaction

were higher than that obtained without catalyst under solar and UV irradiation.

The sonolysis of Basic Blue 41 dye in aqueous solution was performed at 35 kHz using ultrasonic power of 160W and temperature of 25±1°C [58]. The nanoparticles of TiO_2 were used as catalyst to assist the sonication process. The effect of experimental parameters such as pH, H_2O_2 concentration and initial dye concentration on the reaction were investigated. It was observed that at lower pH values the dye removal rate decreased. However, the rate increased with increase in H_2O_2 concentration and decrease in the initial dye concentration. The intermediate compounds were detected by integrated gas chromatography–mass spectrometry (GC/MS) and ion chromatography (IC). During the decolorization, all nitrogen atoms and aromatic groups of Basic Blue 41 were converted to urea, nitrate, formic acid, acetic acid, oxalic acid, etc. Kinetic studies revealed that the degradation process followed pseudo-first order mechanism with a correlation coefficient of 0.9918 under experimental conditions. The results showed that power ultrasound can be regarded as an appropriate tool for degradation of azo dyes to non-toxic end products.

Eren and Ince [59] carried out studies on the degradation of two azo dyes at low and high frequency ultrasound (US) to compare their reactivity and to assess the impacts of frequency, $^{\bullet}OH$, chemical structure and soluble/nonsoluble additives. Low frequency US alone was totally ineffective for bleaching the dyes even after 2 h irradiation, while high frequency provided significant color decay in 30-min contact. The result was attributed to larger number of oscillations at high frequency that

allowed a larger fraction of $^{\bullet}OH$ ejection to the bulk liquid. The difference in the rates of dye degradation was due to different substituents around the azo bonds that dictated the reactivities of the dyes with $^{\bullet}OH$ and other species. The performance of low frequency US was remarkably improved and exceeded that of high frequency in the presence of CCl_4, nano-sized TiO_2 and zero-valent copper. The effect was attributed to the advantage of low frequency for long life time of the bubbles, high collapse temperatures, turbulent flow conditions and high sonoluminescence intensity. The efficacies of the additives in terms of the reduction in dye concentration per unit mass of additive were: $TiO_2 > CCl_4 > Cu$, regardless of the dye structure and the operation frequency. Better performance of TiO_2 than Cu was attributed to its larger surface area with a slight positive charge on it and to the effect of stable sonoluminescence that may have induced photocatalytic properties on semiconductor surface.

Lops et al. [60] proposed an environmental friendly sonophotocatalytic approach to decontaminate polluted waters from industrial dyes efficiently by exploiting ZnO micro- and nano-materials. The generation of reactive oxygen species (ROS) under ultrasound stimulation is demonstrated by Electron Paramagnetic Resonance Spectroscopy (EPR) for five different zinc oxide (ZnO) micro- and nano-structures, i.e. Desert Roses (DRs), Multipods (MPs), Microwires (MWs), Nanoparticles (NPs) and Nanowires (NWs). Rhodamine B (RhB) was used as the test molecule. The DRs microparticles demonstrated the best sonocatalytic performance (100% degradation of RhB in 180 min) and the highest generation of OH radicals under ultrasonic irradiation. Strikingly, the

coupling of ultrasound and sunlight irradiation in a sonophotodegradation approach led to 100% degradation efficiency, i.e. color reduction, of RhB in just 10 min, revealing a great positive synergy between the photocatalytic and sonocatalytic processes. The RhB sonophotocatalytic degradation was also evaluated at different initial dye concentrations and in the presence of anions in solution. The combination technique has demonstrated good stability over repeated cycles of dye treatment, which points to the potential applicability of this technique for the treatment of industrial effluents.

Triphenylmethane (TPM) dyes are an important category of dyes with a variety of industrial applications and consequently, these are found in the aquatic environment at relatively higher concentrations. The sonodegradation of two Triphenylmethane (TPM) dyes, ie para rosaniline (PRA) and ethyl violet (EV) was investigated using an ultrasonic frequency of 350 kHz and power of 60 W [61]. Complete degradation of EV and PRA was observed with a pseudo first order rate constant of 0.2339 min^{-1} and 0.1956 min^{-1}, respectively. The product analyses using high-resolution mass spectrometry (LC-Q-TOF-MS) revealed the formation of hydroxylated, de-alkylated, and other collapsed conjugated structure destructed products. The evolution of these products in the presence of various inorganic ions (Cl^-, SO_4^{2-}, NO_3^-, and CO_3^-) showed that only carbonate ions had a significant impact. The carbonate ions facilitated the formation of conjugated structure destructed product for both the dyes, probably due to the high reactivity of carbonate radical, and consequently accelerated interaction. The carbon-centered radicals

thus formed undergo further reaction leading to the destruction of conjugated structures. The scavenging effect of carbonate ions was also confirmed from the reduction in the formation of most of the hydroxylated products. Since one of the major inorganic species in any wastewater is carbonate ions this result is very relevant to the understanding of oxidation based treatment protocol.

Another recent study on the sono decomposition of C.I. Reactive Orange 107 (RO107) azo dye showed that more than 80% of decolorization could be achieved within 4 h. of sonication [62]. Degradation of the dye followed pseudo-first-order kinetics. The results also showed that sonication is controlled by hydroxyl radicals together with pyrolysis. Sulfanilic acid (m/z:172) was identified as the main intermediate by using liquid chromatography–tandem mass spectrometry (LC/MS) analysis. Possible pathways for the formation of the degradation products were proposed in this report.

1.3.11 Electrochemical degradation as an AOP (EAOP)

Another emerging AOP based technology for wastewater remediation is electrochemical degradation. The wide acceptance of this technology is due to its environmental compatibility because of the fact that it uses electron as the main reagent. Electron is a clean reactant and it operates under mild conditions [63]. Various other advantages including its versatility, high energy efficiency, availability of automation etc. makes this technique, a perfect tool for water purification [64]. Various AOP techniques which can be combined with the EAOPs for water purification are listed in figure 1.8.

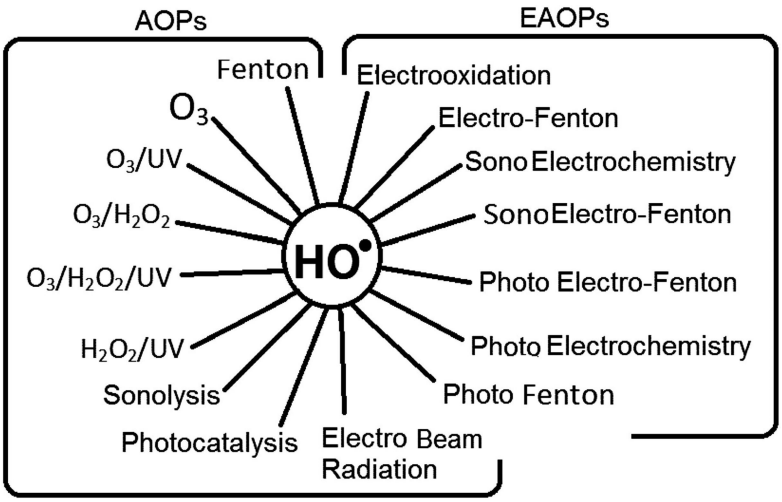

Fig. 1.8: Various AOPs and EAOPs with potential for water treatment

Anodic oxidation is the most appropriate electrochemical method for the treatment of wastewater containing organic pollutants [65]. A typical electrochemical system is represented in figure 1.9.

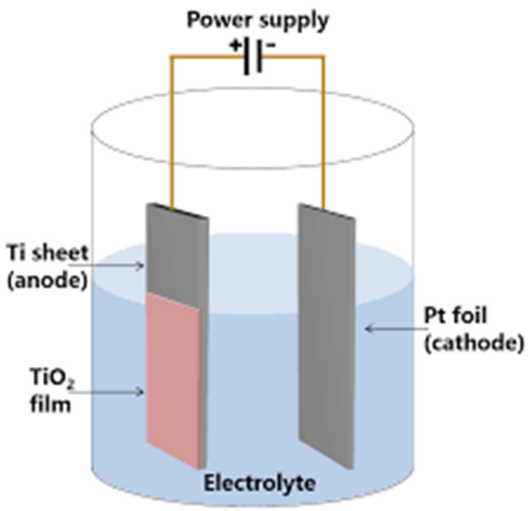

Fig. 1.9: Schematic diagram of an electrochemical reaction

Hydroxyl radicals ($^{\bullet}OH$) are generated at a high oxygen evolution potential anode (M) and the organic pollutants are expected to be degraded by interaction with the radicals [66, 67].

$$M + H_2O \rightarrow M(^{\bullet}OH) + H^+ + e^- \quad ....(1.18)$$

Graphite, platinum, dimensional stable electrode (DSA), stainless steel (SS), and air diffusion electrode (ADE) are frequently used as cathodic materials. When graphite or ADE is used as cathode, it is often fed with air or pure oxygen to generate H_2O_2 through the electrochemical reduction of O_2. This process is called AO-H_2 which also belongs to the scope of anodic oxidation. Na_2SO_4 is usually selected as the supporting electrolyte for the following reasons [68]: (i) it is relatively cheap, (ii) it could be oxidized into $S_2O_8^{2-}$ which also participate in the degradation of organics, (iii) it would not produce hazardous compounds during treatment and (iv) presence of Na_2SO_4 would promote the degradation of the substrate.

In presence of chloride, oxidation of organic compounds is mediated by active chlorospecies. The main reactions at the electrode are:-

$$\text{Anode: } 2Cl^- \rightarrow Cl_2 + 2e^- \quad ....(1.19)$$

$$\text{Cathode: } 2H_2O + 2e^- \rightarrow H_2 + 2OH^- \quad ....(1.20)$$

In the bulk solution, Cl_2 hydrolysis takes place as follows:

$$Cl_2 + H_2O \rightarrow HOCl + H^+ + Cl^- \quad ....(1.21)$$

$$HOCl \leftrightarrow H^+ + OCl^- \quad ....(1.22)$$

At the anode, O_2 evolution competes with Cl_2 evolution according to the equation,

$$H_2O \rightarrow 2H^+ + 1/2O_2 + 2e^- \quad ....(1.23)$$

This process is often called indirect electrolysis or chlorine-mediated electrolysis.

1.3.11.1. Anodic oxidation

In this process, pollutants are degraded either directly on the anode surface or by the reaction mediated by reactive oxygen species. Two types of mechanism are proposed in the case of EAOPs; (i) the pollutants are transferred from bulk liquid region to the anode surface where they undergo direct electrochemical reaction by electron transfer to the pollutants (ii) the pollutants undergo degradation by the reactions with the high oxidants generated from the anodic oxidation of water molecule or ions present in the water. The major oxidizing species is $^{\bullet}OH$ and they are generated by the direct conversion of water molecule as given below;

$$H_2O \rightarrow {}^{\bullet}OH_{ads} + H^+ + e^- \quad ....(1.24)$$

$$OH^- \rightarrow {}^{\bullet}OH_{ads} + e^- \quad ....(1.25)$$

1.3.11.2 Selected relevant earlier studies in electrochemical degradation of organic pollutants

The degradation of cationic turquoise blue GB (GB) by electrochemical oxidation with typical rare earth doped PbO_2 electrodes was reported [69]. The Ce- doped PbO_2 electrode was prepared by thermal decomposition-electrodeposition technique. The effects of electrodes used as anodes in the electrochemical oxidation system were

carefully studied for GB degradation. The effects of Ce-doped and undoped electrodes were compared and the former was found to be more efficient. Optimal degradation conditions were experimentally verified by studying the effects of different parameters, such as current density and electrolyte concentration. The characteristics of undoped and Ce-doped electrode were analyzed using the SEM images. The mechanism of GB degradation in electrochemical oxidation with Ce-doped electrode was discussed based on the intermediates which are identified by 'inductively coupled' and 'gas chromatographic' MS.

Kusuma et al. [70] studied the degradation of malachite green dye by using a voltage source potential and certain current is passed through carbon/TiO_2 electrodes as anode and silver electrodes as cathode. Degradation was measured by varying the potential, pH and time in a solution of malachite green containing supporting electrolyte 0.1 M NaCl. Optimum conditions were identified as pH 7-8 and potential 10 V. Based on the voltammogram, reactions that occur are identified as electrochemical-chemical-electrochemical (E-C-E) and irreversible. This method can reduce the COD value of 25 ppm dye solution up to 81.89% in 30 minutes. The degradation of the dye during this period is 100%.

de Silva et al. [71] investigated the electrochemical oxidation of the dye reactive blue 4 (RB-4) and reactive orange 16 (RO-16) on RuO_2 using dimensionally stable anode (DSA®). The electrolyses is performed both in the presence and the absence of NaCl as supporting electrolyte. In both cases efficient color removal was achieved. Moreover, at low chloride concentration (0.01 mol L^{-1}), total color removal was obtained

after just 10 min of electrolysis, and a significant increase in total dye combustion was achieved for all the studied anodes in chloride medium (reaching *ca.* 80% COD removal). No significant enhancement in color removal or mineralization was observed upon increasing chloride concentration. The influence of oxide composition on dye elimination seems to be significant in both media (with or without chloride), Thus $Ti/Ru_{0.30}Ti_{0.70}O_2$, is identified as the most active material for organic compound oxidation. The oxygen evolution reaction (OER) is a limiting factor in both supporting electrolytes; *i.e.*, NaCl and Na_2SO_4, and its competition with organic compound oxidation remained an obstacle. There is slight consumption of the undesirable adsorbable organo halogens (AOX) species formed within the first minutes of the electrolysis in the system $Ti/(RuO_2)_{0.70}(Ta_2O_5)_{0.30}$. Hence it may be inferred that even though the electrode system is an environmentally friendly composition, both anode composition and chloride concentration lead to the formation of undesirable compounds.

The degradation of an industrial textile dye Acid Blue 113 (AB113) by electrochemical oxidation (EO) approach has been performed in an aqueous medium [72]. The galvanostatic electrolysis was done using platinum supported on Ti (Ti/Pt), Pb/PbO_2 and TiO_2-nanotubes decorated with PbO_2 supported on Ti (Ti/TiO_2-nanotubes/PbO_2) as anodes. The electrochemical flow cell consists of 1.0 L of solution containing 250 mg dm^{-3} AB 113 with Na_2SO_4 as supporting electrolyte. The power applied was 20, 40 and 60 mA cm^{-2}. The electrolytic process was monitored by UV–visible spectrometry and the chemical oxygen demand (COD). The results showed that the dye was successfully degraded by

hydroxyl radicals electrogenerated from water on the Ti/TiO_2-Nanotubes/PbO_2 electrode surface. Compared with Ti/Pt and Pb/PbO_2, the Ti/TiO_2-nanotubes/PbO_2 anode is more efficient in oxidation rate, current utilization and energy consumption.

Morsi et al. [73] investigated the degradation of three types of textile dyes by electrochemical oxidation on lead dioxide anode. The influence of pH, current density, time of electrolysis, temperature, the conductive salt concentration and the initial dye concentrations were critically examined. Highest electrocatalytic activity was achieved in the presence of NaCl (3 g/l), 30 mA/cm^2, pH of 3 and temperature of 30°C which could be attributed to indirect oxidation of the dyes by the electrogenerated hypochlorite ions formed from the chloride oxidation. In addition, contribution from direct oxidation also could be possible via reaction of these dyes with the electrogenerated hydroxyl radicals adsorbed on the lead dioxide surface.

The electrooxidation as an environmentally clean technology has been investigated for the degradation of Mordant Blue 13 azo dye (MB13) using boron-doped diamond (BDD) and oxide ruthenium titanium (Ti/$Ru_{0.3}Ti_{0.7}O_2$ (DSA)) anodes. Various water matrices: distilled water (DW), hot tap water (HTW) and simulated wastewaters (SWS) with and without surfactant (SW) were used in the study [74]. The influence of reaction parameters, such as current density, initial dye concentration, electrolysis time/specific charge and pH on the MB13 degradation rate, current efficiency and energy consumption has been determined. The enhanced rate of both color and chemical oxygen demand (COD) removal

in sulfate aqueous solutions with BDD was observed. This indicates that sulfate ($SO_4^{-\bullet}$) radicals along with $^{\bullet}OH$ might be responsible for the degradation process. The MB13 decolorization process obeyed a pseudo-first-order reaction kinetics with the apparent rate constant varying from 7.36×10^{-2} min^{-1} to 4.39×10^{-1} min^{-1} for BDD and from 9.2×10^{-3} min^{-1} to 2.11×10^{-2} min^{-1} for DSA depending on the electrolysis conditions. Inorganic ions, mordant salt and surfactant contained in simulated effluents decelerated the COD decay for both the anodes. Comparison of the specific energy consumption for each electrocatalytic material under different experiment conditions has been made. The BDD electrode was more efficient than the DSA to oxidize the MB13 dye in all kinds of water. The same electrode system was tested and similar results were reported in the case of the dye Disperse Yellow 3 (DY3) too [75].

The treatment of synthetic wastewater polluted with the dye Procion Red MX-5B by different Electrochemical Advanced Oxidation Processes (EAOP) based on diamond anodes is reported recently [76]. The influence of current density and the supporting electrolyte on the efficiency of dye removal and mineralization has been studied. Results show that electrolysis with diamond electrodes is a potential technology for the efficient degradation of dye. The efficiency increases when chloride is used as the supporting electrolyte because of the electrochemical generation of hypochlorite in wastewater which contributes significantly to the dye removal. On the contrary, the total mineralization of the organic matter is more efficient in sulfate media. In this case, large amounts of peroxodisulfate are electrogenerated, favoring the complete removal of total organic carbon (TOC). Coupling of UV light irradiation

or ultrasound to electrolysis significantly improves the process performance; photoelectrolysis being the most efficient technology for the treatment of wastewater polluted with Procion Red MX-5B. The enhancement is attributed to the potential production of free chlorine or sulfate radicals that takes place by the activation of the electrogenerated oxidants. These species are more reactive than the oxidants and, therefore, they attack the organic matter present in wastewater more efficiently.

1.3.12 Fenton and Fenton-based reactions as AOP for water treatment

Fenton (F) and related processes encompass reactions of peroxides (usually H_2O_2) with iron ions to form active oxygen species that oxidize organic or inorganic compounds. The Fenton reaction was discovered by H.J.H. Fenton in 1894. He showed that H_2O_2 could be activated by ferrous (Fe^{2+}) salts to oxidize tartaric acid [77]. In the last few decades, the importance of OH^- reactions has been recognized and over 1700 rate constants for OH^- reactions with organic and inorganic compounds in aqueous solution have been tabulated [78]. In the recent past, Fenton reaction was efficiently utilized for the removal of many hazardous organics from wastewater [79, 80.].

In Fenton reactions, Fe^{2+} along with other oxidants (mainly H_2O_2) is used to generate $^{\bullet}OH$ [81-84] . The main reactions are given in equations 1.26 to 1.29.

$$Fe^{2+} + H_2O_2 \rightarrow Fe^{3+} + {}^{\bullet}OH + OH^- \qquad ....(1.26)$$

The rate of production of $^{\bullet}OH$ is enhanced when the above system is irradiated by UV light (Eq.1.27). One of the main advantages of UV

irradiation is the regeneration of the ferrous ion from the ferric ions (Eq. 1.28)

$$H_2O_2 + UV \rightarrow 2\ ^{\bullet}OH \quad ....(1.27)$$

$$Fe^{3+} + H_2O + UV \rightarrow {}^{\bullet}OH + Fe^{2+} + H^+ \quad ....(1.28)$$

Thus the Fe^{2+} can be recycled multiple times. Apart from ferrous ion regeneration, hydroperoxyl radicals ($^{\bullet}O_2H$) are also produced (Eq. 1.29).

$$Fe^{3+} + H_2O_2 \rightarrow Fe^{2+} + {}^{\bullet}O_2H + H^+ \quad ....(1.29)$$

The hydroperoxyl radicals may also attack organic contaminants though they are less reactive than hydroxyl radicals. It should be noted that, the iron added in small amount acts as a catalyst while H_2O_2 is continuously consumed to produce hydroxyl radicals.

The general mechanism of the Fenton process is shown in Fig. 1.10

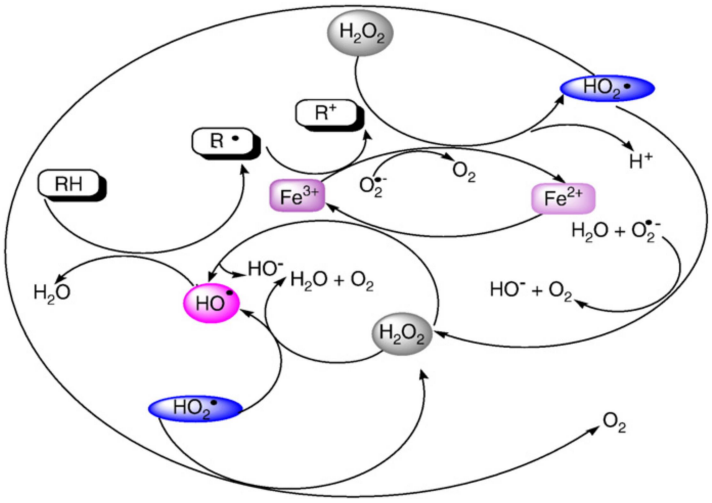

Fig. 1.10: Mechanism of oxidation of organic compounds with Fe^{2+} and H_2O_2 [84]

The use of persulphates (both peroxy mono and disulphates) in place of H_2O_2 is also reported in Fenton processes [79]. Persulphates generate $SO_4^{\bullet -}$ which are also equally efficient as the $^{\bullet}OH$.

1.3.12.1 Effect of Ferrous ion concentration

Usually the rate of degradation increases with an increase in the concentration of ferrous ion [85]. However, the extent of increase is sometimes only marginal above a certain concentration of ferrous ion as reported by Lin et al. [86, 87], Kang and Hwang [88] and Rivas et al. [89] reported that an enormous increase in the ferrous ions will lead to an increase in the unutilized quantity of iron salts, which will contribute to an increase in the total dissolved solids content of the effluent stream. This is not acceptable environmentally and hence, laboratory scale studies are required to establish the optimum loading of ferrous ions for efficient mineralization of the organics.

1.3.12.2 Effect of Hydrogen peroxide concentration

Concentration of H_2O_2 plays a crucial role in deciding the overall efficiency of the degradation process. Usually the % degradation of the pollutant increases with increase in the dosage of hydrogen peroxide [86-88]. However, care should be taken while selecting the operating oxidant dosage. The unused portion of H_2O_2 during the Fenton process contributes to COD [90] and hence excess amount is not recommended. Also, the presence of H_2O_2 is harmful to many of the organisms [86] and will affect the overall degradation efficiency significantly where Fenton oxidation is used as a pretreatment to biological oxidation. Another negative effect is the scavenging of the generated hydroxyl radicals, when large quantities

of H_2O_2 are used. Thus, the dosage of H_2O_2 should be adjusted in such a way that the entire amount is beneficially utilized and this can be decided based on laboratory scale studies.

1.3.12.3 Photo, Sono and Electro-Fenton processes

A combination of hydrogen peroxide and UV radiation with Fe^{2+} or Fe^{3+} oxalate ion (photo-Fenton (PF) process) produces more hydroxyl radicals compared to conventional Fenton method or photolysis and in turn increases the rate of degradation of organic pollutants [91-93]. Fenton reaction accumulates Fe^{3+} ions in the system and the reaction does not proceed once all Fe^{2+} ions are consumed. The photochemical regeneration of ferrous ions (Fe^{2+}) by photo-reduction (Eq. (1.30) of ferric ions (Fe^{3+}) occurs in photo- Fenton reaction [94]. The newly generated ferrous ions react with H_2O_2 and generate hydroxyl radical and ferric ion, and the cycle continues:

$$Fe(OH)^{2+} + h\upsilon \rightarrow Fe^{2+} + {}^{\bullet}OH \qquad ....(1.30)$$

The combination of Fenton reaction with conventional radiation zone of the visible and near ultraviolet gives better degradation of organic pollutants such as 4-chlorophenol [95], nitrobenzene, anisole [96], herbicides [97] and ethylene glycol [98] compared to the individual Fenton or photoprocesses. Direct photolysis of H_2O_2 produces hydroxyl radicals which can be used for the degradation of organic compounds. However, in the presence of iron complexes, which strongly absorb radiation, this reaction will contribute only to a lesser extent for the photo-degradation of organic contaminants [99,100].

The photo-Fenton process offers better performance at pH 3.0, when the hydroxy–Fe^{3+} complexes are more soluble and $Fe(OH)^{2+}$ are more photoactive [101-103]. The photo-Fenton process was reported as more efficient than Fenton treatment [102]. The use of sunlight instead of UV irradiation can reduce the costs. However, the solar process is less efficient. De Oliveira et al. [100] compared the performance of Fenton and photo-Fenton processes for the treatment of paint industry effluent (COD = 80.75 mg/L) and reported higher COD and TOC removal with solar-assisted photo-Fenton process compared to Fenton treatment or when an artificial radiation source was used. The performance was compared with three iron sources, i.e., $FeSO_4$, $Fe(NO_3)_3$ and potassium ferrioxalate ($K_3[Fe(C_2O_4)_3]$ (obtained by mixing $Fe(NO_3)_3$ with $K_2C_2O_4$ solutions). The formation of Fe^{3+} complex, when $Fe(NO_3)_3$ was used, resulted in poor performance whereas the addition of $K_3[Fe(C_2O_4)_3]$ increased the carbon loading of the wastewater. In the presence of 15 mM of Fe^{2+} and 300 mM of H_2O_2, 99.5% COD reduction was reported in 6 hr when the wastewater was irradiated with solar radiation.

The possibility of using ultrasound as the source of AOP activation is indicated in Section 1.3.10. The oxidation of organic contaminants in water by ultrasound, with and without catalyst (sonolysis/sonocatalysis) has received considerable attention in recent years [104]. The efficiency of the sonolytic process can be considerably enhanced by appropriately optimizing relevant reaction parameters (105-112). Similar enhancement by ultrasound irradiation has been reported in the Fenton process also [113-115]. However, such studies are relatively fewer to draw any specific conclusion except the accelerated generation of $^{\cdot}OH$ in presence

of US. More investigations are needed to establish the viability of the sonoFenton process in wastewater treatment.

In electro-Fenton (EF) process, pollutants are destroyed by the action of Fenton's reagent in the bulk together with anodic oxidation at the anode surface. Electro-Fenton process is classified into four types. In type 1, H_2O_2 and ferrous ion are electro-generated using a sacrificial anode and an oxygen sparging cathode [116]. In type 2, H_2O_2 is externally added while ferrous ion is produced from sacrificial anode as shown in Eq. (1.31) [117.]:

$$Fe \rightarrow Fe^{2+} + 2e^- \quad ....(1.31)$$

In type 3, ferrous ion is externally added and hydrogen peroxide is generated using an oxygen sparging cathode [118,119]. In type 4, hydroxyl radical is produced using Fenton reagent in an electrolytic cell and ferrous ion is regenerated through the reduction of ferric ions on the cathode [120,121]. However, electro-Fenton processes have problems with respect to H_2O_2 production. The generation of H_2O_2 is slow because oxygen has low solubility in water and the current efficiency is lower under reduced pH (pH < 3) [122]. In principle, the most promising electro-Fenton method is type 4, in which ferric ion is reduced to ferrous ion at the cathode. However, in this case too, Fe^{2+} regeneration is slow even at an optimal current density. The efficiency of electro-Fenton process depends on the nature of the electrode, pH, catalyst concentration, electrolytes, dissolved oxygen level, current density and temperature.

The continuous generation of $^{\bullet}OH$ and regeneration of Fe^{2+} is presented in equations 1.32-1.34.

$$O_2 + 2H^+ + 2e^- \rightarrow H_2O_2 \quad ....(1.32)$$

$$Fe^{2+} + H_2O_2 \rightarrow Fe^{3+} + H_2O + {}^{\bullet}OH \quad ....(1.33)$$

$$Fe^{3+} + e^- \rightarrow Fe^{2+} \quad ....(1.34)$$

The typically employed electrode materials in electro as well as electroFenton process are graphite, RVC (Reticulated Vitreous Carbon), Activated Carbon Fibre (ACF), carbon felt, and Gas Diffusion Electrodes (GDEs). The cell design is also an important factor in determining the efficiency of the reaction at varying concentrations of the pollutants. Various operational parameters that determine the rate of degradation in this technology are O_2 feeding, stirring rate or liquid flow rate, temperature, solution pH, electrolyte composition, applied potential or current, concentration of the catalyst as well as of the pollutant.

1.3.12.4 Selected relevant reports on the Fenton degradation of dyes

Bouasla et al. [123] studied the degradation of methyl violet dye in aqueous solution using Fenton process. Effects of various experimental parameters on the oxidation reaction were investigated. The parameters include the initial pH, temperature, stirring velocity and the initial concentrations of $FeSO_4$, of H_2O_2 and of the dye. The effect of $FeSO_4$ as catalyst has been compared with those of other catalysts $FeCl_3$ and Fe $(NO_3)_3$. The efficiency of degradation after 60 min of reaction, was 97.6% under optimized conditions i.e., initial pH=3; $[H_2O_2]_0$=2.1mM; $[Fe^{2+}]$=0.06mM; for a concentration of dye $[MV]_0$=0.06mM; temperature =

30°C. The results showed that the Fenton's reaction was effective for the degradation of methyl violet dye even with a low concentration of H_2O_2 and Fe^{2+}.

The oxidative decolorization of Reactive Black 5 (RB5) in aqueous solution has been studied by Lucas and Peres using Fenton (H_2O_2/Fe^{2+}) and photo-Fenton (H_2O_2/Fe^{2+}/UV) processes [124]. Both methods can remove the color of RB5. Batch experiments were carried out to determine the optimal operational conditions and make the process competitive with other processes. The optimal conditions were $[H_2O_2]_0/[RB5]_0$ of 4.9:1, $[H_2O_2]_0/[Fe^{2+}]_0$ of 9.6:1 and pH of 3.0. The decolorization experiments indicated that RB5 can be effectively decolorized using Fenton and photo-Fenton processes with almost same efficiency of 97.5% and 98.1%, respectively under optimal conditions. However, the difference is more in the case of TOC removal. With photo-Fenton process the TOC removal is 46.4% while with Fenton process it is only 21.6% after 1hr of reaction. This indicates that although UV irradiation has only little enhancing effect on the decolorization of the dye, it is important in the mineralization.

Combination of US and low concentration Fe^{2+} (<3 mgL^{-1}) (US/Fenton) has been used to treat wastewater containing Acid black 1 (AB1) [125]. The results show that the oxidation power of low concentration of Fenton reagent could be significantly enhanced by ultrasonic irradiation. Many operational parameters, such as ultrasonic power density, the pH value, the Fe^{2+} and H_2O_2 dosage, AB1 concentration and the temperature, affecting the degradation efficiency were investigated.

Under the given test conditions, 98.83% degradation efficiency was achieved after 30 min reaction by US/Fenton. The effects of various inorganic anions (such as Cl^-, NO_3^-, CO_3^{2-}, etc.) on the oxidation efficiency of US/Fenton were also studied. These anions inhibit the degradation of the dye significantly. The inhibiting effect of various inorganic anions was in the following order:

$$SO_3^{2-} > CH_3COO^- > Cl^- > CO_3^{2-} > HCO_3^- > SO_4^{2-} > NO_3^-$$

The results show that the US/Fenton can be an effective technology for the treatment of organic dyes in wastewater, provided the input parameters are identified and optimized.

Youssef et al. [126] investigated Fenton reaction at normal temperature and atmospheric pressure for the degradation of Methyl orange. The effects of different parameters like H_2O_2 and Fe^{2+} dosages, initial concentration of the dye and pH of the solution on the oxidation of the dye are studied in detail. The results indicate that the dye can be most effectively oxidized at dye:Fe^{2+}: H_2O_2 molar ratio of 1:3.5:54.2. It was found that more than 97.8% removal of the dye could be achieved in 15 min at pH 2.79 at room temperature. The results are useful in designing proper treatment systems for wastewater containing various dyes.

Ertugay et al. [127] investigated the degradation of Direct Blue 71 (DB71) by Fenton's oxidation process. The effect of initial pH, dosages of Fe^{2+} and H_2O_2, dye concentration and temperature on the color and COD removal was optimized in a batch reactor. Under optimal conditions, i.e., pH =3.0, Fe^{2+}= 3 mgL^{-1} and H_2O_2 =125 mgL^{-1}, 94%

color and 50.7% COD removal efficiency of the dye (100 mgL^{-1} aqueous solution) were achieved after 20 min of reaction. The Behnajady–Modirshahla–Ghanbery (BMG) kinetic model provided the best correlation of the experimental data compared to the pseudo-first and second-order kinetic models.

Comparison of classic and ultrasound Fenton process for treatment of industrial textile wastewater showed that the latter is more economical because the use of H_2O_2 and ferrous ions is comparatively less [128]. The degradation and mineralization of petrochemical wastewater containing phenol and nitrophenol with chemical oxygen demand (COD) at 260 mg/L and total organic carbon (TOC) at 100 mg/L, were investigated by sono–photo-Fenton process [129]. The influence of operational variables such as pH, initial concentration of H_2O_2 and Ferrous ions on the removal of COD was investigated. The graphical response surface plots were employed to determine the optimum conditions. The operational variables optimized by the model were as follows: $[Fe^{2+}]$ = 24 mg/L, pH = 3 and $[H_2O_2]$ = 500 mg/L. The results showed that at the predicted optimum conditions, the degradation and mineralization (removal of TOC) were 76.1 and 68.7%, respectively after 60 min of reaction. Enhancement in the efficiency of the Fenton process, by combining it with oxidants such as O_3, hypochlorite etc. and electrolysis, for the degradation of various dyes as well as their precursors and reaction intermediates also has been reported [130,131].

Some of the recent reports on the application of various AOPs for the treatment of wastewater containing different types of dye

pollutants were reviewed above. Of the many AOPs discussed, photolysis/photocatalysis, sonolysis, electrolysis and Fenton process (and its combination with various forms of activation) are investigated in detail in the current study for the mineralization of Indigo Carmine dye pollutant. The best technique identified from the study, i.e. solar photocatalyticFenton, is applied for the removal of a variety of pollutants from water. The 'previous' wastewater is thus rendered reusable by this technique.

.....ꕥ.....

Chapter

2

OBJECTIVES OF THE STUDY, MATERIALS USED, GENERAL PROCEDURES, PLAN OF THE THESIS

Contents

2.1 Main Objective

Identification of eco-friendly, efficient and economical Advanced Oxidation Processes (AOPs) based on Electro, Sono, Photo and Fenton chemistry for the decontamination of water from multiple chemical pollutants in order to enable the reuse of the treated water appropriately.

2.1.1 Specific Aims under the main objective

- In depth investigation of photocatalysis using sunlight as the energy source and commercially available semiconductor oxides such as ZnO as catalyst for the removal of chemical pollutants from water.
- Evaluation of the potential of inexpensive electrochemical processes for the decontamination of water from selected category of pollutants such as dyes.

- Extension of the investigations on sonolysis and sonocatalysis already in progress in our laboratory, towards the removal of toxic dye pollutants from water.
- Investigations on the classic Fenton process from a different angle including its combination with other AOPs and the use of sunlight as the natural source of energy for the efficient decontamination of water with minimum Fe sludge formation.
- Application of the most efficient AOP as identified from the study for the decontamination of water from multiple chemical pollutants.

2.2 Analytical Procedures

Analytical procedures used for the studies reported commonly in all Chapters i.e., H_2O_2 analysis, oxalic acid analysis, Chemical Oxygen Demand (COD), adsorption, $^{\cdot}OH$ radical detection etc are as given below. Specific procedures pertaining to specific study are provided in respective Chapters.

2.2.1 Estimation of H_2O_2

H_2O_2 was analyzed by standard iodometry [132]. The oxidation of iodide ions by H_2O_2 was carried out in 1N sulphuric acid in presence of a few drops of saturated ammonium molybdate solution, which acts as a catalyst. The reaction was allowed to go to completion (5 minutes) in the dark. The liberated iodine was then titrated against a standard solution of sodium thiosulphate, (usually of 5×10^{-3} N) prepared freshly from 10^{-1} N stock solution. Freshly prepared starch was used as the indicator.

2.2.2 Estimation of oxalic acid

Oxalic acid is estimated by the standard redox titration using potassium permanganate. Oxalic acid is the reducing agent and $KMnO_4$ is the oxidizing agent. A standard solution of $KMnO_4$ is prepared. H_2SO_4 is added to the oxalic acid solution before titration. The reaction between $KMnO_4$ and oxalic acid is slow and hence the solution is heated to 60°C to accelerate the rate of reaction. End point is change in color from colorless to light pink.

2.2.3 Chemical Oxygen Demand (COD)

Open reflux method is used to determine COD of the samples [132]. 50 mL of the sample was pipetted out into a refluxing flask. $HgSO_4$ (1g) was added along with several glass beads. 5 mL of sulfuric acid reagent (5.5g Ag_2SO_4 in 543 mL conc. H_2SO_4) were added slowly with mixing to dissolve $HgSO_4$. The sample was cooled while mixing to avoid the possible loss of volatile material. 25 mL of 0.05 N $K_2Cr_2O_7$ solution was also added and mixed well. Remaining (70 mL) sulfuric acid reagent was added through the open end of the condenser. The whole mixture was refluxed for 2 hours and cooled thereafter to room temperature. The mixture was diluted to 150 mL and the excess $K_2Cr_2O_7$ was titrated against 0.05 N ferrous ammonium sulfate (FAS) solution using ferroin as the indicator. The end point was sharp change in color from blue-green to reddish brown. A blank was also carried out under identical conditions using the reagents and distilled water in place of the sample.

COD is calculated using the following Eq;

$$\text{COD as mg } O_2/L = \frac{(A-B)\times M \times 8000}{\text{mL Sample}} \quad .....(2.1)$$

A = mL FAS used for blank

B = mL FAS used for sample

M = Molarity of FAS

8000 = milli equivalent weight of oxygen × 1000 mL/L

2.2.4 Detection of hydroxyl radicals using photoluminescence spectra

The formation of $^{\cdot}OH$ radicals in the reaction system during the solar photocatalytic activation was tested by the photoluminescence (PL) technique using terephthalic acid (TPA) as the probe molecule [133]. Shimadzu model RF-5301 PC fluorescence spectrophotometer was used for recording the spectrum. If $^{\cdot}OH$ is formed in situ in the system, it will react with TPA and form 2- hydroxyterephthalic acid (HTPA), which is a fluorescent molecule. The intensity of its PL will be proportional to the quantum of $^{\cdot}OH$ present in the system. In this method, the reaction solution of the required concentration is mixed with aqueous solution of TPA (2×10^{-4}M) and NaOH (2×10^{-3}M) and irradiated by the activation source (light, ultrasound etc). The PL spectrum of the product HTPA is recorded periodically in the range of 400-450 nm. The PL intensity at 425 nm corresponds to the concentration of HTPA and hence of the $^{\cdot}OH$ radicals formed in the system.

2.3 Materials Used

2.3.1 Indigo Carmine

Indigo Carmine (IC) (AnalaR Grade 99.5% purity) from Sisco Research Laboratories Pvt. Ltd (India) was used as such without further purification. IC (5, 5′-indigodisulfonic acid sodium salt) is an organic salt derived from indigo by sulfonation, which comes from tropical leguminous plants, *Indigoferra species*. IC is a redox indicator, turning yellow upon reduction. Toxicity of IC in terms of LD_{50} in rat is >2000 mg/kg. It has been used as an indicator substance in a number of analytical methods due to its sharp absorption peak. It is used as microscopic stain and also as diagnostic dye. It is also used as a food additive as well as in cosmetics and pharmaceuticals. IC is classified as a highly toxic indigoid dye. Contact with it can cause skin and eye irritation [134,135]. The chemical structure of Indigo Carmine is given in Fig. 2.1.

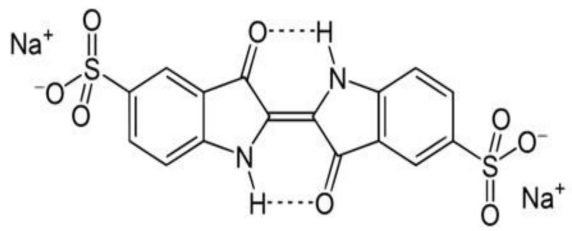

Fig. 2.1: Structure of Indigo Carmine

The main physicochemical properties of Indigo Carmine are given in Table 2.1

Table 2.1: Physicochemical properties of Indigo Carmine

Chemical formula	**$C_{16}H_8N_2Na_2O_8S_2$**
Molecular mass	466.35 g/mol
Appearance	Dark blue powder with coppery luster
Solubility	1 g/L, Soluble in water, ethanol, insoluble in organic solvents
Melting point	>300°C (572°F)
Absorption maximum (water)	608-612 nm
Bulk density	700-900 kg/m^3
pH value	7 (10 g/L, H_2O, 20°C)
Decomposition	When heated to decomposition it emits very toxic fumes of sulfur oxide, nitrogen oxide, and sodium oxide

2.3.2 Rhodamine B

Rhodamine B (RhB) {molecular formula $C_{28}H_{31}N_2O_3Cl$, molecular weight: 479.01g/mole, IUPAC name: N-[9-(ortho-carboxyphenyl)-6-(diethylamino)-3H-xanthen-3-ylidine]diethyl ammonium chloride}, used in the study (>99.6% purity) was from Sigma Aldrich India and was used as such without further purification. The dye exists in two molecular forms i.e., cationic and zwitter ionic forms. The absorbance of RhB solution at 554 nm (n → π* transition of C=N, C=O groups) in the UV-Vis spectra is used to monitor the decolorization. It has wide applications such as in dyeing and printing in textile, paper, paints, leathers etc., and as intermediate in the production of pesticides, synthetic polymers etc. It is primarily a water pollutant and the removal of color from effluents is

aesthetically as well as environmentally important. Further, even a small quantity of the dye in water can be toxic to humans. Harmful health effects include mutations, cancer, allergic dermatitis, skin irritation, burning of the eyes, excessive tearing, nasal burning, chest pain/tightness, cough, headache, nausea etc. [136]. The toxicity in terms of LD_{50} (mice) is 887 mg/kg. The chemical structure of RhB is given in Fig. 2.2.

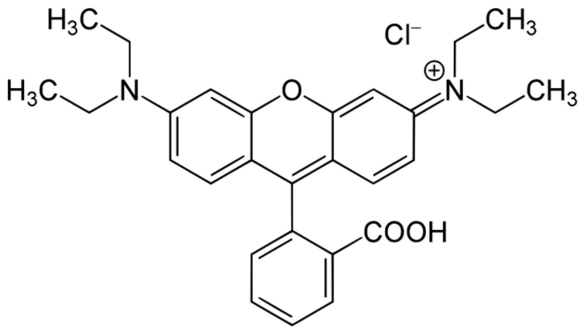

Fig. 2.2: Structure of Rhodamine B

Since RhB is suspected to be carcinogenic, products containing the dye must carry a warning on its label. Cases of economically motivated adulteration, where RhB was illegally used to impart red color in food and cosmetics industry have been reported from some countries. Typical properties of RhB are presented in Table 2.2.

Table 2.2: Physicochemical properties of Rhodamine B

Chemical formula	**$C_{28}H_{31}ClN_2O_3$**
Molecular mass	478.68 g/mol
Appearance	Red to violet powder
Solubility in water	~15 g/L (20°C)
Melting point	210-211°C (410 to 412°F, 483-484K) (Decomposes)
Specific Gravity	1.31
Stability	Stable. Incompatible with strong oxidizing agents

2.3.3 Diquat

Diquat dibromide monohydrate (99.9%) obtained from Sigma-Aldrich was used as such without further purification. Diquat is a dipyridyl compound which is the active ingredient in some herbicide compounds and most often available as the dibromide; Diquat dibromide. It produces desiccation and defoliation. On a global basis, two-thirds of the volume of Diquat is used for preharvest desiccation to aid the harvesting of seed and fodder crops whereas one-third is sold as a weed killer. Diquat is also used (at or below 1 mg/L) as an aquatic herbicide for the control of free-floating and submerged aquatic weeds in ponds, lakes and irrigation ditches. It acts quickly to damage only those parts of the plant where it is applied. Diquat bonds strongly to mineral and organic particles in soil and water and remains without significant degradation for years [137]. The structure of Diquat is given in Fig. 2.3.

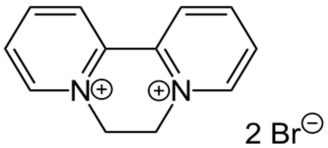

Fig. 2.3: Structure of Diquat

Diquat is moderately toxic. It may be fatal to humans if inhaled, swallowed or absorbed through skin in large quantities. Rapid and extensive photochemical degradation occurs in presence of sunlight. The LD_{50} of Diquat is 25 to 50 mg/kg (oral, rat). Some of the relevant properties of Diquat are given in Table 2.3.

Table 2.3: Physicochemical properties of Diquat

Chemical formula	**$C_{12}H_{12}Br_2N_2$**
Molar mass	344.05 $gmol^{-1}$
Appearance	Yellow crystals
Boiling point	Decomposes at or below boiling point
Melting point	335°C (635°F, 608K)
Density	1.22-1.27 g/cm^3
Vapor pressure	< 0.00001 mmHg (20°C)
Solubility	Soluble in water (70% at 20°C), practically insoluble in organic solvents
Specific gravity	1.61 g/cm^3
Hydrolysis	pH 5-7 (stable); pH 9 (slight hydrolysis)

2.3.4 Diclofenac

Diclofenac from Alfa Aesar (purity 99%) was used as such without further purification. Its chemical name is 2- (2, 6-dichloranilino) phenylacetic acid. Diclofenac is a non-steroidal anti-inflammatory drug (NSAID) used to treat pain associated with conditions like migraine, rheumatoid arthritis, gout, sprains of muscles and joints. Use of Diclofenac reduces these symptoms and helps the patient to lead normal daily activities. Diclofenac is widely detected in surface waters and can potentially cause deleterious effects in fish and can adversely affect marine ecosystem. It is extremely toxic and can readily undergo phototransformation reactions in the environment [138]. Toxicity is LD_{50}=390 mg/kg (orally in mice). The structure of Diclofenac is given in Fig. 2.4.

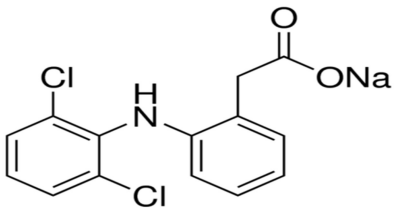

Fig. 2.4: Structure of Diclofenac

Table 2.4: Physicochemical properties of Diclofenac

Chemical formula	$C_{14}H_{11}C_{l2}NO_2$
Appearance	Crystals from ether-petroleum ether
Molecular mass	296.148 g/mol
Solubility in water	2.37mg/L (at 25°C)
Melting point	283-285°C
Vapour pressure	0.0 ± 1.0 mmHg at 25°C
Density	1.4 ± 0.1 g/cm^3
Boiling point	412.0 ± 45.0°C at 760 mmHg

2.3.5 Phenol

Phenol of AnalaR Grade (99.5% purity) from Qualigen (India) was used as such without further purification. Phenol is often used as a model pollutant in wastewater remediation studies. Phenol is commonly employed in the manufacture of phenolic resins, bisphenol A, caprolactam and chlorophenols [139]. Phenols are being discharged into the waters from various industrial processes such as oil refineries, ceramic plants, petrochemical plants, coal conversion processes and phenolic resin industries. It is toxic and harmful to living organisms even at low concentrations. Phenol and its derivatives pose serious threat to many ecosystems, water supplies and human health because of their toxicity, inertness, endocrine disrupting abilities and carcinogenic behavior. The use of phenol-contaminated waters causes protein degeneration, paralysis of the central nervous system and also damages the kidney, liver and pancreas in human bodies. Based on the recommendations of World Health Organization (WHO), the permissible concentration of phenolic contents in potable water is 1 g/L and the regulations by the Environmental

Protection Agency (EPA), call for lowering phenol content in wastewaters to less than 1mg/L. The removal of phenols from water and wastewater is an important issue in order to protect public health and the environment [140]. The structure of phenol is shown in Fig. 2.5.

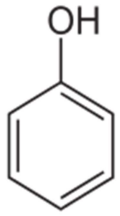

Fig. 2.5: Structure of Phenol

Table 2.5: Physicochemical properties of Phenol

Chemical formula	**C_6H_6O**
Molecular mass	94.11 g/mol
Appearance	Transparent crystalline solid
Solubility in water	8.3 g/100 mL (20°C) 40.5°C (104.9°F, 313.6K)
Boiling point	181.7°C (359.1°F, 454.8K)
Stability	Stable. Incompatible with strong oxidizing agents
Density	1.07 g/cm^3
UV-vis (λmax)	270.75 nm

2.3.6 Carbendazim

Carbendazim is a systemic benzimadazole fungicide that has extensive application. It is used to control diseases in cereals, fruits, vegetables and ornamental plants. It is also used for seed pre-planting treatment and postharvest food storage. The fungicidal action of carbendazim involves inhibition of the development of the fungi by

interfering with spindle formation at mitosis (Mitosis is a process where a single cell divides into two identical daughter cells). The LD_{50} of carbendazim is 10,000 mg/kg [141]. Carbendazim is identified as an endocrine disruptor. It also affects the number of chromosomes in human even at low exposures by inhibition of polymerization of tubulin, the protein that is essential for segregation of chromosome during cell division. Carbendazim gets strongly adsorbed to sediments thereby affecting the aquatic organisms. It is toxic to earthworm and non-target plants. The structure of carbendazim is shown in Fig. 2.6. The physico-chemical properties of carbendazim are shown in Table 2.6.

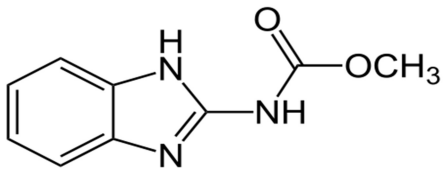

Fig. 2.6: Structure of Carbendazim

Table 2.6: Physico-chemical properties of carbendazim

IUPAC name	**Methyl *1H*-benzimidazol-2-ylcarbamate**
Chemical formula	$C_9H_9N_3O_2$
Appearance	Light Grey Powder
Molar mass	191.187g/mol
Density	1.45 g/cm^3
Melting point	302 to 307 °C (576 to 585 °F; 575 to 580 K)
Solubility in water	8mg/L
Acidity (pKa)	4.48
UV- Vis (λ max)	284 nm

2.3.7 Paracetamol

Paracetamol, also known as acetaminophen or APAP, is a medicine used to treat pain and fever. It is classified as a mild analgesic. Acute overdoses of paracetamol can cause potentially fatal liver damage. Gastrointestinal complications such as stomach bleeding are also reported when high doses are taken chronically. Kidney damage is seen in rare cases, most commonly in overdose. It can also cause severe skin reactions like Stevens–Johnson syndrome and toxic epidermal necrolysis. It is the most common cause of acute liver failure in both the United States and the United Kingdom. Hence accumulation of paracetamol in water bodies, soil, and other components of environment can ultimately reach humans and other living beings which will be extremely harmful to the biodiversity. The LD_{50} of paracetamol is 2000 mg/kg**.** The structure of paracetamol is shown in Fig. 2.7. Important physical properties are listed in table 2.7

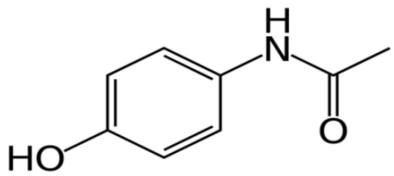

Fig. 2.7: Structure of Paracetamol

Table 2.7: Physico-chemical properties of Paracetamol

Molecular formula	**$C_8H_9NO_2$**
Molar mass	151.163 g/mol
Density	1.263 g/cm^3
Melting point	169 °C (336 °F)
Boiling point	420 °C (788 °F)
Solubility in water	12.78 g/kg (20 °C) ~14 mg/mL (20 °C)
UV- Vis (λ max)	243nm

2.3.8 Acteophenone (ACP)

Acetophenone is a colourless to yellow-tinted liquid with a sweet strong odour resembling the odour of oranges. It is the simplest aromatic ketone. Acetophenone comes mainly as a byproduct of the phenol-acetone synthesis in the cumene oxidation process to cumene hydroperoxide. It is used as a solvent for synthesis of pharmaceuticals, chemicals, dyestuffs and corrosion inhibitors; as flavouring ingredient in fruit flavours; as catalyst for the polymerization of olefins; as fragrance ingredient in soaps, detergents, creams, lotions, perfumes etc.. Structure of ACP is given in Figure 2.8. Physico chemical properties are given in Table 2.8.

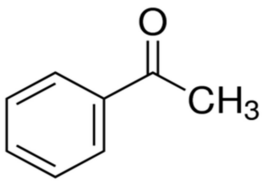

Fig. 2.8: Structure of Acteophenone

Table 2.8: Physico-chemical properties of Paracetamol

Chemical Name	**Acetophenone**
Molecular formula	C_8H_8O
Molecular weight	120.16 g/mole
Melting point	19.7°C
Boiling point	201.7°C
Specific gravity	1.0296 @ 20°C
Density	1.028 g/cm^3
Vapour pressure	0.33 mm Hg @ 20°C
Solubility in water	5.5 g/L @ 25°C
Viscosity	1.62 cP @25°C

The LD_{50} is 815 mg/kg [142]. Acute exposure of humans to acetophenone vapour may produce skin irritation and transient corneal injury.

Oral exposure has been observed to cause hypnotic or sedative effects, haematological effects, and a weakened pulse in humans, gastrointestinal irritation with nausea, vomiting and diarrhoea, central nervous system depression characterized by excitement followed by headache, dizziness, drowsiness, and nausea. Advanced stages may cause collapse, unconsciousness, coma and possible death due to respiratory failure.

2.3.9 Zinc oxide (ZnO)

ZnO (99.5%) used in the study was from Merck India Limited. Zinc oxide usually appears as a white powder, nearly insoluble in water. It is present in earth crust as a mineral, zincite. It is often called II-VI semiconductor because zinc and oxygen belong to the 2nd and 6th groups of the periodic table, has ionicity at the borderline between the covalent and ionic semiconductors. Most of the group II–VI binary compound semiconductors crystallize in either cubic zinc blende or hexagonal wurtzite (Wz) in which each anion is surrounded by four cations at the corners of a tetrahedron, and vice versa. This tetrahedral coordination gives rise to polar symmetry along the hexagonal axis, which is the reason for a number of specific properties of ZnO. The wurtzite structure is thermodynamically stable at ambient pressure and temperature. Zinc blende is stable only by growth on cubic structures and the rocksalt structure is a high-pressure metastable phase which is formed at~10 GPa

[143]. The structures of rocksalt (or Rochelle salt), zinc blende, and wurtzite forms of ZnO are schematically shown in Figure 2.9 [144].

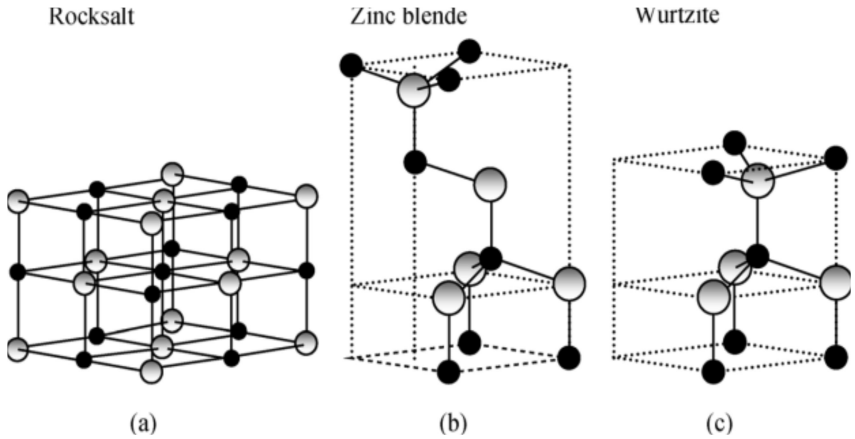

Fig. 2.9: Structure of ZnO: Stick-and-ball representation of ZnO crystal structures: (a) cubic rocksalt, (b) cubic zinc blende, and (c) hexagonal wurtzite. Shaded gray and black spheres denote Zn and O atoms, respectively

Zinc oxide is a non-toxic amphoteric oxide. It is nearly insoluble in water and alcohol, but is soluble in most of the acids. It has high catalytic efficiency, low cost, moisture stability and reusability. It is abundant in nature. The powder is widely used as an additive for numerous materials and products including semiconductors, plastics, ceramics, glass, cement, rubber, lubricants, paints, ointments, adhesives, sealants, pigments, foods, batteries, ferrites, fire retardants, first-aid tapes etc. Zinc oxide also has antibacterial and deodorizing properties. It has a band gap of Eg=3.4 eV at low temperature and 3.37 eV at room temperature. The free exciton binding energy is 60 mV at room temperature. Because of large band gap, it has the ability to sustain large electric fields, higher breakdown voltages, lower electronic noise, high temperature and high-power operations.

ZnO crystals are almost always n-type, even in the absence of intentional doping. Controllable n-type doping can be easily achieved by substituting Zn with group-III elements such as Aluminium, Galium, Indium or by substituting oxygen with group-VII elements like chlorine or iodine. These facts combined with its lower cost make ZnO a promising alternative to TiO_2 in photocatalysis. Photodegradation mechanism is also similar in the case of ZnO and TiO_2, though, at acidic pH range ZnO is considered to be less efficient due to its corrosion. The electronic and photocatalytic properties of ZnO solely depend on its crystal structure, surface area, particle morphology, density and crystallographic orientation which in turn depend on the method of preparation. Crystalline zinc oxide is thermochromic in nature, changing from white to yellow colour on heating and reverting to white on cooling in air. Some of the physical, chemical and electronic properties of ZnO are listed in Table 2.9

Table 2.9: Properties of Zinc oxide

Crystal structure	**Quartzite**
Molar mass	81.408 g/mol
Appearance	White solid
Odor	Odorless
Solubility in water	0.16 mg/100 mL (30°C)
Density	5.606 g/cm^3
Melting point	1975°C (decomposes)
Boiling point	2360°C
Band gap	3.3 eV (direct)
Photoluminescence	375 nm
Exciton binding energy	60 meV
Refractive index (nD)	2.0041
Electron effective mass	0.24
Hole effective mass	0.59

In addition to above mentioned properties, ZnO also has advantages such as large piezoelectric constant, large non-linear optical coefficient, availability of large single crystals, amenability to wet chemical etching, radiation hardness etc [145,146]. It also has several favorable properties like good transparency, high electron mobility, strong room-temperature luminescence etc., which are important in photocatalysis.

2.3.10 Potassium persulphate ($K_2S_2O_8$) (PS)

Potassium persulphate (~99%) from Qualigen (India) was used as such without further purification. Persulfate ($S_2O_8^{2-}$) is one of the strongest oxidants and has higher potential (E_0=2.01 V) than H_2O_2 (E_0=1.76 V). Persulphate (PS) is also called peroxydisulphate or peroxodisulphate (PDS). It has some advantages over other oxidants. It is a solid at ambient temperature, is easy to store and transport, has high stability, high aqueous solubility and relatively low cost. At ambient temperature, reactions of persulphate with organic pollutants are generally slow and activation of persulphate is necessary to accelerate the process. It is commonly activated by UV light, MW, transition metals, heat, use of ferrous ion, minerals, carbon etc resulting in the formation of reactive free radicals such as $SO_4^{\bullet-}$ [147]. The activation initiates radical formation through reduction of persulphate forming sulfate radical ($SO4^{\bullet-}$) [148,149]. These radicals can enhance the degradation of organics. Important properties of typical persulphate salt (Potassium persulphate) are given in Table 2.10.

Table 2.10: Properties of Potassium persulphate

Molecular formula	**$K_2S_2O_8$**
Crystal structure	Triclinic
Molecular weight	270.309 g/mol
Colour	Colourless (white crystalline)
Odour	Odourless
Density	2.477 g/L
Stability	Gradually decompose losing avail Oxygen
pH	Acidic

2.3.11 Hydrogen peroxide (H_2O_2)

H_2O_2 (30.0% w/v) obtained from Qualigen (India) was used as such without further purification. Hydrogen peroxide (HP) in its pure form is a colorless liquid and is used as a powerful oxidizing agent. However it can act as strong reducing agent for strong oxidants. The major by-product of H_2O_2 reaction is water and is hence considered to be safer environmentally. Therefore it is a preferred oxidizer in many industries, as it does not create any hazardous wastes. For safety reasons it is normally used as an aqueous solution. H_2O_2 is denser than water, but is miscible with water in all proportions. Aqueous solution of H_2O_2 appears like water but has a faint, pungent odor. It is a non-combustible liquid, but heat and oxygen released during decomposition can ignite combustible materials [150]. It is used as a bleaching agent and disinfectant. Concentrated hydrogen peroxide is used as a propellant in rocketry. When it decomposes, it forms water and releases oxygen (Eq. 2.2).

$$H_2O_2 \rightarrow H_2O + 1/2\ O_2 \qquad .....(2.2)$$

The primary factors which must be controlled to prevent increased rate of H_2O_2 decomposition are temperature, contamination and pH. Heterogeneous decomposition of hydrogen peroxide is localized on the surface of solid catalysts, usually metals. Excessive concentration of H_2O_2 would act as a radical scavenger reducing the rate of oxidation, while too low H_2O_2 dosage generates insufficient hydroxyl radicals and decrease the oxidation rate. The characteristics of H_2O_2 are summarized in Table 2.11 [150].

Table 2.11: Characteristics of Hydrogen peroxide

Molecular formula	**H_2O_2**
Structure	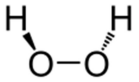
Molar mass	34.0147 g/mol
Appearance	Colorless in solution
Odor	Odorless
Density	1.135 g/cm^3 (20°C) (30%), 1.450 g/cm^3 (20°C, pure)
Melting point	-0.43°C (31.23°F; 272.72K)
Boiling point	150.2°C (302.4°F; 423.3K) (decomposes)
Freezing point	-26°C-15°F (30%)
Solubility in water	100%
Oxidizing Properties	Strong oxidizer
pH	< = 3.7 5.0-6.0 @ 25°C (1% solution)
Stability	Stable (heat and contamination could cause decomposition)
Refractive index (D)	I.4139

2.3.12 Ferrous sulphate ($FeSO_4$)

$FeSO_4.7H_2O$ (FS) used in the study was obtained from Qualigen (India). It is a greenish or yellow-brown colored crystalline solid. It has a density of 2.84 g/cm^3, melts at 64°C and loses hydration at 90°C. It is used in AOP as an important reagent in Fenton reactions for water purification. It is a white orthorhombic crystal, hygroscopic and soluble in water. Ferrous sulphate rapidly oxidizes and becomes coated with brownish yellow ferric sulphate in presence of moist air. The rate of oxidation is enhanced by the addition of alkali or by exposure to light. FS is known as copperas and as green vitriol. Upon dissolving in water, the ferrous sulphate forms metal aquo complex $[Fe\ (H_2O)_6]^{2+}$, which is almost a colorless, paramagnetic ion. Decomposition of iron (II) sulphate begins at about 680°C (1,256°F) as in Eq. (2.3).

$$2\ FeSO_4 \rightarrow Fe_2O_3 + SO_2 + SO_3 \qquad .....(2.3)$$

Typical characteristics of $FeSO_4$ are given in table 2.12

Table 2.12: Characteristics of Ferrous sulphate

Chemical formula	**$FeSO_4$**
Appearance	Greenish or yellow-brown crystalline solid
Molar mass	151.908 g/mol
Density	2.84 g/cm³
Melting point	70 °C
Soluble in	Water

2.3.13 Miscellaneous materials

Relevant information on various other materials used in the study and their characteristics are provided in the respective Chapters.

2.4 Plan of the Thesis

The current thesis is presented 8 Chapters. Each Chapter has its own specific objectives, experimental procedures, results, discussion and conclusions.

Chapter 1: Introduction

This Chapter gives an overview of the relevant literature and discussions on various types of AOPs with special focus on the application of activation sources such as UV light, sunlight and ultrasound (US). Recent developments in electrochemical and Fenton based processes for water purification are also discussed. The advantages of combination processes are highlighted and critically analyzed.

Chapter 2: Objectives of the study, Materials used, General Procedures, Plan of the Thesis

This Chapter describes the main objective and specific aims of the study and outlines the activities undertaken to accomplish the objectives/aims. Relevant characteristics of various materials used, in particular, are also briefly discussed. The Chapter also provides the general layout of the Thesis.

Chapter 3: Solar photocatalysis mediated by ZnO for the decontamination of water from Indigo Carmine dye pollutant

This Chapter deals with studies on the photocatalytic degradation of IC in presence of semiconductor oxide catalyst ZnO and oxidants such as peroxide and persulphate. Details of experimental procedures followed, analytical methods and the results are presented and dicussed. Solar photocatalysis mediated by ZnO is identified as an efficient environment-friendly method for mineralization of the dye IC in water and bring down the chemical oxygen demand (COD) to 'nil'. The previous wastewater thus becomes fit for reuse for the purpose for which the corresponding fresh water was initially used.

Chapter 4: Electrochemical AOPs for the decontamination of water from Indigo Carmine dye pollutant.

This Chapter deals with the electrochemical degradation of IC using different combination of electrode-electrolyte systems. BiO_2-TiO_2/Ti anode and graphite rod cathode with Na_2SO_4 as the electrolyte (BiO_2-TiO_2/Ti - graphite -Na_2SO_4) is identified as the most efficient system for the complete mineralization of Indigo Carmine. Absence of any consumable chemicals or other additives makes the process a potential economically viable candidate for water treatment. The system is efficient even at its normal pH which makes it

even more attractive. BiO_2-TiO_2/Ti – SS - NaCl is more efficient for the decolorization of the dye. However insitu formation of chloro compounds which degraded only slowly makes the process inefficient for mineralization. The observations are discussed in detail and tentative conclusions are derived.

Chapter 5: Ultrasound as the source of activation in AOPs for the decontamination of water from Indigo Carmine dye pollutant

The sonochemical degradation of IC under various reaction conditions is experimentally tested and the results are analyzed in this Chapter. Sonocatalysis mediated by ZnO and promoted by persulphate is a moderately efficient AOP for the decolorization and mineralization of IC. The efficiency of electrolysis, photocatalysis and sonocatalysis for the mineralization of IC is compared and discussed in this Chapter.

Chapter 6: Fenton and Fenton based hybrid AOPs for the decontamination of water from Indigo Carmine dye pollutant

This Chapter discusses the application of various types of Fenton processes in water treatment. Classic Fenton reaction using simple ferrous salt and H_2O_2 under ambient conditions is identified as an effective AOP for the removal of traces of IC from water. The disadvantage of Fe sludge formation from

accumulated Fe^{3+}/Fe^{2+} is overcome by enhancing the efficiency of the process through hybridization with other AOPs, ie, sonolysis, photolysis and electrolysis.

Solar photoFenton is identified as a highly efficient process for the decolorization of IC while Solar photocatalyticFenton mediated by ZnO is the most efficient hybrid process for mineralization. The efficiency of various processes for the decolorization/mineralization of IC is compared and discussed in this Chapter in detail.

Chapter 7: Solar photocatalyticFenton process as a highly efficient AOP for the mineralization of multiple chemical pollutants in water

This Chapter describes the results of the investigation on the efficiency of solar photocatalyticFenton process for the mineralization of multiple chemical pollutants. Dyes, pesticides, petrochemicals and pharmaceuticals were used in the study under laboratory conditions as well as field conditions. Natural river water is used as the matrix for field conditions. Cross contamination by various organic chemicals does not influence the efficiency of the process which makes it an economically viable and environmentally safer method for water decontamination.

Chapter 8: Summary and Conclusions

This Chapter summarises the findings of the investigation and the salient conclusions. Photocatalysis, Electrolysis, Sonolysis, Classic Fenton, SolarFenton, SonoFenton, Solar photocatalyticFenton and ElectroFenton have been identified as potential AOPs for the decontamination of water from chemical pollutants. Solar photocatalyticFenton process mediated by ZnO is identified as the most efficient AOP for the mineralization of multiple chemical pollutants from water. The versatility of the process as an environment-friendly tertiary water treatment tool is demonstrated by the complete mineralization of diverse chemical pollutants such as pesticides, pharmaceuticals, petrochemicals and dyes. The technique is applicable even under field conditions with natural river water as the matrix.

.....ꕥ.....

Chapter

3

SOLAR PHOTOCATALYSIS MEDIATED BY ZnO FOR THE DECONTAMINATION OF WATER FROM INDIGO CARMINE DYE POLLUTANT

Contents

3.1 Introduction

Dyes are used extensively in many of the modern day materials including textiles, paints, food, pharmaceuticals, printing and a host of industries. The production, processing and application of various dyes will result in contamination of water with toxic and recalcitrant materials which are resistant to destruction by conventional physicochemical and biological treatment. In particular, the textile industry consumes large quantities of water during the dyeing and finishing operations. Even the best treatment method may not be capable of removing the last traces of coloring agents completely. In addition to the toxicity and other health hazards, the dye pollutants also reduce the light penetration through the contaminated water resulting in inhibition of photosynthesis and ultimate destruction of organisms living in those water bodies. Conventional

techniques such as adsorption, ultra filtration, reverse osmosis, extraction etc. are non-destructive and they simply transfer the organic pollutants from water to another medium or end up as sludge. Thus the pollution continues unabated from a different source. Hence it is imperative that viable environment-friendly techniques are developed for the mineralization of the pollutants and the decontamination of water to make it safer and reusable.

Semiconductor oxide-mediated photocatalysis is fast becoming an efficient Advanced Oxidation Process (AOP) for the removal of chemical and bacterial pollutants from water [151-157]. The pioneering discovery of the photosensitization effect of TiO_2 electrodes on the electrolysis of water into H_2 and O_2 by Fujishima and Honda [158] has laid the foundation for extensive research on this phenomenon. Among the semiconductors tested so far, TiO_2 and ZnO are identified as highly efficient for the removal of variety of water pollutants. Semiconductor photocatalysis has also been widely investigated as a potential candidate for the efficient conversion of solar energy into chemical energy. Photocatalysis is also attracting the attention of researchers worldwide as a 'green technology' for the detoxification of harmful compounds in both water and air without utilizing or producing hazardous materials [159-162].

The advantages of ZnO and TiO_2 as photocatalysts include their favorable physicochemical properties, low cost, easy availability and low toxicity. They have identical band gap, i.e. (ZnO)E_{bg} = 3.2 eV, anatase (TiO_2) E_{bg} = ~3.2 eV and rutile (TiO_2), E_{bg} = ~3.0 eV. They can absorb light mainly below 400 nm, which is in the UV range that constitutes less

than 5% of sunlight. Many studies have been reported on the modification of semiconductor oxides in order to extend the absorption of light into the visible range. These include dye sensitization, semiconductor coupling, impurity doping, use of coordination metal complexes and noble metal (Pt, Pd, Au, Ag etc) deposition [163-165]. The resulting enhancement in the photocatalytic degradation of organics is attributed partially to the increased light absorption. The metals also act as electron traps promoting the interfacial charge transfer and thus delaying the recombination of the electron-hole pair. Current status of visible light active TiO_2 photocatalysis for environmental applications has been summarized in recent reviews by Pelaez et al. [164] and Wang et al. [165].

In spite of the comparable physicochemical characteristics of ZnO and TiO_2, the former is more active in the visible region for the photocatalytic decontamination of water containing variety of organic pollutants such as pulp mill bleaching wastes, phenol, dyes and/or heavy metals [166-169]. The advantages of ZnO for visible light harvesting arise from its relatively better absorption of larger fraction of solar spectrum and light quantum [28]. Most widely used form of ZnO in photocatalysis is of wurtzite structure. The light scattering effect of ZnO is comparatively less due to its lower refractive index (ZnO: 2.0, TiO_2: 2.5-2.7) which is also favorable for better photocatalytic efficiency. In spite of these advantages, the number of research publications on the use of ZnO as an effective environmental photocatalyst is much less compared to TiO_2. This may be due to the perceived instability or photo-corrosion of ZnO under acidic conditions resulting in catalytic inactivation over time.

Indigo Carmine (IC) (3,3'-dioxo-1,3,1',3'-tetrahydro-[2,2']-bi-indolylidene-5,5'-disulphonic acid disodium salt), also known as acid blue 74 (AB74), is an important industrial dye used for dyeing of clothes and also for medical diagnostic purposes. It can also help to target biopsies even better since the homogeneously stained or unstained areas can be correlated with intraepithelial neoplasia [170]. More details on the chemistry of the dye, its physicochemical characteristics etc are provided under Section 2.3.1, Chapter 2.

Few investigations on the removal of IC from water using AOPs have been reported [171-175]. Our earlier studies revealed that ZnO can be used as an effective photocatalyst for the degradation of many organic pollutants such as phenol, α- methyl styrene, acetophenone, diquat (herbicide) etc. in water using sunlight as the source of energy [176]. In the current study the possibility of using ZnO as a solar photocatalyst for the removal of IC is investigated. The dye is chosen since it is one of the least investigated dye pollutants under photocatalysis. The influence of various operational parameters such as concentration of the pollutant, pH, catalyst loading, temperature, presence of salt contaminants, dissolved O_2 etc. on the rate of removal of the dye and the reaction kinetics are investigated. Probable intermediates are also identified.

3.2 Experimental details

3.2.1 Materials Used

Zinc oxide (~99% pure) supplied by Merck (India) Ltd. is used as such without further purification. The average particle size was around 15×10^{-2}μm and the BET surface area was ~12 m^2/g. Characterization

using Scanning Electron Microscopy (SEM) and X-ray diffractogram (XRD) measurements (as reported later in this Chapter) confirmed the consistency of the physicochemical characteristics of ZnO used with those reported in literature [28]. H_2O_2 (30.0% w/v) and Persulphate (PS) (purity ~99%) were from Qualigen (India). IC (Extra Pure Grade > 99.5% purity) was from Sisco Research Laboratories Pvt. Ltd (India) and was used as such without further purification. Double distilled water was used in all the experiments. All other chemicals used were of AnalaR Grade or equivalent unless indicated otherwise. Detailed chemistry of various materials used is discussed in Chapter 2.

3.2.2 Solar photocatalytic Experimental set up

The solar photocatalytic experiments were performed in a pyrex glass reactor. The reactor was placed in a tray through which water from a thermostat maintained at the required temperature was constantly circulated. The dye solution, ZnO and the additives (as and when required) were taken in the reactor. The suspension was stirred frequently to ensure uniform mixing. The experimental setup is presented in figure 3.1. For solar experiments, the reactor assembly was placed on the roof top of our laboratory at Kochi, Kerala, India (9^0 57' 51" N, 76^0 16' 59" E) during sunny days from October (2015) to May (2017). UV irradiation was done in the laboratory using a 400 W medium pressure mercury vapor lamp. A reference sample under exactly identical conditions is kept with every experiment to ensure consistency and reproducibility of the data especially with solar irradiation. In case

the reference sample data is not reproducible such experiments are repeated multiple times until the results are reproducible.

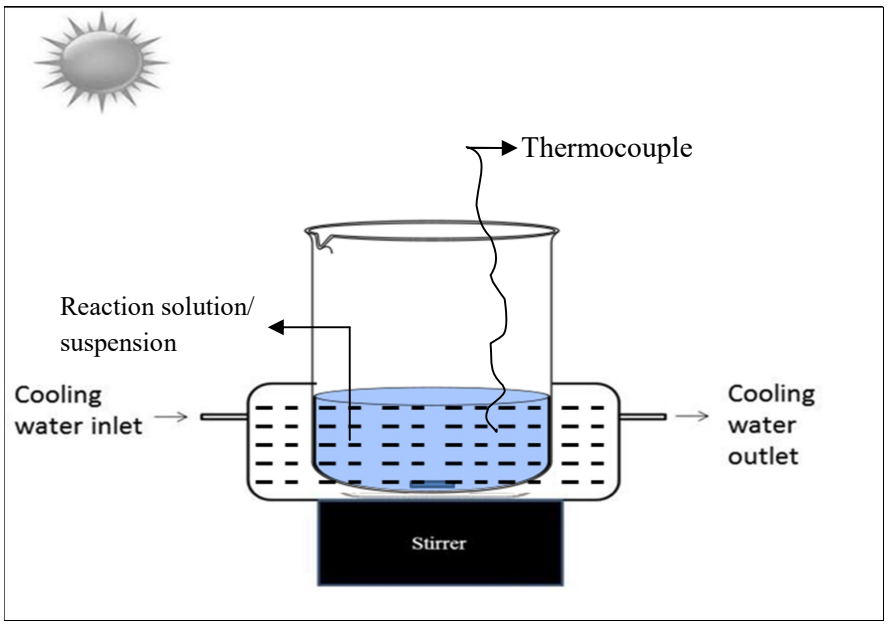

Fig. 3.1: Solar photocatalytic experimental set up

3.2.3 Analytical procedures

Samples from the reactor were drawn periodically, centrifuged for removing traces of fine suspended particles, if any and analyzed for the IC concentration by UV-VIS Spectrophotometry at 609 nm. High Performance Liquid Chromatography coupled with Mass Spectrometry (HPLC/MS) (Waters Xevo G2 Q-TOF) was used to identify the reaction intermediates. Suspension kept under identical conditions in the dark was used as the reference in each case to eliminate the contribution from adsorption towards the reduction in the IC concentration. H_2O_2 was

estimated by standard iodometry. COD was determined at different times of reaction as explained in Section 2.2.3, Chapter 2.

3.3 Results and Discussion

3.3.1 Catalyst Characterization

The catalyst ZnO used in the study was characterized by various methods such as surface area measurements, particle size analysis, pore size distribution, adsorption, X-ray Diffraction (XRD), Scanning Electron Microscopy (SEM) and Transmission Electron Microscopy (TEM). The BET surface area of ZnO is~ 12 m^2/g. Pore size analysis was made using Micrometrics Tristar surface area and porosity analyser. The results are shown in Fig. 3.2. The distribution of pore size is in the range 30-180 Å. The average pore width and pore volumes are 139 Å and 3.5×10^{-4} cm^3/g respectively.

XRD analysis of the ZnO powder using Bruker D2 PHASER X-Ray powder analyzer within the diffraction angle (2θ) of 10-80^0 shows highly crystalline phase of pure hexagonal wurtzite structure. XRD pattern of ZnO is shown in Fig. 3.3. The profile is matching with the reference provided by the International Centre for Diffraction Data (ICDD) PDF of 00-003-0888 for ZnO. 100% intensity peak was observed at 2θ of 36.04. Other major characteristic peaks are at 2θ values of 31.360, 34.210, 56.370 and 69.010. The five peaks correspond to the crystalline planes 100, 002, 101, 011 and 110 respectively.

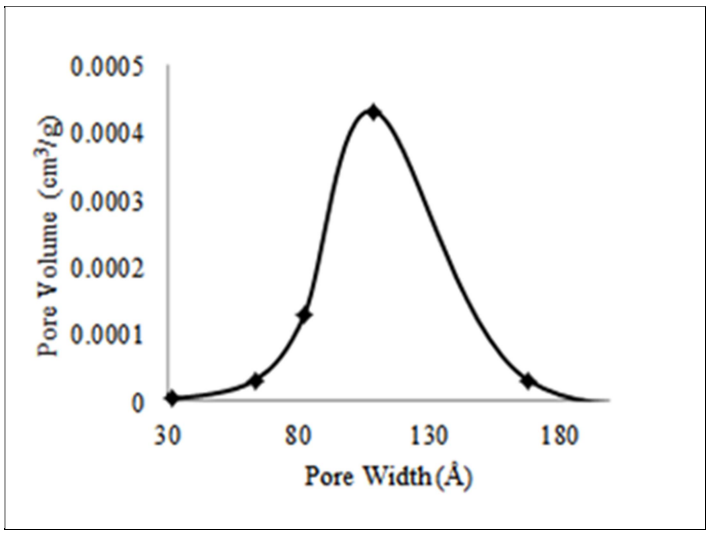

Fig. 3.2: Pore size distribution of ZnO

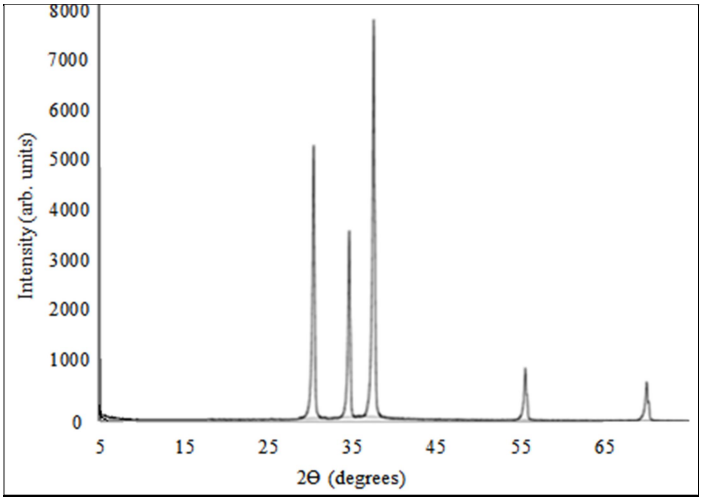

Fig. 3.3: XRD pattern of ZnO

The SEM image of ZnO is recorded using JEOL Model JSM - 6390LV. Fig. 3.4 gives the SEM image. The particles are rod-shaped with an average particle size of ~ 0.1 μm.

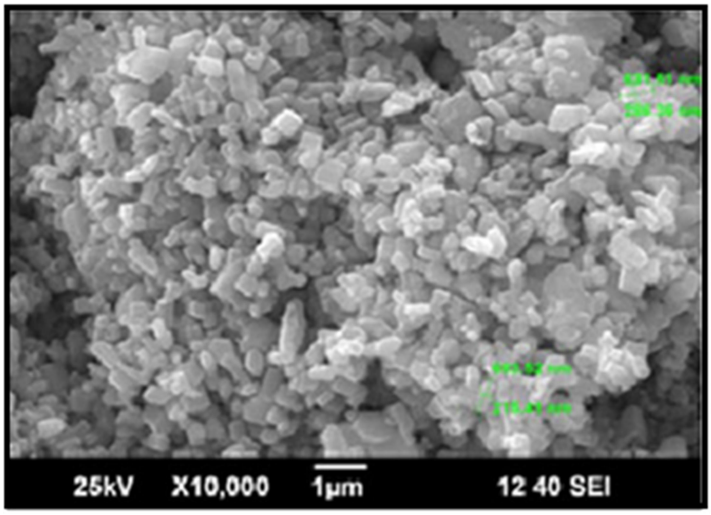

Fig. 3.4: SEM image of ZnO

The morphology, size distribution and surface characterization of ZnO were further verified by Transmission Electron Microscopy (TEM) using JEOL JEM-2100 equipment. Fig. 3.5 gives the TEM image of ZnO used.

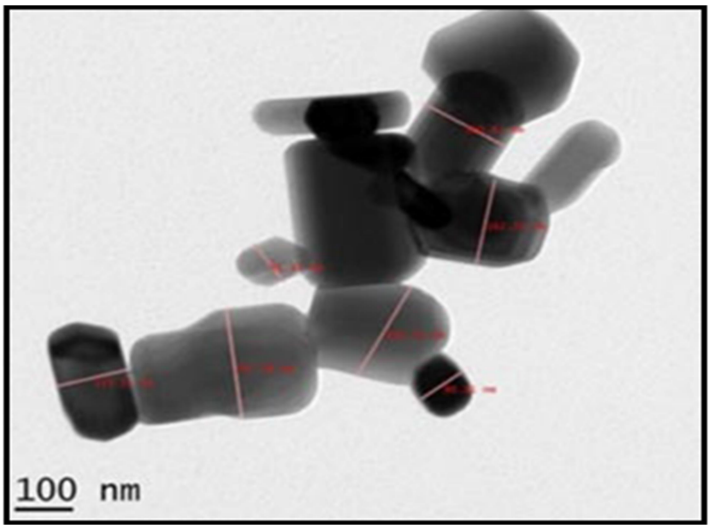

Fig. 3.5: TEM image of ZnO

The particles are of rod shape in the size range 0.09 to 0.2 μm. In general, the particle size distribution is in the range of 0.1 to 0.2 μm.

The reflectance spectrum of ZnO (Fig. 3.6) shows that it absorbs light mostly in the UV region below 400nm.

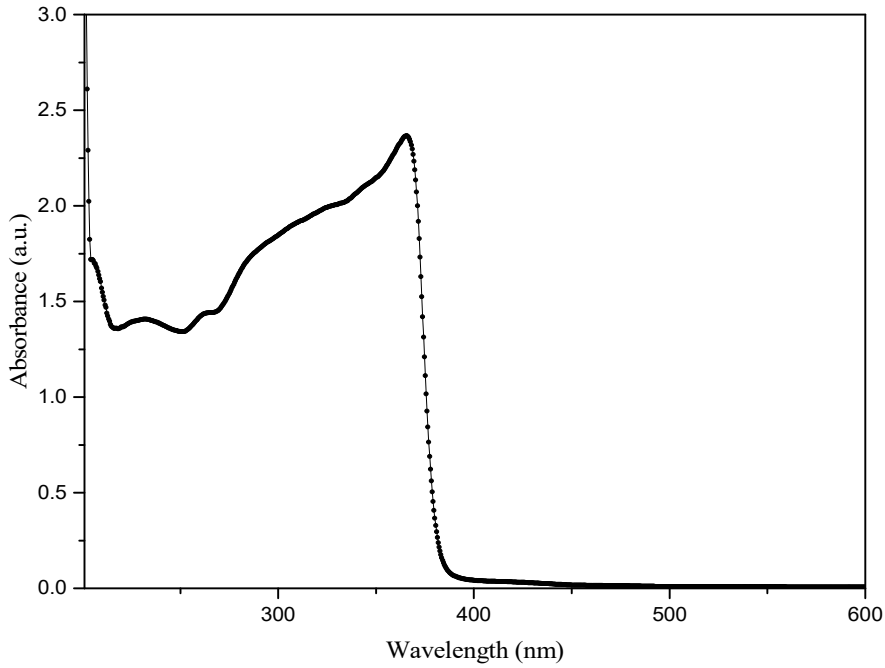

Fig. 3.6: Reflectance spectrum of ZnO

The characteristics of the FTIR spectrum (Fig 3.7) of the sample used are comparable with those reported in literature for ultra pure ZnO.

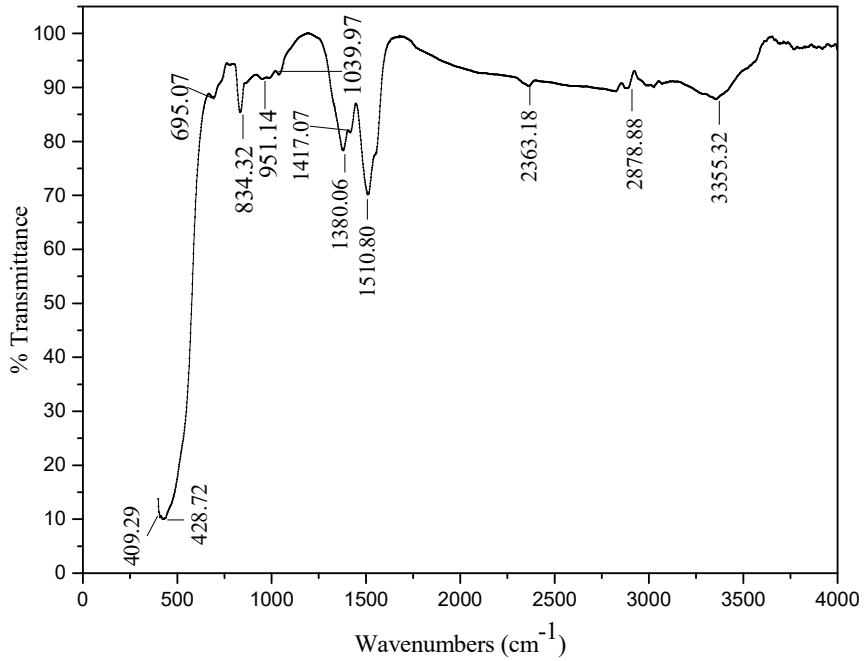

Fig. 3.7: FTIR spectrum of ZnO

The identity of ZnO used in the study is reconfirmed from the characterization as above.

3.3.2 Preliminary photocatalytic experimental results

Sunlight (SL) induced photocatalytic degradation of trace amounts of IC in water in presence of ZnO is investigated under various reaction conditions. No degradation of IC takes place in the absence of catalyst and light indicating that these two components are essential for the degradation. The results are shown in figure 3.8. The pH of the reaction system was maintained at the natural value for ZnO-water suspension, i.e. 4.8 unless indicated otherwise. The results clearly show that the decrease in the concentration of IC is not due to its adsorption on the catalyst or

direct solar degradation of the dye. The maximum equilibrated dark adsorption of IC observed under the reaction conditions is less than 5%.

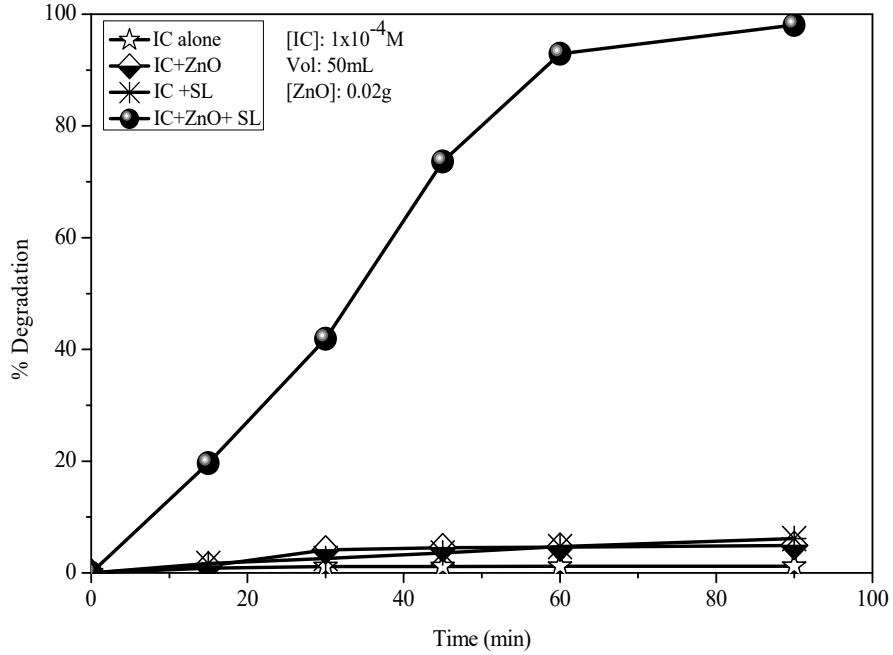

Fig. 3.8: Solar photocatalytic degradation of IC

Evaluation of the comparative photocatalytic effect of ZnO and TiO_2 in presence of sunlight under identical conditions shows that the former is much more efficient (~90% compared to ~40% of the latter in 60 minutes) for the degradation of IC. Hence all further studies were carried out using ZnO as the catalyst.

The comparative degradation of IC in presence of ZnO in presence of UV light and sunlight under otherwise identical conditions is shown in figure 3.9. The IC itself undergoes moderate degradation in presence of UV (~30% in 60min) even in the absence of the catalyst. However, the

sunlight induced degradation of the dye is negligible. The photocatalytic degradation is more under sunlight than under UV irradiation. This is surprising because ZnO is essentially a UV-active photocatalyst, with only modest capability to get activated under sunlight. The high solar catalytic activity may be due to the sensitization of ZnO induced by IC which is an anionic dye capable of absorbing visible light with λ_{max} of ~ 600 nm.

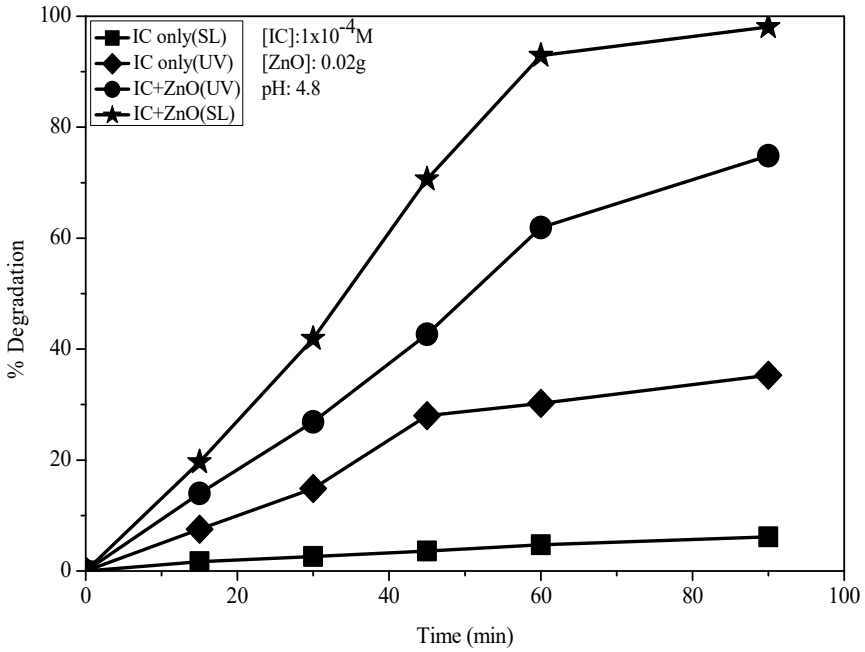

Fig. 3.9: Comparative photocatalytic degradation of IC under sunlight (SL) and UV light irradiation

Consequently, electrons from the sunlight-excited dye are injected into the conduction band of ZnO more easily than the promotion of an electron from the valence band of ZnO to its conduction band under UV irradiation. The conduction band electron forms superoxide radical anion ($O_2^{-}\cdot$) by reaction with dissolved/adsorbed O_2, resulting in the formation

of reactive oxygen species (ROS) such as hydroxyl radicals. These ROS are responsible for the oxidation of the organic contaminants including the dye itself or other co-existing organics [28]. The general mechanism of dye sensitization is shown in figure 3.10.

Thus it is observed that ZnO mediated photocatalytic degradation of IC is more efficient under sunlight compared to UV light. Hence further studies are undertaken with sunlight as the source of irradiation.

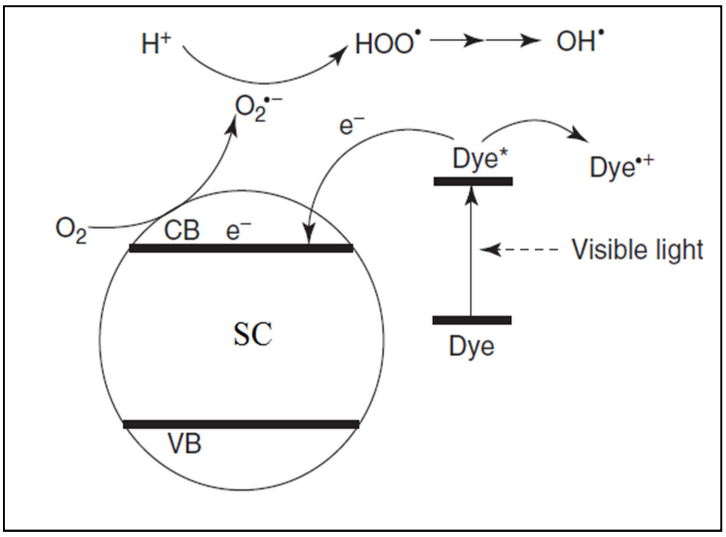

Fig. 3.10: Mechanism of dye sensitization of ZnO under sunlight

3.3.3 Effect of catalyst dosage

The effect of catalyst loading on the solar photocatalytic degradation of IC is investigated and the results are presented in figure 3.11. The % degradation increases steeply with increase in catalyst loading, reaches an optimum, decreases slightly thereafter and stabilizes. Higher degradation at higher dosages can be attributed to increase in catalyst surface area,

increased adsorption of the substrate, efficient light absorption and consequent generation of higher number of active species. However beyond the optimum, in the same reactor, some of the catalyst particles will be effectively in the dark and there is decrease in the light penetration. Scattering of light at higher catalyst loading also reduces the efficiency of light absorption. Further, it is difficult to maintain the suspension homogeneous at high catalyst dosage as the catalyst particles have a tendency to settle at the bottom of the reactor. Variation in the degree of settling may also influence the uniformity of the reaction system and the consistency of the sampling process. At higher loadings, the photo-activated particles may interact more frequently with the abundant ground state particles and get deactivated as in equation 3.1 [28].

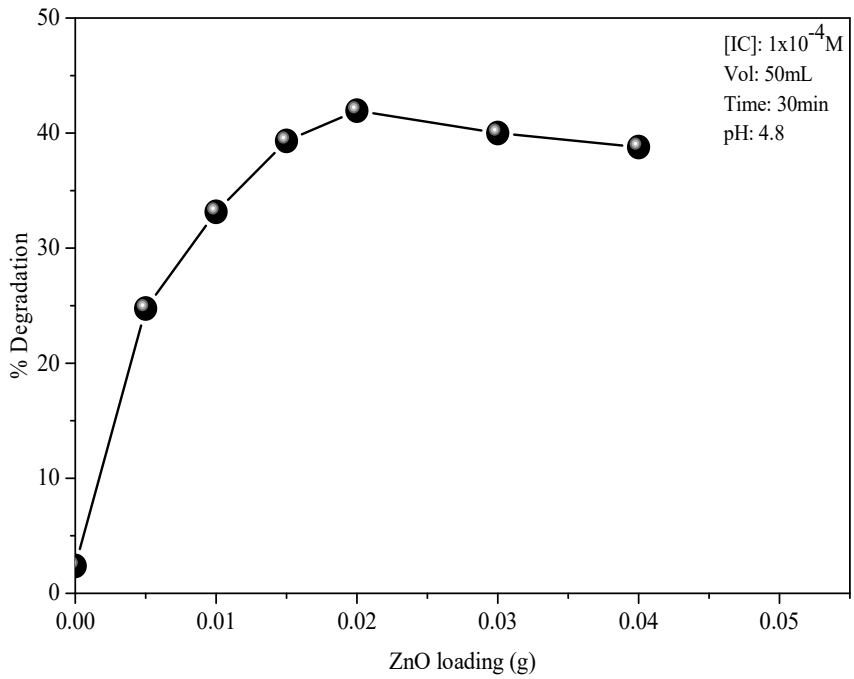

Fig. 3.11: Effect of ZnO loading on the photocatalytic degradation of IC

$$MO^* + MO \rightarrow MO^{\#} + MO \qquad .....(3.1)$$

where

MO represents ZnO. MO* and $MO^{\#}$ are the activated and deactivated forms respectively.

These factors together contribute to stabilization/decrease in the efficiency of the catalyst at loadings above the optimum level. The optimum dosage of the catalyst under the reaction conditions in the current reactor is 0.02g/50 mL. However, the optimum will be different for a reactor of different size and geometry as well as other reaction parameters. Hence the catalyst dosage has to be optimized every time when the reaction and reactor parameters are different. In the current instance, all further studies were carried out at the optimized dosage of 0.02g/50 mL, unless indicated otherwise.

3.3.4 Effect of pH

The effect of pH on the photocatalytic behavior of semiconductor oxides is often correlated with their oxidation potential and surface charge which determine the adsorptive properties. However other factors such as characteristics of the substrate and reaction intermediates, presence of pH-sensitive contaminants etc. also influence the effect of pH. In the current study, the effect of pH on the degradation of IC is investigated and the results are given in figure 3.12. Optimum degradation is observed at pH 4 which decreases thereafter with increase in pH. Hence all further studies are made at the natural pH of 4.8 of the suspension. The low degradation at pH <3 is due to the corrosion and photo-dissolution of ZnO which are

enhanced by reaction with insitu generated valence band holes as in reaction 3.2.

$$ZnO + 2h_{VB}^{+} \rightarrow Zn^{2+} + O^{-} \qquad .....(3.2)$$

The lower degradation above pH 4.5 can also be due to the presence of Cl^{-} anions (from the HCl used for pH adjustment) which can react with hydroxyl radicals leading to inorganic radical anions. These radical anions show much lower activity than $^{\bullet}OH$. There will also be competition between the dye and the anion for $^{\bullet}OH$ resulting in decreased degradation.

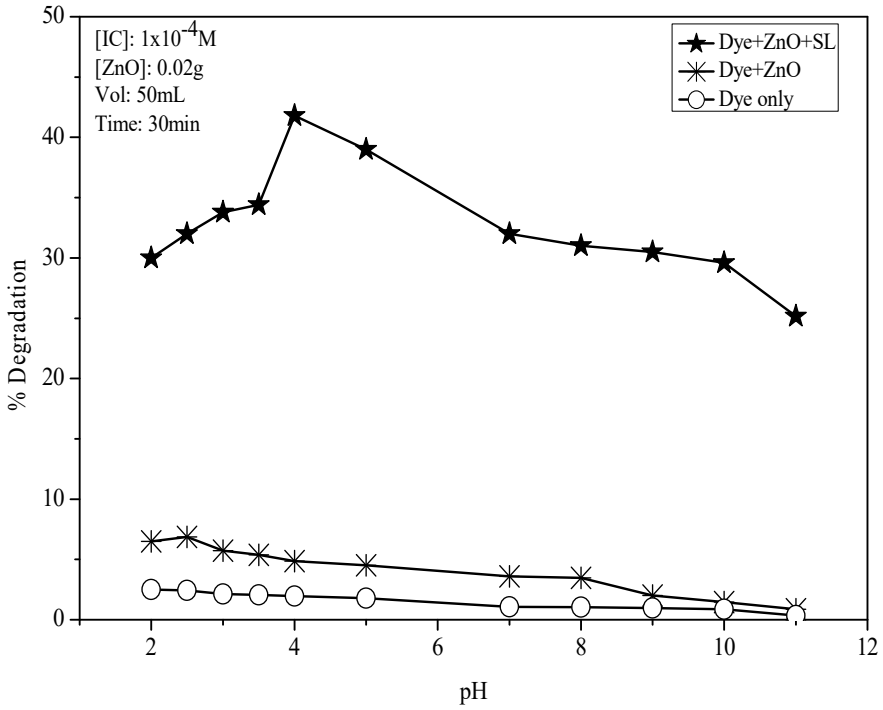

Fig. 3.12: Effect of pH on the degradation of IC

The effect of pH on the degradation/disappearance of IC is not due to adsorption as seen from the results of adsorption studies (dye + ZnO) at different pH (figure 3.12). The data in the figure also shows that the effect of pH on the dye as such is not much.

As expected, the adsorption remains fairly steady at ~ 5% in the acidic to neutral range of 3-7 (after adjusting for the mild decolorization of ~ 2 % in this pH range). IC is a weak acid which dissociates less towards acidic pH and will be in neutral electric form φ-SO_3H [177]. Hence adsorption is moderate in the acidic range with no electrostatic repulsion between the surface and the dye. The adsorption is negligible under alkaline condition. This may be attributed to the surface characteristics of ZnO. The PZC of ZnO is 9±0.3. The surface of ZnO will be negatively charged above this pH and hence the anionic dye IC (φ-SO_3^-) will get repelled. The degradation of IC also is less in this range.

The ZnO may also form complexes in the basic pH range (reaction 3.3) leading to partial insulation of the catalyst surface and consequent inactivation.

$$ZnO + H_2O + 2OH^- \rightarrow [Zn(OH)_4]^{2-} \qquad .....(3.3)$$

The moderate degradation observed in the alkaline condition may be due to the increase in $^{\cdot}OH$ radicals formed from the hydroxyl ions OH^-.

In many instances, adsorption is considered to be an important prerequisite for heterogeneous catalytic processes. However, in the current case, the adsorption of IC is much smaller compared to the high

percentage degradation of the dye. This shows that a sizeable part of the photocatalytic degradation of IC is taking place in the bulk. Similar observations are reported in the case of photocatalytic degradation of other substrates as well [178, 179, 180].

It is well recognized that the effect of pH on the photocatalytic process is complicated and cannot be explained based on individual parameters in isolation because it depends on multiple factors such as electrostatic interaction between the semiconductor surface, solvent molecules, substrates, intermediates and charged radicals formed during the reaction process [178].

3.3.4 Effect of initial concentration of IC

As can be seen from figure 3.8, the photocatalytic degradation of IC slows down with time. This is mainly because the residual concentration of IC becomes lower and lower with time and the insitu formed intermediates and other products may compete for the same active adsorption sites on the surface and for the reactive free radicals at the surface and in the bulk. Further, just as in the case of catalyst dosage, there will be an optimum for the substrate concentration for effective interaction with the ROS and subsequent degradation under specific experimental parameters. This is verified by studying the degradation at different concentrations of IC at the optimum catalyst dosage and natural pH of the reaction system.

The results plotted in figure 3.13 show the percentage degradation of IC at different concentrations. The rate of degradation at different

concentrations of IC is shown in figure 3.14. The percentage degradation decreases with increase in concentration. However, the initial rate of degradation increases with increase in concentration before it eventually levels off at higher concentrations (>1.5×10^{-4}M). This is in line with many photocatalytic reactions which follow pseudo first order kinetics at lower concentrations of the substrate in accordance with the Langmuir-Hinshelwood model modified to accommodate reactions occurring at solid-liquid interface [177-179]. The rate decreases and slowly stabilizes at higher concentration indicating lower order and eventual zero order kinetics.

Once the concentration of IC is adequate to interact with the optimum available ROS and other reactive free radicals, further increase in concentration cannot result in any increase in the reaction and the removal of IC becomes independent of its concentration. At higher substrate concentration, some of the insitu formed reaction intermediates may get adsorbed onto the surface or remain in the bulk for relatively longer period resulting in less frequent interaction between fresh dye molecules and the ROS. Complete domination of the reaction system by the reactant/intermediates/products can also result in suppression of the generation of surface initiated reactive free radicals. However, at any point in time, there will be an optimum for the number of substrate molecules that can interact with the reactive free radicals generated by the surface.

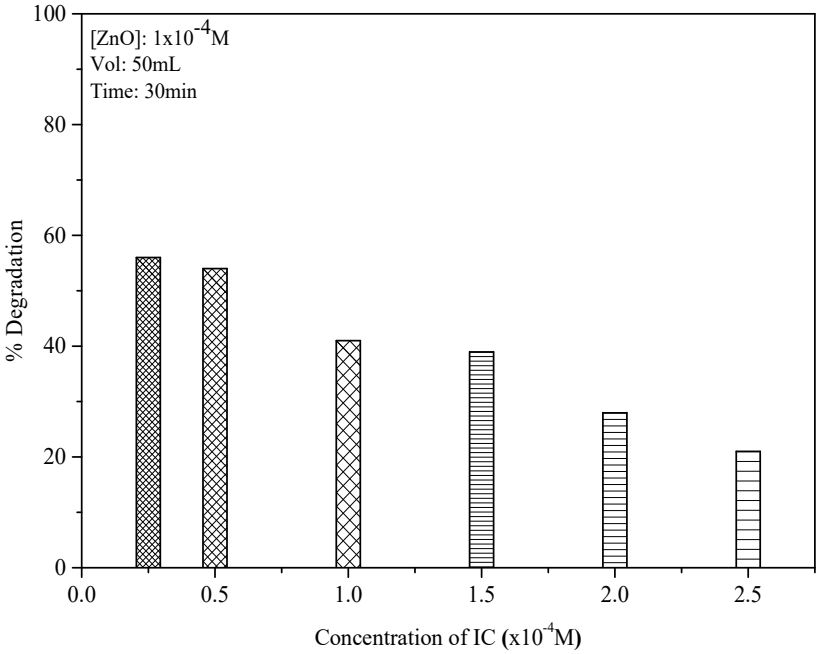

Fig. 3.13: Effect of concentration of IC on its % degradation

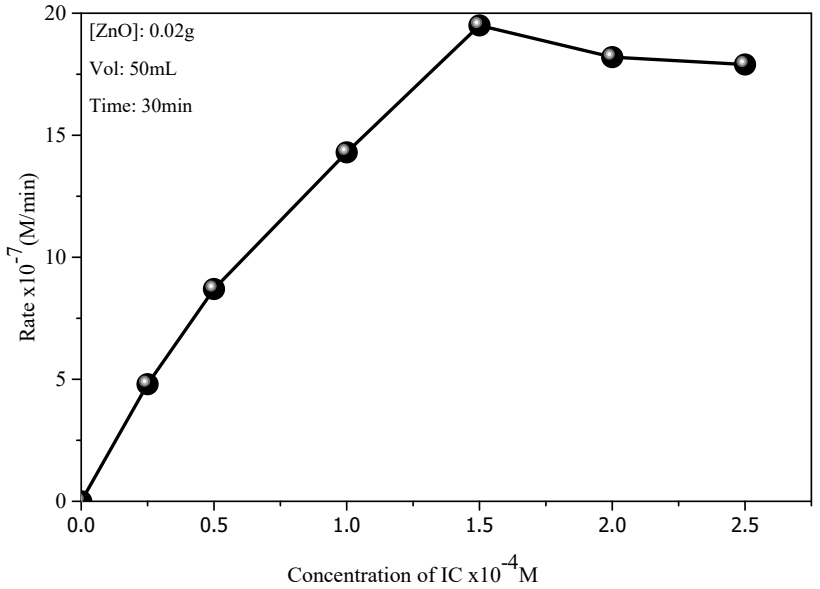

Fig. 3.14: Rate of degradation of IC vs Concentration (of IC)

This optimum will depend on a number of parameters such as initial concentration of the substrate, intensity of illumination, wavelength of light, mass and type of photocatalyst, type and geometry of photoreactor etc. Consequently, the measurements and calculations apply only to the specific reaction conditions and cannot be generalized.

According to the Langmuir-Hinshelwood model, modified to accommodate reactions occurring at solid-liquid interface [177, 178] the simplest way to represent the degradation, assuming that there is no competition with reaction by-products, is

$$R = -dC/dt = k_r K C_0 / (1+KC_0) \qquad .....(3.4)$$

R is the rate of disappearance of the substrate (mg L^{-1} min^{-1}), C_0 (mg L^{-1}) is the initial concentration, K is the equilibrium adsorption coefficient and k_r is the reaction rate constant at maximum surface coverage. Equation 3.4 can be rewritten as

$$1/R = 1/k_r + 1/k_r K \times 1/C_0 \qquad .....(3.5)$$

Plot of 1/R against $1/C_0$ yields a straight line in the concentration range $0.25\text{-}1.5\times10^{-4}$M indicating first order kinetics and L-H mechanism (figure3.15)

Further, integration of equation 3.5 yields

$$\ln (C_0/C) + K (C_0-C) = k_r K t \qquad ..... (3.6)$$

When C_0 is very small, above equation becomes

$$\ln (C_0/C) = k_r K t = k't \qquad .....(3.7)$$

The plot of $\ln(C_0/C)$ versus irradiation time (t) for the concentration range of $0.5\text{-}1.5\times10^{-4}$M yields straight lines (figure 3.16) thereby reconfirming pseudo first order kinetics. The slope of each line is the apparent rate constant of degradation *k'* at the corresponding concentration of the substrate. The rate constants thus computed are given in table 3.1.

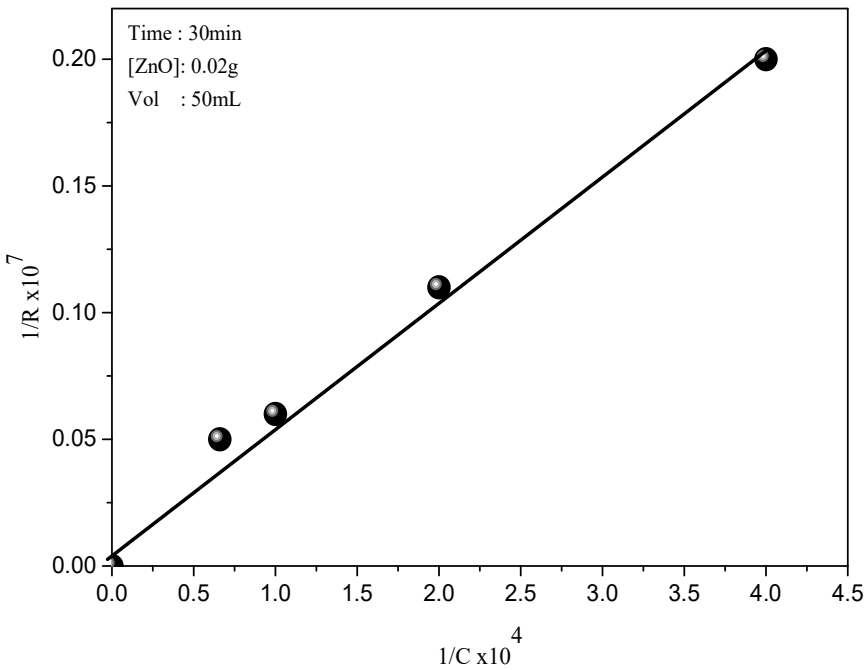

Fig. 3.15: Reciprocal plot of initial rate vs initial concentration

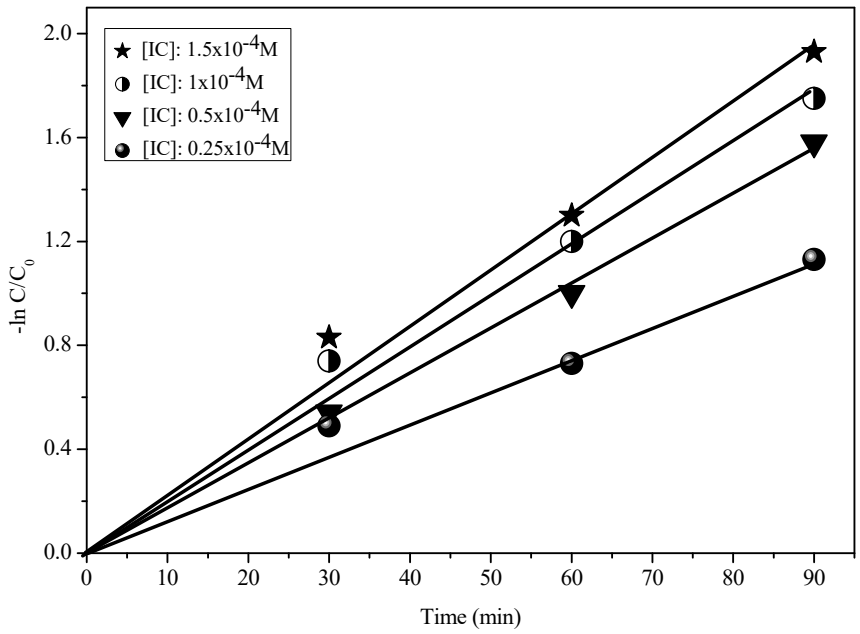

Fig. 3.16: Logarithmic plot of pseudo first order kinetic for the degradation of IC

Table 3.1: Pseudo first order rate constants for the photocatalytic degradation of IC over ZnO

Sl. No.	ZnO (g/50mL)	IC ($x10^{-5}$M)	$k' \times 10^{-2}(min^{-1})$
	0.02	2.5	2.00
	0.02	5.0	1.75
	0.02	10.0	1.47
	0.02	15.0	1.27

The rate constant decreases with the increase in concentration of IC, which is consistent with the results reported in the case of many photocatalytic degradation studies [179, 180]. For a fixed amount of catalyst and hence finite number of surface-generated ROS available for interaction, the number of substrate molecules is excessive at higher

concentrations. This reduces the relative % fraction of substrate which can successfully interact with the ROS, leading to decrease in the apparent rate constant. However, it is to be noted that the above rate constant values apply only under the current specific experimental conditions and are hence not absolute.

Decrease in the rate of photocatalytic degradation and hence in the order of the reaction at higher concentrations of the substrate has been reported earlier [181-183]. Variation in the kinetics of the degradation with concentration of the substrate has been reported in the case of ZnO mediated sonophotocatalytic reactions also [184, 185].

The basic mechanism of semiconductor-mediated photocatalysis involves the formation of highly reactive oxygen species such as ·OH, HO_2·, H_2O_2 etc. which interact with the substrate molecules on the surface as well as in the bulk. The most reactive among these ROS is the ·OH radicals though their lifetime is very short (only few nanoseconds). Hence they can react more efficiently with the organic pollutant molecules in the immediate proximity of their formation. At higher substrate (IC) concentration there will be more number of its molecules per unit volume and hence the probability of collision between the oxidizing species and IC also will be higher. However at very high concentration, an inner filter effect is possible and the incident light will be largely wasted for the excitation of the substrate rather than the excitation of the catalyst particles and the generation of reactive free radical species [181]. The path length of light entering the system also decreases with increase in concentration of the substrate. Similar screening effect was reported

earlier also [184]. Another reason for the lower rate of degradation at higher concentration (which is dependent on the reactor geometry also) is that the major portion of the reaction occurs in the reaction zone close to the irradiated side where the irradiation intensity is much higher [185]. Consequently, a substantial fraction of the substrate (which is on the other side) will not get adequately activated to effect the degradation. As a result of all or some of these factors, the reaction rate is stabilized or even decreases at higher concentration of IC. The stability beyond the optimum concentration suggests that the reaction rate becomes independent of the concentration of the substrate. Hence it is logical to assume that the photocatalytic degradation happens in two stages. In the first stage, the reaction is faster and follows pseudo first order kinetics. In the second stage, the reaction rate is slow reaching zero order eventually. Duration of the first stage decreases with increasing concentration of the substrate.

As the initial concentration of the substrate is increased, the requirement of energy, catalyst surface for adsorption and number of ROS for effective interaction also increase correspondingly. But when the catalyst and the light source are kept the same, the ROS generated will be constant. The stabilization effect at higher concentration beyond the optimum implies that the substrate cannot interact with correspondingly more ROS. In other words, the relative concentration of ROS for interaction with the substrate becomes lower and this leads to stable/reduced degradation. Thus it may be confirmed that absorption of light by the catalyst, intensity of illumination, wavelength of light, number of available catalyst surface sites and relative abundance of reactive free radicals vs the substrate are the major factors which may

influence the effect of concentration of the pollutant on the degradation. Addition of extra amount of catalyst which leads to generation of additional reactive radicals at the stage of stabilization enhances the degradation. This also supports the contention that relative concentration of reactive free radicals with respect to the substrate is an important factor that drives the efficiency of the photocatalytic degradation of pollutants.

3.3.5 Insitu formation and effect of added H_2O_2

H_2O_2 is formed as a by-product/intermediate in many photocatalytic reactions. Recent studies on the sono, photo and sonophotocatalytic degradation of organic pollutants revealed that the H_2O_2 formed undergoes concurrent decomposition resulting in oscillation in its concentration [186]. In the current study also H_2O_2 formation is observed (figure 3.17).

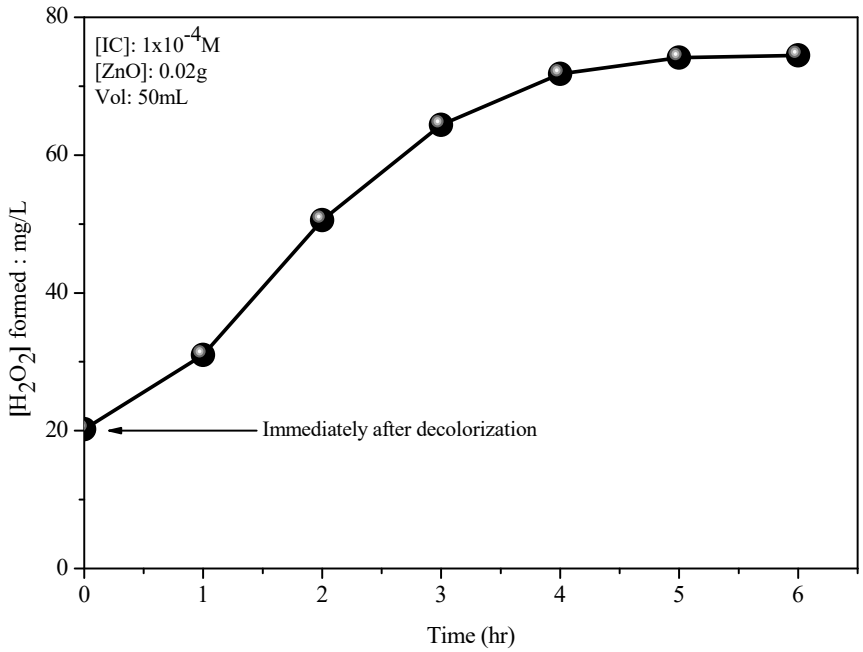

Fig. 3.17: Formation of H_2O_2 during the degradation of IC

Since the precise estimation of H_2O_2 in the system in presence of the colored dye is difficult, the same is not done while the degradation/decolorization of the dye is in progress. The concentration of H_2O_2 is determined immediately after the decolorization is complete. At this stage, the H_2O_2 concentration in the system is 20 mg/L. Since IC is known to produce a number of relatively stable intermediates which also degrade very slowly, the irradiation is continued and the H_2O_2 is also measured periodically. The H_2O_2 continues to increase for some more time and stabilizes after about 4 hr. However, the mineralization is still in progress which takes about 6 hr (see Section 3.3.10) to be completed. During this period, the concentration of H_2O_2 does not increase corresponding to the mineralization and gets stabilized indicating simultaneous formation and decomposition as reported earlier. When the rates balance each other, the concentration of H_2O_2 is stabilized.

Being a good oxidant of photocatalytic reactions, the insitu formed H_2O_2 (oxidation potential is 1.77 V) can influence the degradation of IC. This is verified by externally adding H_2O_2 at different concentrations to the reaction system and evaluating the effect on the degradation of IC. The results are shown in figure 3.18. The slow photodegradation in the absence of any catalyst is practically unaffected by added H_2O_2. ZnO catalyzed photodegradation is enhanced significantly by H_2O_2. With increase in concentration of H_2O_2 (>10 mg/L), the degradation increases slowly upto 40 mg/L. Thereafter, the degradation is stabilized and addition of more H_2O_2 has no extra effect on the already stabilized degradation rate.

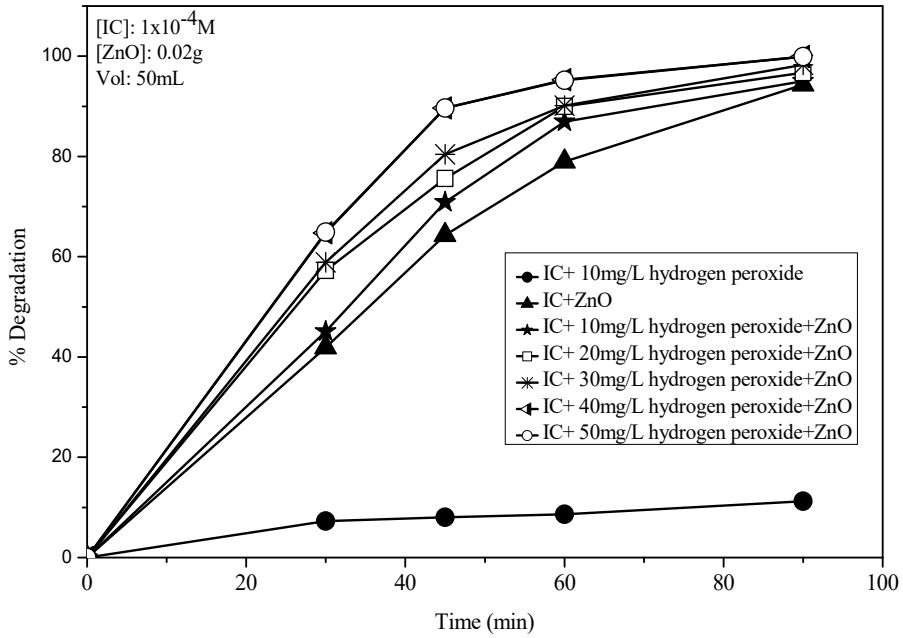

Fig. 3.18: Effect of H_2O_2 on the solar photocatalytic degradation of IC

(Data points for 40 and 50 mg/L are overlapping and hence not distinct)

In the case of ZnO, the adsorption of H_2O_2 is negligible and hence most of the latter will be in solution [186]. H_2O_2 is known to serve as a reservoir of reactive free radicals such as $^{\bullet}OH$ and $HO_2^{\bullet}$, in addition to being a good oxidant by itself. Further, more ROS are formed on irradiation of ZnO in presence of O_2. They interact with the pollutant IC leading to its degradation. The H_2O_2 decomposes in parallel through multiple interactions as in reactions 3.8-3.12 thereby resulting in stabilization in its concentration [186-188]. Thus, above a critical concentration of H_2O_2, instead of generating more ROS such as $^{\bullet}OH$, it becomes a major competitor to the substrate to consume the oxidizing species in the system (reactions 3.11 and 3.13). This leads to decreased or stabilized degradation of IC.

$H_2O_2 + e_{CB}^- \rightarrow {}^{\bullet}OH + OH^-$ ..... (3.8)

$O_2^{-\bullet} + H_2O_2 \rightarrow {}^{\bullet}OH + OH^- + O_2$ ..... (3.9)

$H_2O_2 + 2\ e_{cb}^- + 2H^+ \rightarrow 2\ H_2O$ ... (3.10)

$H_2O_2 + 2\ h_{vb}^+ \rightarrow O_2 + 2H^+$ ... (3.11)

$H_2O_2 + h\nu \rightarrow 2\,{}^{\bullet}OH$ ... (3.12)

$H_2O_2 + {}^{\bullet}OH \rightarrow HO_2^{\bullet} + H_2O$ ....(3.13)

At higher concentration, H_2O_2 absorbs more light, its decomposition is enhanced and more reactive ${}^{\bullet}OH$ radicals are produced (reaction 3.12). These radicals can competitively interact with the H_2O_2 itself, the substrate IC or the reaction intermediates. Scavenging of the radicals by H_2O_2 reduces the efficiency of pollutant degradation.

HO_2 radicals (oxidation potential = ~1.70 eV) are less reactive than ${}^{\bullet}OH$ (oxidation potential = ~2.80 eV) towards the organic pollutants [189]. Hence the contribution of H_2O_2 at its higher concentration (when more of the $HO_2^{\bullet}$ radicals are in the system) towards the degradation of the dye is relatively less and eventually the degradation is stabilized.

3.3.6 Effect of persulphate (PS)

Persulphate ($S_2O_8^{2-}$) is a more powerful oxidant (E_0 = ~2.01 V) than even H_2O_2 (E_0 = ~1.77 V). It is a solid at room temperature and offers advantages of stability, ease of handling and transportation, high aqueous solubility and relatively lower cost. PS has been proven to be a good enhancer of UV photocatalytic degradation of many pollutants while the enhancement is 'moderate' to 'negligible' under sunlight irradiation [176]. In the current instance of ZnO mediated solar photocatalysis, the

enhancement in the degradation of IC by PS is only moderate as seen in figure 3.19. The effect of concentration of PS on the degradation is given in the inset which also confirms that the enhancement is only moderate.

At smaller concentration of PS (upto 20 mg/L) the effect is negligible. However, as the concentration increases further, the degradation increases slowly, reaches an optimum at 30 mg/L and stabilizes thereafter. At the respective optimum concentrations of PS (30 mg/L) and H_2O_2 (40 mg/L) the degradation of IC effected is more or less the same (~ 60% in 30 min.). Combination of H_2O_2 and PS at the respective optimum concentrations does not produce any extra enhancement in the degradation of IC which remains same as in the case of 'H_2O_2 only'.

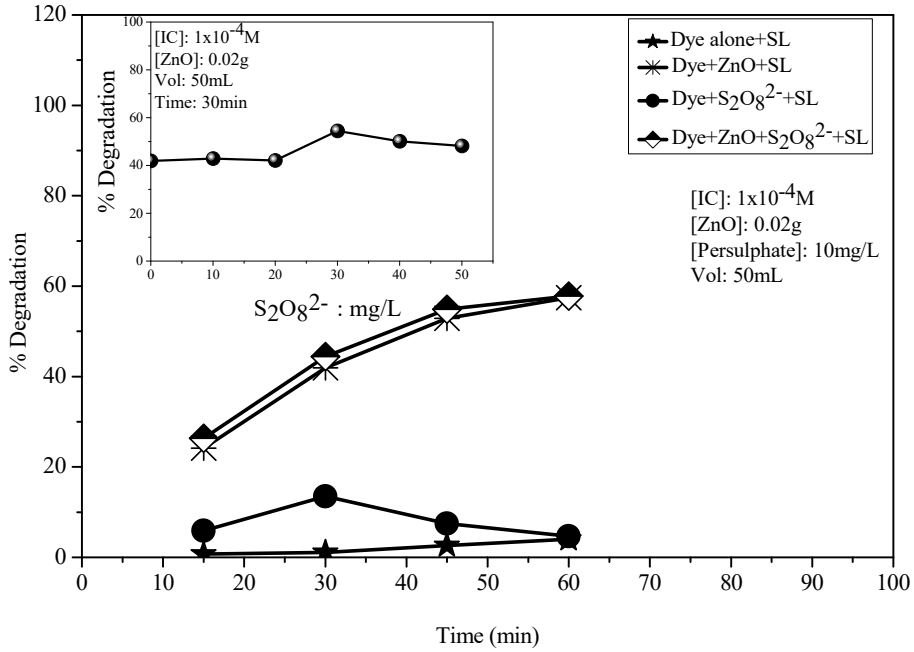

Fig. 3.19: Effect of PS on the degradation of IC

[Inset]: Effect of concentration of PS on the degradation

The reactions leading to the enhancement in the photocatalytic degradation of IC by PS can be generally explained as follows:

PS generates highly reactive $SO_4^{-}\cdot$ radical anions insitu under photocatalytic conditions. These radicals interact with the substrate IC and initiate/enhance their degradation. Higher concentration of PS will generate more $SO_4^{-}\cdot$ radicals under UV irradiation leading to a series of chain reactions as follows (equations 3.14-3.24) [189-191]:

$S_2O_8^{2-} \rightarrow 2SO_4^{-}\cdot$ ....(3.14)

$S_2O_8^{2-} + RH \rightarrow SO_4^{-}\cdot + HSO_4^{-} + R\cdot$ .....(3.15)

RH: organic pollutant

$SO_4^{-}\cdot + H_2O \rightarrow SO_4^{2-} + H^{+} + \cdot OH$ ....(3.16)

$SO_4^{-}\cdot + RH \rightarrow R\cdot + HSO_4^{-}$ ....(3.17)

$\cdot OH + RH \rightarrow R\cdot + H_2O$ ....(3.18)

$R\cdot + \cdot OH \rightarrow$ Intermediates → products ....(3.19)

$SO_4^{-}\cdot + R\cdot \rightarrow$ Chain termination ....(3.20)

$SO_4^{-}\cdot + \cdot OH \rightarrow$ Chain termination ....(3.21)

$2SO_4^{-}\cdot \rightarrow S_2O_8^{2-}$ Chain termination ....(3.22)

$2\cdot OH \rightarrow H_2O_2$ Chain termination ....(3.23)

$2R\cdot \rightarrow$ RR Chain termination/ Further degradation....(3.24)

Various ROS such as H_2O_2, $HO_2\cdot$, $\cdot OH$ etc. and $SO_4^{-}\cdot$ formed during the irradiation interact with IC on the surface of the catalyst as well as in the bulk, leading to its degradation into various intermediates and eventual mineralization. However, the enhancement in the degradation in the present case under solar irradiation is not as significant as under UV

light irradiation. Visible light activation of PS and the formation of reactive species as above are relatively weak under solar radiation compared to UV light [176, 179, 180]. The reactive $SO_4^{-}\cdot$ radicals may also get deactivated as in reactions 3.20-3.22 thereby making the enhancement in the degradation of IC only marginal. The $SO_4^{-}\cdot$ radicals can also interact with PS and form less reactive $S_2O_8^{-}\cdot$ radicals as follows:

$$SO_4^{-}\cdot + S_2O_8^{2-} \rightarrow SO_4^{2-} + S_2O_8^{-}\cdot \quad ....(3.25)$$

Consequent to the above reactions combined with the lower rate of generation under sunlight, the net concentration of $SO_4^{-}\cdot$ in the system is diminished. Hence, the enhancement in the solar photocatalytic degradation of IC in presence of PS also is relatively less.

It has been reported earlier [192] that PS can be even three times more effective than H_2O_2 for the UV-photocatalytic degradation of polyethylene plastics (PEP) pollutant. This is attributed to the trapping of photoproduced electrons by PS (reaction 3.26) thus inhibiting the electron-hole recombination. The resulting reactive sulphate radical anions which are even more powerful oxidants can further enhance the degradation.

$$S_2O_8^{2-} + e^{-} \rightarrow SO_4^{2-} + SO_4^{-}\cdot \quad ....(3.26)$$

The SO_4^{2-} can get adsorbed on the surface and interact with the photoproduced holes producing even more $SO_4^{-}\cdot$ radicals.

$$h^{+} + SO_4^{2-} \rightarrow SO_4^{-}\cdot \quad ....(3.27)$$

Since S is a strong oxidizing agent, the $SO_4^{-\cdot}$ (Reduction potential: 2.6 eV) can accelerate the degradation process by itself as well as by producing more $^{\cdot}OH$ radicals (reactions 3.28, 3.29).

$$SO_4^{-\cdot} + H_2O \rightarrow SO_4^{2-} + \cdot OH + H^+ \quad ....(3.28)$$

$$SO_4^{-\cdot} + \text{Pollutant} \rightarrow SO_4^{2-} + \text{degradation/mineralization products} \quad ....(3.29)$$

The absence of any additive or synergic effect on the degradation of IC in presence of the combination of PS and H_2O_2 under ZnO/sunlight shows that the formation of $SO_4^{-\cdot}$ and other ROS is weak under visible light. Further, the interactions leading to the deactivation of insitu generated reactive ·OH and other free radicals may be still active even in the combined presence of the oxidants. Hence the enhancing effect of PS or PS/H_2O_2 on the degradation of IC is only moderate or even negligible.

3.3.7 Temperature effect

The effect of temperature on the photocatalytic degradation of IC in presence of ZnO is tested in the range of 15-50°C. The degradation increases with increase in temperature upto 30°C and stabilizes thereafter (figure 3.20). The rate constant k_{app} is determined at various temperatures and the apparent activation energy (E_a) is calculated from the Arrhenius equation

$$\ln k_{app} = (-Ea/kT) + \ln A \quad ....(3.30)$$

by plotting $\ln k_{app}$ vs (1/T).

T is the temperature of reaction in Kelvin and A is the Arrhenius factor.

The E_a as computed is 16.0 $kJmol^{-1}$. This is the total activation energy of both adsorption and photocatalytic degradation [177]. However, in the case of ZnO the adsorption of IC is relatively small (<5%) and hence the value can be considered as true activation energy. This value is close to the Ea value of 14.4 $kJmol^{-1}$ reported by Barka et al. [177] for the photocatalytic degradation of IC on TiO_2 coated nonwoven fibres. The activation energy for the photocatalytic degradation of acid blue dye on Degussa P-25 also is comparable as reported by Bouzaida et al. [193].

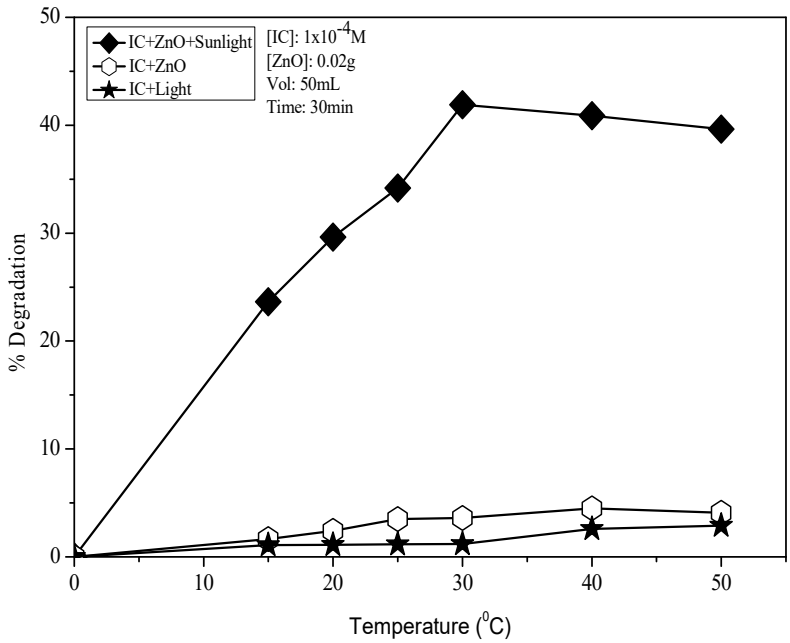

Fig. 3.20: Effect of temperature on the degradation of IC

As the temperature increases, adsorption of the dye which is already very low, decreases further. At low temperature, the degradation is lower in spite of better adsorption because the energy is not enough. At 40°C when the adsorption is less, the degradation is more. This again confirms

that adsorption is important though it is not the sole parameter that determines the degradation. Once the catalyst is activated by thermal and/or photo energy, the reactive free radicals are generated and the reaction can take place in the bulk as well.

3.3.8 Effect of anions

Many of the anionic contaminants which are naturally present in water inhibit the efficiency of AOPs for the degradation of organic pollutants [194, 195]. Instances of anions functioning as enhancers of the degradation of pollutants also have been reported [196, 197]. In this context, the effect of some of the commonly occurring anions in water, i.e. SO_4^{2-}, Cl^-, PO_4^{3-}, CO_3^{2-} and HCO_3^- on the efficiency of solar photocatalytic degradation of IC is tested and the results are presented in figure 3.21.

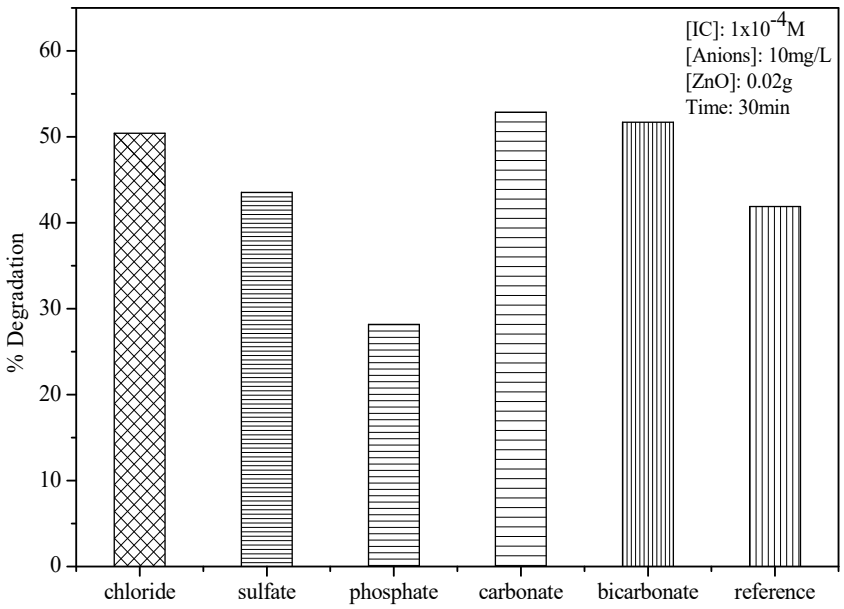

Fig. 3.21: Effect of various salts/anions on the degradation of IC

The results showed that the anion sulfate (SO_4^{2-}) has no effect while chloride (Cl^-), carbonate (CO_3^{2-}) and bicarbonate (HCO_3^-) enhance the degradation moderately. As expected based on previous results, [179, 180, 197-199] PO_4^{3-} is a strong inhibitor of the degradation of IC.

The effect of concentration of the anions on the degradation is also tested. In the case of the enhancing anions Cl^-, CO_3^{2-} and HCO_3^-, the degradation of IC increases with increase in their concentration (Fig. 3.21 A-C). In the case of SO_4^{2-}, the concentration effect is less (Fig. 3.21D). In the case of PO_4^{3-}, the inhibition increases with increase in its concentration (3.21E).

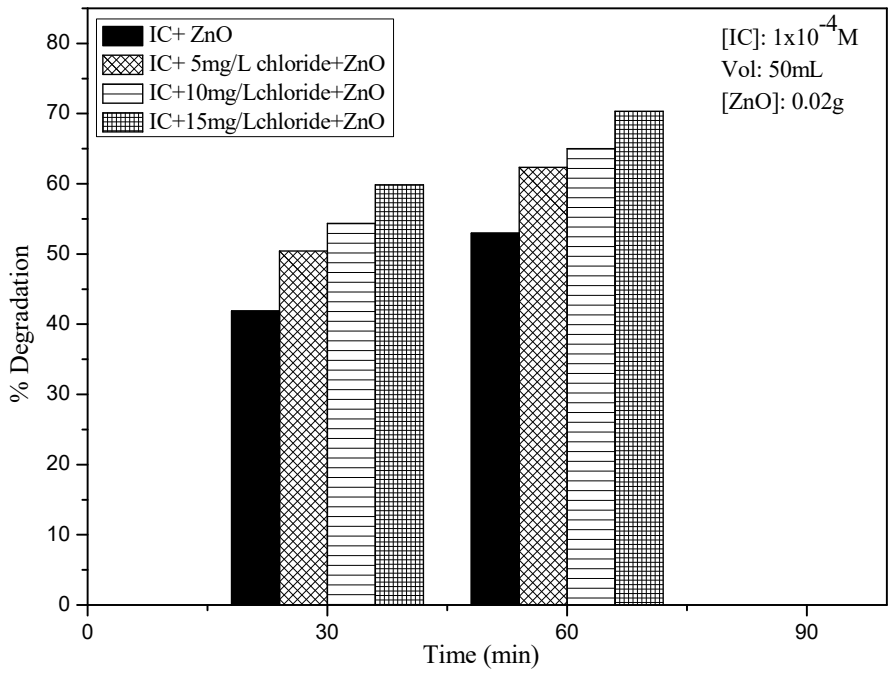

Fig. 3.21.A: Effect of Cl^- on the degradation of IC

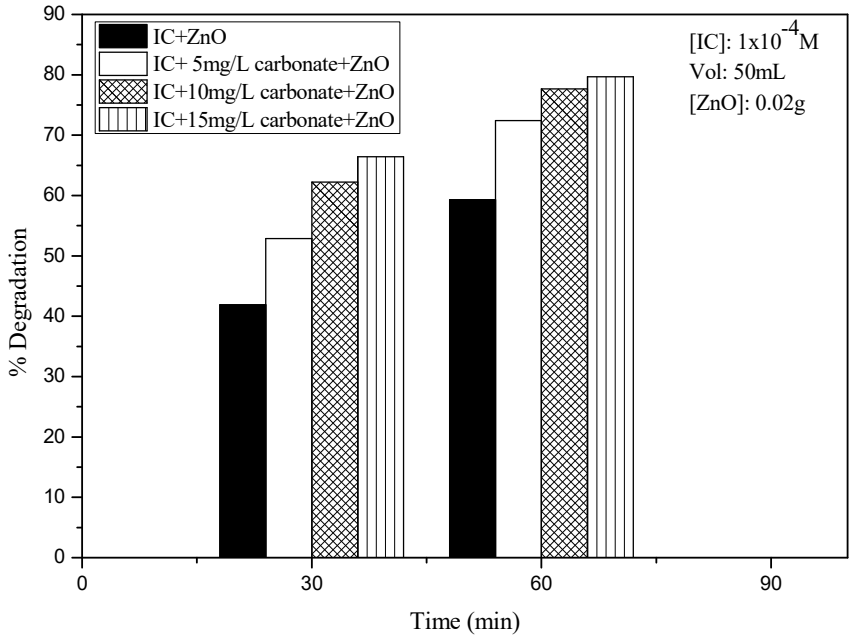

Fig. 3.21.B: Effect of CO_3^{2-} ion on the degradation of IC

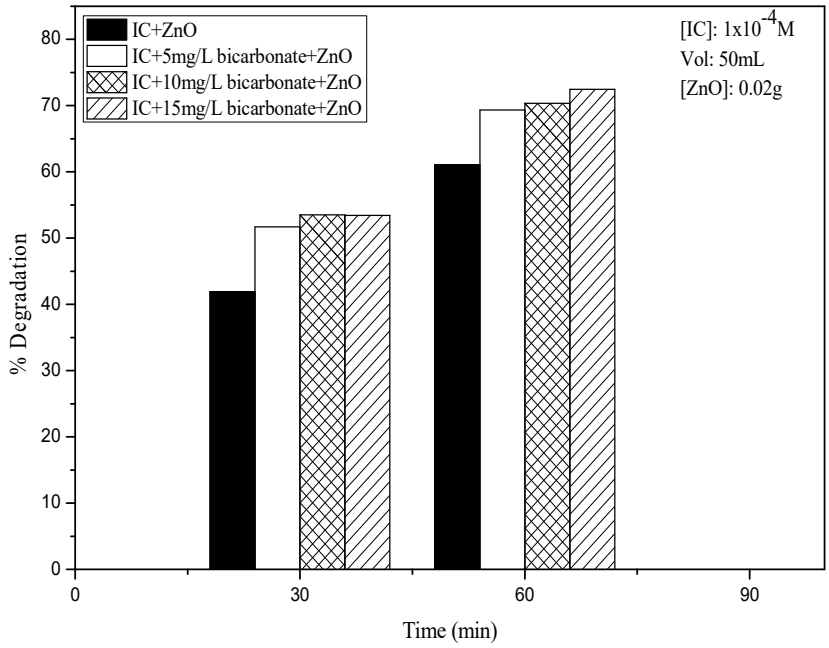

Fig. 3.21.C: Effect of HCO_3^- ion on the degradation of IC

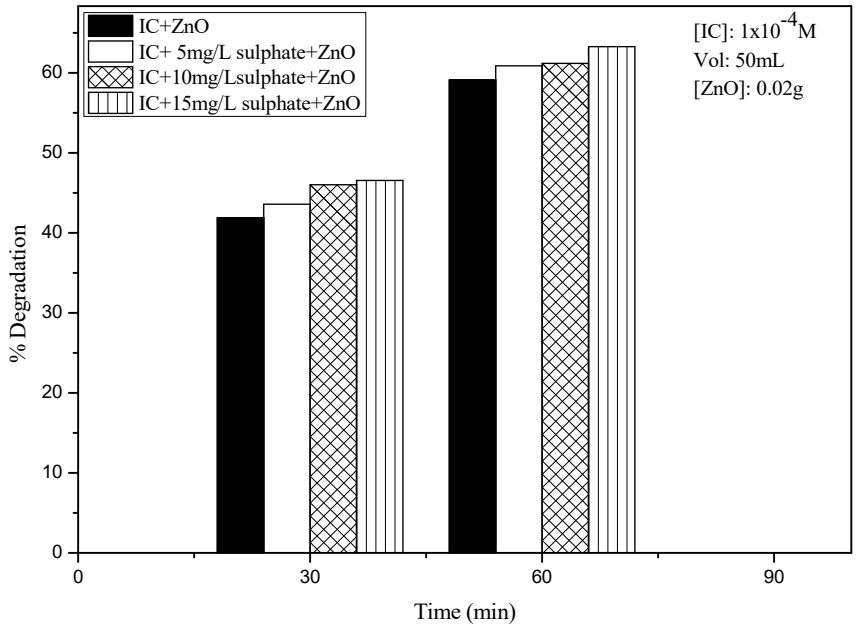

Fig. 3.21.D: Effect of SO_4^{2-} ion on the degradation of IC

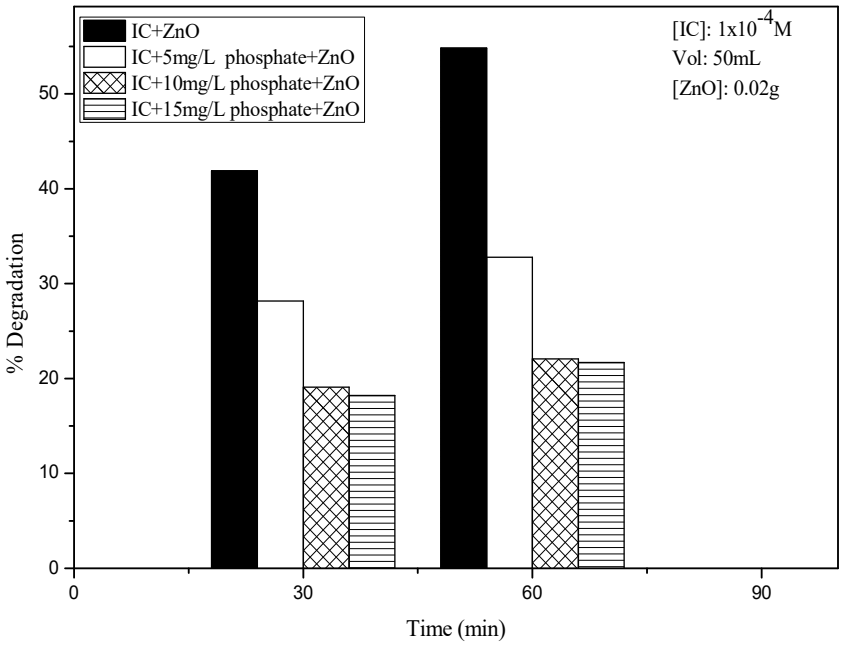

Fig. 3.21.E: Effect of PO_4^{3-} ion on the degradation of IC

The inhibiting anions become better inhibitors and the enhancing anions become better enhancers with increase in their concentration. In all cases, the effect is stabilized eventually resulting in no further enhancement or inhibition as the case may be, beyond a critical concentration. However, the concentration of anions in all these cases was varied within a narrow range only (0-15 mg/L) and any conclusion based on the limited data may not be appropriate. More in-depth investigation is needed in view of the complexity and inconsistency of the effect of anions on AOPs, as reported in previous studies [200, 201].

The inhibition of the photocatalytic degradation of organics by anions/salts is often explained based on blocking of the active surface sites on the catalyst by preferential adsorption (of the anions), surface layer formation and/or scavenging of reactive ·OH radicals. Since the Point of Zero Charge (PZC) of ZnO is ~9±0.3 the surface is positively charged when the pH is lower than this value and negatively charged when the pH is higher. Hence, at the natural pH of ~ 5 of the system all the anions tested here can get strongly adsorbed on ZnO. The adsorption of IC on ZnO in presence of the anions is measured experimentally (figure 3.22).

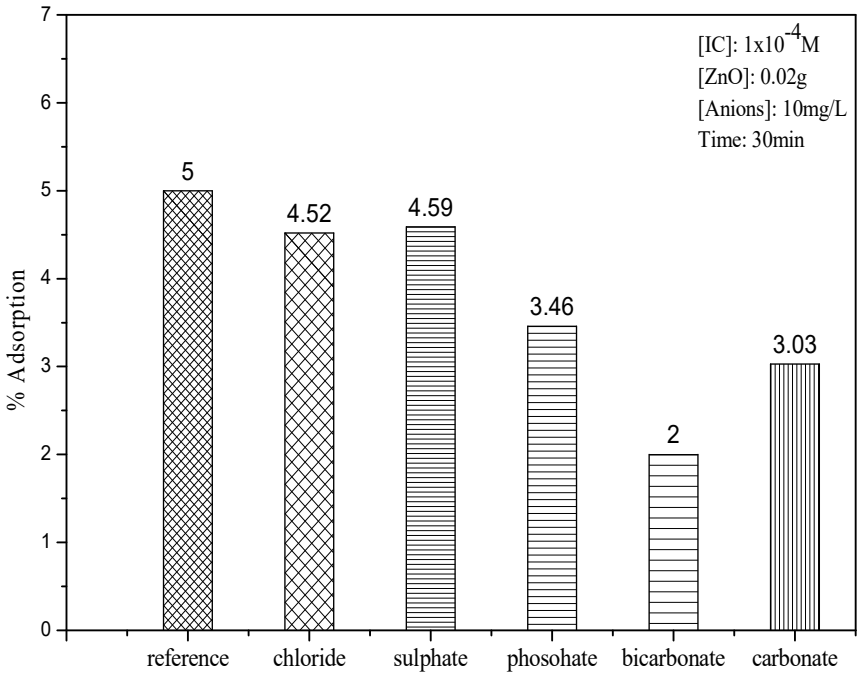

Fig. 3.22: Adsorption of IC in presence of anions

It is seen that the adsorption is slightly inhibited in presence of PO_4^{3-}, CO_3^{2-} and HCO_3^- while other anions do not influence the adsorption much. The cation was kept the same in all cases, i.e., Na^+. Had the competitive adsorption of the anions been the main cause of the anion effect, all of them should have been inhibitors and the inhibition should have been in the order:

$$SO_4^{2-} \sim Cl^- > PO_4^{3-} > CO_3^{2-} > HCO_3^{2-} \quad ....(3.31)$$

This sequence is not followed except in the case of PO_4^{3-} which is the only strong inhibitor of the degradation of IC. Other anions are enhancers or have 'no effect'. Hence, the preferential adsorption by the

anion is not the major cause of inhibition, though it may be one of the many causes. This is even more true in the case of poorly adsorbing substrates such as IC on ZnO. The degradation proceeds primarily in the bulk of the medium and it is not a surface initiated process.

Presence of anions can also reduce the diffusion coefficient of the organic pollutant in the reaction medium. Consequently, the pollutant molecules will be less accessible to the reactive ·OH and this also can contribute to the inhibition. Another possible reason for the inhibition by anions is the formation of an inorganic layer on the catalyst surface. The efficiency of layer formation depends on the solubility of the salts [201]. The higher the solubility of the salt the lower will be the layer formation. The solubility of the salts (in mg/g of water at 20^0C) tested here is in the order;

$$Na_2SO_4\ (40.8) \geq Na_2CO_3\ (39.7) > NaCl\ (36.1) > Na_3PO_4\ (16.3) > NaHCO_3\ (11.1) \quad ....(3.32)$$

Correspondingly the layer formation, if any, will be in the order:

$$HCO_3^- > PO_4^{3-} > Cl^- \geq CO_3^{2-} \geq SO_4^{2-} \quad ....(3.33)$$

If layer formation is the major cause, the inhibition must be in the same order as above. The experimentally observed anion effect in the current instance is not fully consistent with equation (3.33) except in the case of PO_4^{3-}. The anions Cl^-, CO_3^{2-}, HCO_3^- and SO_4^{2-} are mild enhancers or have 'no effect'. In many other AOPs, these anions function as inhibitors. In the present case, they are mild enhancers and hence it may be presumed that their inhibiting efficiency (part of which is attributed to

layer formation) is compensated for or even overpowered by other factors.

Many anions are known to scavenge the reactive ·OH radicals. The scavenging rate constants in the case of some of the anions are summarized in Table 3.2 [201].

Table 3.2: Scavenging rate constants of ·OH by various anions

Anion	Scavenging Rate constants ($mol^{-1}s^{-1}$)
Cl^-	4.3×10^9
CO_3^{2-}	3.9×10^8
SO_4^{2-}	1×10^{10}
$H_2PO_4^{3-}$	2×10^4
HCO_3^-	8.5×10^6

However, scavenging of the reactive ·OH radicals by the anions can explain only inhibition (of PO_4^{3-} in this case) and not the 'no effect' (of SO_4^{2-}) or enhancement (by the anions Cl^-, CO_3^{2-} and HCO_3^-). Hence there must be more efficient alternative processes taking place to effect the enhancement even after compensating for the potential inhibition caused by adsorption of the anions on the surface, surface layer formation and the trapping of reactive ·OH radicals.

Scavenging of the ·OH by anions would yield respective radical anion species which are also reactive towards organic compounds, although less efficiently than ·OH [198]. In the case of the anions with 'enhancing effect' or 'no effect' in the present case, the radical anions are formed as follows:

$$\cdot OH + HCO_3^- \rightarrow H_2O + CO_3\cdot^- \quad \text{.....(3.34)}$$

$$\cdot OH + CO_3^{2-} \rightarrow OH^- + CO_3\cdot^- \quad \text{.....(3.35)}$$

$$\cdot OH + Cl^- \rightarrow OH^- + Cl\cdot \quad \text{.....(3.36)}$$

$$Cl\cdot + Cl^- \rightarrow Cl_2^-\cdot \quad \text{.....(3.37)}$$

$$\cdot OH + SO_4^{2-} \rightarrow OH^- + SO_4\cdot^- \quad \text{.....(3.38)}$$

These radical anions $CO_3\cdot^-$, $Cl_2^-\cdot$, etc. undergo slower recombination or deactivation compared to ·OH. Hence they are more readily available for longer time than ·OH to react with the substrate and effect degradation. Thus their relatively lower reactivity is compensated by their better availability for reaction with the substrate. Many of the $^{\bullet}OH$ radicals would undergo recombination and get deactivated if they are not reacting with the anions. Enhancement in the degradation of the substrate occurs when the reaction rate between added anions and $^{\bullet}OH$, forming radical anion, is higher than that between substrate and $^{\bullet}OH$. However, both the rates would be much lower than radical-radical recombination. Even those radical anions which are formed at or near the surface of the catalyst can diffuse into the solution bulk and react with the substrate. The $^{\bullet}OH$ radical concentration is relatively less in the bulk compared to the surface and/or its immediate neighborhood and hence their recombination also is slow. Consequently, the $^{\bullet}OH$ will interact with the more abundant substrate molecules and anions, both of which can lead to enhanced degradation as explained above. Hence, it may even be said that the anions are protecting the $^{\bullet}OH$ radicals from unproductive recombination by transforming them into radical anions. However, this process is dependent on the concentration of the anions and other reaction parameters [198]. Above a particular concentration of the anion, the relative concentration of $^{\bullet}OH$ radicals available to interact with

them is less. Similarly, once the degradation of the substrate has progressed substantially and its concentration in the system is less (towards the later stages of reaction), the radical anion $X^{-\cdot}$ which has only substrate as the sink, cannot sustain the enhanced degradation rate. From that point onwards, the anion-caused enhancement slows down gradually and eventually the effect is stabilized as in the present case or even reversed to inhibition as reported in literature [198].

It is well known that pH of the reaction medium has strong influence on the AOP degradation of many water pollutants. Anions, especially carbonate and bicarbonate, are expected to increase the pH of the medium. Hence the possibility of anion effect arising at least partially from the variation in pH is examined. In the presence of HCO_3^- and CO_3^{2-} (10 mg/L each), the pH of the reaction medium increases to 6.3 and 7.1 respectively from 4.8. The variation in pH in the presence of other anions tested here is not significant. Comparison of the degradation of IC at these pH values after 30 minutes of irradiation shows decrease from ~42% (pH = 4.8) to ~35% (pH = 6.3) and ~33% (pH = 7.1). Thus, based on sole pH variation, the effect of HCO_3^- and CO_3^{2-} should have been decrease in degradation of IC. However, in presence of these anions, the photocatalytic degradation of IC is enhanced moderately. Hence it may be inferred that the effect of anions, at least under the experimental conditions tested here, is not primarily due to any change in the pH of the system.

The above results clearly show that a universally applicable explanation to account for the effect of anions in different kinds of photocatalytic systems with different catalysts, substrates and reaction

conditions is not possible and it will be more appropriate to consider individual systems to explain specific effects in specific cases.

3.3.9 Effect of oxygen

All mechanisms proposed for the photocatalytic degradation of organics involve the participation of O_2 through the formation of reactive oxygen species (ROS) such as $O_2^{-}\cdot$, $HO_2\cdot$, $\cdot OH$, H_2O_2 etc. In order to confirm the effect of O_2 on the photocatalytic degradation of IC, the reaction system is degassed with N_2 and the experiments were carried out under otherwise identical conditions. The degradation is almost fully inhibited in the degassed system (Fig. 3.23) thereby illustrating that O_2 (and ROS resulting from it) is essential for the photocatalytic degradation of IC. The formation of H_2O_2 also is negligible in the degassed system.

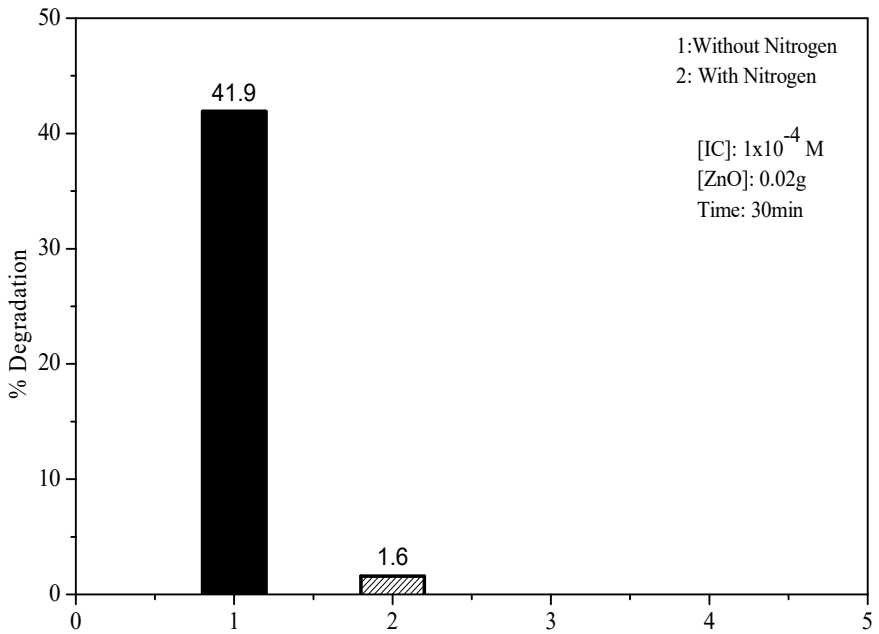

Fig. 3.23: Effect of oxygen on the solar photocatalytic degradation of IC

Thus it can be seen that the photocatalytic degradation of IC on ZnO is almost completely inhibited in the absence of O_2. Adsorption of the dye on the catalyst is only moderate and hence the main role of the catalyst and its activated surface is the generation of ROS from dissolved as well as adsorbed O_2. These reactive species interact with the substrate as well as the insitu formed reaction intermediates mainly in the bulk resulting in eventual mineralization. Hence adsorption of the substrate is not important in this case. Turchi and Ollis [202] have also demonstrated that adsorption of the substrate is not an essential requirement for photocatalytic reactions, even though the adsorption characteristics of the components can influence the rate of degradation of the organic compounds on the surface.

3.3.10 Chemical Oxygen Demand and (COD) effect of intermediates

The decolorization of dyes need not necessarily lead to mineralization and the possibility of formation of even more toxic intermediates cannot be ruled out. In order to verify the mineralization of IC under the current experimental conditions, the chemical oxygen demand (COD) of the optimized reaction system ZnO /IC under sunlight irradiation at various intervals is determined. The results presented in figure 3.24 show that decolorization does not result in corresponding mineralization. However, when the decolorization is complete (in 90 minutes), the COD decreases significantly. Thereafter it remains steady for long (over 250 minutes) even when the irradiation is continued. The stable COD for long duration shows that after the initial decolorization and partial mineralization of relatively unstable intermediates formed insitu, the more stable intermediates take longer time for mineralization. Eventually they also get mineralized and the COD becomes almost zero.

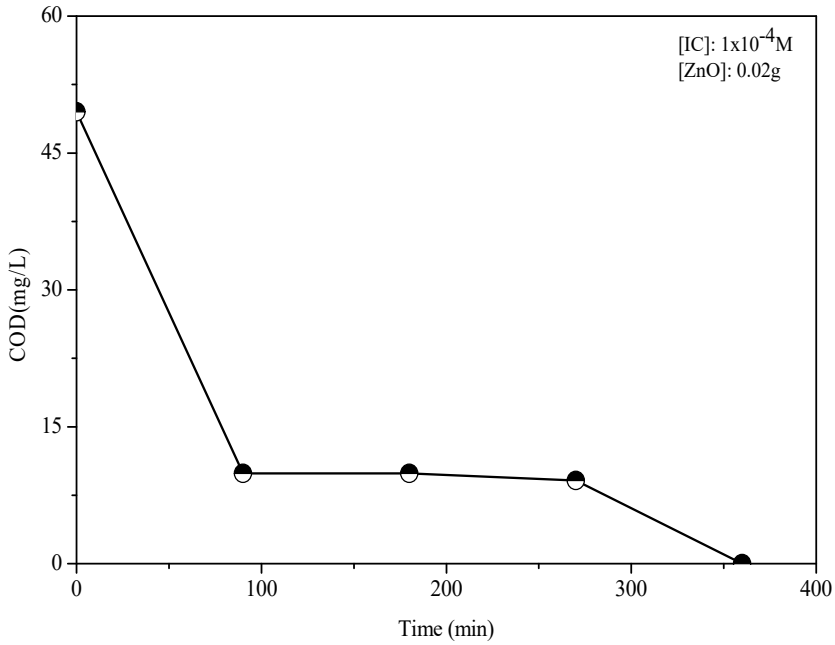

Fig. 3.24: Chemical oxygen demand (COD) of the IC/ZnO system during solar photocatalytic degradation of IC

3.3.11 Reaction intermediates

It has been reported that the degradation of IC under AOP yields stable intermediates such as acetic acid, tartaric acid, malic acid, oxalic acid, anthranilic acid etc. [172, 203, 204]. In the current study, only two of these could be detected consistently; oxalic acid and acetic acid, even though the possibility of formation of other intermediates cannot be ruled out. In any case, the effect of the likely intermediates on the degradation of IC is evaluated and the results are shown in figure 3.25.

The carboxylic acids likely to be present in the reaction system are added, one at a time to the system. Intermediates formed during the photocatalytic degradation process do affect the degradation of the

original compounds. Higher initial concentration of substrate will result in higher concentration of intermediates, which will affect the overall rate of the reaction.

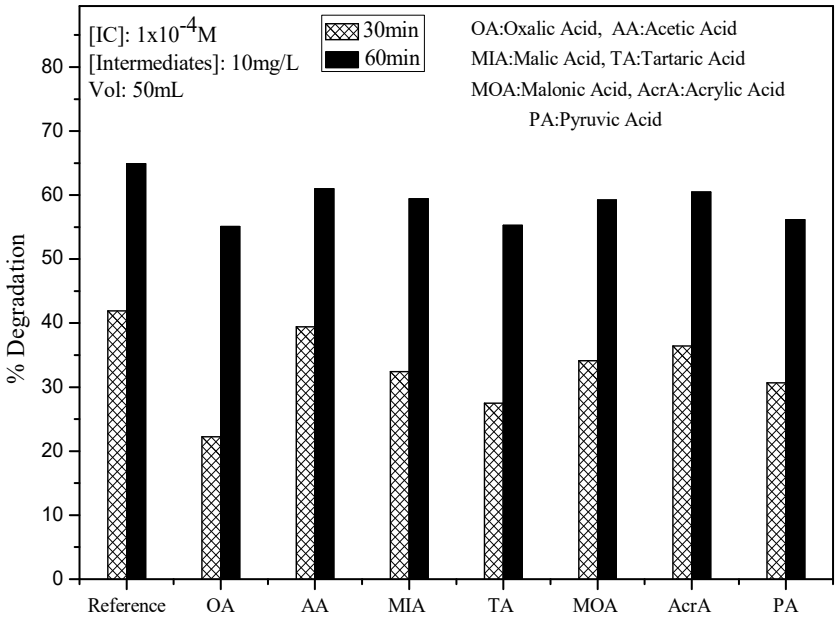

Fig. 3.25: Effect of likely intermediates on the degradation of IC

The results show that the degradation is inhibited by all intermediates at least in the concentration studied here. Maximum inhibition is observed in the case of oxalic acid. The inhibition is in the decreasing order:

Oxalic acid ≥ Tartaric acid > Pyruvic acid > Malic acid ≈ Malonic acid > Acrylic acid ≈ Acetic acid ....(3.39)

The effect of varying concentration of the intermediate carboxylic acids on the degradation of IC is investigated in detail and the results are shown in figures 3.25 A-E.

Oxalic acid (OA) is the strongest inhibitor, with inhibition increasing with increase in concentration of OA. However in the case of acrylic acid and tartaric acid, clear inhibition is observed only at higher concentrations. In the case of acetic acid, malic acid and pyruvic acid, the effect varies from mild inhibition to no effect depending on the concentration. At lower concentration, the intermediate acids also get photodegraded faster without interfering with the degradation of IC. However with time, they get accumulated and at higher concentration, they will compete with the substrate IC for surface sites as well as the reactive free radicals resulting in mild to moderate inhibition.

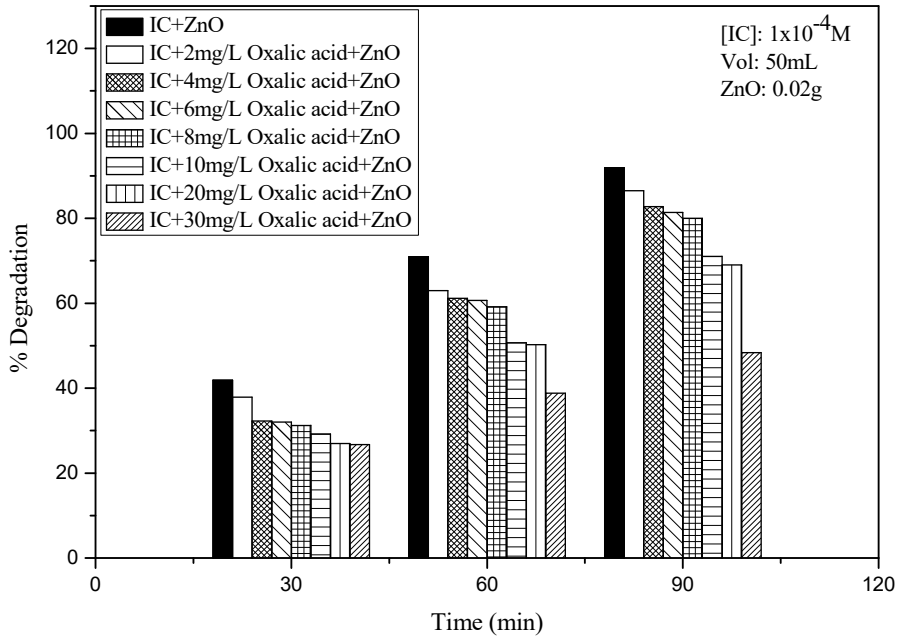

Fig. 3.25.A: Effect of varying concentrations of oxalic acid on the photocatalytic degradation of IC

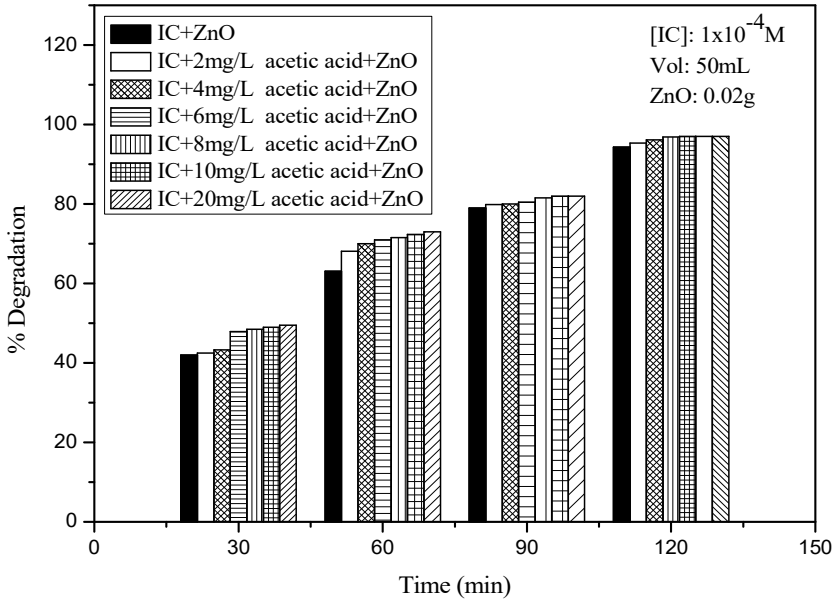

Fig. 3.25.B: Effect of varying concentrations of Acetic acid on the photocatalytic degradation of IC

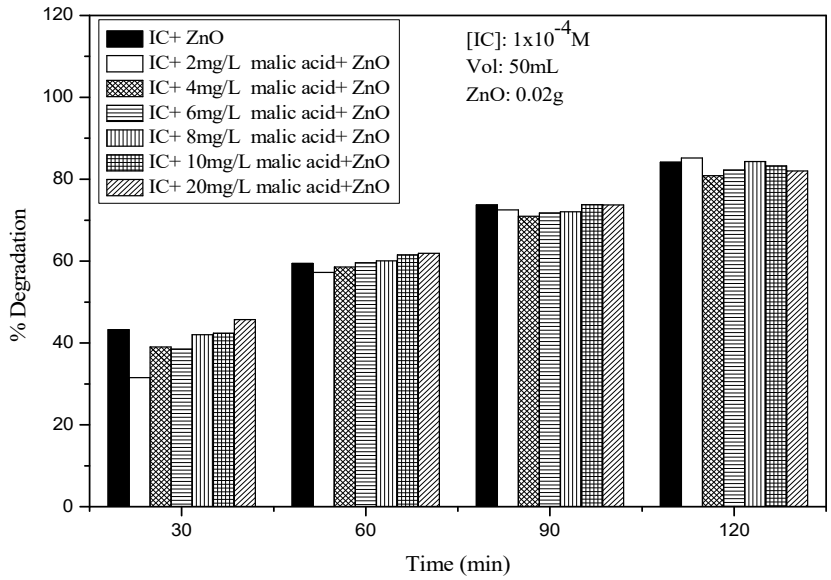

Fig. 3.25.C: Effect of varying concentrations of Malic acid on the photocatalytic degradation of IC

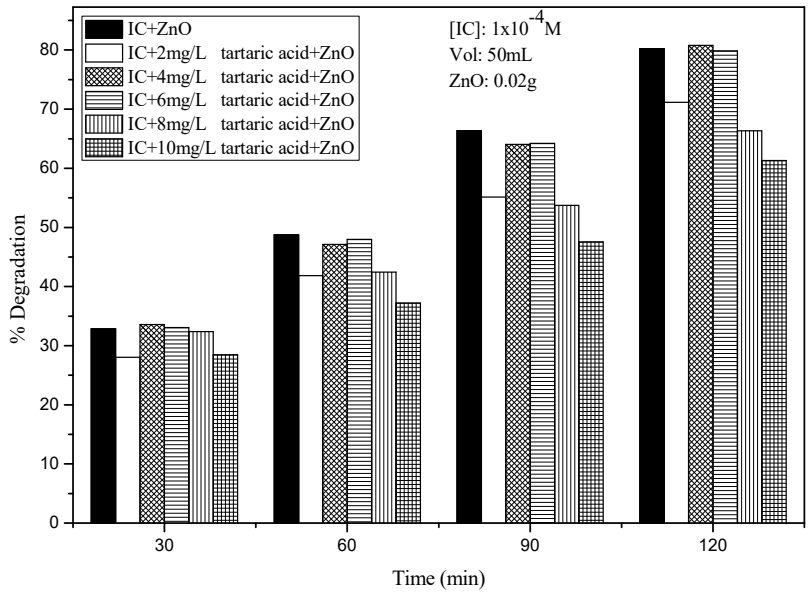

Fig. 3.25. D: Effect of varying concentrations of Tartaric acid on the photocatalytic degradation of IC

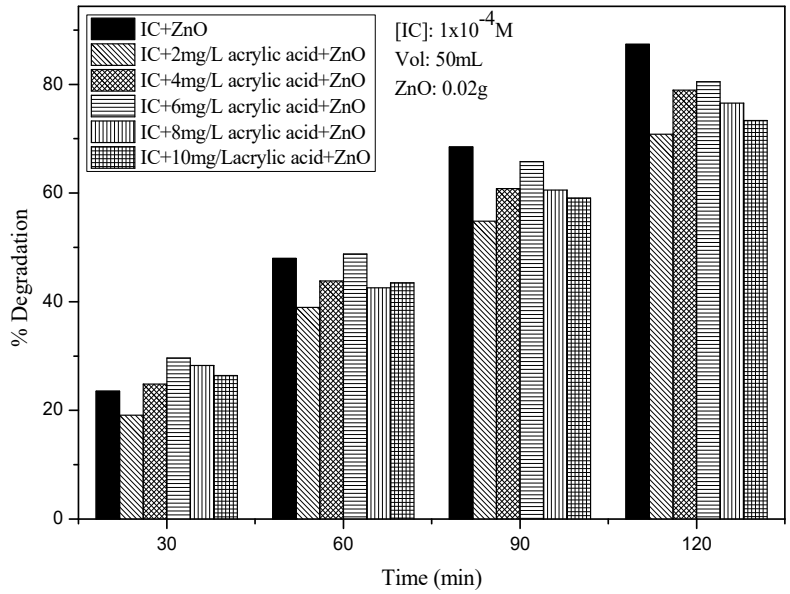

Fig. 3.25. E: Effect of varying concentrations of Acrylic acid on the photocatalytic degradation of IC

The effect of concentration of the strongest inhibitor among the intermediates, i.e., oxalic acid, at different reaction time intervals is verified and the results are shown in Table 3.3.

Table 3.3: Effect of oxalic acid at different concentrations on the degradation of IC at different reaction times, [IC]: 1×10^{-4}M, [ZnO]: 0.02 g

Intermediate added	Concentration (mg/L)	% Degradation of IC after (in min)			
		30	60	90	120
Nil (Reference)	0	42.0	62.5	74.0	89.5
Oxalic acid	2	37.7	55.0	67.2	84.2
	4	32.8	49.4	64.2	80.5
	10	28.2	45.5	61.0	76.0
	20	24.8	42.7	54.5	67.9

The degradation and eventual mineralization of the intermediates is further tested with oxalic acid as the test molecule. The degradation of oxalic acid is performed in the presence of catalyst ZnO and oxidants such as peroxide and persulphate, individually as well as in combination of the two. The results are presented in figure 3.26.

The results show that oxalic acid is degraded in the presence of sunlight and the degradation is accelerated in the presence of oxidants and catalyst. The combination of the catalyst and the oxidant is the most efficient and the efficiency is in the order:

$$(S_2O_8^{2-}+H_2O_2+ZnO) > (S_2O_8^{2-}+ ZnO) > (H_2O_2+ZnO) \geq ZnO > (S_2O_8^{2-}+H_2O_2) > S_2O_8^{2-} > H_2O_2 \quad ....(3.40)$$

The results clearly show that oxalic acid, the most stable among the intermediates also get degraded slowly but steadily and can be completely mineralized in presence of catalyst and oxidant (ZnO + PS). Hence ZnO

mediated oxidant assisted degradation of IC is a viable method for its complete mineralization in water.

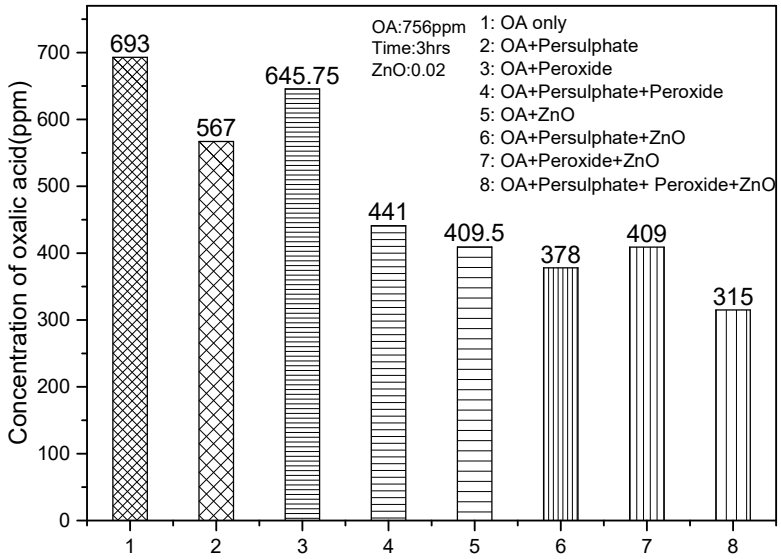

Fig. 3.26: Solar photocatalytic degradation of oxalic acid under different conditions

Major transient intermediates present in the system immediately after decolorization as identified by LC/MS are listed in Table 3.4. However, eventually they also get degraded and mineralized as seen from the 'Nil' COD value and the mass chromatogram (Fig. 3.27).

3.3.12 General Mechanism of the photocatalytic degradation

The basic mechanism of semiconductor oxide photocatalysis consists of initial light absorption by the catalyst which promotes the electron from the valence band to the conduction band resulting in the creation of hole in the valence band (reaction 3.41).

$$\text{Semiconductor (ZnO)} + h\nu \rightarrow h^+ + e^- \qquad ....(3.41)$$

Table 3.4: Major transient intermediates formed during the mineralization of IC

Sl No.	m/z	Molecular formula	Proposed structure
1	189	$C_6H_7NSO_4$	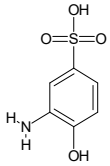
2	201	$C_7H_7NSO_4$	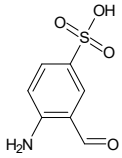
3	217	$C_7H_7NSO_5$	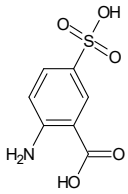
4	227	$C_8H_5NSO_5$	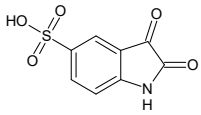
5	259	$C_8H_5NSO_7$	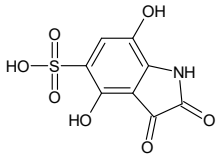
6	261	$C_8H_7NSO_7$	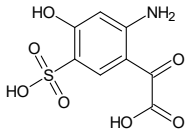
7	358	$C_{16}H_{10}N_2SO_6$	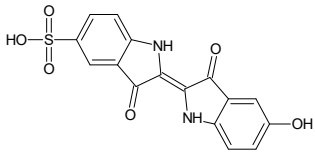
8	424	$C_{16}H_{12}N_2SO_{10}$	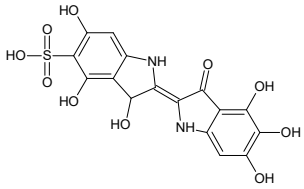

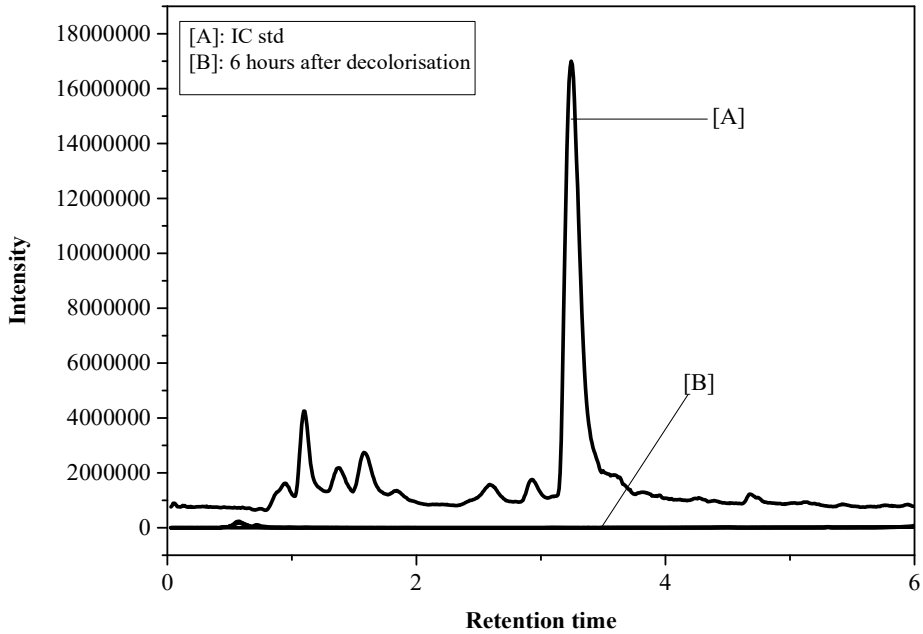

Fig. 3.27: Mass chromatogram of the reaction mixture [A] initially and [B] after 6 hr irradiation

Both the electron and hole must be consumed so that the material can act as an efficient catalyst. It is generally believed that both the electrons and holes can find low energy trap sites on a sub-picosecond time scale in the semiconductor [205]. These electrons and holes can either recombine and dissipate the input energy as heat (reaction 3.42) or react with electron donors and electron acceptors which are adsorbed on the semiconductor surface or trapped within the surrounding electrical double layer of the charged particles to produce strong oxidizing hydroxyl radicals. These radicals can promote the oxidation of organic compounds [206]. Dissolved oxygen and surface oxygen play important role by scavenging the electrons generated on photoactivated ZnO and forming

superoxide radical anion and other reactive species. Various reaction steps involved in the process can be presented as follows:

$h^+ + e^- \rightarrow$ Heat ... (3.42)

$O_2 + e^- \rightarrow O_2^{-}\cdot$ ....(3.43)

$O_2^{-}\cdot + 2\,H^+ + e- \rightarrow H_2O_2$ ....(3.44)

$h^+_{VB} + H_2O \rightarrow H^+ + \cdot OH$ ....(3.45)

$O_2^{-}\cdot + H^+ \rightarrow HO_2\cdot$ ....(3.46)

$2\,HO_2\cdot \rightarrow H_2O_2 + O_2$ ....(3.47)

$HO_2\cdot + O_2^{-}\cdot + H_2O \rightarrow H_2O_2 + O2 + .OH$ ....(3.48)

$H_2O_2 + e^- \rightarrow \cdot OH + OH^-$ ... (3.49)

$\cdot OH + \cdot OH \rightarrow H_2O_2$ ....(3.50)

$h^+_{VB} + OH^- \rightarrow \cdot OH$ ....(3.51)

The ROS formed as above interact with the organic molecules (IC in this case), resulting in the formation of various intermediates and eventual mineralization.

$\cdot OH + RH \rightarrow H_2O + R\cdot$ ....(3.52)

RH is the dye or the intermediates formed insitu

$R\cdot + O_2 \rightarrow ROO\cdot \rightarrow \ldots \rightarrow$ mineralized products ....(3.53)

The general mechanism of semiconductor photocatalysis can be schematically presented as in figure 3.28

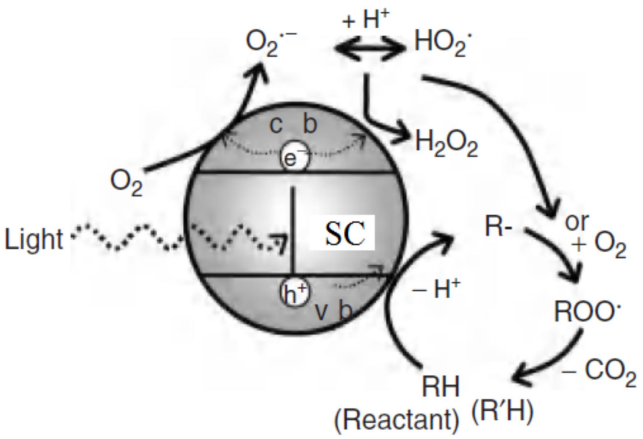

Fig. 3.28: Schematic presentation of the general mechanism of semiconductor photocatalysis

Surface sensitization of a wide band gap semiconductor photocatalyst such as ZnO by physisorbed or chemisorbed dyes can expand the wavelength range of excitation for the photocatalyst and/or increase the efficiency of the excitation process. The first step is the excitation of the sensitizer followed by charge transfer to the semiconductor. The excited state can inject either a hole, or more commonly, an electron to the particle. When a monolayer of a dye is dispersed on the photocatalyst with high surface area, the charge injection will be more efficient. Extension of the photoactive wavelength range of the catalyst to the visible range is important for the harnessing of sunlight. Photosensitization of semiconductors by various dyes has been monitored by nanosecond and picosecond flash photolysis as well as femtosecond spectroscopy. The rates of injection of electron as well as the back electron-transfer from the dye to the photocatalyst depend upon the nature of the dye molecules, properties of the catalyst particles and the interactions between the dye and particles [207].

3.4 Conclusion

Solar photocatalysis using ZnO as the catalyst is found to be an efficient method for the removal of trace amounts of Indigo Carmine dye pollutant from water. The degradation follows pseudo first order kinetics at lower concentrations of the substrate. H_2O_2 formed insitu in the process undergoes concurrent decomposition resulting in stabilization in its concentration. Oxidants H_2O_2 and persulphate enhance the degradation moderately. The salt/anion contaminants present in water influence the degradation differently with the effect varying from inhibition to 'no effect' or even enhancement depending on the nature of the anion and the multitude of interactions involving the substrate, reaction intermediates and the catalyst. The degradation proceeds through many transient intermediates which degrade further on continued irradiation to give organic acids such as oxalic acid and acetic acid. They inhibit the degradation of IC though eventually they also get mineralized. The inhibition is attributed to the competition between the substrate and the insitu formed intermediates for surface sites as well as reactive oxygen species. The degradation is practically negligible in nitrogen flushed systems thereby confirming the role of O_2 (and the reactive oxygen species formed insitu) in the degradation. The results are discussed in detail and suitable mechanisms for the observed effects are proposed.

.....ꕥ.....

Chapter

4

ELECTROCHEMICAL AOPs FOR THE DECONTAMINATION OF WATER FROM INDIGO CARMINE DYE POLLUTANT

Contents

4.1 Introduction

Manufacture and use of synthetic dyes, especially in textiles, is a massive industry today. Around 30% of the dyes used in the textile industry does not get fixed on the target and are discharged in the respective factory effluent. Dyes are highly visible and even minor release into the water bodies may be unacceptable aesthetically as well as environmentally. Dyes can also obstruct light penetration into the water bodies, thus inhibiting the biological processes based on photosynthesis. Many of these dyes are also toxic, carcinogenic, mutagenic or teratogenic to various microbiological or animal species. Due to low biodegradability of dyes, the conventional treatment process is not very efficient for their removal from wastewater. Such techniques simply transfer the pollutants from one medium to another (water to water, water to soil and water to air) causing secondary pollution. In this context, advanced oxidation

processes (AOP) are gaining importance as tertiary treatment techniques for the removal of even small concentration of chemical pollutants [12, 208-210].

In recent years, electrochemical techniques have been gaining acceptance as powerful tools for wastewater remediation [63, 211, 212]. The advantage of this technology is its environmental compatibility because the main reactant is the electron which is not a pollutant [63]. Other advantages are related to its versatility, high energy efficiency, availability of automation, safety and mild reaction conditions. It can also be operated in combination with other techniques, i.e. sonoelectrochemical [213], photoelectrochemical [214] processes etc.

Among the electrochemical methods, anodic oxidation is perhaps the most popular one for the treatment of wastewaters containing persistent organic pollutants (POPs). The pollutants are removed using high oxygen evolution potential anode which generates highly reactive hydroxyl radicals ($^{\bullet}OH$) insitu [215,216].These radicals instantly interact with the pollutant leading to the degradation and eventual mineralization. The reaction involved in the formation of $^{\bullet}OH$ is:

$$M + H_2O \rightarrow M(^{\bullet}OH) + H^+ + e^- \quad \text{..... (4.1)}, \quad M\text{: Electrode}$$

In presence of chloride, AOP oxidation of organic compounds proceeds through chlorinated intermediates. The organochlorine compounds (RCl) formed during the degradation of the pollutant have different genotoxic, carcinogenic and/or mutagenic effects depending on the chemical structure. Hence it is important that the chemistry of the

pollutant and its possible interactions in chloride medium are verified before the electrolytic method is proposed for wastewater treatment.

Graphite, platinum, dimensional stable electrode (DSA), stainless steel (SS) and air diffusion electrode (ADE) are frequently used as cathodic materials. When graphite or ADE is used as cathode, it is often fed with air or pure oxygen to generate H_2O_2 through the electrochemical reduction of O_2. This process which can be considered as anodic oxidation [217-222] is normally termed as AO-H_2O_2. Use of Na_2SO_4 as the supporting electrolyte is usually preferred because it is; (i) relatively cheap, (ii) could be oxidized into $S_2O_8^{2-}$ which also participates in the degradation of organics and (iii) does not produce hazardous compounds during the process in most cases. Further, the presence of Na_2SO_4 is also reported to promote degradation of organics in many AOPs. [202].

In the study reported in this Chapter electrolytic oxidation is investigated as a potential method for the removal of small quantities of chemical pollutants from water with special reference to the characteristics of the electrodes and electrolytes. Indigo Carmine (IC) which is used as the test pollutant in the earlier Chapter is used in this case as well.

4.2 Materials & Methods

4.2.1 Materials

The Indigo Carmine dye used in the study was the same as in Chapter 3, i.e., AnalaR grade (99%) from Sigma-Aldrich (India). Synthetic wastewater containing IC of desired concentrations was prepared by dissolving the dye in double distilled water. Other materials

such as zinc oxide (99.9%), H_2O_2, persulphate, various salts etc. are the same as described in Chapter 3. All other materials/chemicals used were of AnalaR grade or equivalent, unless indicated otherwise.

4.2.2 Electrodes used

The following electrodes used in the study were purchased from Titanium Tantalum Products limited Chennai, India:

- Ti Cathode – 50 × 25 ×1 (mm)
- Nb Cathode - 50 × 25 × 1 (mm)
- MMO/Ti-50×25×1(mm), MMO coating of 6μ thickness, MMO: Mixed metal oxide
- Pt/Ti-50 × 25 × 1 (mm), Pt plating of 3μ thickness
- Pt/Nb-50 × 25×1 (mm), Nb plating of 3μ thickness
- Further, the following electrodes were from in-house:
- Graphite rod (made by separating the electrode from a used dry cell)
- Bismuth oxide doped titanium dioxide, coated on titanium plate ($BiO_2/TiO_2/Ti$) which was used as the anode and Stainless steel plate (SS) which was used as the cathode are gifted by the Inter University Instrumentation Centre, Mahatma Gandhi University, Kottayam, India.

4.2.3 Electrolysis Experiments

The experimental setup is shown in figure 4.1. Two single compartment electrolytic cells are used in parallel. The anode and the cathode were immersed vertically in an aqueous solution of the target IC pollutant mixed with 0.05M NaCl or Na_2SO_4 as the case may be. The height of the electrodes dipped in the solution is 3.5 cm with an inter-electrode distance of 4.0 cm, unless indicated otherwise. A constant cell current (3.4V) was applied to the electrodes with a DC power supply.

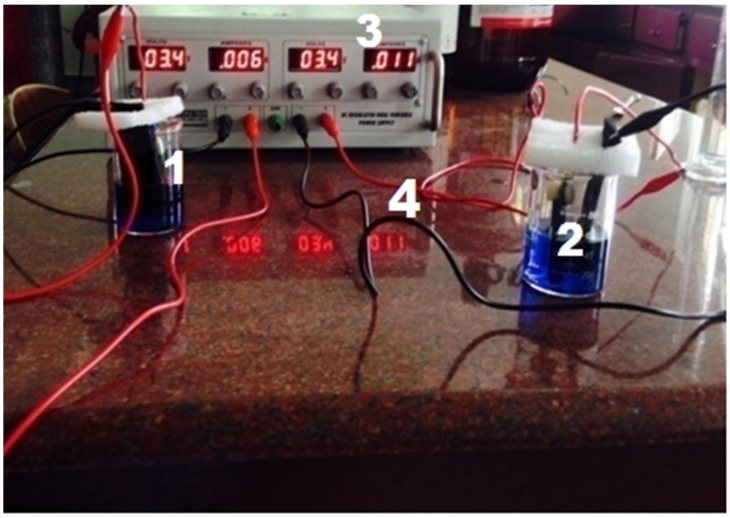

Fig. 4.1: Electrolytic experimental set up
1,2: Electrolytic cells, 3: Power supply unit,
4: Anode (red) and Cathode (black)

The samples were drawn periodically during the electrolytic process, filtered if needed and are analyzed for IC remaining in the system using UV/Vis spectrophotometry at a wavelength of 609 nm. The reaction intermediates were identified by using LC-MS (Q-TOF)

instrument (Waters Xevo G2 Q-TOF). Open reflux method is used to determine the COD of the samples [132].

4.3 Results and Discussion

Preliminary studies were made on the electrolytic oxidation of IC in water using different anode/cathode/electrolyte system. These include $BiO_2/TiO_2/Ti$, MMO/Ti, Pt/Ti or Pt/Nb as anode and SS, graphite, Ti or Nb as cathode. NaCl or Na_2SO_4 was used as the electrolyte. The anodes, cathodes and electrolytes were used in different permutations and combinations. Most of the systems, except those listed in Table 4.1 were not efficient for the decolorization/degradation of IC and were hence not investigated further.

Table 4.1: Preliminary results on potential electrolytic systems for the degradation of IC [IC]: $1x10^{-4}$M, [Electrolyte]: $5x10^{-2}$M

Anode	Cathode	Electrolyte	Preliminary electrolysis data
$BiO_2/TiO_2/Ti$	SS	NaCl	Decolorization in 10min
$BiO_2/TiO_2/Ti$	Graphite	NaCl	Decolorizationin 10 min
$BiO_2/TiO_2/Ti$	Graphite	Na_2SO_4	Decolorizationin 90 min
MMO/Ti	Graphite	Na_2SO_4	Decolorizationin 120 min
Pt/Ti	Graphite	NaCl	Decolorizationin 10 min
Pt/Ti	Graphite	Na_2SO_4	Decolorizationin 90 min

Based on the above data, the electrode-electrolyte system i.e., $BiO_2/TiO_2/Ti/SS/NaCl$, $BiO_2/TiO_2/Ti/graphite/NaCl$ and BiO_2-$TiO_2/Ti/$ $Graphite/Na_2SO_4$ were selected for further investigation on the electrochemical degradation of IC. The efficiency of the system is determined from the time taken for the decolorization and total

mineralization of the dye. The system with Pt/Ti anode, though efficient, is not investigated further, since it is relatively more expensive.

4.3.1 Electrolytic degradation of Indigo Carmine using $BiO_2/TiO_2/Ti$ anode and stainless steel (SS) cathode with NaCl as supporting electrolyte ($BiO_2/TiO_2/Ti/SS/NaCl$)

The degradation/decolorization of IC is tested using 50mL of 1×10^{-4}M solution of the dye. The supporting electrolyte (NaCl) concentration was 0.05 M. Potential applied was 3.4V. The length of the electrode dipped in the solution was 3.5cm. Complete decolorization is obtained in 10 minutes as confirmed by UV/Vis spectrophotometry. Figure 4.2 shows the complete disappearance of the absorbance at 609 nm (which corresponds to IC) after 10 minutes of electrolysis.

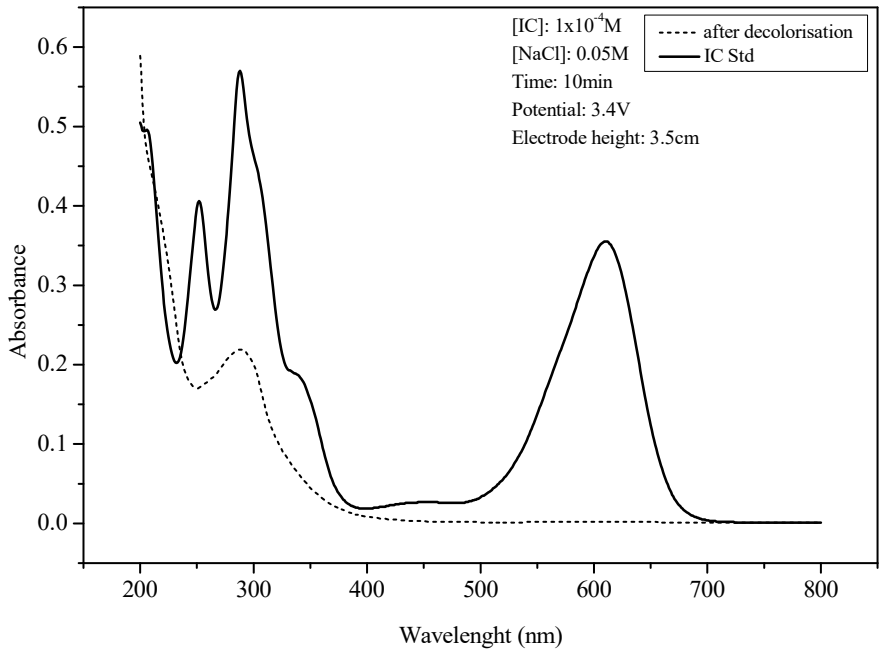

Fig. 4.2: UV/Vis spectrum of IC: before and after decolorization [$BiO_2/TiO_2/Ti/SS/NaCl$]

The effect of various reaction parameters on the efficiency of the system is evaluated as follows:

4.3.1.1 Effect of pH on the degradation of IC

The effect of variation of initial pH on the time taken for decolorization of IC during electrolytic oxidation is shown in figure 4.3. The decolorization is faster in extreme acidic medium (pH~2-3), probably because at low pH, the chlorine resulting from the Cl^- ions present in the solution forms hypochlorous acid, which has higher oxidation potential (1.63V) than hypochlorite (0.89V) [223]. Under comparable pH conditions and reaction times, the decolorization is very small and even negligible in the absence of electrolysis, as shown in the inset of the figure.

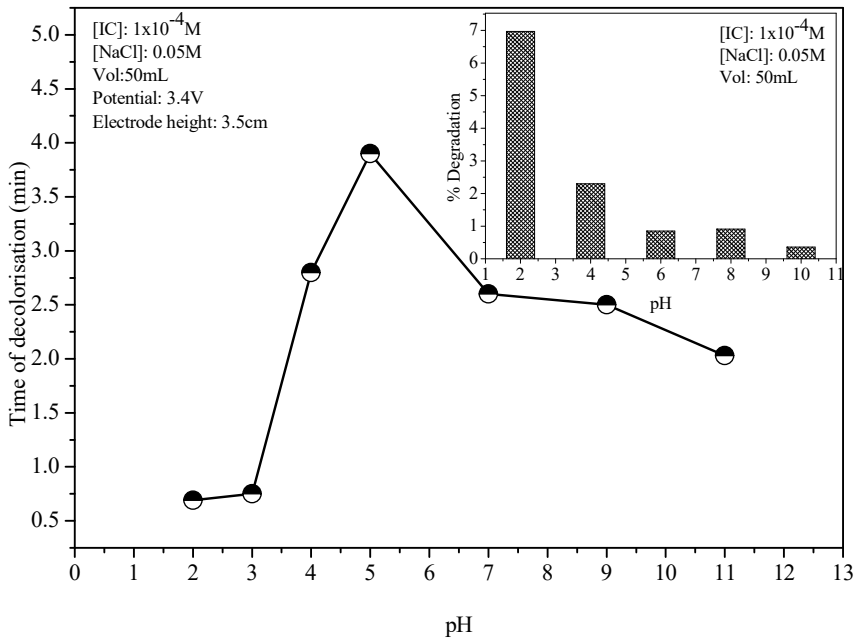

Fig. 4.3: Effect of pH on the electrochemical degradation of IC [BiO_2/TiO_2/Ti/SS/NaCl]

[Inset]: Degradation of IC at different pH without electrolysis

The reactions leading to the formation of HClO are;

$$\text{Anode: } 2Cl^- \rightarrow Cl_2+2e^- \quad .....(4.2)$$

$$\text{Cathode: } 2H_2O+2e^- \rightarrow H_2+2OH^- \quad .....(4.3)$$

In the bulk solution, Cl_2 hydrolysis takes place as follows:-

$$Cl_2+H_2O \rightarrow HClO+H^++Cl^- \quad .....(4.4)$$

Under alkaline medium, deprotonation of the HClO as well as the interaction with the OH^- ions provides hypochlorite (ClO^-) as follows:

$$HClO \leftrightarrow H^++ClO^- \quad .....(4.5)$$

$$HClO + {}^-OH \rightarrow ClO^- + H_2O \quad .....(4.6)$$

At the anode O_2 evolution competes with Cl_2 evolution according to the equation,

$$H_2O \rightarrow 2H^++½O_2+2e^- \quad .....(4.7)$$

Acidity increases the efficiency of Cl_2 discharge and the rate of dye oxidation. The type and concentration of the active chlorine species present in solution is dependent on its pH [224]. The predominant species at various pH are: Cl_2 (pH<3), HClO (pH: 3-7.5) and ClO^- (pH>7.5). If the Cl^- concentration in solution is decreased, the pH interval for the predominance of the HClO species will extend further towards lower pH. For e.g., at very low [Cl^-] of 0.005 mol L^{-1} at 25°C, the predominance of HClO occurs approximately at pH 1-7.5. However, extreme acidic pH may not be advisable for large scale applications and hence the natural pH of the system (~7.4) at which the degradation rate is still good is chosen for further studies. Moreover faster decolorization reactions do not

guarantee the mineralization of the dye or reduction in toxicity, which is the yardstick for measuring the efficiency of the purification process.

4.3.1.2 Effect of Initial Concentration of IC

The influence of the initial concentration of IC on its decolorization was studied in the range of 2-60 mg/L. The time for decolorization increases with increase in concentration (figure 4.4). The rate of decolorization increases with increase in the concentration and is eventually stabilized or decreases thereafter (inset of figure 4.4). This is consistent with the variable kinetics with concentration, reported for many AOP degradation of organics [187, 225].

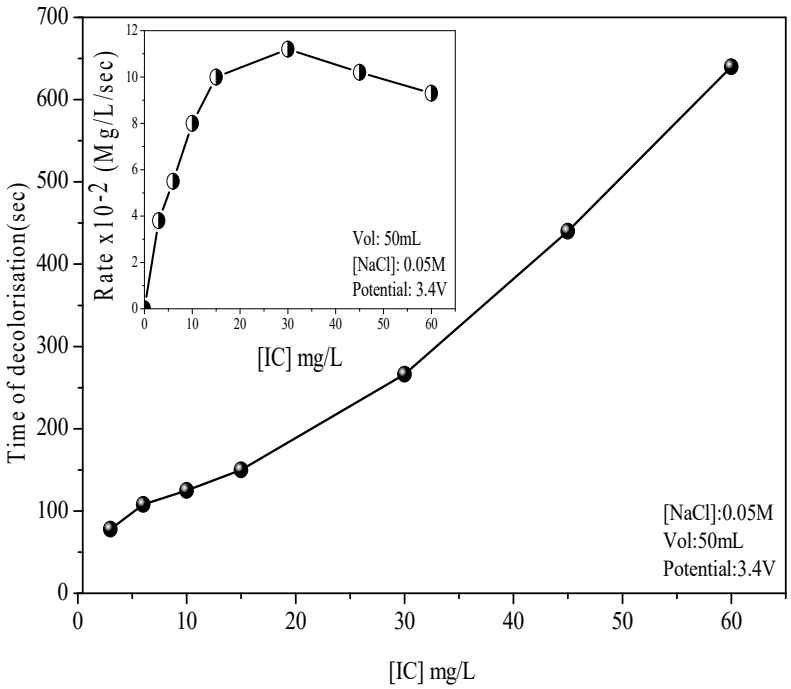

Fig. 4.4: Effect of concentration of IC on its electrolytic degradation [BiO_2/TiO_2/Ti/ SS/NaCl], {Inset: Conc. Vs Rate plot}

With increase in concentration of the dye, there will be more number of interactions with the reactive free radicals and hence increase in the degradation. However at a particular concentration of the dye, the optimum number of molecules which can effectively utilize the reactive oxygen species (ROS) is reached and the rate becomes constant. Above this optimum, increase in concentration will not lead to increased interaction. It is also possible that more and more intermediates are formed in the system especially at higher concentrations of IC and they will be competing with the substrate for the ROS. This will result in gradual decrease in rate of degradation of the parent compound. Also at higher concentration, the dye molecules tend to associate into larger molecules. This lowers the rate of diffusion of the dye to the anode surface with consequent decrease in the removal rate [226].

4.3.1.3 Effect of electrolyte (NaCl) concentration

Figure 4.5 shows the effect of NaCl electrolyte concentration on the rate of dye removal. Increased chloride concentration increases the rate of removal of the dye thereby reducing the time needed for decolorization. This enhancement can be attributed to the increased efficiency of Cl_2 discharge with increase in the concentration of NaCl. At the anode, O_2 evolution competes with Cl_2 evolution as in equation 4.7. As the concentration of NaCl increases, the discharge potential of Cl_2 will be less than that of O_2. Consequently the formation of the oxidant will be more and the decolorization of IC will be faster [227]. However, beyond an optimum concentration of NaCl, the potential applied being constant, the evolution of Cl_2 and O_2 as well as the formation of reactive species will

be stabilized and the decolorization also levels off. At this stage, the decolorization can be enhanced probably by increasing the applied potential which is verified in the subsequent sections.

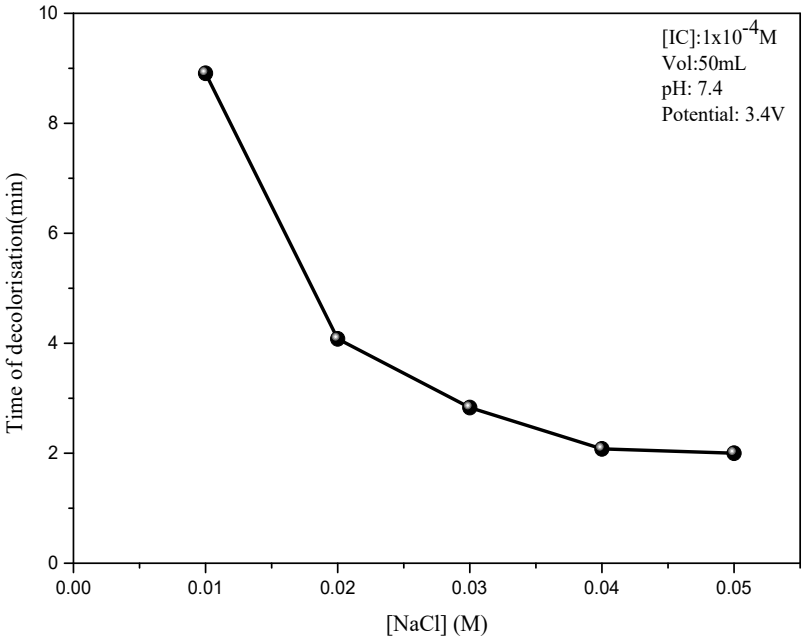

Fig. 4.5: Effect of electrolyte (NaCl) concentration on the decolorization of IC [$BiO_2/TiO_2/Ti/SS/NaCl$]

4.3.1.4 Effect of potential on the degradation of IC

The effect of applied potentials (1.0-3.4V) on the electrochemical degradation of IC is verified. The results presented in figure 4.6 show that the efficiency increases with increase in potential, as reflected in decrease in the time taken for complete decolorization, and reaches an optimum at potential of 3.0 V. This can be attributed to increase in the evolution of Cl_2 and consequently of HClO generation resulting in increased degradation

of IC. This also implies that with increase in the area of the electrodes immersed in the electrolyte, the generation of reactive species will also be increasing leading to increasing interaction with the dye and decrease in the time taken for decolorization. This is illustrated in the following section.

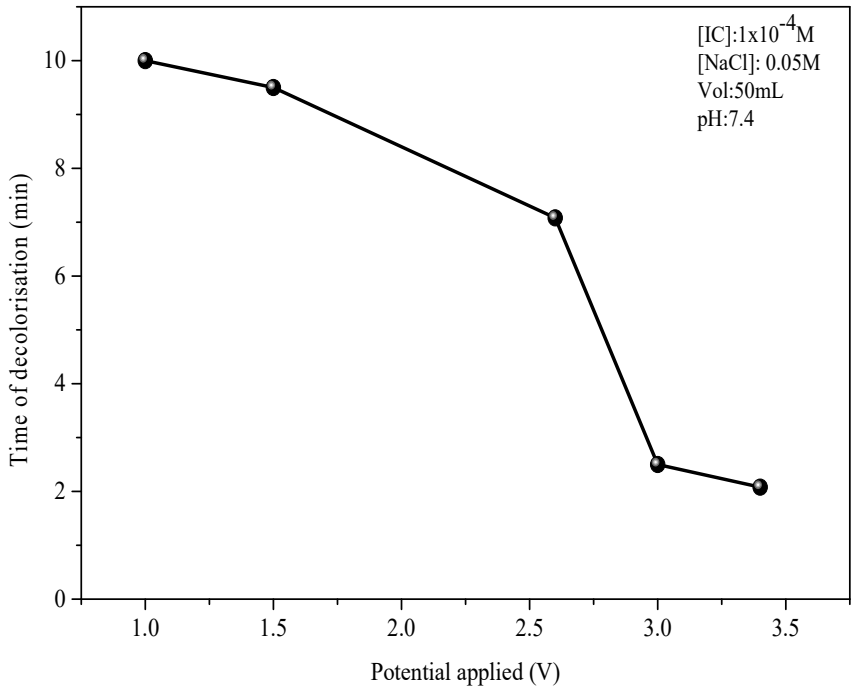

Fig. 4.6: Effect of applied potential on the electrolytic degradation of IC [BiO_2/TiO_2/Ti/SS /NaCl]

4.3.1.5 Effect of area/length of electrode immersed in the electrolyte

As the area of electrode immersed in the electrolyte is increased (by increasing the height of the electrode dipped in the solution), the time required for decolorization of IC decreases (figure 4.7). With increase in

the exposed area of the electrode more number of reactive Cl_2 and HOCl ions are generated in the solution leading to faster decolorization of IC.

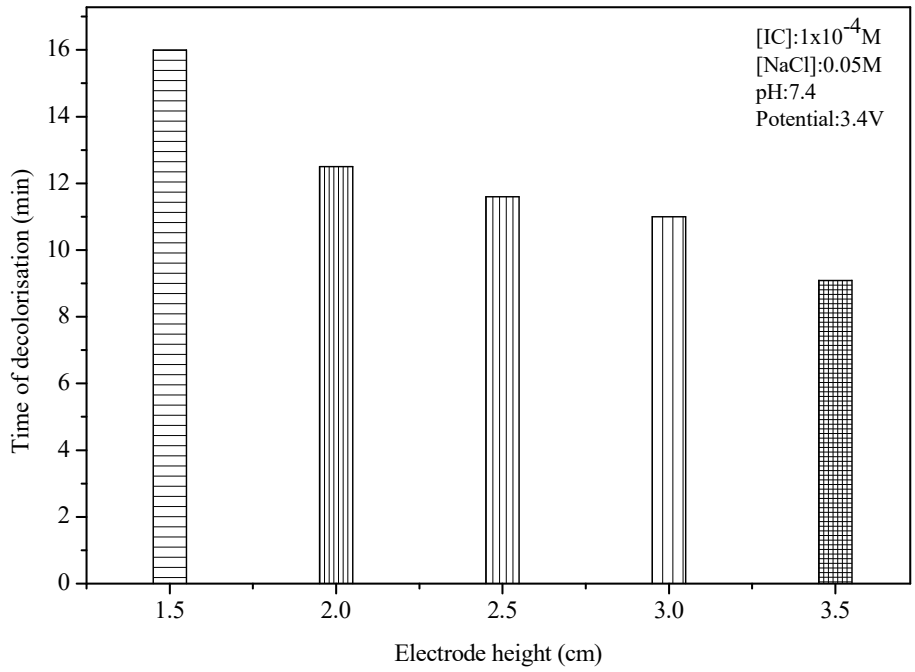

Fig. 4.7: Effect of electrode length immersed in the electrolyte on the electrolytic degradation of IC [$BiO_2/TiO_2/Ti/SS/NaCl$]

4.3.1.6 Effect of inter-electrode distance

Another parameter which determines the efficiency of electrolytic process is the distance between the electrodes, i.e., inter electrode distance. In this context, the effect of inter electrode distance on the efficiency of degradation of IC is verified. The results are shown in figure 4.8.

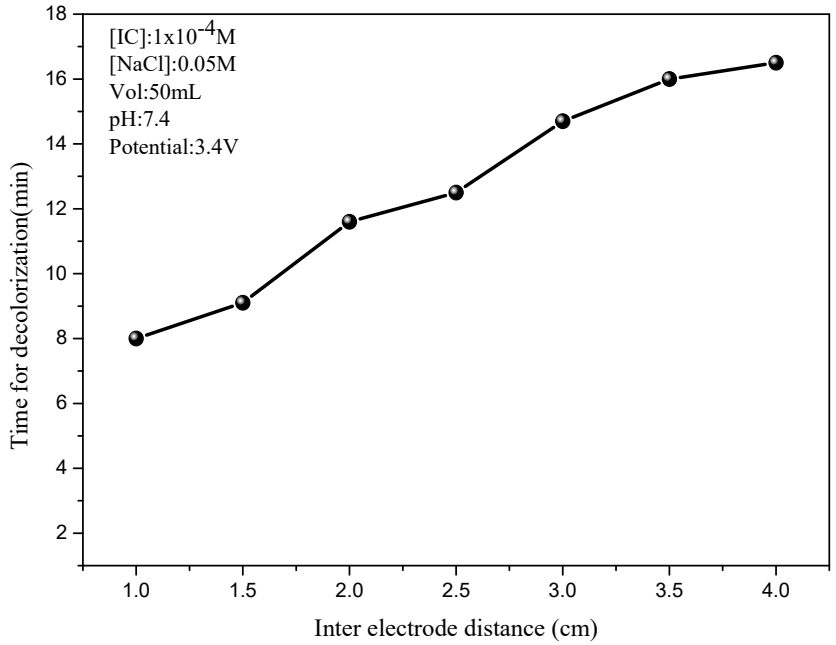

Fig. 4.8: Effect of inter electrode distance on the electrolytic degradation of IC [$BiO_2/TiO_2/Ti/SS/NaCl$]

Color removal efficiency is enhanced by reducing the distance between cathode and anode. This can be explained based on the increase of electrical current with decreasing the inter-electrode distance and consequent increase in the frequency of collisions of the ions. Decrease of the space between anode and cathode leads to low resistance of the electrolyte which also in turn results in increased generation of reactive species and consequently increase in the reaction rate. In this study, the inter electrode distance is optimized at 1.0 cm.

4.3.1.7 Effect of the type of electrode system used

The effect of number of electrodes on the efficiency of the electrolytic degradation of IC is tested by comparing the results using 'three electrode'

and 'two electrode' systems. 'Two electrode' system was the same as discussed earlier, i.e., ($BiO_2/TiO_2/Ti/SS/NaCl$). In three electrode system, additionally a graphite electrode is also used. In two electrode system, the decolorization occurred in 10 minutes, while in the three electrode system, the degradation occurred much faster in 2 minutes. This suggested the potential of enhancing the efficiency of electrolytic oxidation by increasing the number of electrodes. However in the present study, two electrode system with moderate rate of decolorization was preferred for evaluating the effects of various parameters on the efficiency of the process, since the 'three electrode' system with faster decolorization was not amenable to precise measurements with consistently reproducible data. However this indicated the viability of using multiple electrode system for the efficient purification of water contaminated with multiple recalcitrant pollutants.

4.3.1.8 Effect of anions/salts

The wastewater from the dyeing process in textile industry will contain considerable amount of salts/anions naturally as well as from the chemicals used in various stages. They may also affect the efficiency of the electrolytic degradation of the dye in water. Hence, the effect of few individually added salts on the electrochemical degradation of IC is evaluated under the conditions standardized earlier. The results are plotted in figure 4.9. Sulfate, phosphate, carbonate, bicarbonate and nitrate anions are found to enhance the degradation. The enhancement is in the order:

$$CO_3^{2-} > HCO_3^- \approx PO_4^{3-} > NO_3^- \approx SO_4^{2-} \qquad .....(4.8)$$

The enhancement of AOP degradation of organic pollutants in water by anions is explained based on the efficient and sustained

formation of respective radical anions which do not get deactivated by recombination as in the case of ·OH radicals [216, 228-230].

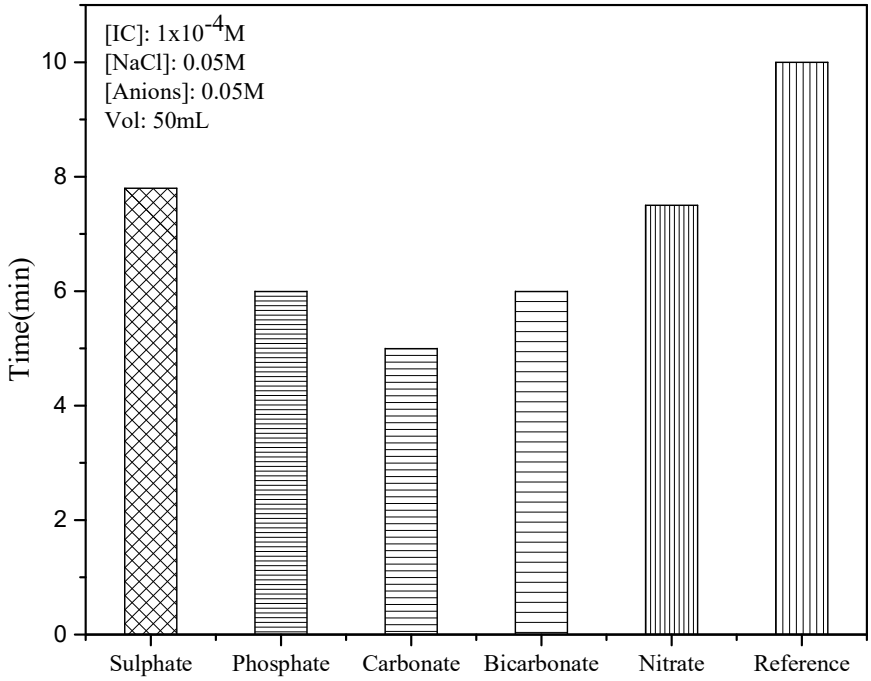

Fig. 4.9: Effect of anions on the electrolytic degradation of IC [$BiO_2/TiO_2/Ti/SS/NaCl$]

The anions are known to get oxidized at the anode surface followed by formation of radical anion species. Such species can continue to produce stable oxidants. Various possible reactions taking place in the case of typical anions are:

$$SO_4^{2-} \rightarrow SO_4^{-\cdot} + e^- \quad .....(4.9)$$

$$PO_4^{3-} \rightarrow PO_4^{2-\cdot} + e^- \quad ....(4.10)$$

$$CO_3^{2-} \rightarrow CO_3^{-\cdot} + e^- \quad ....(4.11)$$

$$NO_3^- \rightarrow NO_3^{\cdot} + e^- \quad ....(4.12)$$

These radicals can combine forming stable peroxide salt oxidants as follows:

$$SO_4^{-\bullet} + SO_4^{-\bullet} \rightarrow S_2O_8^{2-} \quad ....(4.13)$$

$$PO_4^{2-\bullet} + PO_4^{2-\bullet} \rightarrow P_2O_8^{4-} \quad ....(4.14)$$

$$CO_3^{-\bullet} + CO_3^{\bullet} \rightarrow C_2O_6^{2-} \quad ....(4.15)$$

$$NO_3^{\bullet} + NO_3^{\bullet} \rightarrow N_2O_6 \quad ....(4.16)$$

The oxidants can also interact with the $^{\bullet}OH$ radicals present in the system forming other radicals and anions as follows:

$$SO_4^{-\bullet} + {}^{\bullet}OH \rightarrow HSO_5^{-} \quad ....(4.17)$$

$$PO_4^{2-\bullet} + {}^{\bullet}OH \rightarrow HPO_5^{2-} \quad ....(4.18)$$

$$CO_3^{-\bullet} + {}^{\bullet}OH \rightarrow HCO_4^{-} \quad ....(4.19)$$

$$Cl^{-} + {}^{\bullet}OH \rightarrow Cl^{\bullet} + OH^{-} \quad ....(4.20)$$

$$Cl^{\bullet} + Cl^{-} \rightarrow Cl_2^{-\bullet} \quad ....(4.21)$$

Thus many new types of oxidants/radicals are formed which can influence the degradation of IC.

The $^{\bullet}OH$ is also formed from water electrolytically as:

$$H_2O \rightarrow {}^{\bullet}OH + H^{+} + e^{-} \quad ....(4.22)$$

However, photoluminescence study [231-233] does not reveal consistent increase in the concentration of $^{\bullet}OH$, probably due to the recombination/interaction of $^{\bullet}OH$ to generate H_2O_2 or $HO_2^{\bullet}$,

$$^{\bullet}OH + {}^{\bullet}OH \rightarrow H_2O_2 \quad ....(4.23)$$

$$^{\bullet}OH + H_2O_2 \rightarrow HO_2^{\bullet} + H_2O \quad ....(4.24)$$

It is also possible that the effect of anions may be due to the change in the pH of the solution in their presence. Hence the pH of the reaction medium in presence of the anions is measured. It is observed that the pH remains practically unaffected by the anions except in the presence of PO_4^{3-}, CO_3^{2-} and HCO_3^- where the pH varies in the range 5.5-8.5. The pH effect on the decolorization of IC in this range is the same as at the natural pH of IC solution in the absence of anions (7.4) (see inset of figure 4.3). Hence change in pH is not the cause of the anion effect at least at the concentration studied here.

4.3.1.9 Chemical Oxygen Demand/Mineralization

The efficiency of any AOP as a decontamination tool depends on its ability to mineralize the pollutants to harmless products such as CO_2, H_2O, and salts, which is verified by the elimination of chemical oxygen demand (COD). In the current study also, the COD of the electrochemical system $BiO_2/TiO_2/Ti/SS/NaCl$ is measured immediately after decolorization (10 min.) and after extended time (300 min.) of electrolysis. The COD remains unchanged even after 300 min. (see Section 4.3.2, Fig. 4.10). This suggests that electrolysis of the system leads to degradation/ decolorization of IC to stable colorless compounds which cannot be degraded further. In this context, the reaction intermediates in the system after decolorization are analyzed by LC-MS. The identified intermediates are listed in table 4.2. Some of the intermediates are chloro compounds which are relatively more stable and mineralize only slowly. The faster decolorization can be attributed to the transformation of IC into various chloro-compounds. However, same chloro compounds make mineralization slower. The source of chlorine is the electrolyte NaCl.

Table 4.2: Major intermediates formed during electrochemical degradation of IC under BiO_2-TiO_2/Stainless steel/NaCl

Mol.weight	Molecular formula	Molecular structure
163	$C_8H_5NO_3$	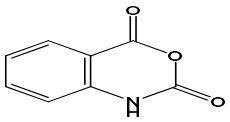
371	$C_{16}H_7N_2O_7S$	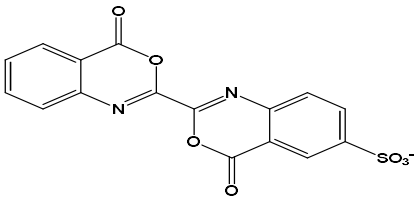
454	$C_{16}H_{10}N_2S_2O_{10}$	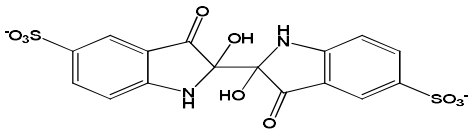
198	$C_7H_4NSO_4$	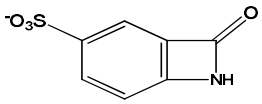
226	$C_8H_4NSO_5$	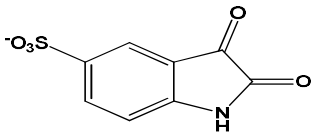
454	$C_{16}H_{10}N_2S_2O_{10}$	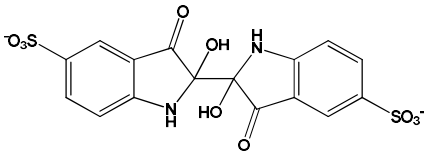
523	$C_{16}H_8Cl_2N_2S_2O_{10}$	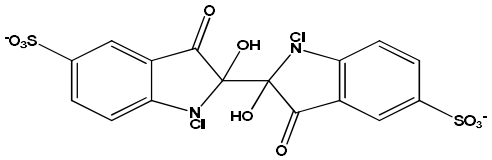
472	$C_{16}H_9N_2ClS_2O_9$	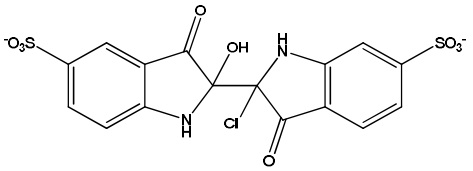

Thus it is clear that the electrolysis system $BiO_2/TiO_2/Ti/SS/NaCl$, which is highly efficient for the decolorization of IC, is not appropriate for its mineralization and hence for the purification of water.

The data in Table 4.1 shows that replacement of SS by graphite as the cathode gives same efficiency for decolorization of IC. Hence, $BiO_2/TiO_2/Ti/graphite/NaCl$ system is tested for mineralization efficiency. In this case also, the COD remains unchanged even after 300 min. of electrolysis thereby indicating that the system with NaCl as the electrolyte is not suitable for the mineralization of IC. In this context, another electrolyte Na_2SO_4 is used in place of NaCl and the experiments are repeated using the electrode system $BiO_2/TiO_2/Ti$ and SS. The color of the dye remains unchanged even after 480 min. of electrolysis indicating that this system is not suitable for the degradation/decolorization of IC. When the cathode SS is replaced by graphite rod ($BiO_2/TiO_2/Ti/graphite/Na_2SO_4$) the decolorization does take place and is complete in 90 minutes. More electrolytes other than NaCl, i.e. Na_2CO_3, $NaHCO_3$, and Na_3PO_4 were also tested with the same electrode combination ($BiO_2/TiO_2/Ti/$ graphite). Of these, Na_2CO_3 has almost same efficiency for decolorization (90 min.) as Na_2SO_4 while the other two electrolytes do not favor decolorization. Based on these observations, Na_2SO_4 is chosen as the convenient and safer electrolyte with $BiO_2/TiO_2/Ti/graphite$ electrode system for further studies.

4.3.2 Studies with Na_2SO_4 as electrolyte

The efficiency of electrolytic decolorization of IC in the $BiO_2/TiO_2/Ti/graphite/Na_2SO_4$ system is not affected by varying the concentration of SO_4^{2-} in the range of 0.25 to 0.60g/L, as is observed experimentally. In this case also, the degradation is more in the acidic pH with maximum in the range 2-4. Similarly, the decolorization is enhanced with increase in the area of the electrode exposed to the electrolyte and with decrease in the inter-electrode distance. Thus the optimized parameters for the decolorization of IC in the $BiO_2/TiO_2/Ti/graphite/Na_2SO_4$ system are: $[Na_2SO_4]$ = 0.05M, pH = 2-4, area of the graphite electrode dipped in the electrolyte: 7.2 cm^2, inter electrode distance: 1.0 cm.

Various intermediates formed during the electrolysis in this case as analyzed by LC-MS are listed in Table 4.3.

There are no chloro-compounds and hence the mineralization is expected to be faster. The COD measurements show ~77% decrease in 5 hr. and complete mineralization in 10 hour of electrolysis. In the case of NaCl electrolyte under identical conditions, the COD decreases by ~23% only in 10 hr. (figure 4.10).

Table 4.3: Intermediates formed during electrochemical degradation of IC in Na_2SO_4 electrolyte

Mol. weight	Molecular formula	Molecular structure
90	$C_2H_2O_4$	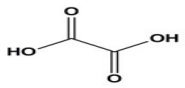
172	$C_6H_6SO_3N$	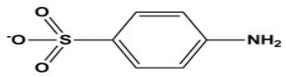
202	$C_6O_5H_4SN$	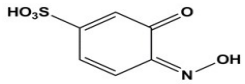
153	$C_7H_7O_3N$	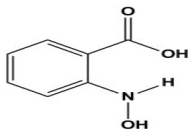
428	$C_{15}H_{12}N_2S_2O_9$	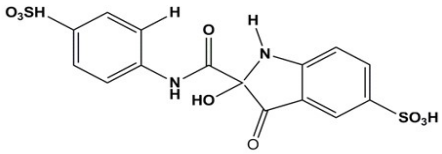
420	$C_{16}H_8N_2S_2O_8$	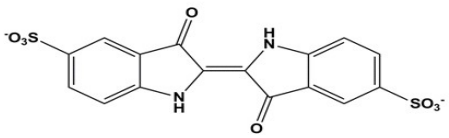
422	$C_{16}H_{10}N_2S_2O_8$	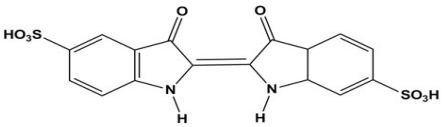
188	$C_6H_6SNO_4$	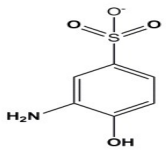
116	$C_4H_4O_4$	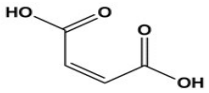

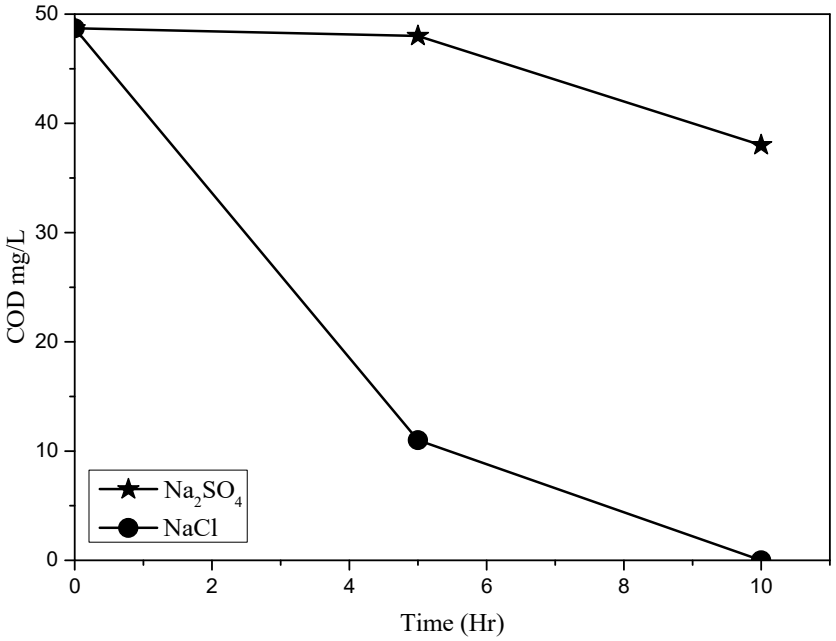

Fig. 4.10: Comparison of NaCl and Na_2SO_4 as electrolytes for the mineralization of IC
[IC] = 1×10^{-4}M, [Electrolyte] = 5×10^{-2}M,
Anode: $BiO_2/TiO_2/Ti$, Cathode: Graphite

The possibility of exploiting the superior decolorization efficiency of NaCl and mineralization efficiency of Na_2SO_4 by using their combination (1:1) as electrolyte is examined experimentally. The COD values at two different time periods of electrolysis, i.e. 5 and 10 hr. are determined and compared with those in electrolytic systems with different electrolyte-electrode combinations. The results are presented in Table 4.4.

Table 4.4: Mineralization efficiency of various systems in Cl^- and SO_4^{2-} electrolytes
[IC] = 1×10^{-4}M, [NaCl] = 0.05M. [Na_2SO_4] = 0.05M, Anode: $BiO_2/TiO_2/Ti$

Cathode	Electrolyte	Initial COD before electrolysis (mg/L)	COD after 5 hr. electrolysis (mg/L)	COD after 10 hr. electrolysis (mg/L)
SS	NaCl	48.7	48.3	37.1
Graphite	NaCl	48.7	48.0	37.3
Graphite	Na_2SO_4	48.7	11.5	0.5 (~ 0)
Graphite	NaCl/Na_2SO_4 (1:1)	48.7	32.5	11.8

The mineralization efficiency in Na_2SO_4 electrolyte (cathode: graphite) is reduced in the presence of Cl^- and the efficiency of the combination is in between that in presence of Na_2SO_4 and NaCl as electrolyte individually (~23% COD decrease in the case of NaCl, ~ 100% COD removal in the case of Na_2SO_4 and ~76% COD decrease in the case of NaCl+Na_2SO_4 combination in 10 hr. electrolysis). The degradation of IC and its mineralization are facilitated by insitu formed (during the electrolysis in Na_2SO_4 electrolyte) $SO_4^{-\bullet}$ radical anions which are very strong oxidants (oxidation potential: 2.5-3.1V) and can facilitate the breakdown of organics by attacking the C-C bond [234]. Unlike in the case of $Cl^\bullet$, the $SO_4^{-\bullet}$ does not give rise to any recalcitrant 'difficult to mineralize' intermediates such as chloro-compounds and this is favorable for the mineralization.

The study clearly shows that $BiO_2/TiO_2/Ti$ /graphite/Na_2SO_4 is a promising electrochemical system for the decontamination of water from IC pollutant.

4.4 Conclusion

Electrochemical Advanced Oxidation Processes (EAOP) with suitably designed and optimized electrode/electrolyte systems is successfully used for the decontamination of water from the dye pollutant Indigo Carmine. The method is based on the electrochemical generation of highly reactive $^{\cdot}OH$ and other radicals in solution which interact with the pollutants and oxidize them irreversibly. Of the different combinations of electrodes and electrolytes tested, the most efficient system consists of $BiO_2/TiO_2/Ti$ anode, Graphite cathode and Na_2SO_4 electrolyte. NaCl as the electrolyte makes the system extremely efficient for the decolorization of the dye, due to the faster formation of various Cl based oxidants. However, these oxidants transform the pollutants into more recalcitrant chloro-compounds thereby making the mineralization difficult and slower. Various intermediates formed during the process are identified by LC-MS. The effect of various reaction parameters on the efficiency of the decolorization/mineralization process is evaluated experimentally and relevant parameters are optimized.

.....ꕥ.....

Chapter

5

ULTRASOUND AS THE SOURCE OF ACTIVATION IN AOPs FOR THE DECONTAMINATION OF WATER FROM INDIGO CARMINE DYE POLLUTANT

Contents

5.1 Introduction

As already discussed in previous Chapters, Advanced Oxidation Processes (AOPs) have high potential for the decontamination of water from chemical and bacterial pollutants. This methodology is based on the insitu production of highly oxidizing hydroxyl radicals (·OH), which can react nonselectively with most of the organic compounds. The commonly used AOPs include photolysis/photocatalysis, UV/H_2O_2, Fenton treatment, photoFenton, sonolysis, sonocatalysis etc. [235-240]. Among these, sonolysis is one of the most versatile techniques which is widely investigated for wastewater treatment due to the advantages of safety, cleanliness and energy efficiency. Several reports are available on the sonolytic degradation of chlorinated organic compounds, phenolic compounds, organic dyes, pesticides, endocrine disrupting compounds, perfluorinated chemicals, pharmaceuticals and microcystins [241-243].

Three types of reactions involved in sonolysis are pyrolysis, reaction of $^{\bullet}OH$ and $^{\bullet}H$ and supercritical water oxidation [244-246]. Ultrasound can produce ·OH and H· by acoustic cavitation (reaction 5.1). Generally hydrophobic and volatile compounds undergo degradation via pyrolysis in the interface region. Supercritical water oxidation process provides an additional route for the degradation. The radical generation in sonolysis is shown in reactions (5.1) - (5.5) [247-249].

$$H_2O +))) \rightarrow {}^{\bullet}H + {}^{\bullet}OH \quad .....(5.1)$$

$$^{\bullet}H + O_2 \rightarrow HO^{\bullet}_2 \rightarrow {}^{\bullet}OH + \tfrac{1}{2} O_2 \quad .....(5.2)$$

$$2{}^{\bullet}OH \rightarrow H_2O_2 \quad .....(5.3)$$

$$2HO^{\bullet}_2 \rightarrow H_2O_2 + O_2 \quad .....(5.4)$$

$$^{\bullet}H + H_2O_2 \rightarrow {}^{\bullet}OH + H_2O \quad .....(5.5)$$

The current Chapter presents the results of our study on the application of sonolysis/ sonocatalysis for the degradation and mineralization of Indigo Carmine dye in water. The effect of various operational parameters such as frequency of US, power density, pH, presence of various additives such as Fe^{2+}, H_2O_2, $S_2O_8^{2-}$ and anions/salts on the efficiency of degradation is investigated in detail and the results are discussed.

5.2 Materials and Methods

5.2.1 Materials

Various chemicals used in this study, i.e. IC, ZnO, H_2O_2 (30.0% w/v) and $K_2S_2O_8$ (PS), are the same as in previous Chapters and are used as such without further purification. Various other chemicals used were also of AnalaR grade or equivalent, unless indicated otherwise.

5.2.2 Sonolysis

Sonication of the reaction system was carried out in a jacketed glass reactor of 500 mL capacity. Ultrasound (US) of different frequencies was generated using an L3 ELAC Nautic ultrasound generator powered by an allied signal R/F generator (T & C power conversion, model AG1006). The variable frequencies used were 200, 350, 620, and 1000 kHz. The power applied varied from 20 to 80W. The temperature was maintained at 25±1°C by circulating cooling water through the jacket from a thermostat. Typical reactor assembly is shown in figure 5.1.

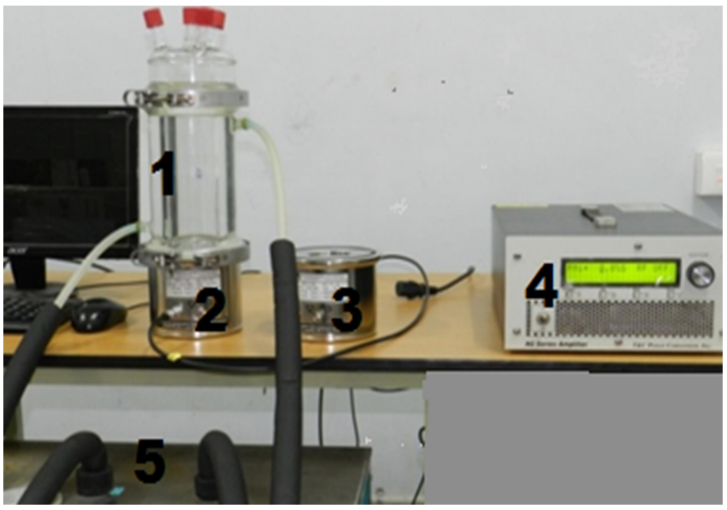

Fig. 5.1: Sonoreaction assembly, 1: Glass reactor, 2, 3: Variable frequency generators, 4: Power supply unit, 5: Thermostat

The disappearance of the dye was followed by using UV/Vis spectrophotometry (609 nm). The intermediates were detected using LC/MS (Waters Xevo G2 Q-TOF). The COD was determined by Open reflux method (as described in Chapter 2).

5.3 Results and Discussion

Preliminary experiments have shown that irradiation by US (sonolysis) is a viable method for the degradation of traces of Indigo Carmine dye pollutant in water. Hence the process and the influence of various reaction parameters on its efficiency are investigated in detail.

5.3.1 Effect of frequency of US

The effect of frequency of US on the degradation of IC is measured by performing experiments at four different frequencies, i.e. 200, 350, 620 and 1000 kHz keeping the power constant (80W). The degradation pattern is given in figure 5.2.

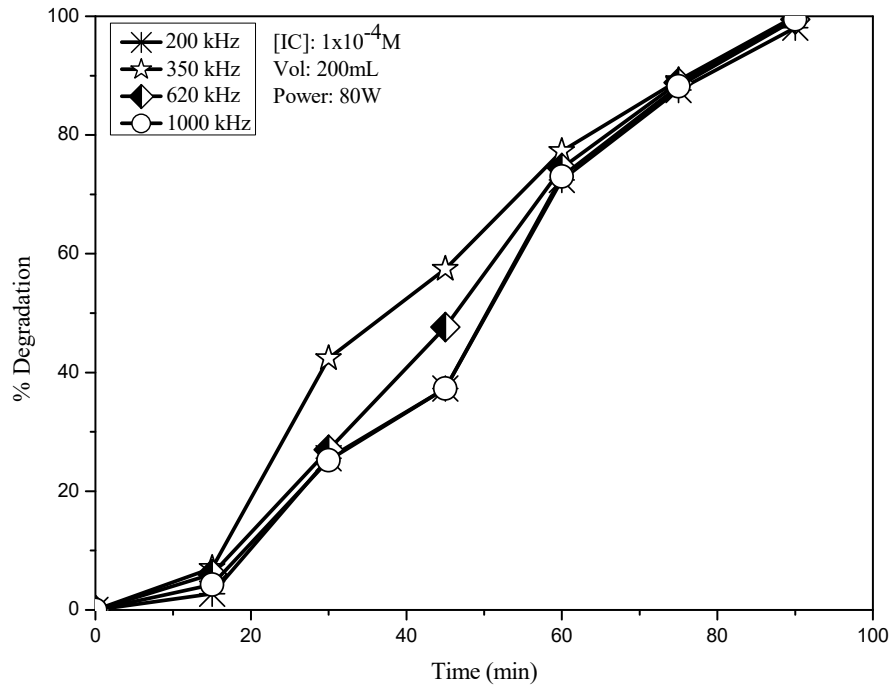

Fig. 5.2: Effect of US frequency on the sonochemical degradation of IC

The rate of degradation does not have any direct correlation with the frequency and is the highest at 350 kHz. The degradation is less at both the lower frequency (200 kHz) and the higher frequency (1000 kHz). Hence simple increase in the frequency does not guarantee increased sonodegradation of the pollutant. A distinct difference in the degradation with change in frequency was observed only during the early stage of sonolysis (upto 60 minutes). Later on, the degradation efficiency was comparable (>80%). The optimum frequency for the degradation of IC is therefore taken as 350 kHz.

The size of the bubble (resonance size), number of bubbles formed, life time of the acoustic bubble in the multibubble field and the intensity of collapse are the important factors in sonolytic degradation which in turn depend on the ultrasonic frequency and power [2501]. The resonant size of the bubbles decreases with increase in the frequency [42], i.e., the size of the bubble will be in the order 200 kHz > 350 kHz > 620 kHz > 1 MHz. At lower frequency, the bubble pulsation occurs slowly and the life time of the cavitating bubble will be more. Thus, chances of recombination of the reactive ·OH in the interface get enhanced. At higher frequency, the size of the cavity is reduced. However the availability of reaction site and the number of cavitational events become higher and consequently more ·OH radicals are generated resulting in faster reaction. The cavitation bubbles become more dispersed and more accessible for the reacting species which also result in enhanced degradation of the substrate [251]. The life time of an acoustic bubble in a multibubble field, which may vary with the applied frequency, is another important factor in

sonolytic degradation of organics. Sunartio et al. [252] reported that the life time of a cavitating bubble increases with decreasing frequency, i.e. in the present case, maximum lifetime is at 200 kHz and the least at 1 MHz. Chowdhuri and Vijayaraghavan [42] compared the sonolytic effects at two different frequencies of 200 and 350 kHz and concluded that the life time of the bubble in the acoustic field is comparable at the two frequencies. However the number of cavitations is higher at 350 kHz thereby generating more hydroxyl radicals. Consequently, degradation of IC is enhanced when frequency is increased from 200 to 350 kHz. But with further increase in the frequency, the relative life time of the bubble becomes lower and therefore the collapse of the bubble will be less violent. This results in decreased formation of $^{\bullet}OH$. This is the likely reason for the lower efficiency of degradation at higher frequencies of 620 and 1000 kHz.

5.3.2 Effect of power

The effect of power of US on the degradation of IC is monitored by varying the power (20W, 40W, 60W and 80W) at a fixed frequency of 350 kHz. The results are shown in figure 5.3. After the initial induction period, efficiency of degradation increases with increase in power, with maximum degradation at 80W. Acoustic intensity dissipated into the solution is directly related to the applied power [253]. At the appropriate power, the bubble growth starts and reaches the resonant size. This is followed by collapse of the bubbles and subsequent formation of $^{\bullet}OH$.

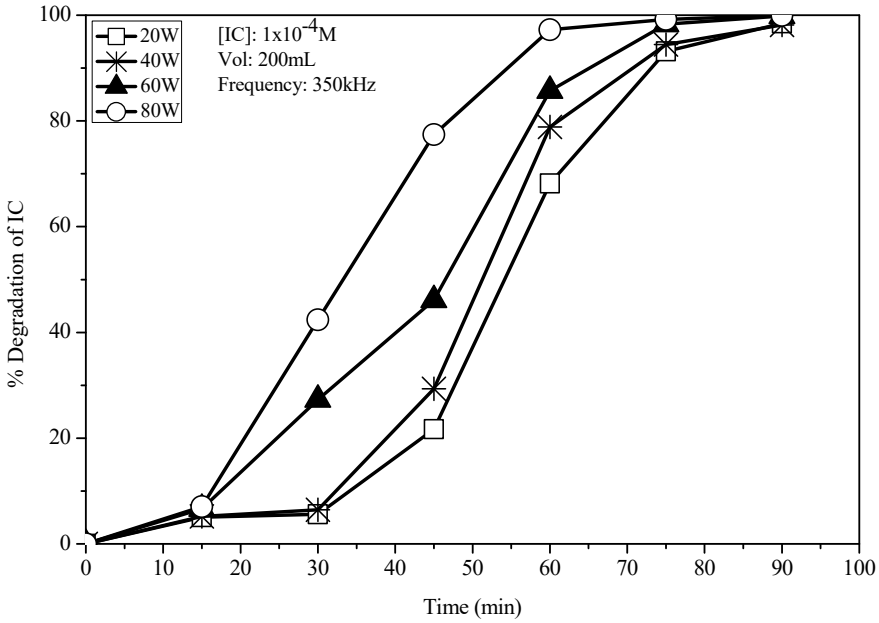

Fig. 5.3: Effect of US power on the sonolytic degradation of IC

The hike in power can also enhance the negative pressure exerted by ultrasound. As a result, the bubble expands more in the rarefaction stage and the cavity reaches the resonance size instantly. Consequently pyrolysis and $^{\bullet}OH$ formation reaction takes place at accelerated rate [254]. In any case, in the current study, the degradation of IC is completed even at the lower power of US and the net time taken for complete degradation is only marginally less at higher power even though the degradation is more dependent on sono power in the early stages of the reaction.

5.3.3 Effect of Concentration of IC

The effect of concentration of IC on its sonochemical degradation is investigated in the range of (0.5-2.0) $\times 10^{-4}$M at the optimized frequency (350 kHz) and power (80W) of US. The percentage degradation decreases

with increase in concentration (figure 5.4). However more appropriate measure of the efficiency is the rate of degradation. The rate of degradation of IC at different concentrations is plotted in the inset of figure 5.4. The rate increases with increase in concentration of IC, reaches an optimum at 1.0×10^{-4}M and decreases thereafter. Accordingly, 1.0×10^{-4}M of IC is chosen as the optimum concentration for further studies.

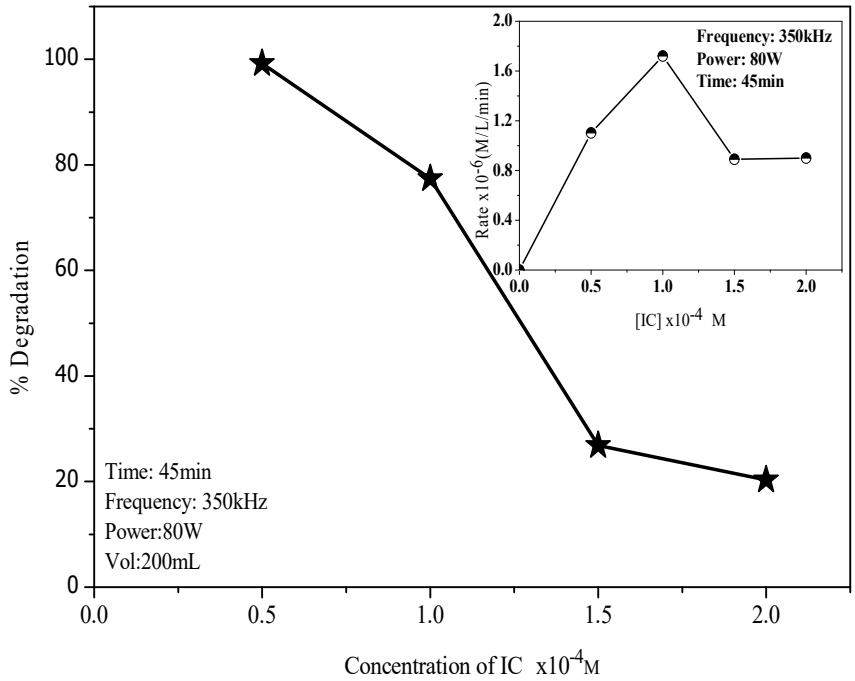

Fig. 5.4: Effect of concentration of IC on its % sonodegradation [Inset]: Rate vs Concentration plot

The degradation of pollutants in water under sonolysis involves their interaction with $^{\bullet}OH$ radicals formed insitu as shown in reactions (5.1) – (5.5). However most of the ·OH will recombine and produce H_2O_2 inside the cavitation bubble and at the gas-liquid interface as shown in

reaction (5.3). H_2O_2 is detected in the present system also. It is also possible that the pollutant molecule inside or in the neighborhood of a disintegrating bubble can get thermally degraded due to the supercritical conditions of high local temperature and pressure [255].

The initial degradation of the dye will be dependent on the relative concentration of dye molecules at the interface of the cavitation bubble and the $^{\bullet}OH$ radicals. IC is a low volatile compound and its relative concentration at the cavitation-bubble interface will be less. Consequently, the sonochemical degradation also will be slower. The rate determining step is the generation of $^{\bullet}OH$ either from water or the deprotonation of insitu formed H_2O_2 or both under sonolysis. At lower dye concentration, the $^{\bullet}OH$ radicals have lesser number of dye molecules to interact with and the rate of degradation is slower. The degradation takes place primarily in the bulk of the solution where the $^{\bullet}OH$ radical concentration is low because only a small part of the radicals generated at the bubble surface can diffuse into the bulk.

With increase in concentration of IC, the frequency of interaction between the substrate and the $^{\bullet}OH$ is more and the rate of degradation increases steadily until the optimum is reached. Beyond the optimum concentration, the rate of $^{\bullet}OH$ radical generation and/or its diffusion into the bulk may not be adequate to interact with correspondingly more of the pollutant molecules and the rate slows down and even decreases. At higher concentration of the dye, the penetration of US into the system and consequently the generation of $^{\bullet}OH$ are inhibited. This also leads to decrease in the degradation. Moreover, as the reaction proceeds, more and

more intermediates are formed which will compete with IC for the $^{\bullet}OH$ radicals resulting in further decrease in the rate. Similarly, the concentration of the dye molecules inside the bubble and the bubble-solution interface also will be relatively less in comparison to its overall concentration. This also results in apparent decrease in the rate of degradation at higher concentration. Hence optimization of the concentration of the dye in water is important for achieving efficient and economical decontamination of the polluted water.

5.3.4 Effect of pH

The pH of the reaction medium is known to have strong influence on all AOPs including US-induced degradation of organic pollutants. Therefore the effect of pH on the sonochemical degradation of IC was studied. The results are shown in figure 5.5. In the absence of US, the effect of pH on the dye is negligible, with mild degradation in the acidic pH. It is observed that the sonodegradation is more efficient in the acidic region than in the alkaline region. At lower pH, the formation of hydrogen peroxide by the recombination of hydroxyl radicals will be less [255]. Therefore, the number of hydroxyl radicals available for the reaction with IC in the liquid region is more. Similarly, the number of reaction sites will increase at this pH due to the increased bubble repulsion caused by the accumulation of hydronium ion in the interface region [256]. This also enhances the degradation at lower pH.

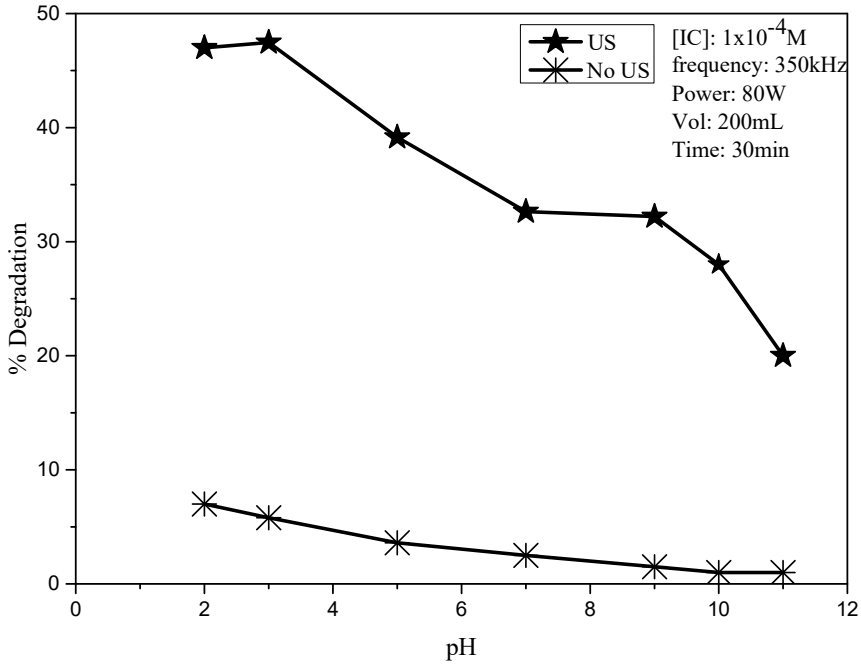

Fig. 5.5: Effect of pH on the sonochemical degradation of IC

5.3.5 Effect of power density

The effect of power density (power/volume) of US on the sonodegradation of IC was studied by taking different volumes of the reaction solution keeping the power applied constant at 80W. By increasing the US power density from 0.16 to 0.8 W/mL (volume decreasing from 500 to 100 mL), the degradation increases steeply initially and slowly thereafter, to level off eventually (figure 5.6). This implies that the relative volume of the reactants and the applied US power have to be optimized in order to achieve efficient sonodegradation.

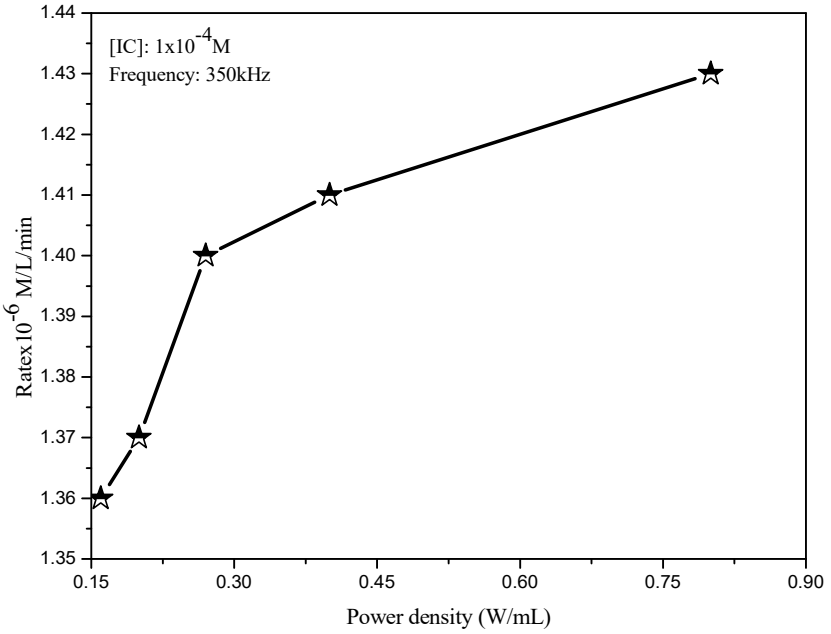

Fig. 5.6: Effect of US power density on the sonodegradation of IC

5.3.6 Formation of H_2O_2

The formation of H_2O_2 during the sonochemical degradation of organics by recombination of insitu formed ·OH has been reported earlier [257]. In the present study also, H_2O_2 is formed in the system and its concentration at different times of sonication is measured after the decolorization. The concentration could not be measured precisely when the system is colored. The results are plotted in figure 5.7. It is seen that even after the decolorization, the concentration of H_2O_2 is increasing showing that formation as well as the recombination of ·OH radicals is continuing. These free radicals interact further with the intermediates formed on decolorization. Eventually, the intermediates also get fully degraded and the system is mineralized completely as is seen in the COD values measured at different times of sonication (Section 5.3.13).

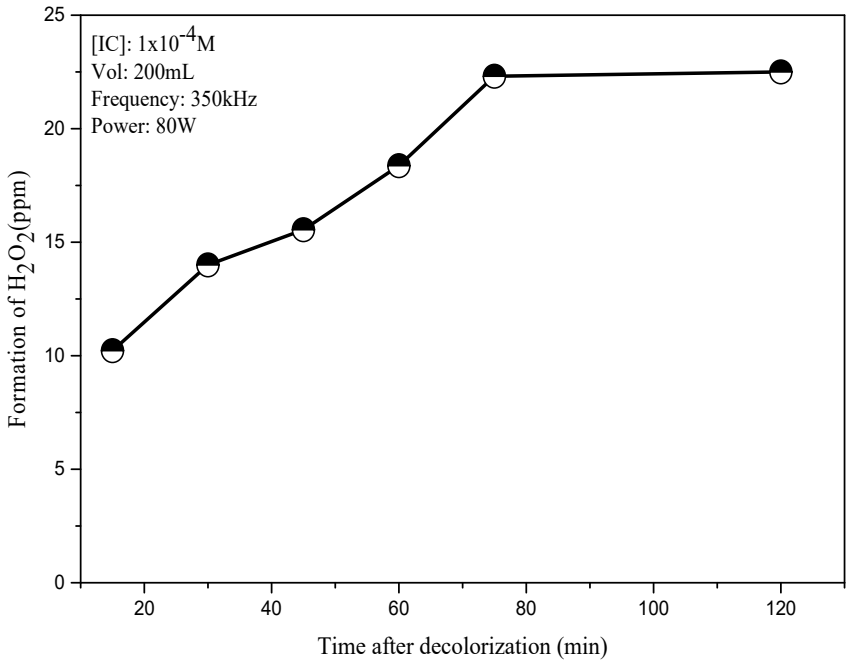

Fig. 5.7: Formation of H_2O_2 during the sonochemical degradation of IC

Under US irradiation, the O_2 present in the solution would be split into reactive $^{\bullet}O$ radicals (reaction 5.6) which interact with H_2O molecules and form reactive $^{\bullet}OH$ and H_2O_2 (reaction 5.7, 5.8). The 'hot spot effect' of US irradiation in water will also enhance the formation of $^{\bullet}OH$ due to the pyrolysis of water molecules as in reaction (5.9). This as well as reaction (5.10) and (5.11) will also result in the formation of more reactive oxygen species (ROS) such as $^{\bullet}OH$, $HO_2\cdot$ and H_2O_2 which will facilitate the degradation and mineralization of the substrate IC (reaction 5.12).

$$O_2 \rightarrow 2\,^{\bullet}O \qquad .....(5.6)$$

$$O + H_2O \rightarrow 2\,^{\bullet}OH \qquad .....(5.7)$$

$$^{\bullet}OH + {}^{\bullet}OH \rightarrow H_2O_2 \qquad .....(5.8)$$

H_2O + >>> → $H^{\bullet}$ + $^{\bullet}OH$ .....(5.9)

$H^{\bullet} + O_2$ → $O + {}^{\bullet}OH$ ....(5.10)

$H^{\bullet} + O_2$ → $HO_2^{\bullet}$ ....(5.11)

IC + ROS ($^{\bullet}OH$, $HO_2^{\bullet}$, H_2O_2 etc.) → → Intermediates → → Mineralization (CO_2, H_2O) ....(5.12)

5.3.7 Effect of hydrogen peroxide

Since H_2O_2, a powerful oxidant, is formed insitu during the sonolytic process, it is quite possible that the rate of degradation of IC is enhanced by its increasing presence in the system. The effect of H_2O_2 on the degradation of IC is investigated by initially adding different concentrations of H_2O_2 (10-50 mg/L) under standardized sonoconditions. The results are shown in figure 5.8.

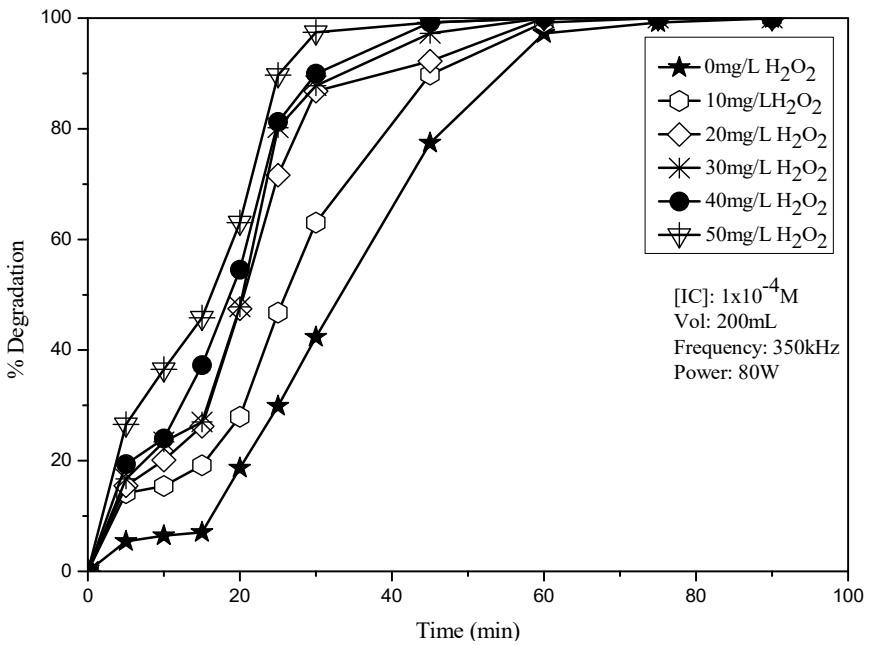

Fig. 5.8: Effect of H_2O_2 on the sonochemical degradation of IC

The degradation is enhanced in the presence of H_2O_2. Control experiments in the presence of H_2O_2 without sonication showed no significant degradation within the time frame of experiments. The degradation increases with increase in the concentration of H_2O_2. At lower concentration, there is an induction period, which is probably due to the slower generation of $^{\bullet}OH$ radicals. However, eventually the rate is enhanced at all concentrations. Complete (100%) degradation is achieved in about 25 minutes with 50 mg/L of added H_2O_2, while it takes approximately 60 minutes at lower concentrations. The enhancement can be attributed to the additional ·OH formed during the sonication by the pyrolysis of hydrogen peroxide as in reaction (5.13) [258, 259].

$$H_2O_2 \rightarrow 2^{\bullet}OH \qquad ....(5.13)$$

However the $^{\bullet}OH$ can also act as a scavenger of H_2O_2 thereby reduces the net concentration of H_2O_2 as follows:

$$H_2O_2 + {}^{\bullet}OH \rightarrow H_2O + HO_2^{\bullet} \qquad ....(5.14)$$

The detrimental effect of H_2O_2 at higher concentration [260-262] on the AOP degradation of organics is not quite evident here. However the enhancement in degradation with increase in H_2O_2 concentration slows down at higher concentration indicating that the scavenging of $^{\bullet}OH$ by H_2O_2 is also taking place in parallel. The enhancement by added H_2O_2 can be explained in two possible ways: i) H_2O_2 molecules that enter the cavitation bubbles during sonication are broken into OH radicals, which enter the solution, interact with and degrade the IC. ii) The H_2O_2 oxidizes IC directly. However the higher rate of enhancement is not sustained later on. This can be explained as follows:

In the beginning, added H_2O_2 decomposes faster in presence of US producing maximum OH radicals which can degrade IC. However, the decomposition of H_2O_2 to water and oxygen ($H_2O_2 \rightarrow H_2O + O_2$) also occurs in parallel which restricts the continued availability of the oxidizing species for IC degradation. Further, even in those experiments without externally added H_2O_2, the H_2O_2 formed in-situ will be accelerating the reaction rate. Hence the effect of initially added H_2O_2 is not that prominent in the later stages of the reaction.

5.3.8 Effect of Fe^{2+}

The insitu formation of H_2O_2 in the reaction system opens up the possibility of enhancing the degradation significantly, by introducing Fe^{2+} to the system and promoting a Fenton like reaction. This will initiate a combination AOP, i.e. SonoFenton and its associated additive or even synergistic effect. In order to verify this possibility, the effect of added Fe^{2+} on the degradation of IC is investigated. $FeSO_4$ is added to the dye solution prior to sonication by keeping the frequency and power constant at 350 kHz and 80W respectively. All reaction parameters are kept the same as those in the case of regular sonolysis. In order to maintain the ideal Fenton condition [263, 264] the initial pH of the solution was maintained at 4-5. The results are compared with those under simple sonolysis as well as comparable Fenton conditions and are shown in figure 5.9. The sonodegradation increases in the presence of Fe^{2+}. The percentage degradation of IC after 15 minutes of sonication in presence of 50 mg/L Fe^{2+} is ~ 99%. During this period, the degradation under simple Fenton is ~ 40% while it is only ~ 5% under simple sonolysis.

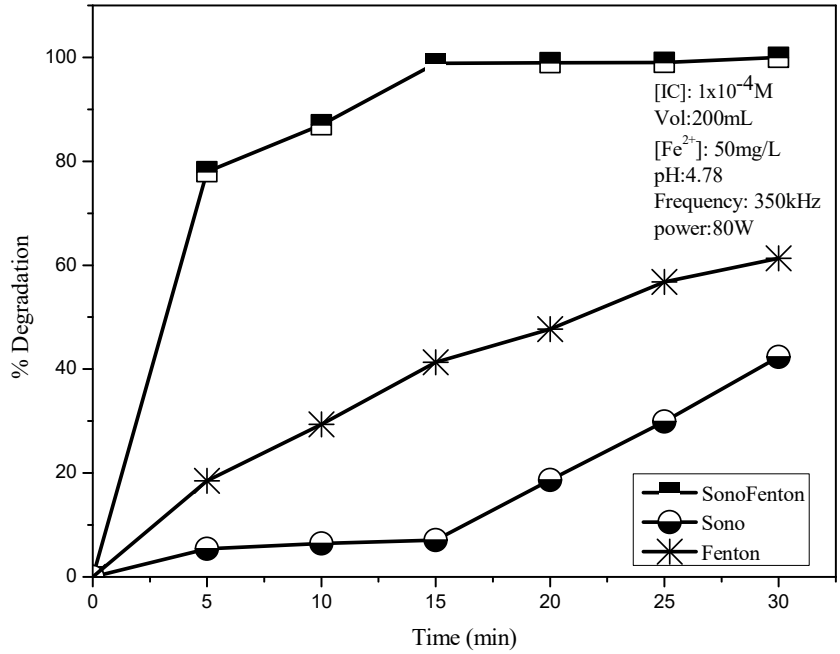

Fig. 5.9: Effect of added Fe^{2+} on the sonochemical degradation of IC

This clearly shows that the effect is more than additive and hence synergistic. The synergy index of sonoFenton process in comparison to the additive effect of sono and Fenton process is calculated for this time period, using the relation,

$$\text{Synergy index (US + Fenton)} = R_{(US+F)} / (R_{US} + R_F) \qquad ....(5.15)$$

where $R_{(US+F)}$, R_{US} and R_F are the rates of degradation under sonoFenton, sono and Fenton conditions respectively. In this case, the synergy index (SI) is 2.2, suggesting very strong synergy by combining the two processes, especially in the early stages of reaction. The synergy at different time periods of reaction is calculated and the values are tabulated in Table 5.1.

Table 5.1: Synergy at different time periods of reaction

Time (minutes)	% Degradation			Synergy
	sonoFenton	Fenton	Sono	
5	78	18.47	5.42	3.39
10	87	29.34	6.45	2.48
15	99.87	41.34	7.07	2.10
20	99.97	47.68	18.67	1.73
25	99	56.78	29.89	1.05(~1.0)
30	99.97	61.34	42.36	0.97(~1.0)

The high synergy reconfirms the formation of H_2O_2 insitu under sonication which makes the Fenton process possible in presence of added $FeSO_4$. The Fenton process results in the formation of more reactive free radicals such as $^{\bullet}OH$, $HO_2^{\bullet}$ etc. as in reactions (5.16) – (5.20). However, with time of reaction, the synergy/additive effect becomes less and less significant (SI decreases to ~1.05 (~1.0) and 0.97 (~ 1.0) after 25 and 30 min. respectively) probably because the concentration of the dye has become too low to show any significant enhancement in the rate of degradation by the combination process (over the sum of the degradation by respective individual processes).

Various reactions taking place in presence of $Fe^{2+}$and H_2O_2 (Fenton reaction) under US irradiation can be summarized as follows:

$$Fe^{2+} + H_2O_2 \rightarrow Fe^{3+} + {}^{\bullet}OH + {}^{-}OH \quad ....(5.16)$$

$$H_2O_2 +))) \rightarrow 2\ {}^{\bullet}OH \quad ....(5.17)$$

$$H_2O_2 + {}^{\bullet}OH \rightarrow H_2O + HO_2^{\bullet} \quad ....(5.18)$$

$$Fe^{3+} + H_2O_2 \rightarrow Fe(OOH)^{2+} + H^{+} \quad ....(5.19)$$

$$Fe(OOH)^{2+} +))) \rightarrow Fe^{2+} + HO_2^{\bullet} \quad ....(5.20)$$

$$2Fe^{3+} \rightarrow 3Fe^{2+} \quad ....(5.21)$$

$$Fe^{3+} + HO_2^{\bullet} \rightarrow Fe^{2+} + H^{+} + O_2 \quad ....(5.22)$$

Thus it is seen that the US induced formation of $^{\bullet}OH$ radicals in aqueous solutions is enhanced in the simultaneous presence of Fe^{2+} and H_2O_2. Complex redox reactions also take place leading to the formation of hydroperoxide radicals and reduced Fe^{2+} ions [264] which also results in enhanced degradation of the pollutant.

5.3.9 Effect of persulphate

The enhancement in the sonochemical degradation of IC in presence of H_2O_2 opens up the possibility of using another powerful oxidant persulphate. Accordingly, sonolysis of IC was done in the presence of persulphate (PS) as an additive. It is observed that the degradation is faster in the presence of PS. The sonodegradation of IC is ~ 30% in the absence of PS while it is ~ 62% in presence of PS (15 mg/L) in 20 minutes. The results are shown in figure 5.10. Sonolysis of PS results in the formation of sulfate radical anion which is a selective oxidant (2.6 V). Oxidative degradation of organic compounds by sulphate radical is well documented [266]. The degradation is increasing with increase in concentration of PS, in the range 10-25mg/L. The degradation is complete in less than 1 hr. even at the lowest concentration of PS, i.e., 10 mgL. PS can diffuse to the interfacial region where pyrolysis also produces sulphate radical.

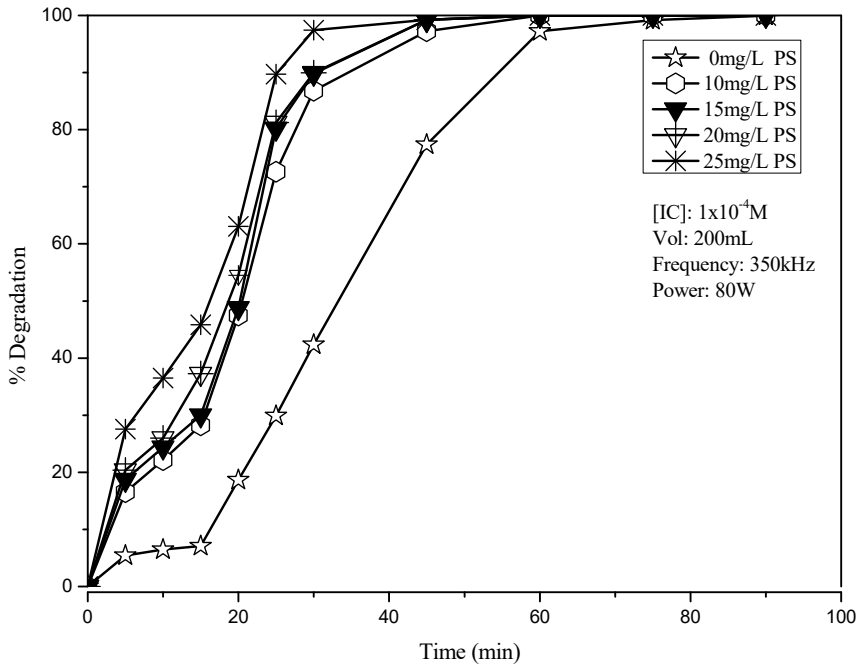

Fig. 5.10: Effect of PS on the sonochemical degradation of IC

Various ROS such as H_2O_2, $HO_2^{\bullet}$, $^{\bullet}OH$ etc. and $SO_4^{-\bullet}$ formed during the irradiation by radical inter conversion reactions interact with IC in the bulk, leading to its degradation into various intermediates and eventual mineralization (reactions 5.24 – 5.32). The results also show that both H_2O_2 and PS have comparable enhancing efficiency. The ·OH radicals also interact with the $SO_4^{-\bullet}$ resulting in the destruction of both by chain termination. Hence addition of more PS is necessary to sustain the generation of $SO_4^{-\bullet}$ and consequently the degradation of IC to drive the reaction to completion, especially so at later stages of reaction when the rate becomes slower. However, too much excess of PS can lead to deactivation of $SO_4^{-\bullet}$ as in reaction (5. 32).

Various reactions leading to the formation and interactions of $SO_4^{-\bullet}$ in presence of added $S_2O_8^{2-}$ are as follows:

$S_2O_8^{2-}$ +))) → $2SO_4^{-\bullet}$ ... (5.23)

$SO_4^{-\bullet}$ + RH → $R^{\bullet}$ + HSO_4^- ..... (5.24) where RH=IC

$SO_4^{-\bullet}$ + H_2O → SO_4^{2-} + H^+ + $^{\bullet}OH$ ....(5.25)

$S_2O_8^{2-}$ + RH → $SO_4^{-\bullet}$ + HSO_4^- + $R^{\bullet}$ ..... (5.26)

$^{\bullet}OH$ + (RH, $R^{\bullet}$) → Intermediates → products ....(5.27)

$SO_4^{-}\cdot$ + ($R^{\bullet}$, $^{\bullet}OH$) → Chain termination ....(5.28)

$2SO_4^{-\bullet}$ → $S_2O_8^{2-}$ Chain termination ....(5.29)

2 $^{\bullet}OH$ → H_2O_2 Chain termination ....(5.30)

$2R^{\bullet}$ → RR Chain termination/Further degradation..(5.31)

$SO_4^{-\bullet}$ + $S_2O_8^{2-}$ → SO_4^{2-} + $S_2O_8^{-\bullet}$ ....(5.32)

5.3.10 Effect of addition of ZnO

ZnO has been proven to be a good catalyst for the sono and photo degradation of many organic pollutants in water. Hence the effect of ZnO on the sono degradation of IC is tested under standardized conditions for sonolysis. The degradation increases moderately in presence of the catalyst (figure 5.11). With increase in catalyst dosage, the degradation increases slowly reaches an optimum at 0.06 g and stabilizes thereafter. The sonodegradation is more in the presence of ZnO compared to that with ultrasound alone. This may be because in presence of ZnO under US

irradiation, more hydroxyl radicals are produced which will react with more of the IC molecules and degrade them. ZnO is an efficient catalyst offering surface sites for the adsorption of the substrate leading to enhanced interaction with the surface generated ˙OH radicals. It is known that presence of suspended particles of appropriate size and amounts in water lead to increase in the acoustic noise and rise in the temperature in the irradiated liquid [187, 202].

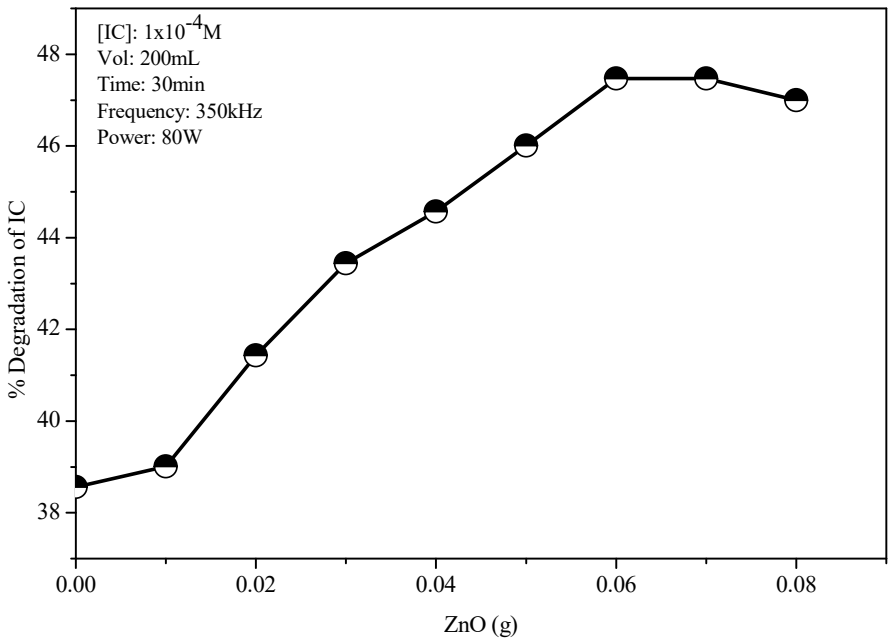

Fig. 5.11: Effect of ZnO at different dosages on the sonochemical degradation of IC

Presence of suspended solids in the liquid can provide more nucleation sites for cavitation bubbles at their surface. This will result in decrease in the cavitation thresholds which is responsible for the increase in the number of bubbles when the liquid is irradiated by US. Increase in the

number of cavitation bubbles increases the pyrolysis of water which also leads to increase in the generation of reactive free radicals and degradation of IC under sonication. However, any increase in the catalyst dosage beyond the optimum will only result in the aggregation of particles which will limit the number of catalytically active accessible sites at the surface. Higher dosage of suspended particles will also disturb the transmission of ultrasound in the aqueous medium. Hence there is no further increase in degradation of the pollutant beyond a particular dosage. The sonoluminescence resulting in UV irradiation may also accelerate the reaction through photocatalysis since ZnO is an efficient photocatalyst [187, 250, 260].

5.3.11 Comparative degradation efficiency of IC in presence of additives

Further to the experiments conducted in presence of various additives individually as above, preliminary studies were made on the efficiency of various combinations for the degradation of IC (in terms of the time taken for complete decolorization). The results are shown in figure 5.12.

Accordingly the most efficient systems for the degradation of IC are:

i) Sonolysis in presence of ZnO and PS (US/PS/ZnO)
ii) Sonolysis in presence of H_2O_2 and PS (US/PS/H_2O_2) and
iii) Sonolysis in presence of PS, H_2O_2 and ZnO (US/PS/H_2O_2/ZnO).

Sonolysis in presence of (i) H_2O_2 and ZnO (US/H_2O_2/ZnO) as well as (ii) PS (US/PS) are also efficient, though slightly less than the above three systems.

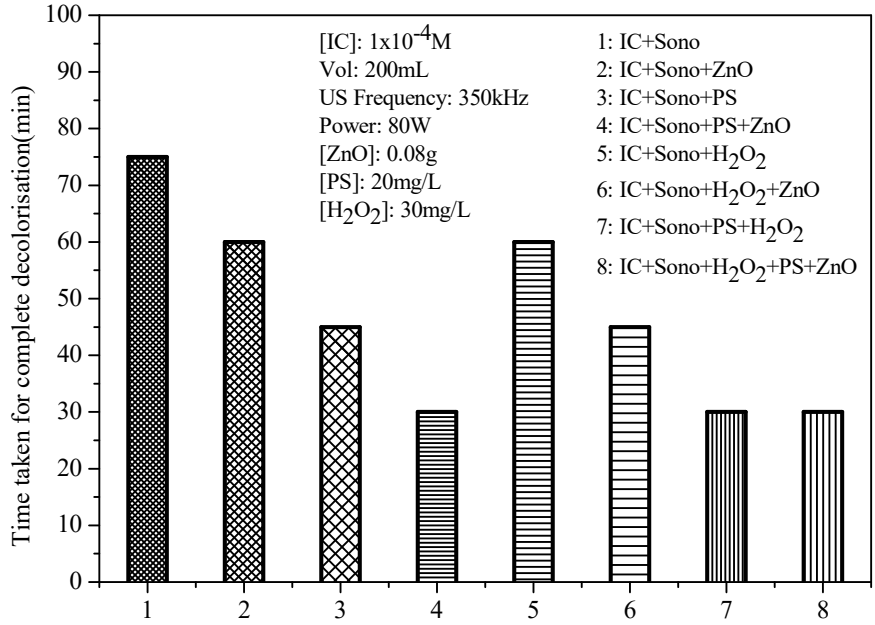

Fig. 5.12: Comparison of the time taken for decolorization of IC in different systems

The relative efficiency of various systems for the decolorization is in the order:

$$(US/PS/ZnO) \approx (US+PS+H_2O_2+ZnO) \approx (US/PS/H_2O_2) > US/H_2O_2/ZnO \approx US/PS > US/H_2O_2 \approx US/ZnO \quad ....(5.33)$$

The relative efficiency of the additives for enhancing the rate of degradation of the pollutant may vary with the concentration of the additives and the reaction conditions. This may be attributed to the multiple interactions of various reactive free radicals at different stages of reaction leading to different transient intermediates [187, 202]. In-depth investigations on such parameters will help to identify optimum conditions for the degradation/mineralization of the pollutant. However,

such an investigation is beyond the scope of this study and is hence not attempted.

5.3.12 Effect of anions

Anions/salts likely to be present in most of natural waters are known to influence the efficiency of many AOPs for water purification. In this context, the effect of few such anions i.e., SO_4^{2-} , Cl^-, CO_3^{2-}, HCO_3^-, and PO_4^{3-} on the rate of sonolytic degradation of IC is investigated and the results are presented in figure 5.13.

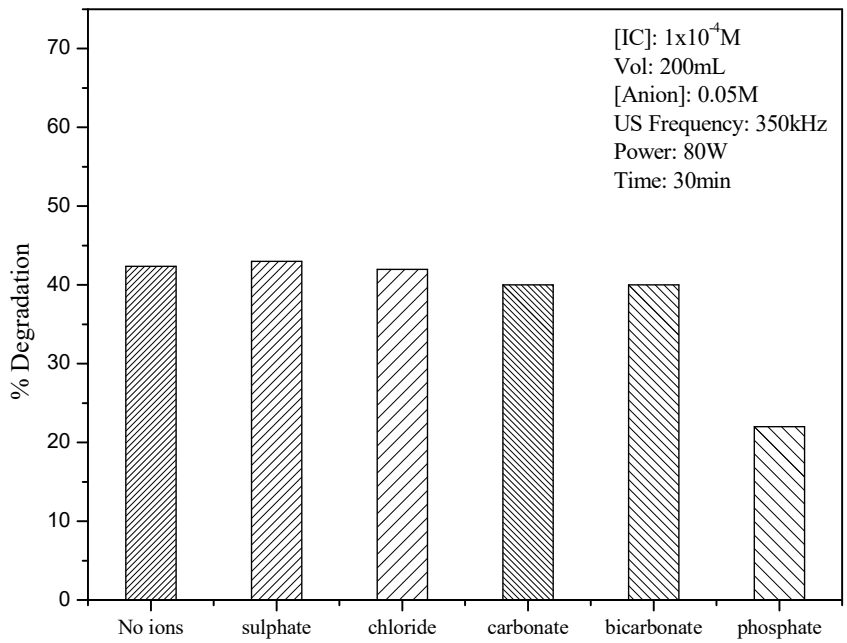

Fig. 5.13: Effect of common anions in water on the sonolytic degradation of IC

The anions have no effect on the degradation of IC at the concentration studied here except in the case of PO_4^{3-} which is known to be a strong inhibitor of most AOPs. Studies at different concentration

ranges of various anions (5-15 mg/L) on the degradation of IC confirm that the concentration effect is negligible at least in this range. This suggests that sonolysis is an efficient source of AOP activation for the removal of IC even from natural water containing dissolved salts. However, at much higher concentration of the anions (which is not natural in most water sources), the possibility of inhibition cannot be ruled out as has been reported in few earlier studies [202].

Since the efficiency of sonolysis for the degradation of IC in water is higher in the presence of additives such as PS, H_2O_2, ZnO and/or their combination, the effect of anions is tested under these conditions as well. In these cases also anions have practically no effect except the inhibition by PO_4^{3-}. This implies that the most efficient systems identified earlier, i.e.US/PS/ZnO, US/PS/H_2O_2/ZnO or US/PS/H_2O_2 can be used for the decontamination of water from IC even in the presence of moderate amount of natural anions.

5.3.13 Mineralization studies

The efficiency of any AOP for the decontamination of water depends on its ability to completely mineralize the pollutants into harmless products. The mineralization in the current instance is tested by measuring the chemical oxygen demand (COD) of the system at different times of sonication. The COD disappears completely in 10 hr. time by simple sonication in the absence of any oxidant or catalyst (figure 5.14).

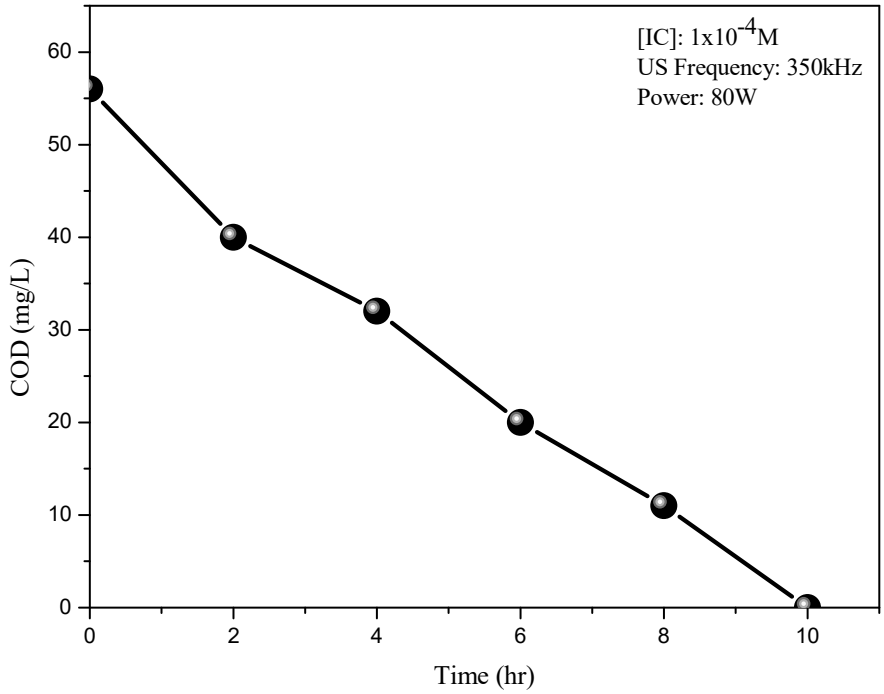

Fig. 5.14: Reduction in COD during sonodegradation of IC

The time taken for complete mineralization of IC is much less in presence of specific additives, as shown in figure 5.15.

The efficiency of mineralization of various systems is in the order:

$$(US/PS/ZnO) \approx (US/PS/H_2O_2) \approx (US+PS+H_2O_2+ZnO) > US/PS > US/H_2O_2 \approx US/ZnO \quad ....(5.34)$$

The mineralization as well as the decolorization follows the same pattern thereby suggesting that the degradation of the intermediates formed during the decolorization is also facilitated by the oxidants.

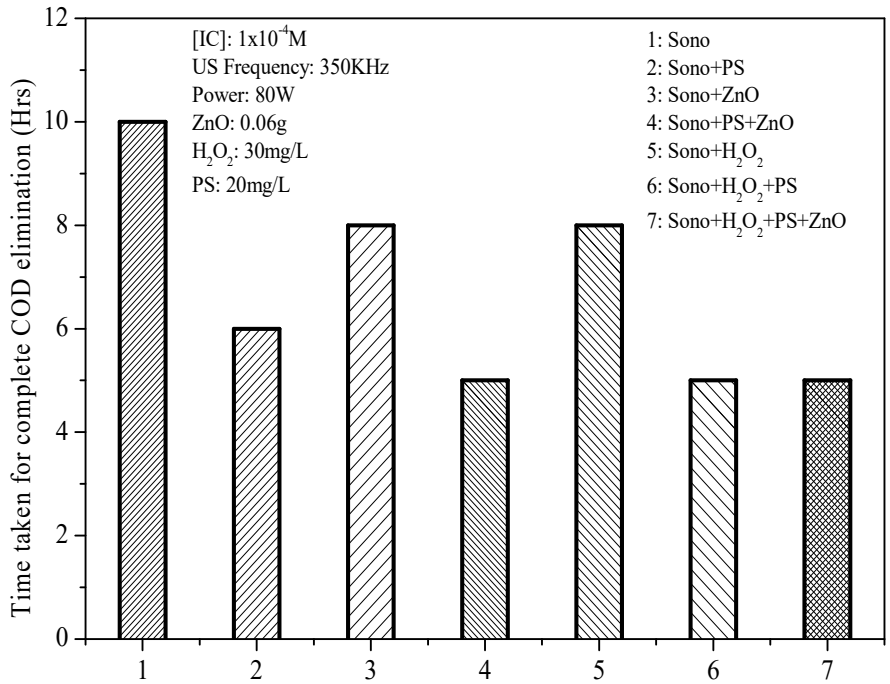

Fig. 5.15: Comparison of the time taken for complete mineralization of IC under sonolysis in presence of different additives

The longer time taken for mineralization compared to decolorization shows that the former proceeds through the formation of recalcitrant intermediates which take longer time to be irreversibly transformed into harmless CO_2, H_2O_2 and salts.

Various intermediates formed during degradation of IC are analyzed by LC/MS and are shown in Table 5.2.

Table 5.2: Major intermediates identified during the sonodegradation of IC

m/z	Mol. formula	Molecular structure
189	$C_6H_7NSO_4$	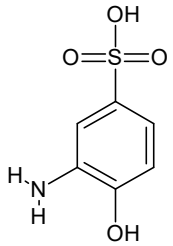
217	$C_7H_7NSO_5$	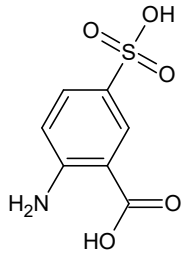
225	$C_8H_5NSO_7$	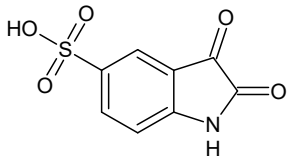
259	$C_8H_5NSO_7$	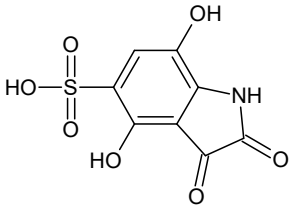
358	$C_{16}H_{10}N_2SO_6$	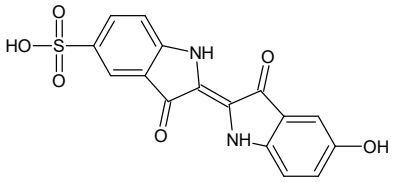
423	$C_{16}H_{11}N_2SO_{10}$	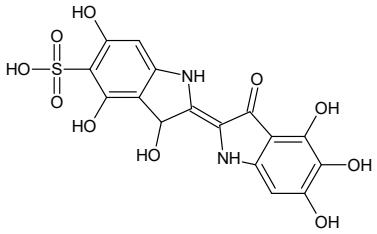

5.4 Conclusion

Ultrasound irradiation at appropriate power and frequency is an efficient mode of activation in advanced oxidation process (AOP) for the decolorization as well as mineralization of Indigo Carmine dye pollutant in water. The mineralization, which is confirmed by measuring the chemical oxygen demand, proceeds through a number of intermediates. These intermediates are identified and characterized by LC/MS. Combination of sonolysis with additives such as Fe^{2+}, H_2O_2, persulphate and ZnO enhances the efficiency of the process for decolorization as well as mineralization. The presence of salts/anions commonly found in water does not inhibit the degradation or mineralization, except in the case of PO_4^{3-} ions. Hence the sonolytic AOP, under suitably standardized conditions, is a potential technique for the decontamination of water from Indigo Carmine (IC) pollutant even in the case of natural effluents containing moderate amounts of salt contaminants.

.....ꕥ.....

Chapter

6

FENTON AND FENTON BASED HYBRID AOPs FOR THE DECONTAMINATION OF WATER FROM INDIGO CARMINE DYE POLLUTANT

Contents

6.1 Introduction

As discussed in earlier Chapters, Advanced Oxidation Processes (AOPs) are environment-friendly and economical techniques for the removal of toxic and hazardous pollutants from water. According to the reactive phase, AOPs are classified into homogeneous and heterogeneous types. Examples of homogeneous type AOPs include Fenton based processes such as classic Fenton (H_2O_2 + Fe^{2+}), Fenton like processes (Fe^{2+} + H_2O_2 + $metal^{n+}$), sono-, photo- and electro-Fenton processes based on O_3, H_2O_2, O_3-UV, H_2O_2-UV and O_3-H_2O_2-UV etc. All processes involving suspended catalysts belong to the category of heterogeneous AOPs. However these processes have gained only limited acceptance so far as viable and effective methods for the large-scale decontamination of wastewater due to complexity of the process, cost, operational constraints etc..

In this context, the simple inexpensive classic Fenton process and its variations become important [266, 267]. The hydroxyl radicals produced insitu in the Fenton process are nonselective in degrading organic pollutants [268]. Fenton's reagent is particularly promising due to its low cost, low toxicity of the reagents (Fe (II) and H_2O_2), and the simplicity of the technology. Several studies have shown that the Fenton's process is effective for the degradation of a number of organic compounds [269-271]. In the present study, the possibility of application of Fenton process under various conditions for the removal of the toxic recalcitrant dye Indigo carmine (IC) from water is examined.

6.2 Experimental details

6.2.1 Materials used

H_2O_2 (30.0% w/v) and $FeSO_4.7H_2O$ (FS) from Qualigen (India) were used as such without further purification. Various other chemicals used were also of AnalaR grade or equivalent, unless indicated otherwise.

6.2.2 Degradation/Mineralization Experiments

In a typical experiment, the dye solution of required concentration is mixed with appropriate combinations of $FeSO_4$ (FS) and H_2O_2 in a 250 ml closed beaker. The reaction mixture is continuously stirred by using a magnetic stirrer. The reaction volume is maintained at 50 mL, unless indicated otherwise. The degradation is monitored by analyzing the IC remaining in the system by using UV-VIS spectrophotometry at 609 nm. H_2O_2 is analysed by standard iodometry. The reaction intermediates and products were identified by LC-MS.

In the case of solar degradation, the experiments were performed in a jacketed pyrex reactor. The dye solution (50 ml) together with the Fenton reagent and/or other additives was taken in the inner compartment and cooling water from a thermostat (29±1°C) was circulated through the outer jacket. The experiments were performed by placing the system at the roof top of our laboratory at Kochi, Kerala, India (9^0 57' 51" N, 76^0 16' 59" E) during sunny days in February-May, September-December 2017 and 2018. The suspension/solution was stirred frequently to ensure uniform mixing. Samples were drawn periodically, filtered through 0.45μm filter in the case of suspensions and analyzed for the remaining dye concentration. Solutions/suspension kept under identical conditions in the dark was used as the reference in each case to eliminate the contribution from adsorption and/or dark reaction, if any, towards the reduction in the dye concentration.

Sonolytic Fenton degradation of IC under different experimental conditions is investigated using ultrasound (US) of frequency in the range 200 kHz - 1 MHz and power in the range of 20-80W as the source of energy. Electrochemical experiments were done using bismuth oxide doped titanium dioxide (BiO_2-TiO_2) coated on titanium plate as the anode and graphite as the cathode in presence of sodium sulphate supporting electrolyte (BiO_2-TiO_2/Ti/graphite/Na_2SO_4). The experiments were conducted under static anodic potential of 3.4V.

6.3 Results and discussions

6.3.1 Optimization of Fe^{2+}/H_2O_2 ratio

Preliminary experiments have shown that IC can be decolorized by Fenton reagent at room temperature. The degradation/decolorization is

practically negligible in presence of the individual components (Fe^{2+} or H_2O_2). The efficiency of the Fenton process for the degradation of any organics depends on the relative concentration of the reagent components; $FeSO_4$ (FS) and H_2O_2. Hence detailed investigations were made for optimizing the ratio of these critical components for the degradation of IC in water. The concentration of IC is kept constant at 1×10^{-4}M. The % degradation of IC at varying ratios of FS and H_2O_2 at different times of reaction is evaluated. The results are plotted in figure 6.1.

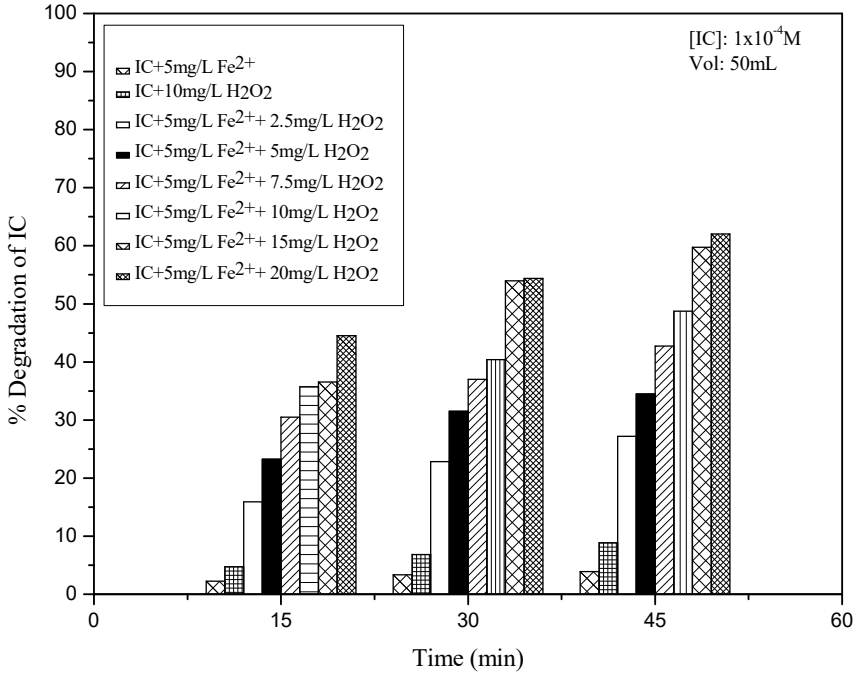

Fig. 6.1: Optimization of Fe^{2+}/H_2O_2 ratio for the degradation of IC

As seen from the figure the optimum ratio of Fe^{2+}/H_2O_2 under the reaction condition is 5:15. Further increase in H_2O_2 dosage leads to stabilization of the degradation. The actual quantity of Fenton reagent in the ratio of Fe^{2+}/ H_2O_2= 5:15 (1:3) is further optimized as follows:

6.3.2 Effect of concentration of Fenton reagent on the degradation of IC

The effect of quantity of the Fenton reagent at the optimized ratio of 1:3 on the decolorization of IC is evaluated and the results are presented in figure 6.2.

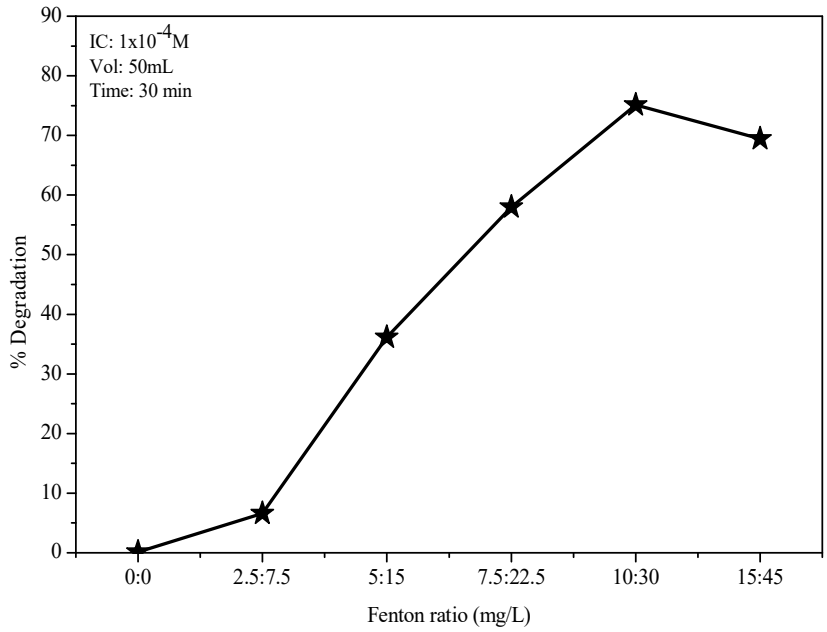

Fig. 6.2: Effect of concentration of Fenton reagent on the rate of degradation of IC

The degradation of IC increases with increase in the concentration of Fenton reagent. Eventually the degradation is stabilized (at Fe^{2+}: H_2O_2 = 10:30) probably because the concentration of the dye has become relatively less for the effective utilization of the higher availability of FR. However, this optimized quantity depends on other reaction and reactor parameters and may vary under another set of conditions. Hence every time when the reaction conditions are changed, the optimum also needs to be reworked.

The degradation of IC at different times, using the optimized quantity [10:30mg/L (Fe^{2+}:H_2O_2)] of the Fenton reagent in the ratio (1:3) is studied keeping the concentration of IC constant. The results are shown in figure 6.3. It is observed that the degradation of IC progresses steadily with time. However, the rate of increase in percentage degradation and consequently the rate of reaction decrease with time, probably because of decrease in the concentration of available IC. Eventually the degradation/decolorization reaches 100%, indicating that the intermediates formed during the degradation does not significantly retard the interaction between the Fenton reagent and IC. This shows that the Fenton process is efficient for the complete decolorization of IC in water.

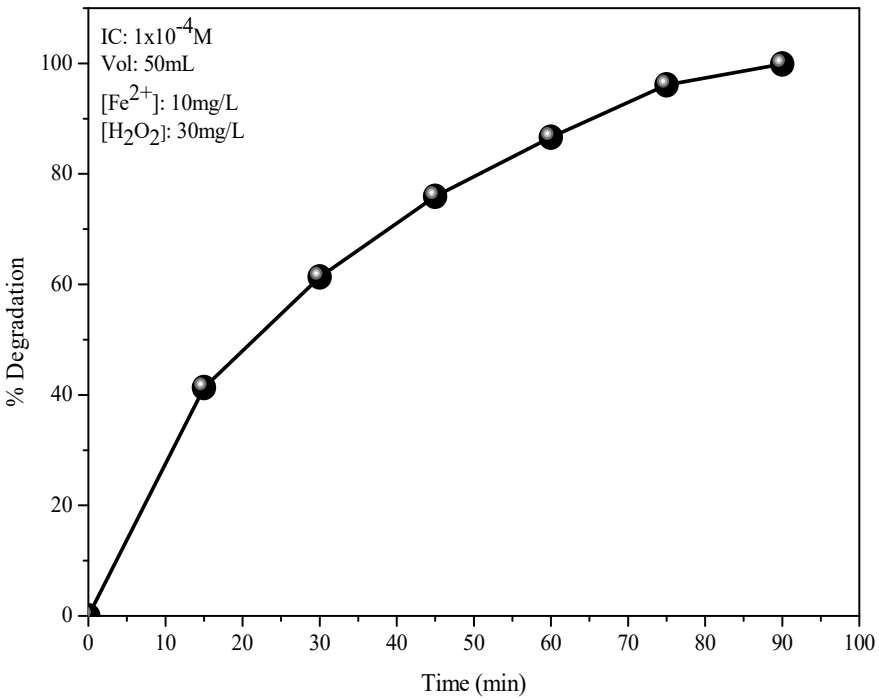

Fig. 6.3: Effect of time on the Fenton degradation of IC

The decreasing rate of decolorization with time indicates that the relative concentration of IC and FR at any point in time of reaction influences the rate of degradation. This is further verified from the effect of initial concentration of IC on its degradation, keeping other parameters constant.

6.3.3 Effect of initial concentration of IC on the Fenton degradation

The effect of concentration of IC on the % degradation is presented in figure 6.4. The % degradation decreases slowly with increase in concentration of IC. However, the rate of degradation increases steadily with increase in the concentration (Inset of Fig. 5).

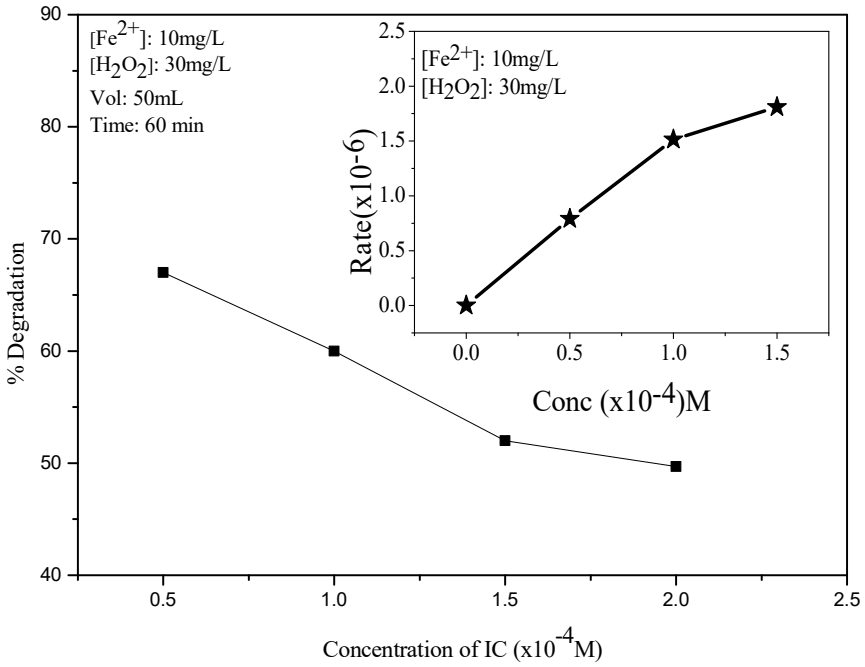

Fig. 6.4: Effect of initial concentration of IC on its Fenton degradation [Inset: Concentration Vs Rate plot]

Beyond a particular optimum concentration (1×10^{-4}M), the rate of degradation slows down. This may be because the concentration of the Fenton reagent is not adequate enough to interact with the higher number of IC molecules available in the system and increase the rate of reaction. Based on these data, 1×10^{-4}M solution of IC is chosen as the optimum for further investigations.

6.3.4 Effect of pH on the Fenton degradation of IC

The pH is a very important and critical parameter that influences the efficiency of the Fenton's process. Change in pH of the solution results in variation in the concentration of Fe^{2+} and consequently the rate of production of ·OH radicals which are responsible for oxidation of IC [272]. The influence of pH on the decolorization of IC was investigated by keeping all other parameters constant and the result are presented in figure 6.5.

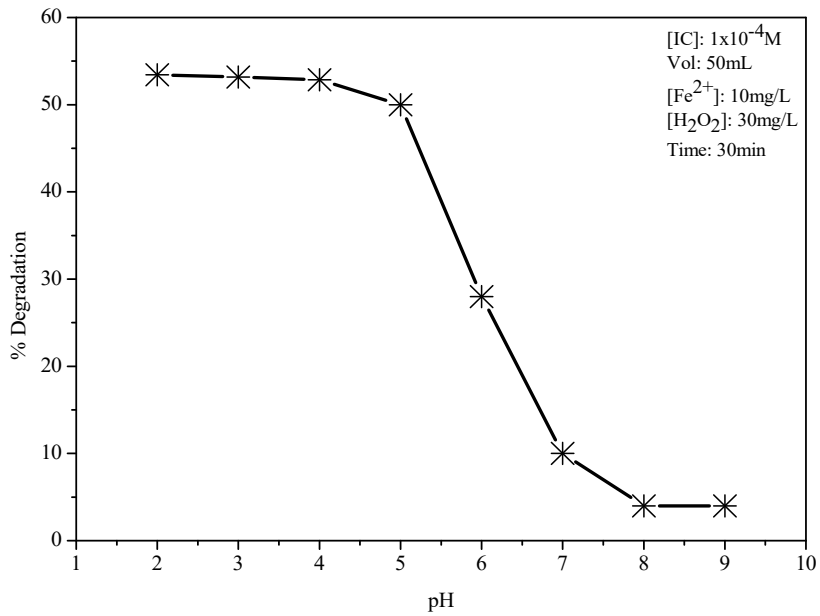

Fig. 6.5: Effect of pH on the Fenton degradation of IC

The results show that Fenton process is favored only in the acidic pH range especially upto pH~ 5. Above pH 5, the generation of $^{\cdot}OH$ decreases sharply due to the formation of Fe^{3+} ions which tend to precipitate in the form $Fe(OH)_3$ as in reaction (6.1).

$$Fe^{3+} + 3^{-}OH \rightarrow Fe(OH)_3 \qquad .....(6.1)$$

This reaction is favored at higher pH [265]. Therefore, the initial pH value has to be in the acidic range (< ~5) to generate the maximum amount of $^{\cdot}OH$ radicals and thus to oxidize the organic compounds.

6.3.5 Effect of Persulphate on the Fenton degradation of IC

Persulphates ($S_2O_8^{2-}$) are proven to be strong oxidants in AOPs due to the insitu formation of highly reactive $SO_4^{-\cdot}$ radical anions. Hence the probability of enhancing the efficiency of the Fenton process by the addition of persulphate (PS) is tested at various concentrations and the results are presented in figure 6.6. The results show that persulphates enhance the Fenton reaction (FR)- induced degradation of IC. Persulphate anion is the most powerful oxidant among the peroxygen family of compounds and one of the strongest oxidants used in environmental remediation. In addition to its direct oxidation capability, persulphates can also yield highly reactive sulphate radicals (as shown in equations 6.2, 6.3), which are also powerful oxidants like the hydroxyl radicals.

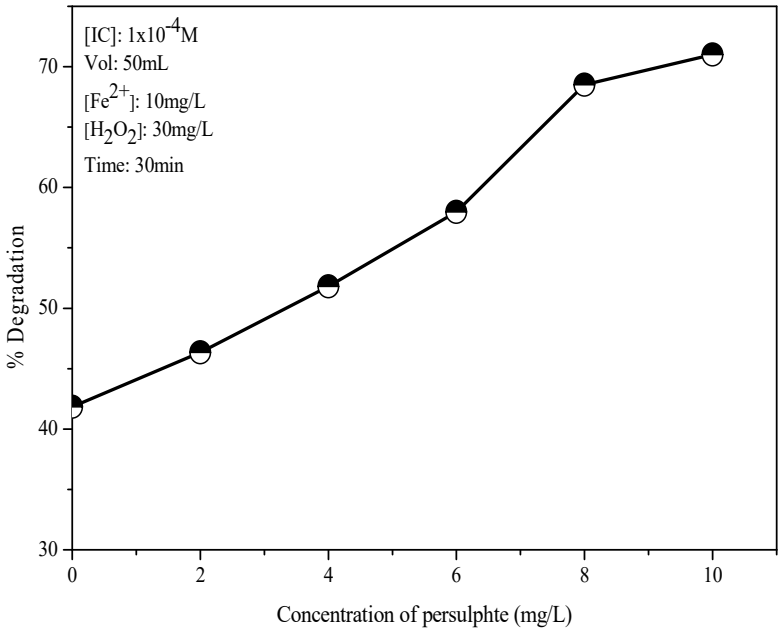

Fig. 6.6: Effect of persulphate at various concentrations on the Fenton degradation of IC

$$S_2O_8^{2-} + 2H^+ + 2e^- \rightarrow 2HSO_4^- \quad .....(6.2)$$

$$S_2O_8^{2-} + \text{Initiator} \rightarrow 2SO_4^{-}\cdot \quad .....(6.3)$$

Both $SO_4^{-\bullet}$ and $^{\bullet}OH$ have similar oxidation potential ($^{\bullet}OH$= 2.80, $SO_4^{-\bullet}$ = 2.60) and hence presence of persulphate is expected to enhance the Fenton degradation at least additively. However, the effect of PS on the Fenton process is not always additive or synergistic. This may be because the $SO_4^{-}\cdot$ generated insitu may be getting deactivated by interactions as follows:

$$SO_4^{-\bullet} + {}^{\bullet}OH \rightarrow \text{Chain termination} \quad .....(6.4)$$

$$SO_4^{-\bullet} + S_2O_8^{2-} \rightarrow SO_4^{2-} + S_2O_8^{-}\cdot \quad ..... (6.5)$$

$$SO_4^{-}\cdot + SO_4^{-}\cdot \rightarrow S_2O_8^{2-} \quad .....(6.6)$$

Hence the economic viability of using PS to accelerate the efficiency of Fenton process for the degradation of pollutants in water needs to be experimentally verified and the parameters optimized in each case as appropriate.

6.3.6 Effect of salts/anions on the Fenton degradation of IC

The presence of chemical contaminants such as salts/anions/cations is known to influence the efficiency of AOPs for the mineralization of pollutants in water. Anions are used at different stages of the dyeing process and are hence likely to be present in the effluent water from dye related operations. In this context, the effect of few common anions (Cl^-, CO_3^{2-}, HCO_3^-, PO_4^{3-}) which are likely to be present in many natural water sources on the efficiency of the Fenton process for the decolorization of IC is examined. The results are presented in figure 6.7.

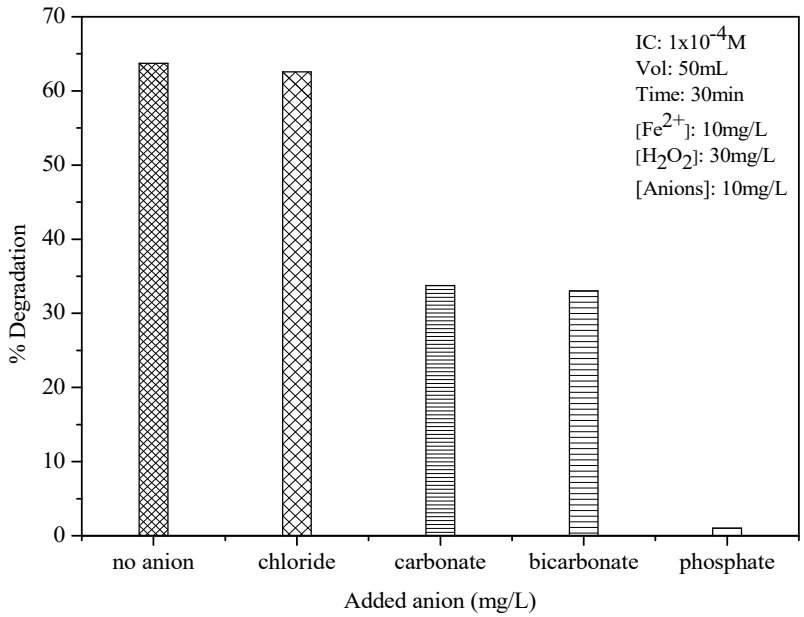

Fig. 6.7: Effect of anions on the Fenton degradation of IC

Anions at the specified concentration are added to the reaction system individually and the Fenton degradation of IC in their presence was compared with the normal system. Results show that chloride has no effect on the degradation while carbonate and bicarbonate are good inhibitors. Phosphate is a strong inhibitor which retards the degradation of IC almost completely.

The main reason for the inhibition by anions may be the scavenging of the reactive ·OH radicals formed insitu during the Fenton reaction resulting in the formation of radical anions as follows [201,265,273]:

$$^{\bullet}OH + HCO_3^- \rightarrow H_2O + CO_3^{\bullet-} \quad .....(6.7)$$

$$^{\bullet}OH + CO_3^{2-} \rightarrow OH^- + CO_3^{\bullet-} \quad .....(6.8)$$

$$PO_4^{3-} + {}^{\bullet}OH \rightarrow PO_4^{2-\bullet} + OH^- \quad .....(6.9)$$

$$^{\bullet}OH + Cl^- \rightarrow OH^- + Cl^{\bullet} \quad ....(6.10)$$

$$Cl^{\bullet} + Cl^- \rightarrow Cl_2^{-\bullet} \quad ....(6.11)$$

The radical anions formed in the process are also moderately active for the degradation of organics. Their concentration will be increasing steadily in the system, unlike the ·OH radicals which decrease progressively by recombination and deactivation as in reactions (6.12) and (6.13).

$$^{\bullet}OH + {}^{\bullet}OH \rightarrow H_2O_2 \quad ....(6.12)$$

$$^{\bullet}OH + H_2O_2 \rightarrow H_2O + HO_2^{\bullet} \quad ....(6.13)$$

Hence, reasonable rate of degradation will continue even in presence of the $^{\bullet}OH$ radical-scavenging anions. The scavenging rate constants for some of the common anions are given in table 3.2 (Chapter 3). Accordingly, if the inhibition was exclusively due to scavenging of the $^{\bullet}OH$ radicals, it should have been in the order:

$$SO_4^{2-} > Cl^- > CO_3^{2-} > HCO_3^- > H_2PO_4^-$$

Since this sequence is not followed, scavenging of the anions cannot be considered as the main reason for the inhibition. The very strong inhibition in presence of PO_4^{3-} in this homogeneous system is surprising even though anions are known to inhibit many heterogeneous AOPs due to the blocking of the catalytically active surface sites. This possibility for inhibition is ruled out in this system with no suspended catalyst particles. In the case of PO_4^{3-} it is possible that the radical anion formed from phosphate is practically not active like other radical anions. It is also possible that the $Fe^{2+}$of the Fenton reagent will interact with PO_4^{3-} thereby decreasing the amount of the cations needed for the formation of $^{\bullet}OH$ by the Fenton reaction.

Another reason for the anion effect in the case of Fenton reaction is the variation in pH in presence of the anions. Even mild variation in the pH, especially from the optimum of ~ 4 can affect the Fenton process strongly. The pH of the system in presence of various anions is shown in figure 6.8.

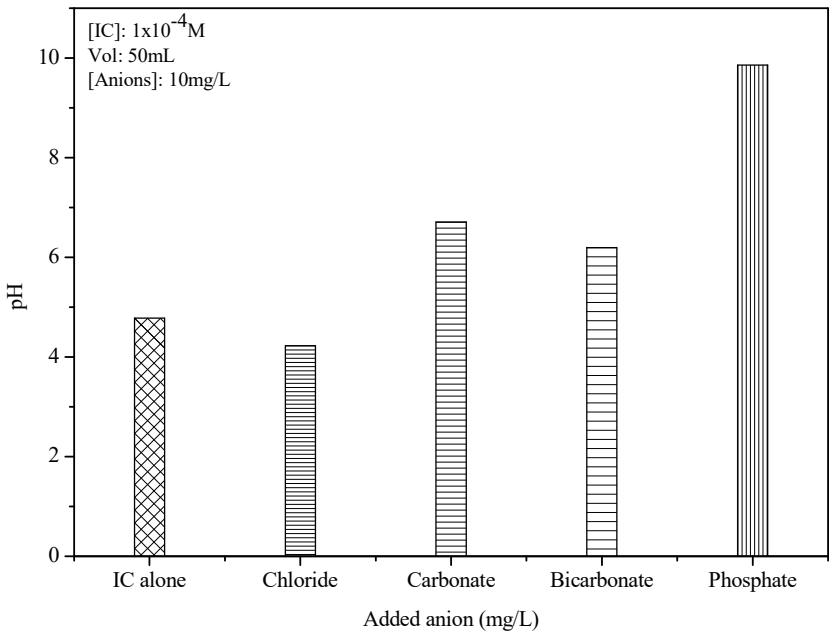

Fig. 6.8: pH of the dye solution in presence of anions

The pH decreases moderately in presence of Cl^- which is a favorable condition for Fenton reaction. As expected, in this case the anion Cl^- has no effect. CO_3^{2-}, HCO_3^- and PO_4^{3-} increase the pH of the medium which is unfavorable for the Fenton degradation. Hence the inhibition in presence of anions, at least in the concentration studied here can be attributed to the variation in pH.

6.3.7 Effect of ZnO on the Fenton degradation of IC

Earlier studies have shown that ZnO and TiO_2 mediated photo, sono and microwave (MW) activated AOP is efficient for the degradation and mineralization of a variety of pollutants [197,262,263]. Of these two widely investigated semiconductor oxides, ZnO has been proven to be more active for solar energy harvesting due to its better absorption

characteristics in the visible range of solar spectrum. In this context, experiments were done to verify whether ZnO can be used beneficially in the Fenton process, either under ambient condition or in presence of powerful activation sources such as sunlight, UV-Vis light or ultrasound. The effect of ZnO on the classic Fenton degradation of IC is shown in figure 6.9.

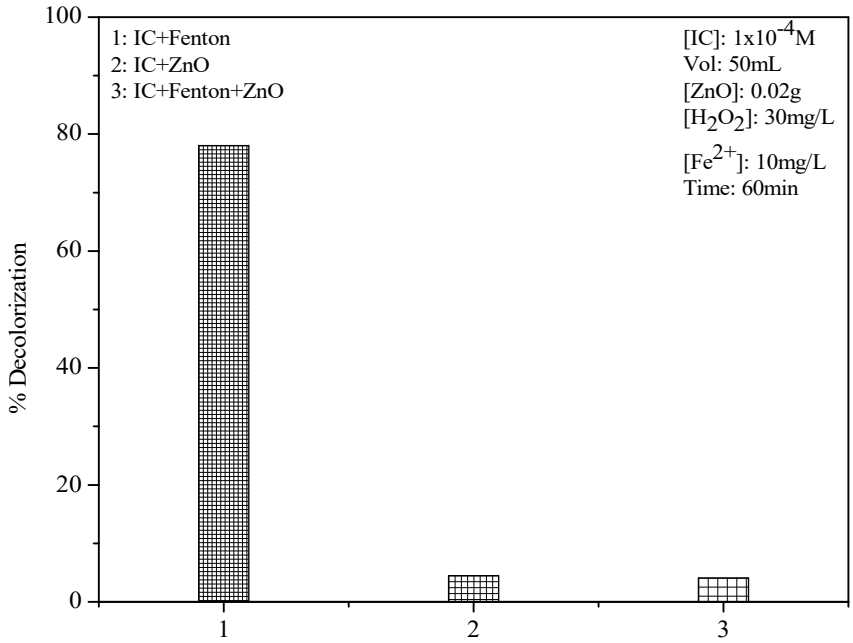

Fig. 6.9: Effect of ZnO on the Fenton degradation of IC

In this heterogeneous system, in the absence of any light irradiation, ZnO inhibits the Fenton degradation of IC almost completely.

The adsorption of H_2O_2 on ZnO and consequent decrease in the concentration of the former as the cause of the inhibition is ruled out since the adsorption has been experimentally observed to be negligible. Hence, the suspended ZnO particles may be inhibiting effective interaction between Fe^{2+} and H_2O_2 thereby reducing the rate of formation of reactive ·OH radicals.

The substrate also may get shielded from interaction with the reactive free radicals by the ZnO particles which also may lead to the inhibition. Presence of ZnO also increases the pH of the medium which is another unfavorable factor for the Fenton reaction as stated earlier. The pH of the standard IC-FR system increases from 4.5 to 7.5 in presence of ZnO (figure 6.10). The effect of pH (Fig. 6.5) clearly illustrates that the degradation is severely inhibited at pH 7. However, when the pH of the IC-FR-ZnO suspension is modified to acidic condition of normal Fenton system, i.e. 4.5, the degradation of IC proceeds faster, though the rate is less compared to that of normal Fenton (without ZnO). The result is shown in figure 6.10 inset. Hence at least one of the main causes for the inhibition by ZnO is its effect on the pH.

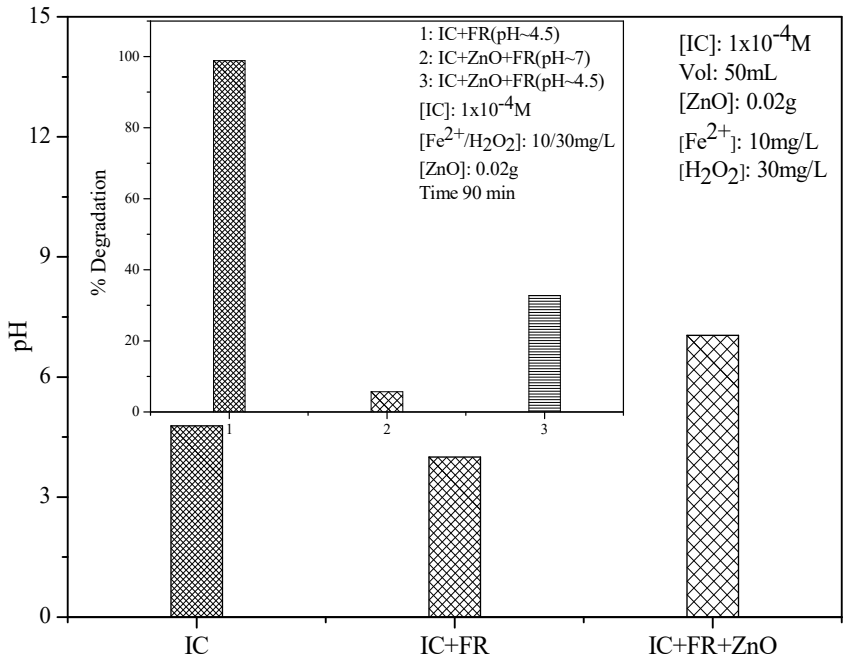

Fig. 6.10: pH of the IC/FR system with and without ZnO [Inset: Effect of ZnO on the Fenton degradation of IC with and without adjusting the pH]

The effect of variation in ZnO dosage on the efficiency of the normal Fenton system is experimentally verified and the results are plotted in figure 6.11. The degradation of IC decreases with increase in the amount of ZnO and is almost completely inhibited above 0.010 g. The effect of varying amounts of ZnO on the pH of the system is shown in the inset of the figure.

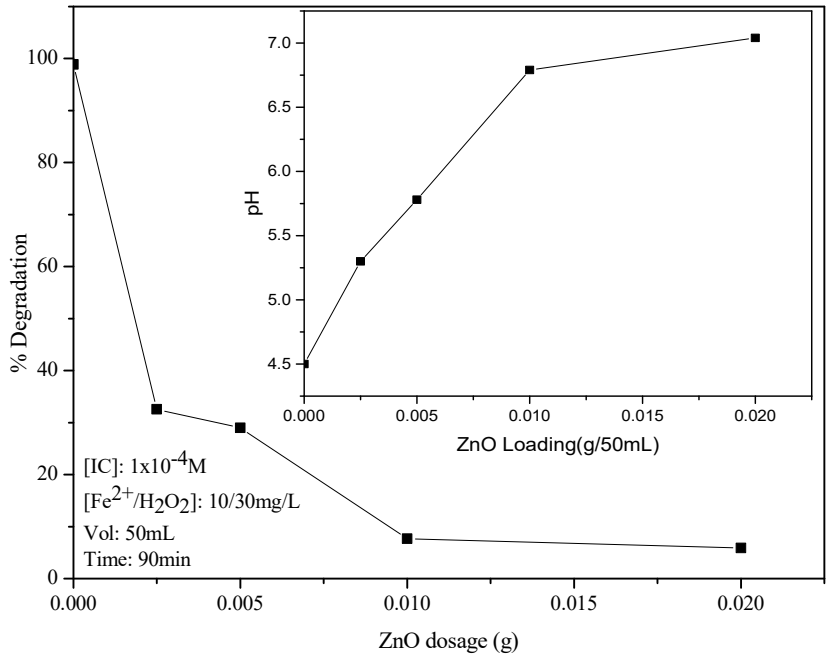

Fig. 6.11: Effect of increasing dosage of ZnO on the Fenton degradation of IC [Inset: Effect of ZnO on the pH of the IC/FR system]

The data clearly shows that increase in the pH of the system is one of the major causes of the inhibition in presence of ZnO.

The inhibiting effect of ZnO is further verified by adding ZnO in between to the Fenton degradation in progress and observing the effect. It is observed that the degradation which was proceeding smoothly, stopped

instantly and stabilized. No further degradation was observed even after long time. The result is shown in figure 6.12.

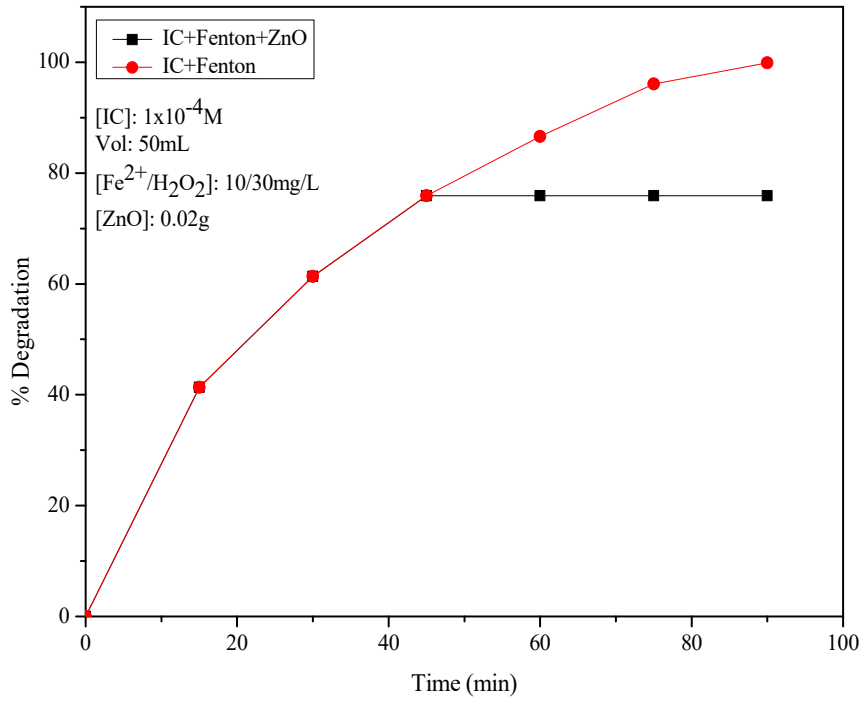

Fig. 6.12: Effect of in between addition of ZnO on the Fenton degradation of IC

6.3.8 Effect of volume of the reactor

Since Fenton reaction is a relatively simple facile process which proceeds smoothly as long as there is sufficient concentration of the reagents and the substrate, the effect of volume of the reaction system on the rate of degradation of IC is tested under optimized reaction parameters in the same reactor. The results which are shown in figure 6.13 confirm the expected outcome, i.e. the rate of degradation is maintained as long as the ingredients are available in required quantities. The initial increase in

degradation with increase in volume from 25 to 50mL shows that there is an optimum volume at which the Fenton process is more efficient compared to very low volume. This also indicates that the volume of the reaction system is not a constraint for the scaling up of the Fenton process at industrial level.

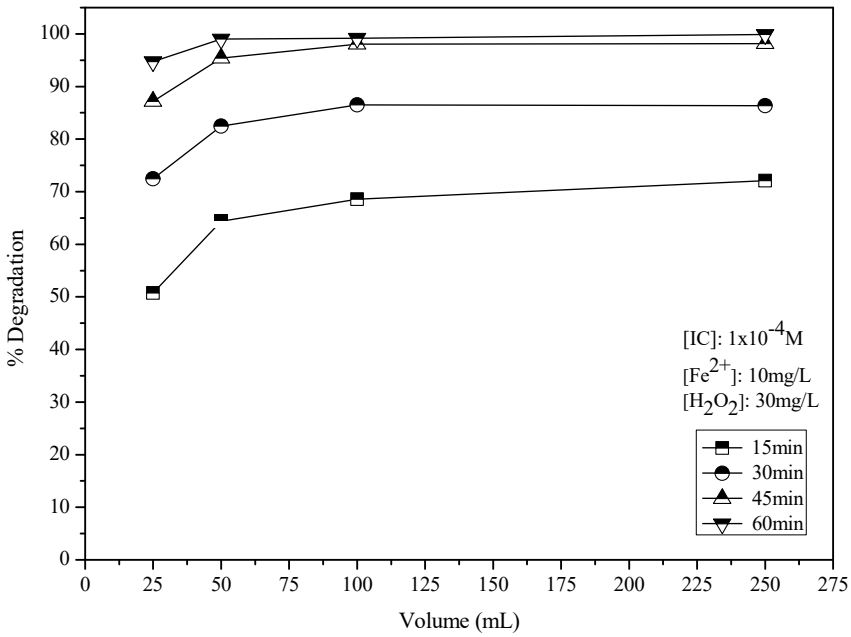

Fig. 6.13: Effect of volume on the Fenton degradation of IC

6.3.9 Mineralization of IC during Fenton degradation

The efficiency of any water purification technique depends ultimately on its ability for mineralizing the chemical pollutant and bringing down the Chemical Oxygen Demand (COD)/total organic carbon (TOC) to 'nil' or acceptable level. In this context, the COD of the IC/Fenton reaction system is measured at different times of reaction and the results are plotted in figure 6.14.

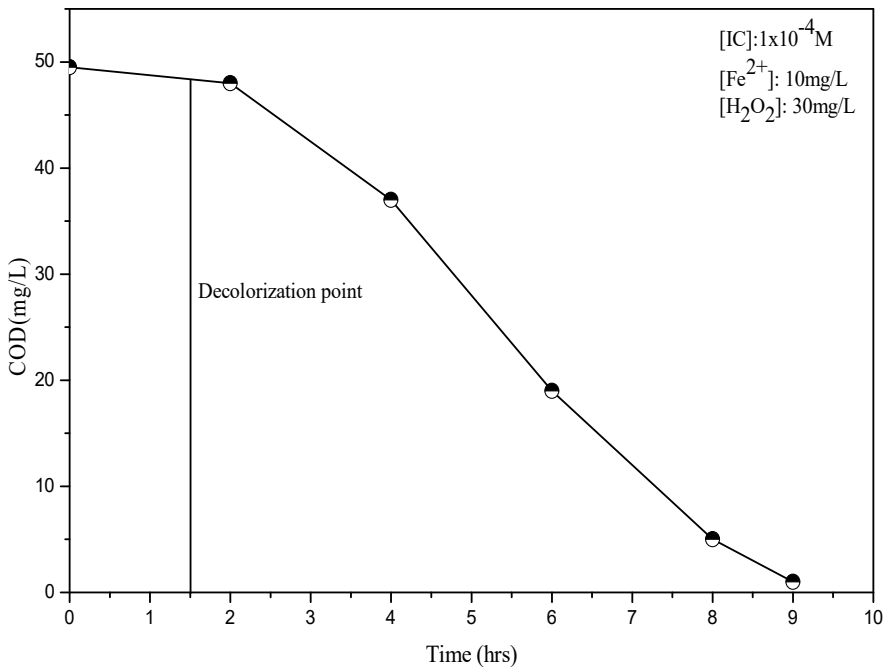

Fig. 6.14: Mineralization of IC during Fenton degradation

As seen in the figure, the COD remains fairly steady till decolorization of IC is complete and decreases steeply thereafter indicating that at least some of the intermediates formed during the decolorization are not stable and get mineralized fast. Continuation of the Fenton reaction results in complete mineralization. Hence it may be confirmed that Fenton process is an efficient inexpensive method for the complete removal of IC pollutant from water. Various intermediates present in the system at 50% degradation are analyzed by LC/MS and the results are shown in table 6.1. Eventually these intermediates also get degraded as seen from the complete elimination of COD in 9 hr. of Fenton reaction.

Table 6.1: Intermediates formed during the Fenton degradation of IC

m/z	Molecular Formula	Molecular structure
424	$C_{16}H_{12}N_2S_2O_8$	
217	$C_7H_7NSO_5$	
203	$C_6H_5NSO_5$	
226	$C_8H_4NSO_5$	
424	$C_{16}H_{12}N_2SO_{10}$	
347	$C_{14}H_7N_2SO_7$	
258	$C_8H_5NSO_7$	
116	$C_4H_4O_4$	

6.3.10 Activation of Fenton process by external energy sources

The efficiency of Fenton process has been reported to be enhanced by activation using external energy sources [274]. In this context, the application of three sources of energy, i.e., light (photoFenton), ultrasound (sonoFenton), and electricity (electroFenton) on the efficiency of the Fenton process for the degradation of IC is tested and the results are as follows:

6.3.10.1 Solar PhotoFenton process

The time taken for complete decolorization of IC in presence of Fenton reagent is reduced from 90 min. to 15min. under solar irradiation (see figure 6.15).

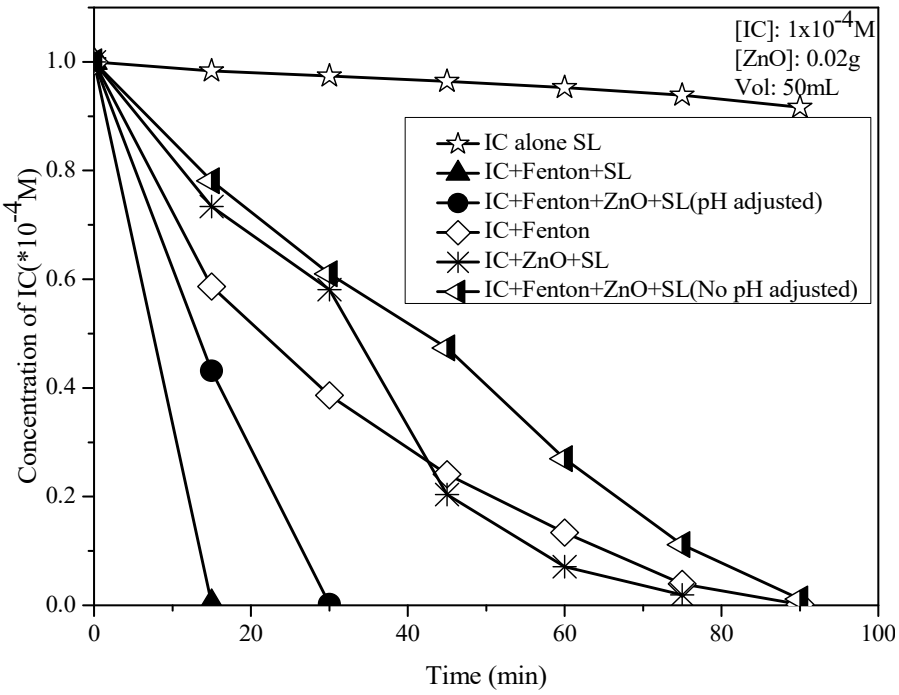

Fig. 6.15: Comparison of different solar photoFenton processes for the decolorization of IC

Presence of ZnO in classic Fenton has been proven to decrease the efficiency of the process, primarily due to change in pH (see Section 6.3.7). However, being a good solar photocatalyst, ZnO is likely to enhance the efficiency of Fenton process under sunlight. This possibility is tested under solar Fenton and the decolorization of IC is compared with and without ZnO under different conditions (figure 6.15). The efficiency of decolorization is in the order:

Solar Fenton > Solar photocatalyticFenton in presence of ZnO (pH adjusted to the regular Fenton pH) > Fenton > ZnO Photocatalysis ≥ photocatalyticFenton in presence of ZnO (no pH adjustment).

The results clearly demonstrate the superiority of the solar Fenton process for the degradation of IC. The presence of ZnO is unable to accelerate the degradation and overtake the efficiency of the simple photoFenton process. This is probably because the extra OH radicals generated by the photocatalytic action of ZnO is not enough to compensate for the ZnO-inhibition of the generation of OH radicals by the interaction of Fe^{2+} and H_2O_2. Thus it is seen that Solar Fenton process is highly efficient for the decolorization of IC in water.

6.3.10.2 SonoFenton Process

The effect of ultrasound (US) with frequency 350 KHz and power 80W as a source of activation on the Fenton degradation of IC is investigated. Experiments were carried out under the conditions optimized for normal Fenton. The results are shown in figure 6.16.

The time taken for complete decolorization of IC under sonoFenton (30 min.) is much less compared to sono only (75 min.) or Fenton only (90 min.). The results also show that the combined process (sonoFenton) is synergistic and is worth investigating in depth. Preliminary results on the synergy of sonoFenton are reported in Chapter 5.

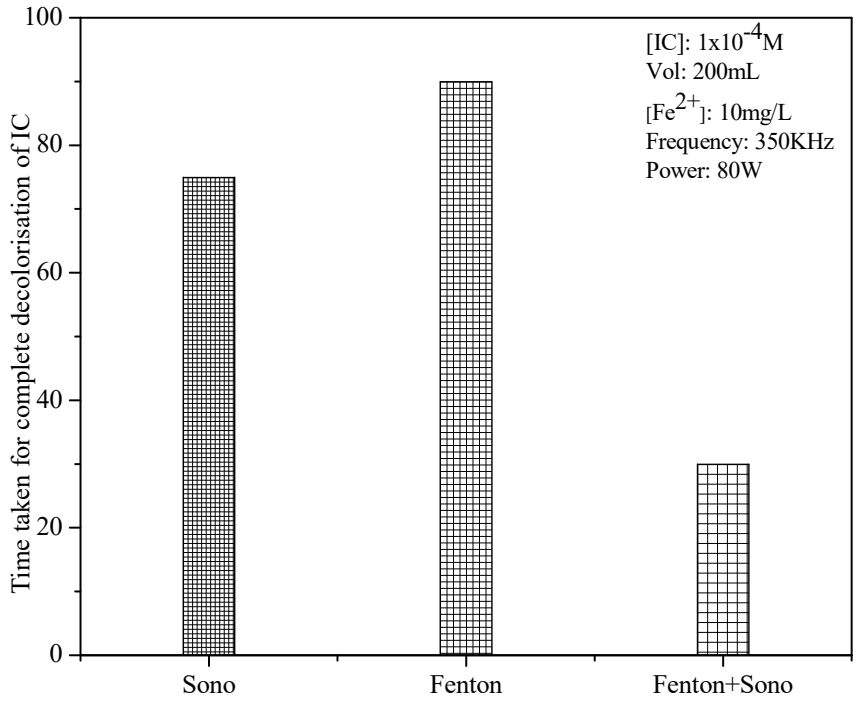

Fig. 6.16: Comparison of Fenton and SonoFenton processes for the degradation of IC

Ultrasound coupled with Fenton's reagent utilizes the advantages of the two methods to generate more $^{\cdot}OH$ radicals which can effectively enhance the degradation of IC. Also cavitation under US gives additional activation through pyrolysis, which will enhance the degradation. In heterogeneous sonoFenton process, acoustic cavitation can enhance mass

transfer, dispersion, and deaggregation of particles [275]. The increased formation of reactive ·OH radicals under Fenton, Ultrasound irradiation and the combination process can be summarized as follows [276,277]:

$$Fe^{2+} + H_2O_2 \rightarrow Fe^{3+} + HO^- + HO^\bullet \quad \text{(Fenton)} \qquad ....(6.14)$$

$$H_2O_2 +))) \rightarrow 2HO\cdot \text{ (US)} \qquad .....(6.15)$$

$$H_2O_2 + HO\cdot \rightarrow H_2O + HO_2^\bullet \quad \text{(Fenton, US)} \qquad ....(6.16)$$

$$Fe^{3+} + H_2O_2 \rightarrow Fe(OOH)^{2+} + H^+ \quad \text{(Fenton)} \qquad ....(6.17)$$

$$Fe(OOH)^{2+} +))) \rightarrow Fe^{2+} + HO_2^\bullet \quad \text{(US)} \qquad ....(6.18)$$

$$Fe^{3+} + HO_2^\bullet \rightarrow Fe^{2+} + H^+ + O_2 \quad \text{(Fenton, US)} \qquad ....(6.19)$$

In Fenton process, the propagation of US waves into the media results in two effects, i.e., enhanced interaction of Fe^{2+} with H_2O_2 and enhanced regeneration of Fe^{2+} in the system. This leads to more efficient generation of ·OH radicals and consequently enhanced degradation of the pollutant. This is in addition to the US-induced generation of free radicals in the gas bubble and/or in the bulk of the system as follows:

$$H_2O +))) \rightarrow H + {}^\bullet OH \qquad ....(6.20)$$

$${}^\bullet H + O_2 \rightarrow HO^\bullet_2 \rightarrow {}^\bullet OH + 1/2O_2 \qquad ....(6.21)$$

$$2\,{}^\bullet OH \rightarrow H_2O_2 \qquad ....(6.22)$$

$$2HO^\bullet_2 \rightarrow H_2O + O_2 \qquad ....(6.23)$$

Various parameters relevant for US-Fenton process such as power and frequency of the US, relative concentration of H_2O_2 and Fe^{2+}, presence of sono active catalyst, effect of cross-contaminants on the

efficiency of the process etc. can be further evaluated and optimized for improving the efficiency of the process. This, being an elaborate investigation, is undertaken as a separate project in our laboratory.

6.3.10.3 ElectroFenton (EF) Process

Earlier studies have shown that electrochemical process can be a viable AOP for the mineralization of pollutants from water [278-280]. Combination of electrochemical and Fenton process (EF) is another hybrid like sono and photoFenton process worth investigating for enhanced efficiency of the Fenton process. Appropriately designed EF process has the advantage of insitu generation of H_2O_2 and Fe^{2+} and can thus avoid the drawbacks of the chemical Fenton process. In the electrochemically assisted Fenton process also, the $^{\cdot}OH$ is produced via the usual Fenton's reaction. However in this case, Fenton's reagent is electrochemically generated in situ, thus avoiding the use of high quantities of H_2O_2 and iron (II) salt [84,281].

In the present study, the electrolytic degradation of IC is combined with the classic Fenton process. Bismuth doped titanium dioxide on titanium as the anode and graphite as cathode in presence of sodium sulphate as supporting electrolyte has been proven to be an efficient electrochemical system for the degradation of IC. Fe^{2+} is added to the system and together with the insitu formed H_2O_2 a Fenton like system is evolved. The degradation of the dye is faster in the case of electroFenton compared with that of the normal electrolytic or Fenton reaction. The results are shown in figure 6.17. As in the case of sonoFenton and photoFenton, electroFenton process also is synergistic, though the

synergy is less compared to other processes. In any case the hybrid process is additive for the degradation of IC (See Table 6.2).

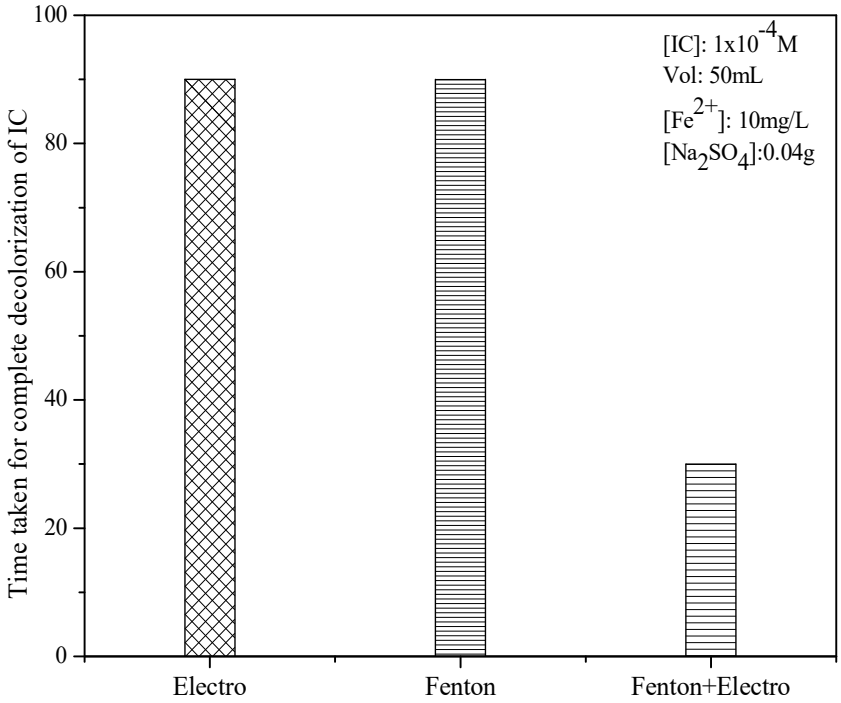

Fig. 6.17: Comparison of Fenton and electro Fenton process for the degradation of IC

In the electroFenton process, pollutants are destroyed by the action of Fenton reagent in the bulk as well as the anodic oxidation at the anode surface. Here the insitu H_2O_2 production is slower because O_2 solubility in water is low and the current efficiency also is low at lower pH of the Fenton reagent. One way to sustain the efficiency of electroFenton process is to continuously add H_2O_2 and Fe^{2+}. However the efficiency of Fe^{2+} regeneration from Fe^{3+} is slow even at optimal current density. Consequently, the rate of degradation will slow down with time. The

efficiency of the electroFenton process depends on the nature of the electrodes, pH, catalyst concentration, electrolyte, dissolved O_2 level, temperature, current density etc.. Detailed investigation on these factors will be important in identifying the optimum conditions. Based on the indicative results presented in this Chapter, detailed investigation on these and other factors are being undertaken separately as another project.

6.3.10.4 Comparison of different hybrid Fenton processes for the decolorization of IC

Comparison of various types of Fenton processes for the decolorization of IC is shown in figure 6.18.

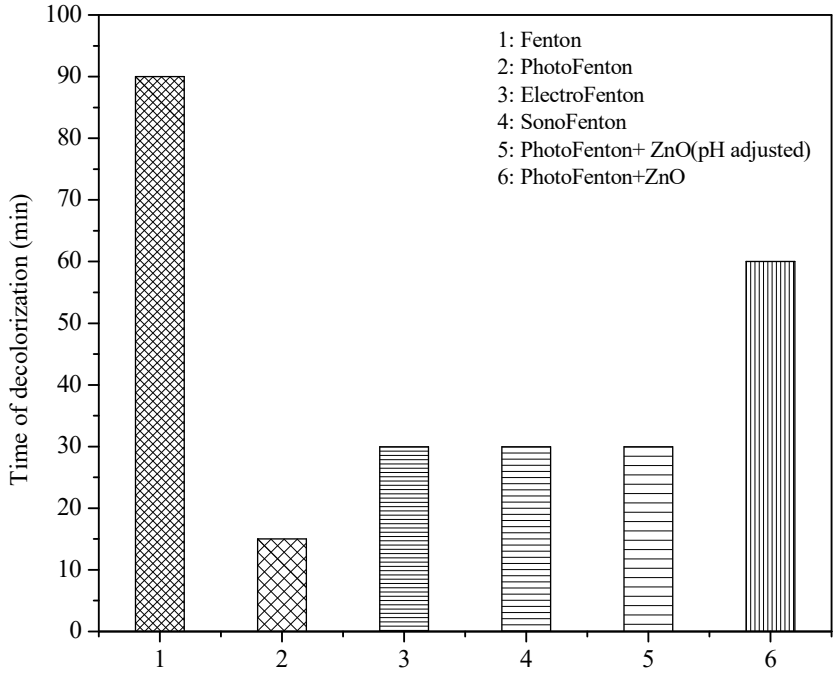

Fig. 6.18: Comparison of different combinations of Fenton process for the decolorization of IC

The combination process is more efficient and synergistic compared to simple Fenton process for the degradation of IC with the efficiency being in the order;

PhotoFenton > ElectroFenton ≈ SonoFenton ≈ Photocatalytic (ZnO) Fenton (pH adjusted) > Photocatalytic (ZnO) Fenton (no pH adjustment) > Fenton

Comparative rate of degradation and synergy of the combination process over respective individual processes are computed and tabulated in Table 6.2.

Table 6.2: Comparative rate of degradation of IC under Fenton and combination Fenton process

Process	Initial rate of degradation × 10^{-7} (mg/L/min.)	Synergy
Fenton	13.7	–
Solar photolysis	8.7	–
Solar PhotoFenton	33.0	1.47
Sono	2.3	–
SonoFenton	19.0	1.19
Electro	8.3	–
ElectroFenton	23.0	1.06

However, the synergy decreases with time of reaction, possibly because of the formation of intermediates which also compete with the substrate for the reactive free radicals. The results in Fig.6.18 reveal that solar photoFenton is the most efficient process (among those tested here) for the decolorization of IC. PhotocatalyticFenton with ZnO as the catalyst (after adjusting the pH to that of classic Fenton) is only as efficient as electro and sonoFenton. Presence of ZnO increases the pH of

the system which is detrimental to the efficiency of Fenton process as has been discussed earlier. Hence adjustment of the pH to the optimum pH of normal Fenton is important in any combination Fenton process. In any case, presence of a solar photocatalyst such as ZnO may be beneficial for the efficiency of the solar process especially for mineralization. This is verified by testing the role of solar photocatalysis in the mineralization of IC (which is tested by COD reduction).

6.3.11 Mineralization (COD reduction) using different combinations of Fenton reaction

The efficiency of various Fenton processes for the total mineralization of IC is verified experimentally by measuring the reduction in chemical oxygen demand (COD) of the system under respective processes. The results are presented in figure 6.19.

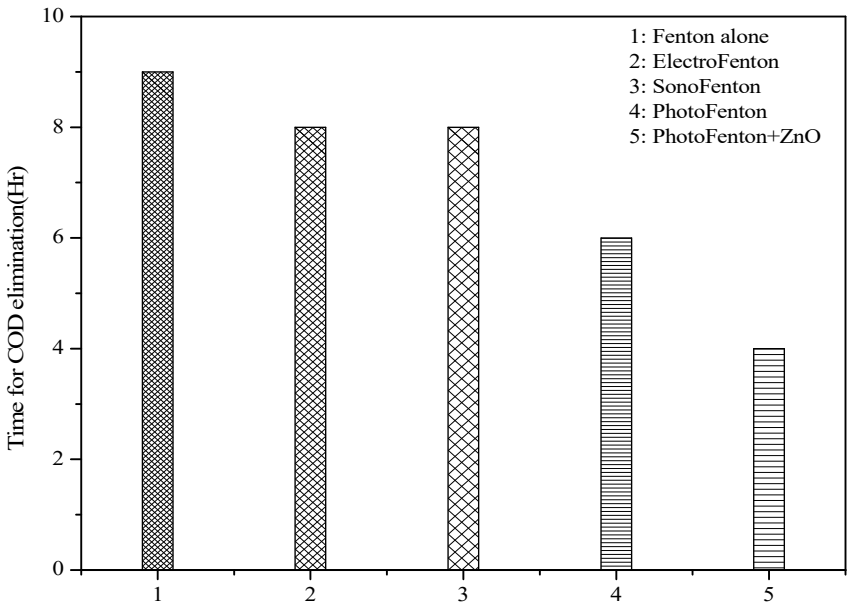

Fig. 6.19: Comparison of the COD reduction using different combinations of Fenton process

Solar photocatalyticFenton with ZnO catalyst is identified as the most efficient process for COD reduction. The comparative efficiency of various processes for the mineralization is in the order;

ZnO- solar photocatalyticFenton > Solar photoFenton > SonoFenton ≈ ElectroFenton > Fenton.

The results show that even though the presence of ZnO inhibits the decolorization of IC under normal Fenton process, it assists the mineralization under photolysis due to the photocatalytic activity of ZnO. Thus photoFenton is the most efficient process for decolorization of IC while photocatalyticFenton is most efficient for its mineralization.

6.3.12 General Mechanism

The first step in the Fenton reaction is the oxidation of ferrous to ferric ions and decomposition of H_2O_2 into $^{\bullet}OH$ radicals as follows:

$$Fe^{2+} + H_2O_2 \rightarrow Fe^{3+} + OH^- + {}^{\bullet}OH \quad ....(6.24)$$

The Fe^{3+} is reduced by excess H_2O_2 to regenerate Fe^{2+} and more free radicals as in reaction (6.25)

$$Fe^{3+} + H_2O_2 \rightarrow Fe^{2+} + HO_2^{\bullet} + H^+ \quad ....(6.25)$$

Other possible reactions are:

$$Fe^{2+} + {}^{\bullet}OH \rightarrow Fe^{3+} + OH^- \quad ....(6.26)$$

$$Fe^{2+} + HO_2^{\bullet} \rightarrow Fe^{3+} + HO_2^- \quad ....(6.27)$$

$$Fe^{3+} + HO_2^{\bullet} \rightarrow Fe^{2+} + O_2 + H^+ \quad ... (6.28)$$

The highly reactive free radicals may get deactivated by self-scavenging, interaction with other radicals and/or H_2O_2 as follows:

$$^{\bullet}OH + {}^{\bullet}OH \rightarrow H_2O_2 \quad ....(6.29)$$

$$^{\bullet}OH + H_2O_2 \rightarrow HO_2^{\bullet} + H_2O \quad ....(6.30)$$

$$HO_2^{\bullet} + HO_2^{\bullet} \rightarrow H_2O_2 + O_2 \quad ....(6.31)$$

$$^{\bullet}OH + HO_2^{\bullet} \rightarrow H_2O + O_2 \quad ....(6.32)$$

In the absence of any organic substrate to be oxidized, H_2O_2 self-decomposes as in reaction (6.33).

$$2H_2O_2 \rightarrow 2H_2O + O_2 \quad ....(6.33)$$

In presence of organic molecules (R), such as IC in the current instance, the degradation can take place as in reactions (6.34) – (6.36) or dimerization occurs as in (6.37). Eventually mineralization takes place as in (6.38).

$$^{\bullet}OH + R \rightarrow H_2O + R^{\bullet} \rightarrow \text{(Partial mineralization + Colorless intermediates)} \quad ....(6.34)$$

$$R^{\bullet} + Fe^{2+} \rightarrow R^{-} + Fe^{3+} \quad ....(6.35)$$

$$R^{\bullet} + Fe^{3+} \rightarrow R^{+} + Fe^{2+} \quad ....(6.36)$$

$$R^{\bullet} + R^{\bullet} \rightarrow RR \quad ....(6.37)$$

$$R^{\bullet} \text{ or } R^{-} \text{ or } R^{+} \text{ or } RR + {}^{\bullet}OH, HO_2^{\bullet}, H_2O_2 \text{ etc.}$$
$$\rightarrow \text{intermediates} \rightarrow \rightarrow \rightarrow CO_2 + H_2O + \text{salts (mineralization)} \quad ....(6.38)$$

Thus at room temperature and pressure itself, a series of reactive free radicals are generated and these can interact with the dye in a variety of ways to produce intermediates and eventually mineralize the pollutant.

The decolorization/mineralization is accelerated by external energy sources such as UV light, sunlight, ultrasound, microwave, electrolysis etc. Relevant mechanisms are discussed in respective sections.

6.4 Conclusion

Classic Fenton reaction involving use of simple Fe^{2+} salt and H_2O_2 at the optimized ratio under ambient conditions is revisited and used as an effective advanced oxidation technique for the removal of traces of the toxic dye pollutant Indigo Carmine from water. pH is a critical parameter in the process. Naturally occurring contaminant salts in water can affect the mineralization of the dye favorably or adversely depending on the nature of the salt and the reaction condition. The volume of the reactants is not a constraint as long as the necessary ingredients are available in the required ratio. These factors together with the relative simplicity of the process make Fenton reaction a promising candidate for economic and efficient waste water treatment. ZnO which is an efficient photocatalyst in many AOPs inhibit the Fenton degradation in the absence of light, probably due to change in pH. The presence of suspended particles which inhibit the interaction between Fe^{2+} and H_2O_2 and thereby the formation of $^{\cdot}OH$ is another cause. The degradation is enhanced synergistically by external sources of activation such as sunlight, ultrasound and electrical energy. PhotocatalyticFenton process with ZnO as the catalyst is more efficient than other processes including photoFenton for the mineralization of the dye pollutant.

.....ꕥ.....

Chapter

7

SOLAR PHOTOCATALYTICFENTON PROCESS AS A HIGHLY EFFICIENT AOP FOR THE MINERALIZATION OF MULTIPLE CHEMICAL POLLUTANTS IN WATER

Contents

7.1 Introduction

The current study has identified solar photocatalyticFenton (SPF) process mediated by ZnO as a highly efficient AOP for the mineralization of the dye pollutant IC in water. The application of this hybrid AOP using the environment friendly and economical solar energy as the source of activation for the decontamination of water from different types of pollutants is tested by selecting four (4) typical families of chemical pollutants: Dyes, Petrochemicals, Pesticides and Pharmaceuticals. Only the qualitative application of the AOP is tested here to establish the suitability of the process. Specific parameters need to be optimized for specific applications, which is outside the scope of the current study.

7.2 Experimental Details

7.2.1 Materials used

The main materials used in the study are, Indigo Carmine and Rhodamine B (dyes), Phenol and Acetophenone (petrochemicals), Paracetamol and Diclofenac (pharmaceuticals), Diquat and Carbendazim (pesticides) and ZnO catalyst. Relevant details about these materials and their characteristics are provided in Chapter 2. Unless indicated otherwise, all materials used are of AnalaR grade or equivalent and are used as such without further purification.

7.3 Results and Discussion

7.3.1 Preliminary experiments

The synthetic polluted water samples were prepared in double distilled water and also in natural field water collected from the river Periyar at Aluva. The location map showing sample collection point is given in figure 7.1. The collected river water sample is analyzed for various characteristics and the results are presented in Table 7.1

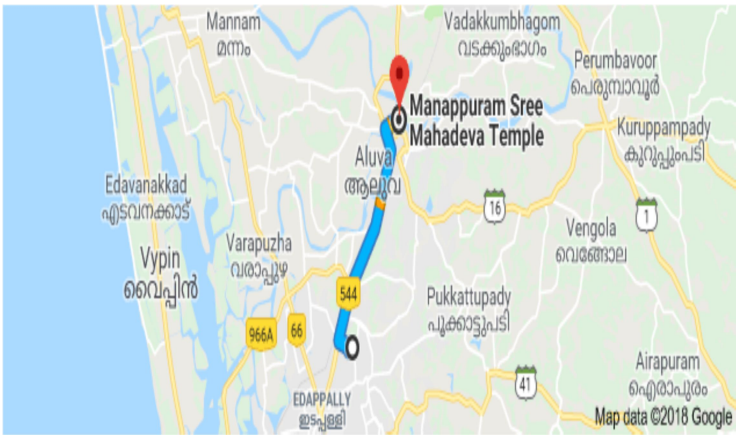

Fig. 7.1: Location of collection of the Periyar river water sample

Table 7.1: Various quality parameters of the river water sample

Sl.No.	Parameter	Value
1	pH	7.34
2	Suspended Solids (NTU)	2
3	Dissolved Oxygen (mg/L)	5.32
4	Redox potential (Eh) (mV)	5
5	EC (µS)	34.71
6	TDS (mg/L)	32.57
7	Salinity (mg/L)	24.91
8	Chloride (mg/L)	2.63
9	Sulphate (mg/L)	1.42
10	Nitrate (mg/L)	2.29
11	Phosphate (mg/L)	ND
12	Sodium (mg/L)	2.6
13	Potassium (mg/L)	3.56
15	Calcium (mg/L)	9.72
16	Magnesium (mg/L)	7.33
16	Aluminium (mg/L)	Not Detected

7.3.2 Dye pollutants

Increased demand for textile production and use of synthetic dyes is causing severe water pollution. Indigo Carmine (IC) and Rhodamine B (RhB) are two major dye pollutants and their complete removal from water is important from environmental and safety angles. In this context, solar photocatalyticFenton (SPF) degradation of RhB and IC is investigated under laboratory conditions using distilled water as well as river water as the matrix.

The structure and relevant physicochemical characteristics of the dyes are provided in Chapter 2. The structures are reproduced below.

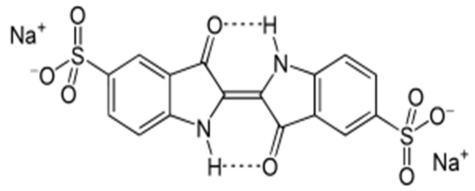

Indigo Carmine (IC)

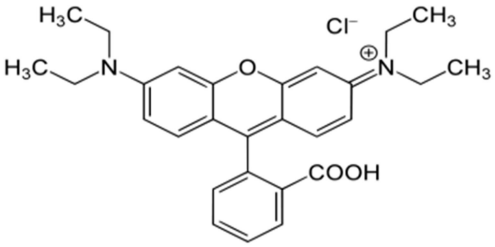

Rhodamine B (RhB)

7.3.2.1 Indigo Carmine, Rhodamine B

IC is an acidic dye widely used for industrial purposes such as printing and dyeing in textiles, paper, paints etc. It is also used as an antibacterial and dermatological agent. It is a recalcitrant toxic pollutant and a potent carcinogen [134,135,282].

The application of SPF process for the mineralization of IC has already been investigated in detail as reported in Chapter 6, with distilled water as the matrix. Reaction conditions optimized with distilled water as the matrix are used in the case of natural river water matrix also for both dyes. The parameters are: [Dye] = 10 mg/L, [ZnO] = 0.02 g, $[Fe^{2+}]$ = 10 mg/L and H_2O_2 = 30 mg/L. The degradation of IC and RhB is measured using

UV-Visible spectroscopy at λ_{max} = 609 and 554 nm respectively. Results on the degradation/decolorization and mineralization of the dyes in distilled water are plotted in Figures 7.2 and 7.3 respectively. The degradation (in terms of decolorization) and complete mineralization are evaluated in natural river water also and the results are presented in figures 7.4 and 7.5 respectively.

The comparative degradation of the two dyes in distilled water (Fig. 7.2) shows that it takes 15 minutes for the decolorization of IC. For RhB and the combination of the two (IC+RhB), the time taken for decolorization is the same, i.e.30 minutes.

In the case of mineralization (Fig. 7.3), IC is faser and takes only 2 hrs. RhB takes 6 hr for complete mineralization. Surprisingly the result shows that the combination of IC and RhB takes less time (4 hr) for mineralization than even RhB alone. It may be because IC is acting as a photosensitizer in this case making ZnO an even more efficient solar potocatalyst. Hence the mineralization of RhB is faster in the presence of IC, thereby making the mineralization of the combination faster.

In the case of river water also the same trend as in distilled water is followed (Fig. 7.4). IC takes 15 minutes for the decolorization. RhB as well as the combination of the two (IC + RhB) take 30 minutes for complete decolorization.

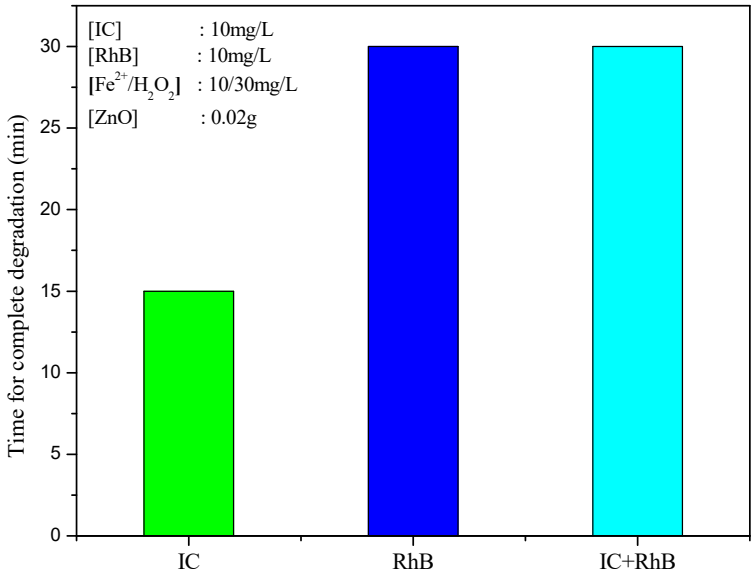

Fig. 7.2: Comparative time taken for decolorization of IC, RhB and (IC+RhB) in distilled water

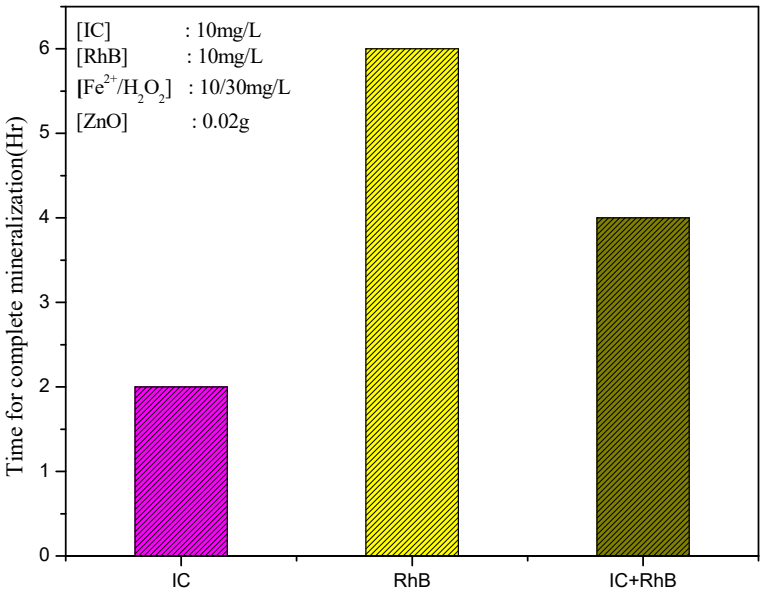

Fig. 7.3: Comparison of the mineralization of IC, RhB and (IC +RhB) distilled water

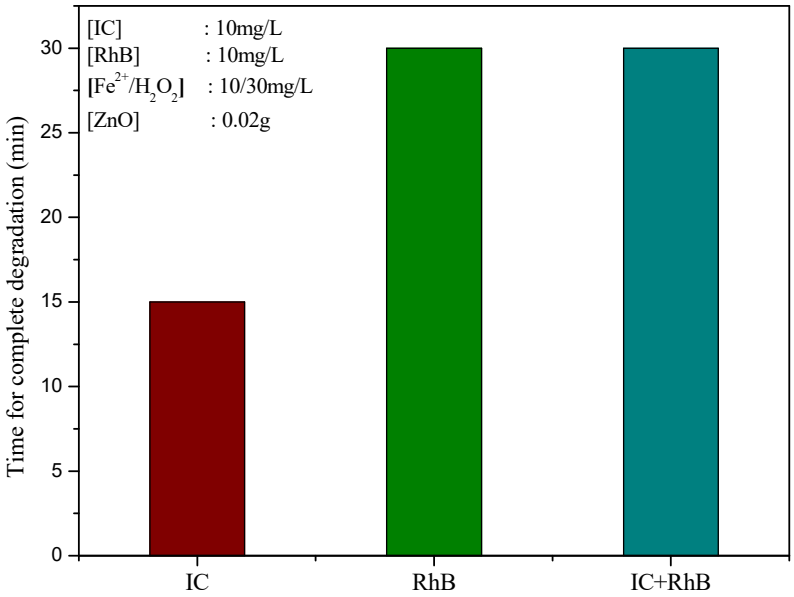

Fig. 7.4: Comparative time taken for decolorization of IC, RhB and (IC+RhB) in river water

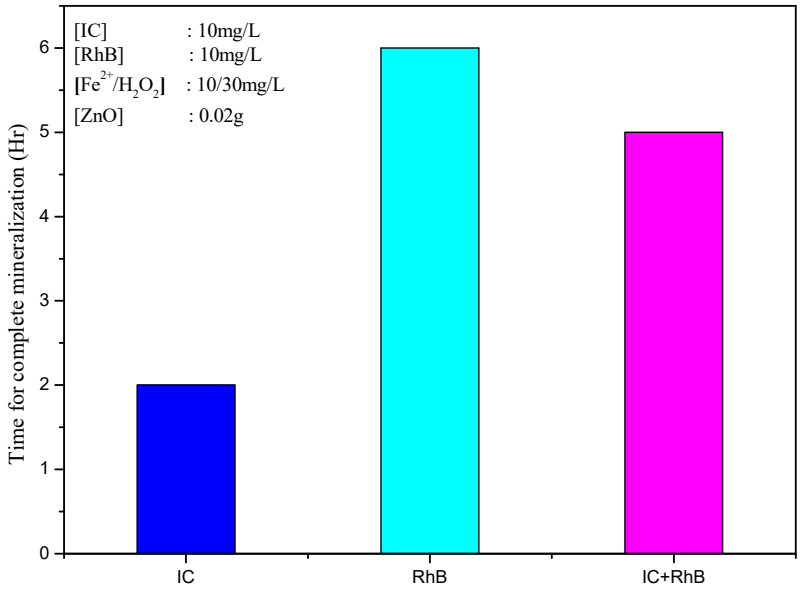

Fig. 7.5: Comparative mineralization of IC, RhB and (IC+RB) in river water

The mineralization also follows the same trend as in distilled water (Fig. 7.5). The rate of mineralization is in the order

IC > (IC+RhB) > RhB

The decolorization of the dye in distilled water and river water is compared in figure 7.6. The mineralization in the two matrices is compared in figure 7.7

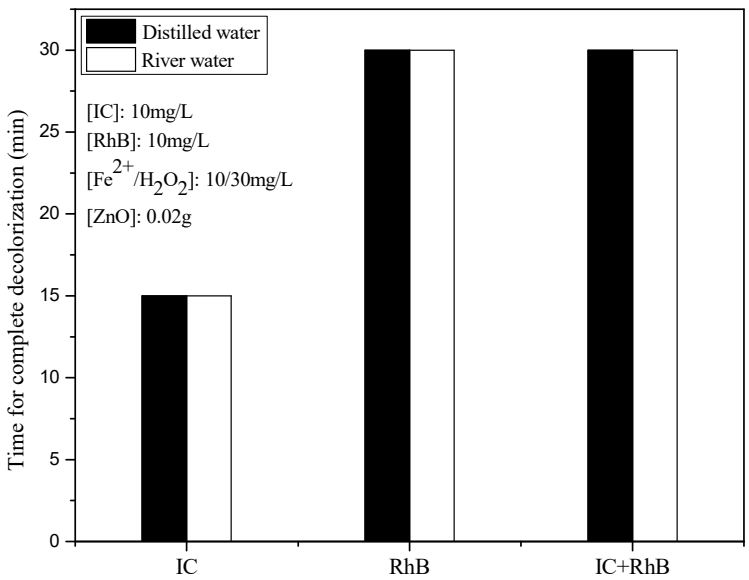

Fig. 7.6: Comparison of the decolorization of the dyes IC, RhB and (IC+RB) in distilled water and river water

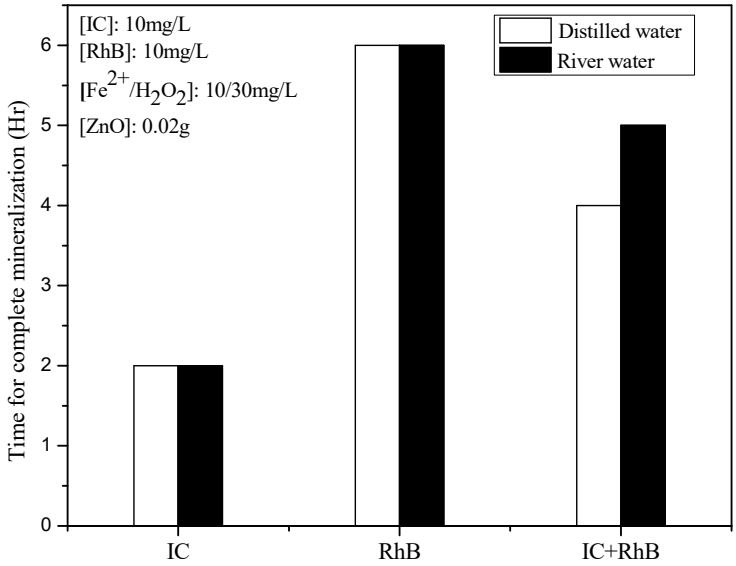

Fig. 7.7: Comparison of the mineralization of the dyes IC, RhB and (IC+RB) in distilled water and river water

The results in figure 7.6 show that the contaminants present in natural river water do not affect the efficiency of solar photocatalyticFenton decolorization of IC, RhB and the combination (IC+ RhB). However, the mineralization of the combination (IC + RhB) is slightly slower in river water (Fig. 7.7) thereby suggesting that the natural contaminants in water inhibit the mineralization moderately.

The results show that this method (SPF) can be a potential candidate AOP for the decontamination of wastewater from these two dye pollutants.

7.3.3 Petrochemicals

7.3.3.1 Phenol and Acetophenone

In this category, two of the most widely used petrochemicals i.e., Phenol and Acetophenone are used as test pollutants to verify the efficiency

of solar photocatalyticFenton mediated by ZnO. Phenolic compounds are present in the effluents of various industries such as oil refining, petrochemicals, pharmaceuticals, resin manufacturing, plastics, paint, pulp, paper products etc.. Discharge of this pollutant without proper treatment may lead to serious health risks to humans, animals, and aquatic systems [283].

Phenol and Acetophenone are analyzed by Gas Chromatography using Flame Ionisation detector, Elite 1301 column and hydrogen as the carrier gas. The structure of phenol is given below;

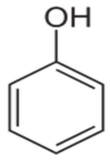

Phenol

Acetophenone (structure given below) is a by-product in phenol-acetone synthesis and finds application in many industries such as polymers, catalysts, food flavors, fragrance, dyes etc.. It is a major pollutant in the effluent water from such industries.

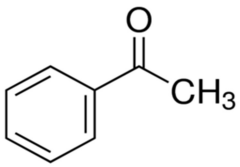

Acetophenone

The degradation of phenol and acetophenone in distilled water is shown in figure 7.8. Phenol is completely degraded in 60 minutes while it takes over 90 minutes for complete degradation of ACP. The primary degradation of the combination (phenol + acetophenone) is not tested due to constraints in the analytical procedure used here. However, the mineralization which is followed by COD measurements could be tested

for the combination also. In distilled water, the mineralization of phenol, acetophenone and (phenol + acetophenone) is complete in 3 hr, 4 hr and 5 hr respectively (figure 7.9). In the case of river water matrix, the degradation of both phenol and acetophenone takes slightly longer time (90 minutes for phenol and 120 minutes for ACP) compared to distilled water matrix (figure 7.10). Correspondingly, the time taken for mineralization is also more in river water compared to that in distilled water for the two pollutants individually and in combination (4 hr for phenol, 5 hr for ACP and 6 hr for the combination) (figure 7.11).

The comparative degradation of phenol and ACP in distilled water and river water is presented in figure 7.12. Similar comparison of the mineralization of the pollutants, individually and in combination is given in figure 7.13.

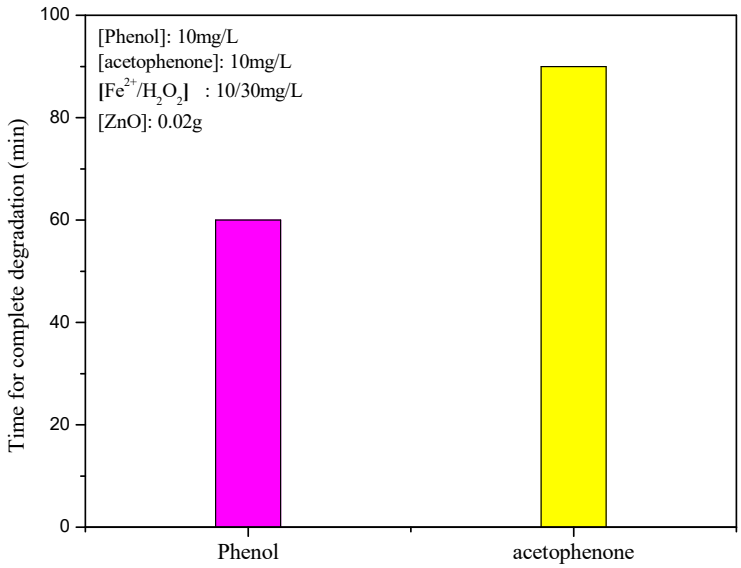

Fig. 7.8: Comparative time taken for degradation of phenol and ACP in distilled water

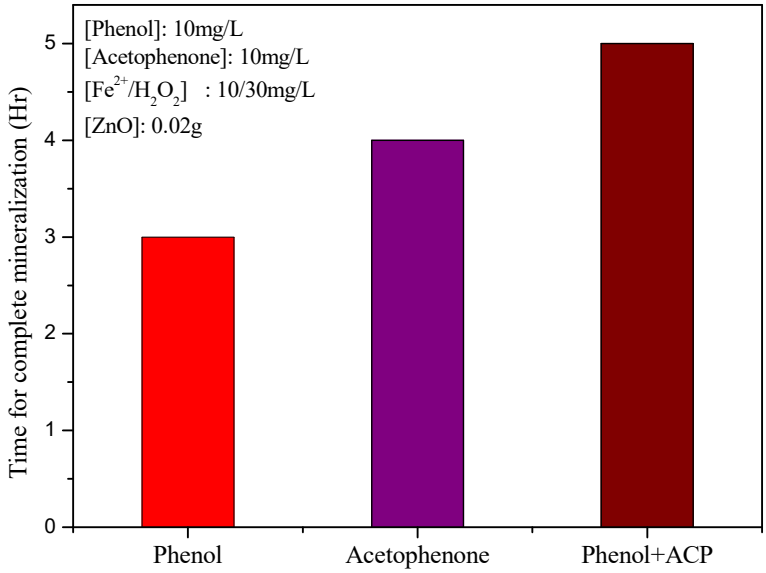

Fig. 7.9: Mineralization of phenol ACP and (Phenol+ACP) in distilled water

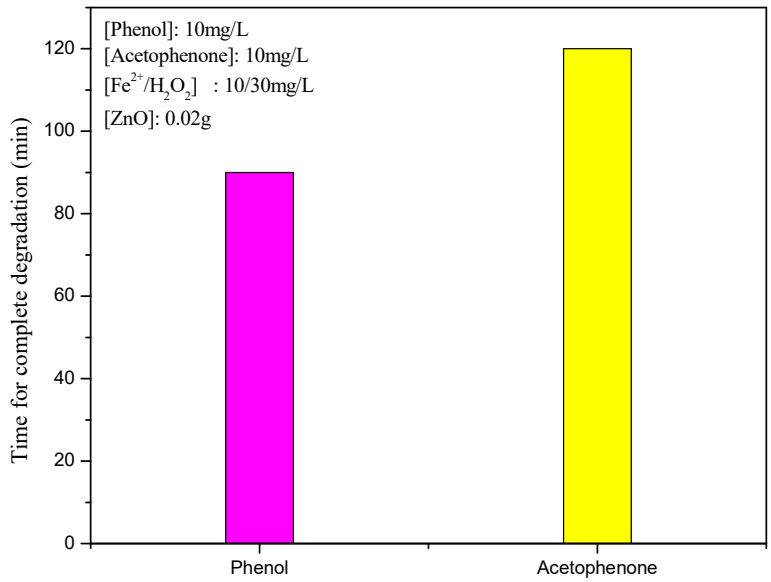

Fig. 7.10: Comparative time taken for degradation of phenol and ACP in river water

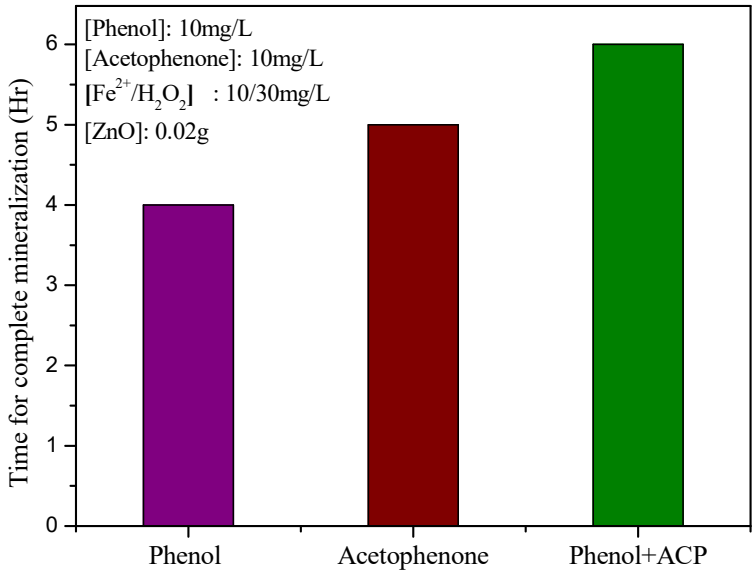

Fig. 7.11: Mineralization of phenol ACP and (Phenol+ACP) in river water

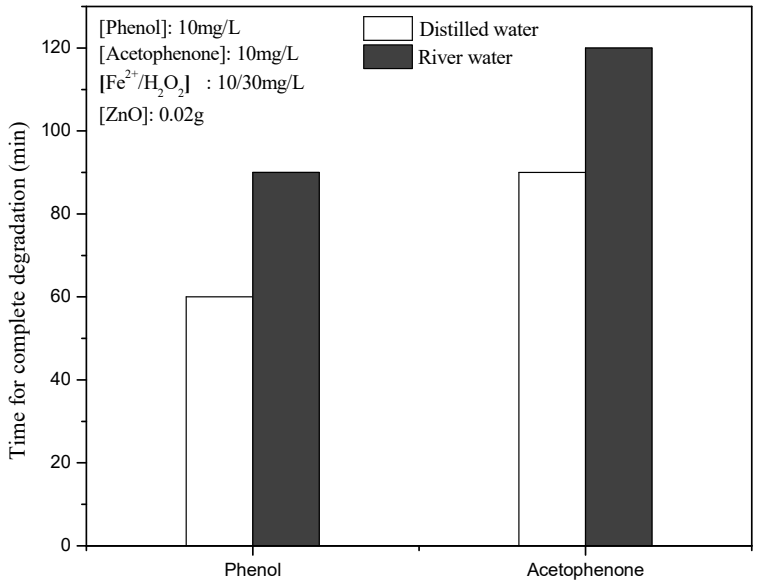

Fig. 7.12: Comparison of the degradation of phenol and ACP in distilled water and river water

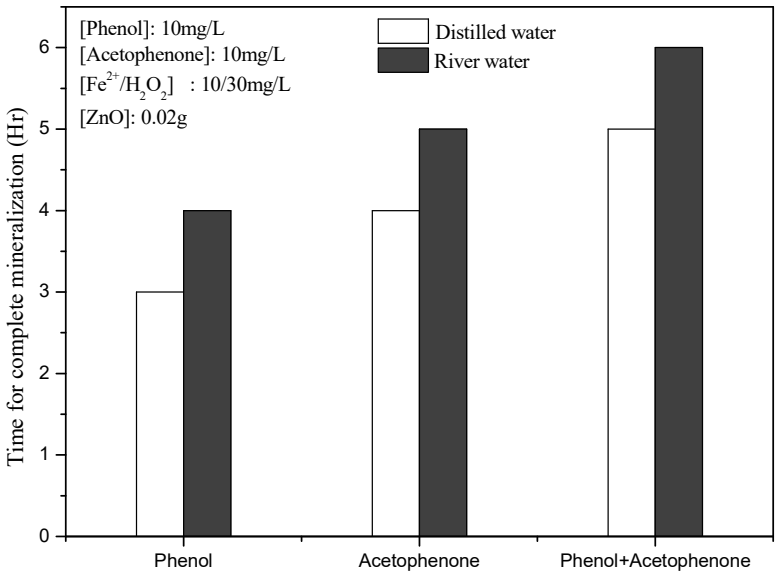

Fig. 7.13: Mineralization of phenol, ACP and (Phenol +ACP) in distilled water and river water

The results show that the time taken for degradation and mineralization of both pollutants, individually and in combination, is more in river water than in distilled water. Hence the dissolved salts/ions present in natural water are interfering with the degradation of the two petrochemical pollutants.

7.3.4 Pharmaceuticals

The effect of the pharmaceutical compounds and their metabolites in the aquatic environment has been recognized as an emerging health issue. Only little is known regarding the potential effects of many pharmaceutical pollutants on organisms present in the aquatic environment except the chronic toxicity and possible additive effects [284]. Hence elimination of even traces of pharmaceutical pollutants is essential from

the ecological angle as well. In this context, the application of solar photocatalyticFenton process is tested for the removal of two typical pharmaceutical pollutants, i.e. paracetamol and diclofenac.

7.3.4.1 Paracetamol, Diclofenac

Paracetamol (structure given below) is a synthetic drug used to relieve and reduce fever. It is often found in effluent water from related industries and also in water and wastewater from hospitals. The concentration of paracetamol in water is analysed by UV-VIS spectroscopy at λ_{max} of 243 nm.

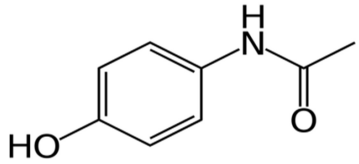

Paracetamol

Diclofenac is one of the important pharmaceutical molecules of widespread use. It is available in various forms such as ointment, tablets, capsules etc. and is one of the most widely used analgesics in the world. Hence the probability of water contamination from manufacturing and formulation sites, hospitals, individual households etc. is very high. Diclofenac is analyzed by UV-VIS spectroscopy at λ_{max} of 275 nm. The structure of diclofenac is given below.

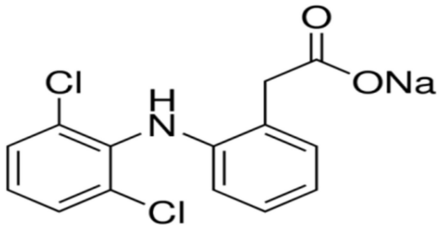

Diclofenac

The photocatalyticFenton degradation of paracetamol and diclofenac in distilled water at different times of irradiation is given in figure 7.14.

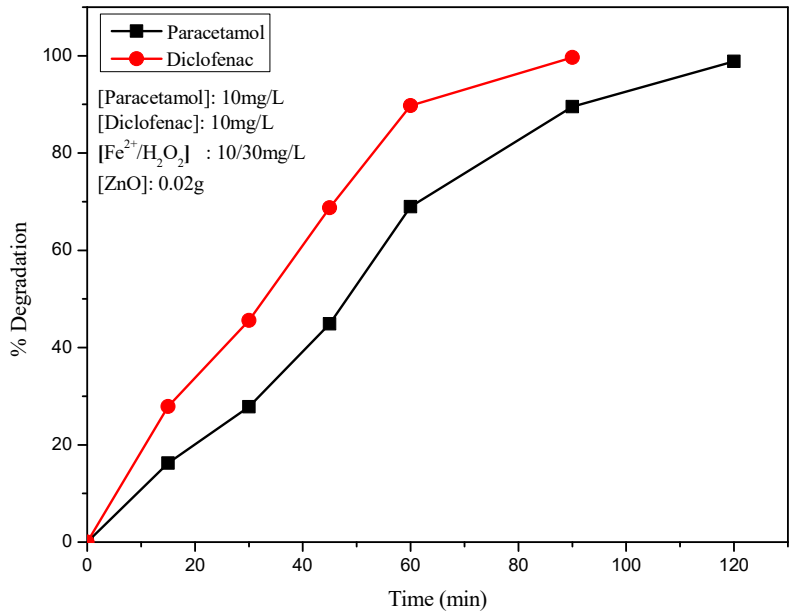

Fig. 7.14: Comparative degradation of paracetamol and diclofenac in distilled water

The degradation is complete in 100 minutes in the case of diclofenac and 120 minutes in the case of paracetamol. The primary degradation of the combination is not tested due to limitation of the analytical technique used (λ_{max} of the two molecules overlap to some extent making the precise determination of the concentration of the individual components in the combination difficult). The mineralization of the two pollutants (determined by measuring the COD) individually and in combination is compared in figure 7.15.

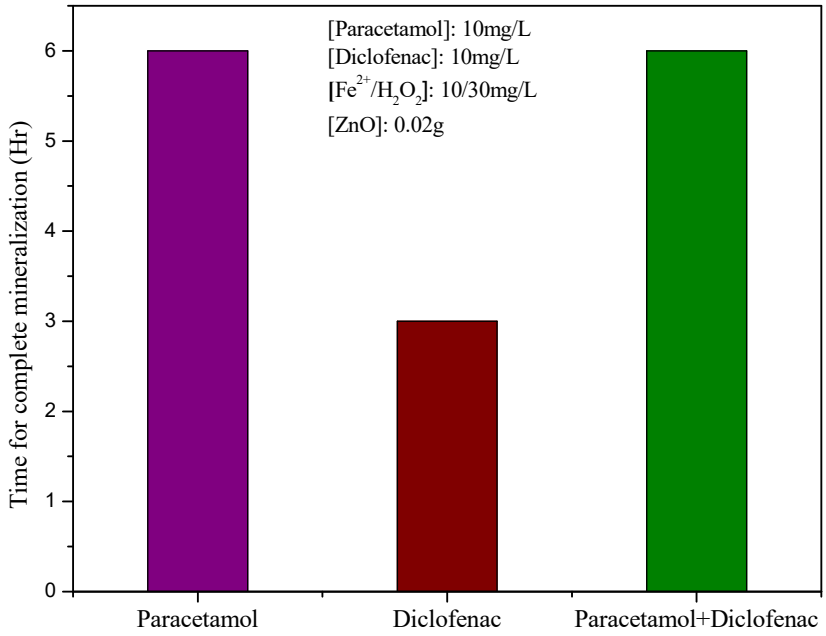

Fig. 7.15: Comparative mineralization of paracetamol, diclofenac and paracetamol+diclofenac in distilled water

Diclofenac gets mineralized much faster compared to paracetamol. The combination of diclofenac and paracetamol also gets mineralized at the same rate as paracetamol. Hence the presence of one component does not affect the mineralization of the other. This is important in the application of the process for the treatment of water contaminated with multiple pollutants. The rate of degradation/mineralization of the two pollutants in river water is also tested under identical condition as in distilled water. The results (figure 7.16) are fairly same as in distilled water. However the mineralization is slower in the case of diclofenac in river water compared to that in distilled water (figure 7.17). The mineralization of the combination also is slower in river water.

In the case of distilled water, the mineralization of the combination (paracetamol + diclofenac) takes the same time as that of the slower mineralizing component (paracetamol), i.e., ~ 6 hr. Hence, the components or their degradation products do not interact in such a way as to affect the mineralization. However, in the case of river water matrix, mineralization of the combination takes more time than that for either of the components. Hence the natural contaminants present in river water are interacting with the intermediates of degradation, thereby inhibiting the mineralization.

Comparative effect of the matrix (distilled water vs river water) on the degradation and mineralization of paracetamol and diclofenac is presented in figure 7.18 and 7.19 respectively. The data confirm the inhibiting effect of contaminants in river water on the mineralization of diclofenac as well as of the combination. The effect is negligible in the case of paracetamol.

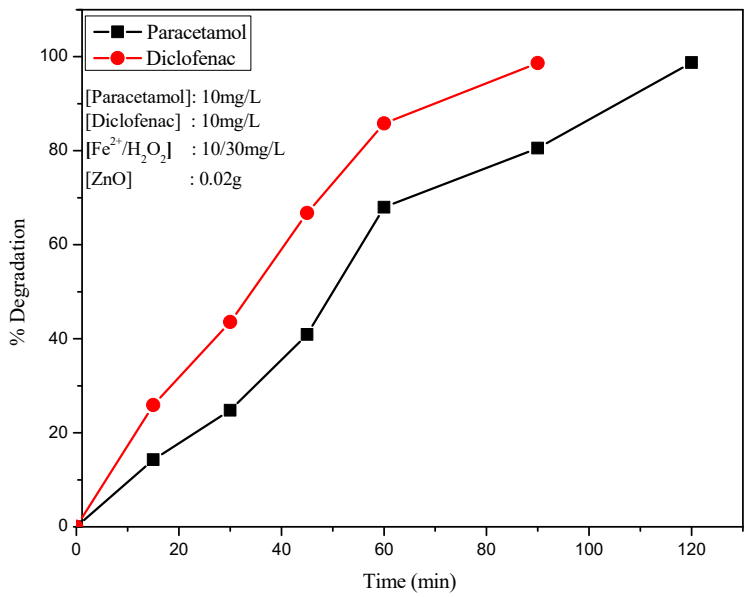

Fig. 7.16: Comparative degradation of paracetamol and diclofenac in river water

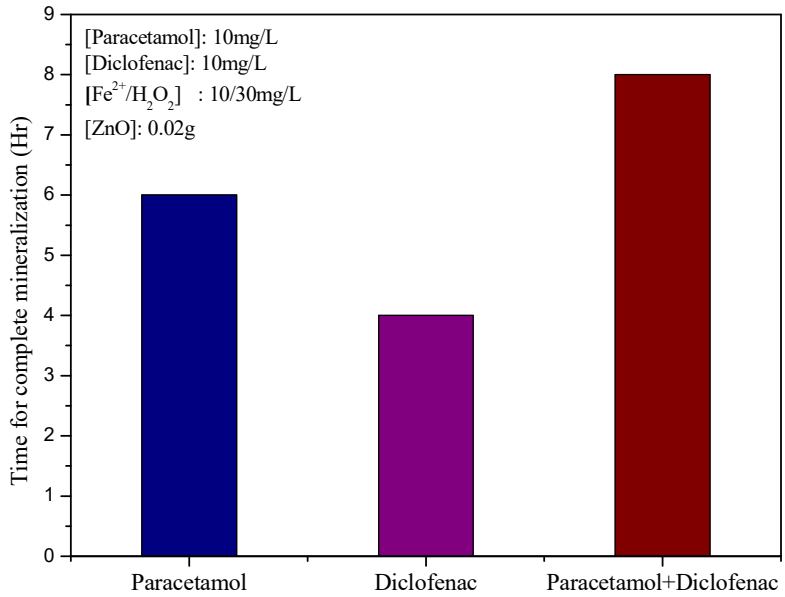

Fig. 7.17: Comparative mineralization of paracetamol, diclofenac and paracetamol+diclofenac in river water

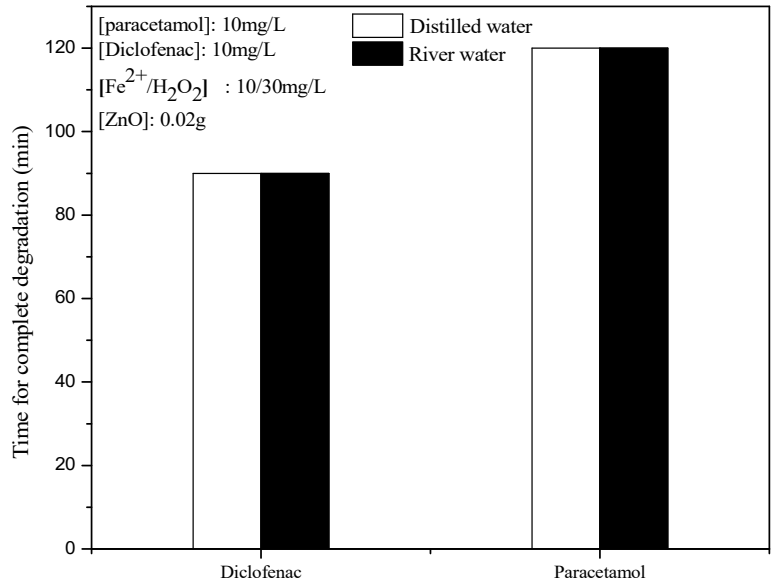

Fig. 7.18: Comparative effect of distilled water and river water matrices on the degradation of paracetamol and diclofenac

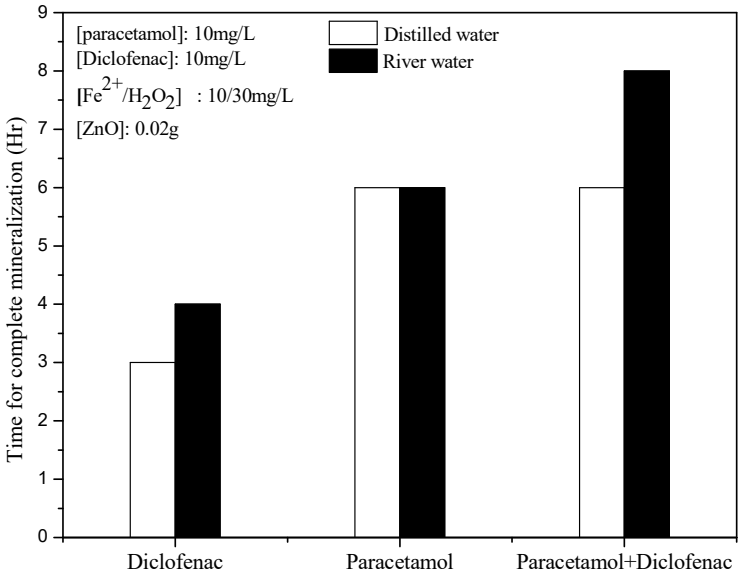

Fig. 7.19: Comparative effect of distilled water and river water matrices on the mineralization of paracetamol, diclofenac and paracetamol+diclofenac

The results show that the presence of contaminants (in natural water) can slow down the decontamination of water at least in the case of the pharmaceutical pollutant diclofenac. The effect is different in the case of diclofenac from that of paracetamol thereby suggesting that the chemistry of the molecule, its degradation products, the water contaminants and their interactions are important in the rate of degradation/mineralization.

7.3.5 Pesticides

Another class of pollutants tested for the efficacy of solar photocatalyticFenton process in water purification is pesticides. Diquat (a herbicide) and carbendazim (a fungicide) are chosen as the test pollutants.

7.3.5.1 Diquat (Dq), Carbendazim (Cz)

Diquat is a widely used herbicide. It is acutely toxic when absorbed through the skin and the possibility for poisoning increases with repeated exposure [137]. It is also a major contaminant of water. The concentration of Dq in water is estimated by UV-Vis spectroscopy at λ_{max}=310 nm. The chemical structure of diquat is given below;

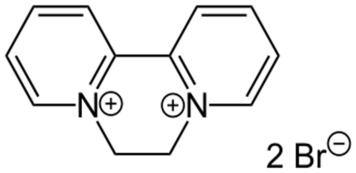

Diquat

Carbendazim is a systemic benzimadazole fungicide that has extensive application. It is used to control diseases in cereals, fruits, vegetables and ornamental plants. It is also used for seed pre-planting treatment and postharvest food storage. The concentration of carbendazim is analysed by UV-VIS spectroscopy at its λ_{max} = 284 nm. The chemical structure of carbendazim is as given below;

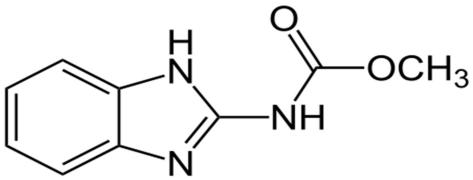

Carbendazim

The SPF degradation of Diquat (Dq) and Carbendazim (Cz) in distilled water is presented in figure 7.20. The degradation is relatively slower in the case of carbendazim. However both pesticides are completely degraded in distilled water.

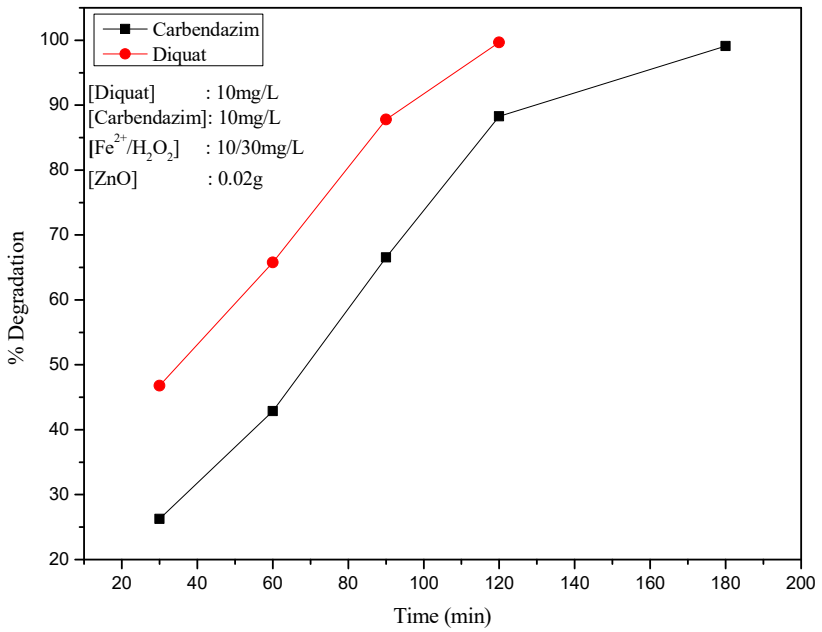

Fig. 7.20: Degradation of Diquat and Carbendazim in distilled water

In this case also, the primary degradation of the combination (Dq+Cz) is not investigated due to analytical constraints. However, in the case of mineralization, the measurement is made by COD and hence the combination also is tested.

The mineralization of the two pollutants in distilled water is tested and the results are presented in figure 7.21. The mineralization of diquat, carbendazim and the combination (Dq+Cz) takes 5 hr, 8 hr and 10 hr respectively.

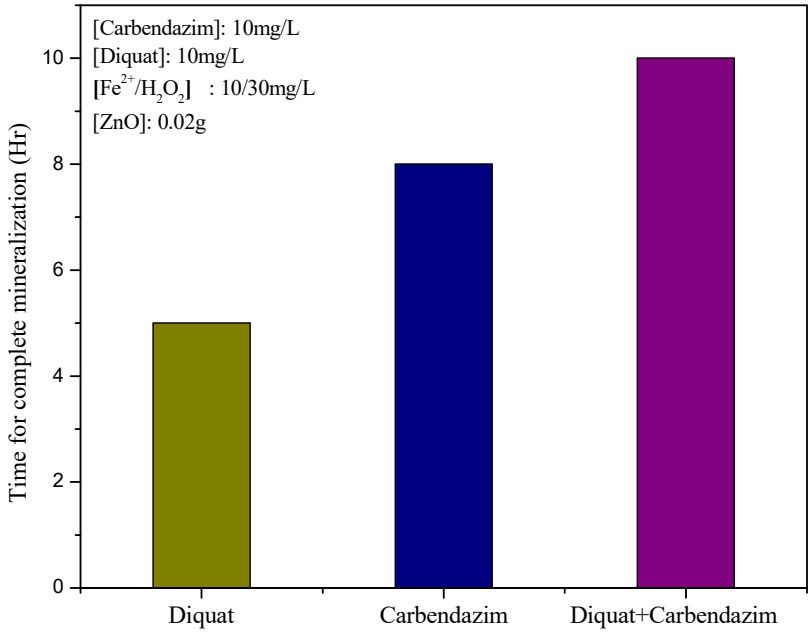

Fig. 7.21: Mineralization of diquat, carbendazim and the combination in distilled water

The combination (Dq+Cz) gets mineralized more slowly compared to individual components. This indicates that the simultaneous presence of the two pesticides in water inhibits the mineralization of one another even though eventually both get completely mineralized.

The trend remains the same in river water. In this case also the degradation of diquat is faster compared to carbendazim (figure 7.22). The time taken for the degradation also remains the same as in distilled water indicating that the contaminants in river water do not affect the degradation of the two pollutants.

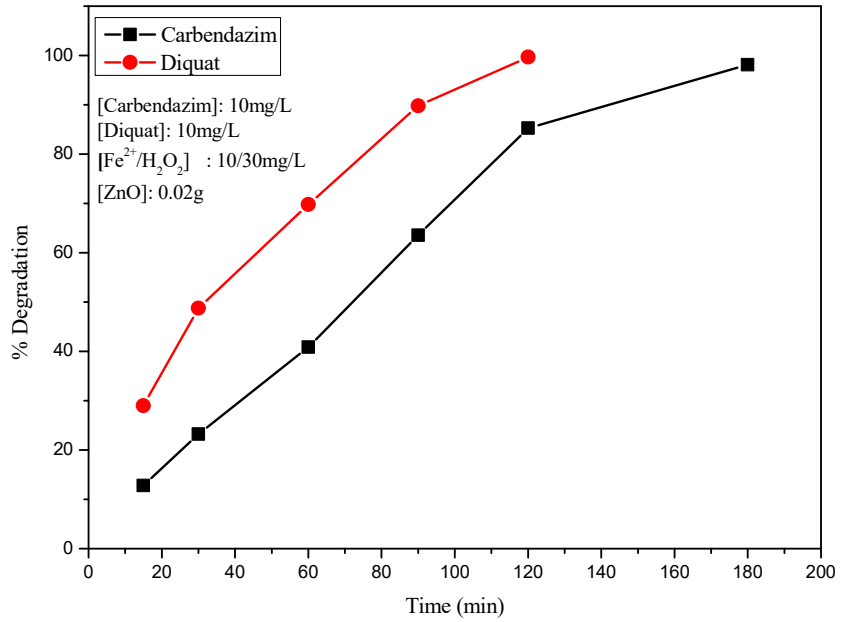

Fig. 7.22: Degradation of Diquat and Carbendazim river water

The mineralization in river water also follows the same trend as in distilled water (Figure 7.23). The efficiency of mineralization is in the order,

Diquat > Carbendazim > (Diquat+ Carbendazim)

Comparative effect of the two matrices, i.e. distilled water and river water, on the degradation and mineralization of the two pollutants is summarized in figure 7.24 and 7.25 respectively.

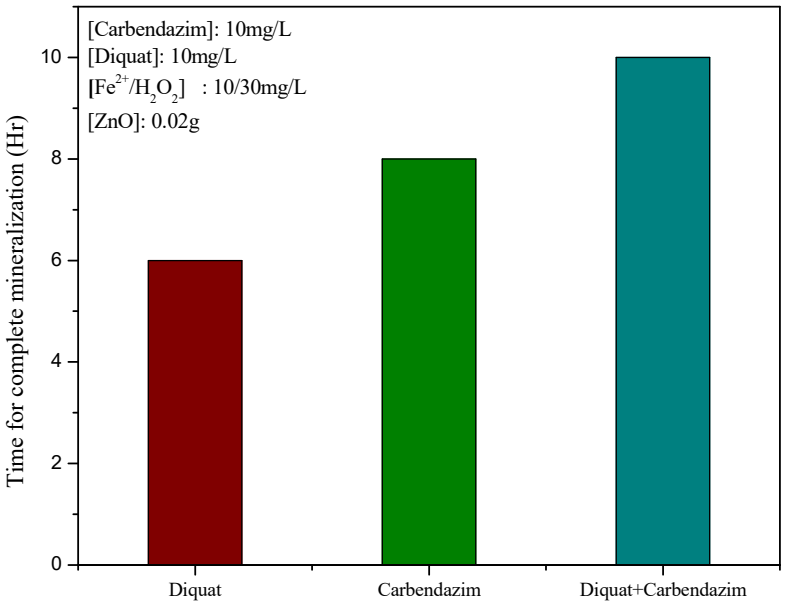

Fig. 7.23: Mineralization of Diquat, Carbendazim and (Diquat + Carbendazim) river water

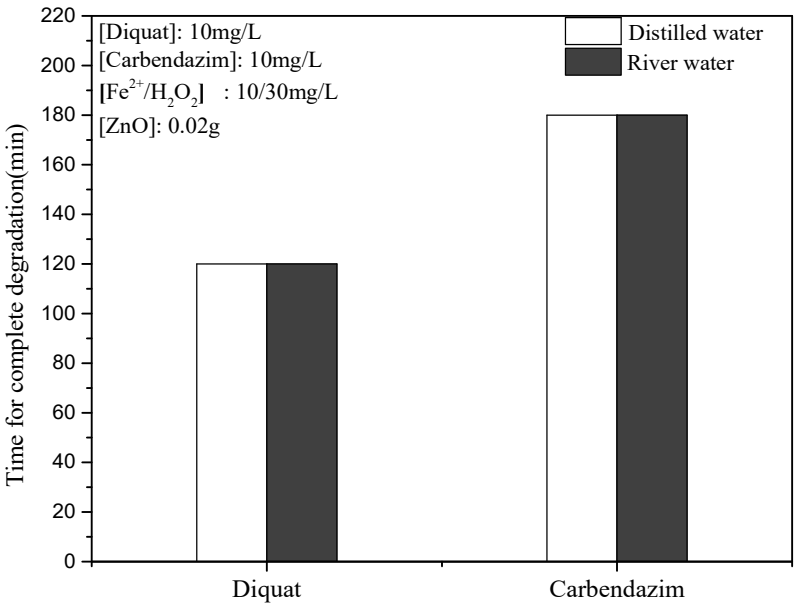

Fig. 7.24: Comparative effect of the matrices (distilled water vs river water) on the degradation of Dq and Cz

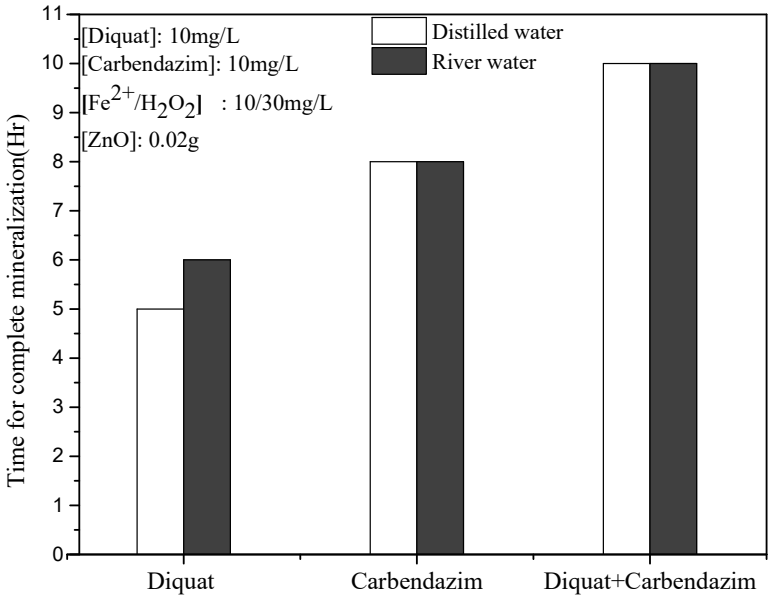

Fig. 7.25: Comparative effect of the matrices (distilled water vs river water) on the mineralization of Dq, Cz and Dq+Cz

The results show that the contaminants in river water inhibit the mineralization in the case of diquat, even though the effect is not significant in the case of carbendazim as well as the combination (diquat + carbendazim). In the combination, by the time Cz is completely mineralized (it takes longer time compared to Dq), Dq also gets mineralized, even though the rate of mineralization is slower in the case of the latter in river water (compared to in distilled water).

7.4 Conclusion

Solar photocatalyticFenton process is identified as a highly efficient AOP for the mineralization of multiple chemical pollutants such as dyes, pesticides, petrochemicals and pharmaceuticals not only under laboratory

conditions but also in natural river water. Cross contaminants of widely varying chemistry do not influence the efficiency of the process significantly though the mineralization is slightly slower in the case of the combination compared to respective individual pollutants. This makes the current process i.e. solar photocatalyticFenton, a potentially viable and environmentally safer water decontamination process. Commercial application of the process needs further evaluation of the effect of various contaminants on the efficiency of the process and corresponding optimization. However, the viability of the process for the decontamination of water from multiple chemical pollutants under suitably optimized conditions is proven beyond doubt in this study.

.....ꕥ.....

Chapter

8

SUMMARY AND CONCLUSION

Photocatalysis, Electrolysis, Sonolysis, Classic Fenton, SolarFenton, SonoFenton, ElectroFenton and Solar photocatalyticFenton have been identified as potential Advanced Oxidation Processes (AOPs) for the decontamination of water from chemical pollutants. There is no direct correlation between the efficiency for primary degradation/decolorization and that for mineralization in the case of many pollutants due to the formation of more recalcitrant intermediates.

Solar photocatalysis mediated by ZnO is an efficient environment-friendly method for the mineralization of the dye pollutant IC in water. The mineralization is facilitated by H_2O_2 while another oxidant persulphate (PS) has surprisingly no effect. The degradation of IC follows pseudo first order kinetics and Langmuir Hinshelwood (L-H) mechanism. Dissolved and/or adsorbed oxygen is essential for the degradation and mineralization highlighting the significance of Reactive Oxygen Species (ROS) in the process. Salts/anions naturally present in water influence the efficiency of solar photocatalysis. The effect is dependent on the concentration of the salt. The degradation proceeds through a number of intermediates which also get eventually mineralized as verified by LC/MS. Solar photocatalysis is thus able to mineralize IC and IC-derived recalcitrant chemical pollutants

in water and bring down the COD to zero. The previous wastewater thus becomes reusable.

Electrolytic process with BiO_2-TiO_2/Ti anode, graphite cathode and Na_2SO_4 as the electrolyte (BiO_2-TiO_2/Ti - graphite -Na_2SO_4) is identified as the most efficient electrolytic system for the complete mineralization of Indigo Carmine. Absence of any consumable chemicals or other additives makes the process an economically viable candidate for water treatment. The system is efficient even at its normal pH which makes it more attractive. Various intermediates formed during the process are identified by LC/MS. Eventually they also get mineralized. BiO_2-TiO_2/Ti – SS - NaCl is more efficient for the decolorization of the dye. However insitu formation of chloro compounds which degraded only slowly makes the process inefficient for mineralization.

Sonocatalysis mediated by ZnO and promoted by oxidants is also an efficient AOP for the decolorization and mineralization of IC. H_2O_2 formed insitu in the system is accelerating the decolorization due to enhanced formation of reactive free radicals.

Another efficient AOP is the Classic Fenton reaction using simple ferrous salt and H_2O_2 under ambient conditions. The disadvantage of Fe sludge formation from accumulated Fe^{3+}/Fe^{2+} and the slow mineralization are overcome by combining the process with photo-, sono- and electro-activation. Solar photoFenton is identified as the most efficient process for the decolorization of IC while Solar photocatalyticFenton mediated by ZnO is the most efficient process for mineralization. The comparative

efficiency of various processes for the decolorization/mineralization of IC is in the order:

Decolorization: Solar photoFenton > Solar photocatalyticFenton ≈ SonoFenton ≈ ElectroFenton > Photocatalysis ≈ Sonocatalysis > Sonolysis > Fenton ≈ Electrolysis > SonocatalyticFenton

Mineralization: Solar photocatalyticFenton > Solar photoFenton ≈ SonoFenton ≈ ElectroFenton > Photocatalysis > Sonocatalysis > Sonolysis > Fenton > Electrolysis > SonocatalyticFenton

Of the above, solar photocatalyticFenton mediated by ZnO is the most efficient AOP for the mineralization of IC in water. The efficiency of the process for the mineralization of multiple chemical pollutants is illustrated using a combination of dyes, pesticides, petrochemicals and pharmaceuticals under laboratory conditions as well as field conditions with natural river water as the matrix. Cross contamination by various organic chemicals does not influence the efficiency of the process significantly. These factors, together with (i) inexpensive safer ZnO as the catalyst (ii) relatively harmless chemicals Fe^{2+} and H_2O_2 for the insitu generation of reactive oxygen species (ROS) and (iii) natural sunlight as the energy source, make the process an economically viable and environmentally safer 'green technology' for the decontamination of water. The otherwise 'waste' or 'used' water can be thus made reusable.

.....ꕥ.....

REFERENCES

[1] I. Arslan, A.I. Balcioglu, Degradation of Remazol black B dye and its simulated dye bath wastewater by advanced oxidation processes in heterogeneous and homogenous media, *Color. Technol., 117 (2001) 38-42*

[2] I.A. Balcioglu, I.Arslan, Partial oxidation of reactive dyestuffs and synthetic textile dye-bath by the O_3 and O_3/H_2O_2 processes, *Water Sci.Technol.,43 (2001) 221-228*

[3] R. Munter, Advanced Oxidation Processes–Current status and prospects, *Proceedings of the Estonian Academy of Sciences, Chemistry., 50 (2001) 59–80*

[4] E. Brillasa, E. Mur, R. Sauleda, L. Sànchez, J. Peral, X. Domènech, J. Casado, Aniline mineralization by AOP's: Anodic oxidation, photocatalysis, electro-Fenton and photoelectro-Fenton processes, *Appl. Catal. B: Environ., 16 (1998) 31-42*

[5] S. Sharma, J. P. Ruparelia, M.L. Patel, A general review on Advanced Oxidation Processes for waste water treatment, *Proc. International Conference on Current Trends in Technology, Nuicone, (2011) 1-7*

[6] G. William, K. Joon-Wun, C. H. Douglas, The chemistry of water treatment processes involving ozone, hydrogen peroxide and UV radiation, *Ozone: Science & Engineering., 9 (1987) 335–352*

[7] T. Oppenlander, Photochemical purification of water and air; advanced oxidation processes (AOPs): Principles, reaction mechanisms, reactor concepts – Wiley-VCH, Weinheim (2003)

[8] J. M. Poyatos, M.M. Muñio, M.C. Almecija, J.C. Torres, E. Hontoria, F. Osorio, Advanced oxidation processes for wastewater treatment: State of the art, *Water Air Soil Poll., 205 (2010) 187–204*

[9] O. Legrini, E. Oliveros, A.M. Braun, Photochemical processes for water treatment, *Chem. Rev., 93 (1993) 671–698*

[10] W.Y. Teoh, R. Amal, J Scott, Progress in heterogenours photocatalysis: From classical radical chemistry to engineering nanomaterials and solar reactors, *J Phys. Chem. Lett., 3 (2012) 629–639*

[11] M. Fox, Photocatalytic oxidation of organic substances. in: Kluwer (ed.) Photocatalysis and Environment: Trends and Applications. Academic Publishers, New York (1988) 445–467

[12] U.I. Gaya, A.H. Abdullah, Heterogeneous photocatalytic degradation of organic contaminants over Titanium dioxide: A review of fundamentals, progress and problems, *J Photochem. Photobiol. C Photochem. Rev., 9 (2008) 1-12*

[13] D.M. Blake, Bibliography of work on the heterogeneous photocatalytic removal of hazardous compounds from water and air; National Renewable Energy Laboratory: Denver, Co, USA, (2001) 1–158.

[14] P. Schmitt-Kopplin, N.K.A. Hertkorn, Structural changes in dissolved soil humic matter during photochemical degradation processes under nitrogen and oxygen atmospheres. *Environ. Sci. Technol., 32 (1998) 2531–2541*

[15] A. Paleologou, H. Marakas, N.P. Xekoukoulotakis, A. Moya, Y. Vergara, N. Kalogerakis, P. Gikas, D. Mantzavinos, Disinfection of water and wastewater by TiO_2 photocatalysis, sonolysis and UV-C irradiation, *Catal. Today, 129 (2007) 136–142*

[16] M.R. Hoffmann, S.T. Martin, W. Choi, D.W. Behnemann, Environmental applications of semiconductor photocatalysis, *Chem. Rev., 93 (1995) 69-96*

[17] S. Liu, C. Li, J. Yu, Q. Xiang, Improved visible-light photocatalytic activity of porous carbon self-doped ZnO nanosheet-assembled flowers, *Cryst. Eng. Comm., 13 (2011) 2533–2541*

[18] J. J Vora, S. K. Chauhan, K. C. Parmar, S. B. Vasava, S. Sharma, L. S. Bhutadiya, Kinetic study of application of ZnO as a photocatalyst in heterogeneous medium, *E-Journal of Chemistry, 6 (2009) 531–536*

[19] F. Barka-Bouaifel, B. Sieber, N. Bezzi, Synthesis and photocatalytic activity of iodine-doped ZnO nanoflowers, *J Mater. Chem., 21 (2011) 10982– 10989*

[20] M. A. Kanjwal, N. A. M. Barakat, F. A. Sheikh, S. J. Park, H. Y. Kim, Photocatalytic activity of ZnO-TiO_2 hierarchical nanostructure prepared by combined electrospinning and hydrothermal techniques, *Macromol. Res., 18 (2010) 233–240*

[21] K. Byrappa, A. K. Subramani, S. Ananda, K.M. Lokanatha Rai, R. Dinesh, M. Yoshimura, Photocatalytic degradation of rhodamine B dye using hydrothermally synthesized ZnO, *Bull. Materials Science, 29 (2006) 433–438*

[22] E. Evgenidou, K. Fytianos, I. Poulios, Semiconductor- sensitized photodegradtion of dichlorovos in water using TiO_2 and ZnO as catalysts, *Appl. Catal. B, Environ., 59 (2005) 81–89*

[23] C. Galindo, P. Jacques, A. Kalt, Photodegradation of aminoazobenzene acids orange 52 by three advanced oxidation process: UV/TiO_2, UV/H_2O_2 and Vis/TiO_2, *J Photochem. Photobiol. A. Chem., 141 (2001) 47–56*

[24] G. Wang, D. Chen, H. Zhang, J. Z. Zhang, J. Li, Tunable photocurrent spectrum in well-oriented zinc oxide nanorod arrays with enhanced photocatalytic activity, *J Phys. Chem. C, 112 (2008) 8850–8855*

[25] M. Miyauchi, A. Nakajima, T. Watanabe, K. Hashimoto, Photocatalysis and photoinduced hydrophilicity of various metal oxide thin films, *Chem. Mater., 14 (2002) 2812-2816*

[26] M. Pera-Titus, V.G. Molina, M.A. Banos, J. Gimenez, S. Esplugas, Degradation of chlorophenols by means of advanced oxidation processes: A general review *Appl. Catal. B, Environ. 47 (2004) 219–256*

[27] C. Hariharan, Photocatalytic degradation of organic contaminants in water by ZnO nanoparticles: Revisited, *Appl. Catal. A: General, 304 (2006) 55–61.*

[28] S. Sakthivel, B. Neppolian, M.V. Shankar, B. Arabindoo, M. Palanichamy, V. Murugesan, Solar photocatalytic degradation of azo dye: Comparison of photocatalytic efficiency of ZnO and TiO_2, *Solar Energy Materials & Solar Cells, 77 (2003) 65–82*

[29] B. Pare, S.B. Jonnalagadd, H. Tomar, P. Singh, V.W. Bhagwat, ZnO assisted photocatalytic degradation of acridine orange in aqueous solution using visible irradiation, *Desalination, 232 (2008) 80–90*

[30] N. Daneshvar, D. Salari, A.R. Khataee, Photocatalytic degradation of azo dye acid red 14 in water on ZnO as an alternative catalyst to TiO_2, *J Photochem. Photobiol. A: Chemistry, 162 (2004) 317–322*

[31] C. Hou, B. Hu, J. Zhu, Photocatalytic degradation of Methylene Blue over TiO_2 pretreated with varying concentrations of NaOH, *Catalysts, 8 (2018) 575-578*

[32] T.C.K. Yang, S. K Ramaraj, S. Balu, K. Uma, G. Pan, Degradation of Methylene Blue Dye in the presence of visible light using SiO_2@α-Fe_2O_3 nanocomposites deposited on SnS_2 flowers, *Materials, 11 (2018) 1030-1034*

[33] Y. Chiu, T. Mark Chang, C. Chen, M. Sone , Y. Hsu, Mechanistic Insights into Photodegradation of organic dyes using heterostructure photocatalysts, *Catalysts, 9 (2019) 430-435*

[34] S. Mortazavian, A. Saber, D. E. James, Optimization of photocatalytic degradation of Acid Blue 113 and Acid Red 88 textile dyes in a UV-C/TiO_2 suspension system: Application of Response Surface Methodology (RSM), *Catalysts, 9 (2019) 360-364*

[35] M.A. Margulis, Fundamental aspects of sonochemistry, *Ultrasonics, 30 (1992) 152-155*

[36] H. Thompson, L.K. Doraiswamy, Sonochemistry: Science and Engineering, *Ind. Eng. Chem. Res., 38 (1999) 1215-1249*

[37] N. Serpone, P. Colarusso, Sonochemistry I: Effects of ultrasounds on heterogeneous chemical reactions - A useful tool to generate radicals and to examine reaction mechanisms, *Res. Chem. Intermed., 20 (1994) 635-679*

[38] P. Colarusso, N. Serpone, Sonochemistry II, Effects of ultrasounds on homogeneous chemical reactions and in environmental detoxification, *Res. Chem. Intermed, 22 (1996) 61-89*

[39] K. Makino, M.M. Mossoba, P. Riesz, Chemical effects of ultrasound on aqueous solutions. Evidence for hydroxyl and hydrogen free radicals ($^{\bullet}OH$ and $^{\bullet}H$) by spin trapping, *J Amer. Chem. Soc., 104 (1982) 3537-3539*

[40] K.S. Suslick, The Chemical Effects of Ultrasound, *Scientific American, 260 (1989) 80-86*

[41] K. S. Suslick, Sonochemistry, *Science, 247 (1990) 1439-1445*

[42] P. Chowdhury, T. Viraraghavan, Sonochemical degradation of chlorinated organic compounds, phenolic compounds and organic dyes – A review*, Science of the total Environment, 407 (2009) 2474-2492*

[43] J. Rae, M. Ashokkumar, O. Eulaerts, C. von Sonntag, J. Reisse, F. Grieser, Estimation of ultrasound induced cavitation bubble temperatures in aqueous solutions, *Ultrason. Sonochem., 12 (2005) 325-329*

[44] C. Petrier, Y. Jiang, M. F. Lamy, Ultrasound and Environment: Sonochemical destruction of chloroaromatic derivatives, *Environ. Sci. Technol., 32 (1998) 1316-1318*

[45] C. Petrier, B. David, S. Laguian, Ultrasonic degradation at 20 kHz and 500 kHz of atrazine and pentachlorophenol in aqueous solution: Preliminary results, *Chemosphere, 32 (1996) 1709-1718*

[46] P. Cintas, J. L. Luche, The sonochemical approach, *Green Chemistry, 1 (1999) 115-125*

[47] I. Hua, M.R. Hoffmann, Kinetics and mechanism of the sonolytic degradation of CCl_4: intermediates and byproducts, *Environ. Sci. Technol., 30 (1996) 864-871*

[48] D. Drijvers, R. De Baets, A. De Visscher, H. Van Langenhove, Sonolysis of trichloroethylene in aqueous solution: volatile organic intermediates, *Ultrason. Sonochem., 3 (1996) S83-S90*

[49] S. Sasi, M.P. Rayaroth, D. Devadasan, U.K. Aravind, C.T. Aravindakumar, Influence of inorganic ions and selected emerging contaminants on the degradation of Methylparaben: A sonochemical approach, *J Hazard. Mater., 300 (2015) 202-209*

[50] Y.G. Adewuyi, Sonochemistry: Environmental Science and Engineering Applications, *Ind. Eng. Chem. Res., 40 (2001) 4681-4715*

[51] R. Kidak, N.H. Ince, Ultrasonic destruction of phenol and substituted phenols: A review of current research, *Ultrason. Sonochem., 13 (2006) 195-199*

[52] J. P. Lorimer, T.J Mason, Sonochemistry. Part 1-The physical aspects, *Chem. Soc. Rev., 16 (1987) 239-274*

[53] S. Merouani, O. Hamdaoui, F. Saoudi, M. Chiha, C. Pétrier, Influence of bicarbonate and carbonate ions on sonochemical degradation of Rhodamine B in aqueous phase, *J Hazard. Mater., 175 (2010) 593–599*

[54] M. Joseph, H. Destaillats, Hui-Ming Hung, M. R. Hoffmann, The Sonochemical degradation of azobenzene and related Azo dyes: Rate enhancements via Fenton's reactions, *J Phys. Chem. A, 104 (2000) 8930-8935*

[55] S. Tang, T. Teng, F. M. A. Alkarkhi, Z. Li, Sonocatalytic degradation of Rhodamine B in aqueous solution in the presence of TiO_2 coated activated carbon, *Int. J Environ. Sci. Dev., 3 (2012) 61-65*

[56] T. Chave, N. M. Navarro, P. Pochon, N. Perkas, A. Gedanken, S. I. Nikitenko, Sonocatalytic degradation of oxalic acid in the presence of oxygen and Pt/TiO_2, *Catal. Today, 241 (2015) 55–62*

[57] N. Ghows, M.H. Entezari, Kinetic investigation on sono-degradation of Reactive Black 5 with core–shell nanocrystal, *Ultrason. Sonochem., 20 (2013) 386–394*

[58] M. Abbasi, N. Razzaghi, Sonochemical degradation of Basic Blue 41 dye assisted by nanoTiO_2 and H_2O_2 , *J Hazard. Mater., 153 (2008) 942–947*

[59] Z. Eren, N. H. Ince, Sonolytic and sonocatalytic degradation of azo dyes by low and high frequency ultrasound, *J Hazard. Mater., 150 (2010) 250-256*

[60] C. Lops, A. Ancona, K. D. Cesare, B. Dumontel, N. Garinoa, G. Canavese, S. Hérnandez, V. Cauda, Sonophotocatalytic degradation mechanisms of Rhodamine B dye via radicals generation by micro- and nano-particles of ZnO, *Appl. Catal. B: Environ., 243 (2019) 629–640*

[61] M.P Rayaroth , U.K Aravind , C.T Aravindakumar , Effect of inorganic ions on the ultrasound initiated degradation and product formation of triphenylmethane dyes, *Ultrason. Sonochem., 48 (2018) 482-491*

[62] O. T. Dede, Z. Aksu, A. Rehorek, Sonochemical Degradation of C.I Reactive Orange 107, *Environ. Eng. Science. 36 (2019) 158-171*

[63] K. Rajeshwar, J. G. Ibanez, Environmental Electrochemistry Fundamentals and Application in Pollution Abatement., Academic Press San Diego, CA, (1997)

[64] C.A. Martínez-Huitle, E. Brillas, Decontamination of wastewaters containing synthetic organic dyes by electrochemical methods: A general review, *Appl. Catal. B. Environ., 87 (2009) 105–145*

[65] N. Borràs, C. Arias, R. Oliver, E. Brillas, Anodic oxidation, electroFenton and photoelectro-Fenton degradation of cyanazine using a boron-doped diamond anode and an oxygen-diffusion cathode, *J Electroanal. Chem., 689 (2013) 158–167*

[66] M. Panizza, G. Cerisola, Direct and mediated anodic oxidation of organic pollutants, *Chem. Rev., 109 (2009) 6541–6569*

[67] JM. Peralta-Hernández, C A. Martínez-Huitle, J L. Guzmán-Mar1, A. Hernández-Ramírez, Recent advances in the application of electro-fenton and photoelectro-fenton process for removal of synthetic dyes in wastewater treatment, *J Environ. Eng. Manage., 19 (2009) 257-265*

[68] C. Comninellis, C. Pulgarin, Electrochemical oxidation of phenol for wastewater treatment using SnO_2 anodes, *J Appl. Electrochem., 23 (1993) 108–112*

[69] M. Weng, Z. Zhou, Q. Zhang, Electrochemical degradation of typical dyeing wastewater in aqueous solution: Performance and Mechanism, *Int. J Electrochem. Sci., 8 (2013) 290 – 296*

[70] H. S. Kusuma, R. I. Sholihuddin, M. Harsini, H. Darmokoesoemo, Electrochemical degradation of Malachite Green dye using Carbon/TiO_2 Electrodes, *J Mater. Environ. Sci., 7 (2016) 1454-1460*

[71] R G. de Silva, S A Neto, A R. de Andrade, Electrochemical degradation of reactive dyes at different DSA® Compositions, *J Braz. Chem. Soc., 22 (2011) 126-133*

[72] D. C. de Moura, M. A. Quiroz, D. R. da Silva, R. Salazar, C. A. Martínez-Huitle, Electrochemical degradation of Acid Blue 113 dye using TiO_2-nanotubes decorated with PbO_2 as anode, *Environmental Nanotechnology, Monitoring &Management, 5 (2016) 13–20*

[73] M.S. Morsi, A.A. Al-Sarawy, W. A. Shehab El-Dein, Electrochemical degradation of some organic dyes by electrochemical oxidation on a Pb/PbO_2 electrode, *Desalination and Water Treatment, 26 (2011) 301–308*

[74] T.A. Kenova , G.V. Kornienko , O.A. Golubtsova , V.L. Kornienko, N.G. Maksimov Electrochemical degradation of Mordant Blue 13 azo dye using boron-doped diamond and dimensionally stable anodes: influence of experimental parameters and water matrix, *Environ Sci. Poll. Res. Int., 30 (2018) 30425-30440*

[75] R. Salazar , M.S. Ureta-Zañartu , C. González-Vargas , C.D.N. Brito , C.A. Martinez-Huitle, Electrochemical degradation of industrial textile dye disperse yellow 3: Role of electrocatalytic material and experimental conditions on the catalytic production of oxidants and oxidation pathway., *Chemosphere., 198 (2018) 21-29*

[76] S. Cotillas, D. Clematis, P. Cañizares, M. P Carpanese, M.A Rodrigo, M. Panizza Degradation of dye Procion Red MX-5B by electrolytic and electro-irradiated technologies using diamond electrodes, *Chemosphere., 199 (2018) 445-452*

[77] H.J.H. Fenton, Oxidation of tartaric acid in the presence of iron, *J Chem. Soc. Trans., 65 (1894) 899–901*

[78] G.V. Buxton, C.L. Greenstock, W.P. Helman, A.B. Ross, Critical review of the rate constants for reactions of hydrated electrons, hydrogen atoms and hydroxyl radicals (·OH/·O) in aqueous solution, *J Phys. Chem. Ref. Data, 17 (1988) 513– 886*

[79] E. Neyens, J. Baeyens, A review of classic Fenton's peroxidation as an advanced oxidation technique, *J Hazard. Mater., 98 (2003) 33–50*

[80] P. Bautista, A.F. Mohedano, J. A. Casas, J. A. Zazo, J. J Rodriguez, An overview of the application of Fenton oxidation to industrial wastewaters treatment, *J Chem. Technol. Biotechnol., 83 (2008) 1323–1338*

[81] P.V. Nidheesh, Heterogeneous Fenton catalysts for the abatement of organic pollutants from aqueous solution: A review, *RSC Advances, 5 (2015) 40552-40577*

[82] A. Dhakshinamoorthy, S. Navalon, M. Alvaro, H. Garcia, Metal nanoparticles as heterogeneous Fenton catalysts, *Sust. Chem, 5 (2012) 46-64*

[83] V S. Gan, H.K. Ng, Current status and prospects of Fenton oxidation for the decontamination of persistent organic pollutants (POPs) in soils, *Chem. Eng. J, 213 (2012) 295-317*

[84] E. Brillas, I. Sirés, M.A. Oturan, Electro-Fenton process and related electrochemical technologies based on Fenton's Reaction Chemistry, *Chem. Rev., 109 (2009) 6570-6631*

[85] C. Bouasla, M. E. Samar, F. Ismail, Degradation of methyl violet 6B dye by the Fenton process, *Desalination, 254 (2010) 35–41*

[86] S.H. Lin, C.C. Lo, Fenton process for treatment of desizing wastewater, *Water Res., 31 (1997) 2050–2056*

[87] S.H. Lin, C.M. Lin, H.G. Leu, Operating characteristics and kinetics studies of surfactant wastewater treatment by Fenton oxidation, *Water Res., 33 (1999) 1735–1741*

[88] Y.W. Kang, K.Y. Hwang, Effects of reaction conditions on the oxidation efficiency in the Fenton process, *Water Res., 34 (2000) 2786–2790*

[89] F.J. Rivas, F.J. Beltran, J. Frades, P. Buxeda, Oxidation of p-hydroxybenzoic acid by Fenton's reagent, *Water Res., 35 (2001) 387–396*

[90] H.R. Eisenhauer, Oxidation of phenolic wastes, *J Water Poll. Control Fed., 36 (1964) 1116–1128*

[91] K. Ito, W. Jian, W. Nishijima, A.U. Baes, E. Shoto, M. Okada, Comparison of ozonation and AOPs combined with biodegradation for removal of THM precursors in treated sewage effluents, *Water Sci. Technol. 38 (1998) 179–186*

[92] G. Ruppert, R. Bauer, G. Heisler, The photo-Fenton reaction – an effective photochemical wastewater treatment process, *J Photochem. Photobiol. A-Chem. 73 (1993) 75–78*

[93] Y. Sun, J. J. Pignatello, Photochemical reactions involved in the total mineralization of 2,4-D by Fe^{3+} /H_2O_2/UV, *Environ. Sci. Technol., 27 (1993) 304–310*

[94] P.R. Gogate, A.B. Pandit, A review of imperative technologies for wastewater treatment II: hybrid methods, *Adv. Environ. Res., 8 (2004) 553–597*

[95] R. Bauer, H. Fallmann, The photo-Fenton oxidation – a cheap and efficient wastewater treatment method, *Res. Chem. Intermed., 23 (1997) 341–354*

[96] R.G. Zepp, B.C. Faust, J. Hoigne, Hydroxyl radical formation in aqueous reactions (pH 3–8) of iron (II) with hydrogen peroxide: the photo-Fenton reaction, *Environ. Sci. Technol., 26 (1992) 313–319*

[97] S.M. Kim, S.U. Geissen, A. Vogelpohl, Landfill leachate treatment by a photoassisted Fenton reaction, *Water Sci. Technol., 35 (1997) 239–248*

[98] B.D. McGinnis, V.D. Adams, E.J. Middlebrooks, Degradation of ethylene glycol in photo Fenton systems, *Water Res., 34 (2000) 2346–2354*

[99] A. Safarzadeh-Amiri, J.R. Bolton, S.R. Cater, *Ferrioxalate-mediated photodegradation of organic pollutants in contaminated water, Water Res., 31 (1997) 787–798*

[100] I.S. De Oliveira, L. Viana, C. Verona, V.L.V. Fallavena, C.M.N. Azevedo, M. Pires, Alkyl resin wastewaters treatment by Fenton and photo-Fenton processes, *J Hazard. Mater., 146 (2007) 564–568*

[101] L.da S. Leite, B.de S. Maselli, G.de A. Umbuzeiro, R.F.P. Nogueira, Monitoring ecotoxicity of disperse red 1 dye during photo-Fenton degradation, *Chemosphere, 148 (2016) 511-517*

[102] P.R. Gogate, A.B. Pandit, A review of imperative technologies for wastewater treatment II: hybrid methods, *Adv. Environ. Res., 8 (2004) 553–597*

[103] O. Legrini, E. Oliveros, A.M. Braun, Photochemical processes for water treatment, *Chem. Rev., 93 (1993) 671–698*

[104] A. Francony, C. Petrier, Sonochemical degradation of carbon tetrachloride in aqueous solution at two frequencies: 20 kHz and 500 kHz, *Ultrason. Sonochem., 3 (1996) S77–S82*

[105] T.J. Mason, E.D. Cordemans, Ultrasonic intensification of chemical processing and related operations: A review, *Chem. Eng. Res. Des., 74 (1996) 511–516*

[106] K.S. Susick, S.J Doktycz, E.B. Flint, On the origin of sonoluminescence and sonochemistry, *Ultrasonics, 28 (1990) 280–290*

[107] O. Dahlem, V. Demaiffe, V. Halloin, J. Reisse, Direct sonication system suitable for medium-scale sonochemical reactors, *AIChE J, 44 (1998) 2724–2730*

[108] J. Liang, S. Komarov, N. Hayashi, K. Eiki, Recent trends in the decomposition of chlorinated aromatic hydrocarbons by ultrasound irradiation and Fenton's reagent, *J Mater. Cycles Waste Management, 9 (2007) 47–55*

[109] A. Kotronarou, G. Mills, M.R. Hoffmann, Ultrasonic irradiation of p-nitrophenol in aqueous solution, *J Phys. Chem., 95 (1991) 3630–3638*

[110] D. Drijvers, H.V. Langenhove, M. Beckers, Decomposition of phenol and trichloroethylene by the ultrasound/H_2O_2/CWO process, *Water Res., 33 (1999) 1187– 1194*

[111] M. Dukkanci, G. Gunduz, Ultrasonic degradation of oxalic acid in aqueous solutions, *Ultrason. Sonochem., 13 (2006) 517-522*

[112] C. Pulgarin, J. Kiwi, Overview on photocatalytic and electrocatalytic pretreatment of industrial non-biodegradable pollutants and pesticides, *Chimia, 50 (1996) 50–55*

[113] C. Comninellis, C. Pulgarin, Anodic oxidation of phenol for waste water treatment, *J Appl. Electrochem., 21 (1991) 703–708*

[114] R. Morselli, J. Garcia-Gomez, P.A. Michaud, M.A. Rodrigo, C. Comninellis, Electro generation of hydroxyl radicals on boron-doped diamond electrodes, *J Electrochem. Soc., 150 (2003) D79–D83*

[115] M. Panizza, G. Cerisola, Application of diamond electrodes to electrochemical processes, *Electrochim. Acta, 51 (2005) 191–199*

[116] F.V.F. Araujo, L. Yokoyama, L.A.C. Teixeira, J. C. Campos, Heterogeneous Fenton process using the mineral hematite for the discolouration of a reactive dye solution, *Braz. J Chem. Eng., 28 (2011) 605-616*

[117] U. Kurt, O. Apaydin, M.T. Gonullu, Reduction of COD in wastewater from an organized tannery industrial region by electro-Fenton process, *J Hazard. Mater., 143 (2007) 33–40*

[118] E. Brillas, J. Casado, Aniline degradation by electro-Fenton1 and peroxi-coagulation processes using a flow reactor for waste water treatment, *Chemosphere, 47 (2002) 241–248*

[119] C. Badellino, C.A. Rodrigues, R. Bertazzoli, Oxidation of pesticides by in situ electrogenerated hydrogen peroxide: Study for the degradation of 2,4-dichlorophenoxyacetic acid, *J Hazard. Mater., 137 (2006) 856–864*

[120] H. Zhang, D. Zhang, J. Zhou, Removal of COD from landfill leachate by electro- Fenton method, *J Hazard. Mater., 135 (2006) 106–111*

[121] H. Zhang, C. Fei, D. Zhang, F. Tang, Degradation of 4-nitrophenol in aqueous medium by electro-Fenton method, *J Hazard. Mater., 145 (2007) 227–232*

[122] W.P. Ting, M.C. Lu, Y.H. Huang, The reactor design and comparison of Fenton, electro-Fenton and photoelectron-Fenton processes for mineralization of benzene sulfonic acid (BSA), *J Hazard. Mater., 156 (2008) 421–427*

[123] C. Bouasla, M. El-Hadi Samar, F. Ismail, Degradation of methyl violet 6B dye by the Fenton process, *Desalination, 254 (2010) 35–41*

[124] M. S. Lucas, J. A. Peres, Decolorization of the azo dye Reactive Black 5 by Fenton and photo-Fenton oxidation, *Dyes and Pigments, 71 (2006) 236-244*

[125] J. Hui Sun, S. Peng Sun, J. Yu Sun, R. Xia Sun, L. Ping Qiao, H. Qin Guo, M. Hong Fan, Degradation of azo dye Acid black 1 using low concentration iron of Fenton process facilitated by ultrasonic irradiation, *Ultrason. Sonochem., 14 (2007) 761–766*

[126] N.A. Youssef, S.A. Shaban, F.A. Ibrahim, A.S. Mahmoud, Degradation of methyl orange using Fenton catalytic reaction, *Egypt. J Pet., 25 (2016) 317-321*

[127] N. Ertugay, F.N. Acar, Removal of COD and color from Direct Blue 71 azo dye wastewater by Fenton's oxidation:Kinetic study, *Arabian J Chem., 10 (2017) S1158-S1163*

[128] S.G. Cetinkaya, M.H. Morcali, S. Akarsu, C.A. Ziba, M. Dolaz, Comparison of classic Fenton with ultrasound Fenton processes on industrial textile wastewater, *Sust. Environ. Res., 28 (2018) 165-170*

[129] A. Shokri, Application of Sono–photo-Fenton process for degradation of phenol derivatives in petrochemical wastewater using full factorial design of experiment, *Int. J Ind. Chem., 9 (2018) 295–303*

[130] L. Szpyrkowicz, C. Juzzolino, S.N. Kaul, A Comparative study on oxidation of disperse dye by electrochemical process, O_3, hypochlorite and Fenton reagent, *Water. Res., 35 (2011) 2129-2136*

[131] V. Kavitha, K. Palanivelu, Destruction of cresols by Fenton oxidation process, *Water. Res. 39 (2015) 3062-3072*

[132] A.D. Eaton, L.S. Clesceri, E.W. Rice, A.E. Greenberg, Standard methods for the examination of water and waste water, American Public Health Association, Washington, (2005) 515-516

[133] M. Sayed, F. Pingfeng, H.M. Khan, P. Zhang, Effect of isopropanol on microstructure and activity of TiO_2 films with dominant facets for photocatalytic degradation of bezafibrate, *Int. J Photoenergy, Article ID 490264, 110 (2014) 11 pages*

[134] S.O. Falodun, S.O. Idris, E.O. Ojo, JF. Iyun, Kinetics and mechanism of the oxidation of Indigo Carmine by permanganate ion in aqueous acidic medium, *Int. J Chem. Biol. Sci., 1 (2015) 255-259*

[135] E.S.Z.E. Ashtoukhy, Removal of Indigo Carmine Dye from synthetic wastewater by electrochemical oxidation in a new cell with horizontally oriented electrodes, *Int. J Electrochem. Sci., 8 (2013) 846-858*

[136] D. J. Dire, J. A. Wilkinson, Acute exposure to Rhodamine B, *J Toxicol. Clin. Toxicol., 25 (1987) 603-7*

[137] Diquat in drinking-water: Background document for development of WHO Guidelines for Drinking-water Quality, WHO/SDE/WSH/03.04/91

[138] D. Cherik, M. Benali, K. Louhab, Occurrence, ecotoxicology, removal of diclofenac by adsorption on activated carbon and biodegradation and its effect on bacterial community: A review, *World Scientific News, 16 (2015) 116-144*

[139] M.C. Labbe, W.A. Shewa, J. A. Lalman, S.R. Shanmugam, Photocatalytic degradation of Phenol and Phenol derivatives using a nano-TiO_2 catalyst: Integrating quantitative and qualitative Factors using Response Surface Methodology, *Water, 6 (2014) 1785-1806*

[140] H.B. Senturk, D. Ozdes, A.A. Gundogdu, C. Durana, M. Soylak, Removal of phenol from aqueous solutions by adsorption onto organomodified Tirebolu bentonite: Equilibrium, kinetic and thermodynamic study, *J Hazard. Mater., 172 (2009) 353-362*

[141] P. Mazellier, É. Leroy, J. De Laat, B. Legube, Degradation of carbendazim by UV/H_2O_2 investigated by kinetic modeling, *Environ. Chem. Lett., 1 (2003) 68 - 72*

[142] E. Amereh, S. Afshar, Photodegradation of acetophenone and toluene in water by nano-TiO_2 powder supported on NaX zeolite, *Materials Chemistry and Physics, 120 (2009) 356-360*

[143] V. A. Coleman, C. Jagadish, Basic properties and applications of ZnO, Zinc oxide bulk, Thin films and Nanostructures, Elsevier Science Direct e Books Ltd, (2006)

[144] H. Morkoç, U. Ozgur, Zinc oxide: Fundamentals, Materials and Device Technology, WILEY-VCH Verlag GmbH & Co, Weinheim, (2009)

[145] A. Janotti, C.G.V.de Walle, Fundamentals of zinc oxide as a semiconductor, *Rep. Prog. Phys., 72 (2009) 1-12*

[146] K. Mondal, A. Sharma, Photocatalytic oxidation of pollutant dyes in wastewater by TiO_2 and ZnO nano-materials – A Mini-review in Nanoscience & Technology for Mankind, Eds.: A. Misra, J R. Bellare, (2014) 36-72

[147] Z. Wang, Y. Guo, Y. Chen, S. Liang, Simulated sunlight enhanced X3B degradation by persulfate activated with steel slag, *J Environ. Eng., 142 (2016) 1-6*

[148] F.O. Kehinde, H.A. Aziz, Heat activated persulfate for decolorization of real textile wastewater, *Adv. Environ. Biol., 9 (2015) 12-16*

[149] X.R. Xu, S. Li, Q. Hao, J. L. Liu, Y.Y. Yu, H.B. Li, Review: Activation of persulfate and its environmental application, *Int. J Environ. Bioenergy, 1 (2012) 60-81*

[150] https://pubchem.ncbi.nlm.nih.gov/compound/hydrogenperoxide

[151] R.W. Matthews, Photocatalytic oxidation of organic contaminants in water: an aid to environmental preservation, *Pure and Appl.Chem, 64 (1992) 1285-1290*

[152] S. Devipriya, Suguna Yesodharan., Photocatalytic degradation of pesticide contaminants in water, *Solar Energy Materials and Solar Cells, 86 (2005) 309-348*

[153] M.N. Chong, B. Jin, C.W.K. Chow , C. Saint, New developments in Photocatalytic water treatment technology; a review, *Water. Res, 44 (2010) 2997-3027*

[154] J. P. Takeuchi, M. Cuong, T.M. Zhang, M. Matsuoka, M. Anpo, Recent advances in visible light –responsive titanium oxide based photocatalysis, *Res. Chem. Intermed, 99 (2010) 327-347*

[155] D. F. Ollis, P. Pichat , N. Serpone, TiO_2 photocatalysis – 25 years, *Appl. Catal. B: Environ, 99 (2010) 377-387*

[156] P. Pichat, Ed., Photocatalysis, Water Purification: From Fundamentals to Recent Applications, Wiley-VCH Verlag GmbH and Co, 2013

[157] M.G. Antoniou, P.A. Nicolaou., JA. Shoemaker, A.A. de la Cruz, D.D. Dionysiou, Detoxification of water contaminated with cyanotoxin microsystin-LR by utilizing thin TiO_2 photocatalyst films, *Appl. Catal. B: Environ, 91 (2009) 165-173*

[158] A. Fujishima, K. Honda, Electrochemical photolysis of water at a semiconductor electrode, *Nature, 238 (1972) 37-38*

[159] S.N. Frank, A. J. Bard, Heterogeneous photocatalytic oxidation of cyanide ion in aqueous solution at titanium dioxide powder, *J Amer. Chem. Soc. 99 (1977) 303-304*

[160] N. Serpone, E. Pelizzetti, Eds. Photocatalysis: Fundamentals and Applications, John Wiley and Sons Inc. New York, 1989

[161] D. F. Ollis, H. Al-Ekabi, Photocatalytic purification and treatment of water and air, Elsevier, Amsterdam, 1993

[162] M. Anpo, P.V. Kamath, Eds., Environment Benign Photocatalysts, Springer, New York, 2010

[163] S. P. Devipriya, SugunaYesodharan, E.P. Yesodharan, Removal of chemical and bacterial pollutants from water using Pt/TiO_2-coated ceramic tiles, *Int. J Photoenergy, Article ID 970474, 2012*

[164] M. Pelaez, N.T. Nolan, S.C. Pillai, M.K. Seery, P. Falaras, A.G. Kontos, P.S.M. Dunlop, J. W. J. Hamilton, J. A. Byrne, K. O'Shea, M.H. Entezari, D.D. Dionysiou, A review on the visible light active titanium dioxide photocatalysts for environmental applications, *Appl. Catal. B: Environ., 125 (2012) 331-349*

[165] Z. Wang, C. Chen, W. Ma, J. Zhao, Photocatalysis and water purification, From fundamentals to recent application, Ed.; Wiley-VCH Verlag GmbH and Co, (2013) 199-240

[166] S.M. Lam, J. C. Sin, A.Z. Abdullah, A.R. Mohamed, Degradation of wastewaters containing organic dyes photocatalysed by ZnO: A review, *Desalination and Water Treatment, 41 (2012) 131- 169*

[167] N. Hariprasad, S.G. Anju, E.P. Yesodharan, Suguna Yesodharan, Sunlight induced removal of Rhodmine B from water through semiconductor photocatalysis, *Res J Material Sci., 1 (2013) 9-17*

[168] N. Daneshvar, D. Salari , A.R. Khataee, Photocatalytic degradation of azo dye acid red 14 in water on ZnO as an alternative catalyst to TiO_2, *J Photochem. Photobiol. A: Chem., 162 (2004) 317-322*

[169] S.K. Kansal, M. Singh, D. Sud, Studies on the photodegradation of two commercial dyes in aqueous phase using different photocatalysts, *J Hazard. Mater, 141 (2007) 581-590*

[170] C.F.I. Jabs, H.P. Drutz, R.I. Summit, The role of intra operative cystoscopy in prolapsed and incontinence surgery, *Am J. Obst.Gynecol, 185 (2001) 1368-1373*

[171] K.E.O. Shea, D.D. Dionysiou, Advanced oxidation processes for water treatment, *J Phys. Chem. Lett., 3 (2012) 2112-2113*

[172] M. Vautier, C. Guillard, J M. Hermann, Photocatalytic degradation of dyes in water: Case study of Indigo and Indigo Carmine, *J Catal., 201 (2001) 46-51*

[173] C. Galindo, P. Jacques, A. Kalt, Photochemical and photocatalytic degradation of an Indigo dye: A case study of acid blue 74 (AB 74), *J Photochem. Photobiol A: Chem, 141 (2001) 47-53*

[174] S. Flox, C. Ammar, E. Arias, A.V. Brillas. Vargas-Zavala. R. Abdelhadi, Electrofenton and photoelectrofenton degradation of indigo carmine in acidic aqueous medium, *Appl. Catal.B: Environ, 67 (2006) 93-99*

[175] R.M.M. Othman, F.M. Ibrahem, Study of photocatalytic oxidation of indigo carmine dye on Mn-supported TiO_2, *J Photochem.Photobiol A: Chem, 189 (2007) 80-85*

[176] O.M. Shibin, B. Rajeev, V. Veena, E.P. Yesodharan, Suguna Yesodharan., ZnO photocatalysis using solar energy for the removal of trace amounts of Alfa-Methylstyrene, Diquat and Indigo carmine from water, *J Adv. Oxid. Technol, 17 (2014) 297-304*

[177] N. Barka, A. Assabane, A. Nounah, I.A. Ichou, I. A., Photocatalytic degradation of Indigo Carmine in aqueous solution by TiO_2 – coated non-woven fibres, *J Hazard. Mater, 152 (2008) 1054-1059*

[178] B. Rajeev, SugunaYesodharan, E.P. Yesodharan, Photocatalytic degradation of alpha-methyl styrene in presence of ZnO, *J Water. Process Eng, 8 (2015) 108-118*

[179] O.M. Shibin, SugunaYesodharan, E.P. Yesodharan, Sunlight induced photocatalytic degradation of herbicide diquat in water in presence of ZnO, *J Env. Chem. Eng, 3 (2015) 1101-1116.*

[180] C. Minero, G. Mariella, V. Maurino, D. Vione, D E. Pelizzetti, Photocatalytic transformation of organic compounds in the presence of inorganic ions. 2. Competitive reactions of phenol and alcohols on a Titanium dioxide−Fluoride System, *Langmuir, 16 (2000) 8964-8972*

[181] S. Rabindranathan, S. Devipriya, SugunaYesodharan, Photocatalytic degradation of phosphamidon on semiconductor oxides, *J Hazard. Mater., 102 (2003) 217-229*

[182] B. Rajeev, Suguna Yesodharan, E.P. Yesodharan, Sunlight induced ZnO mediated photocatalytic degradation of acetophenone in water, *IOSR J Appl. Chem.,3 (2016) 55-70*

[183] S. Anandan, A. Vinu, N. Venkatachalam, B. Arabindoo, V. Murugesan, Photocatalytic activity of ZnO impregnated Hβ and mechanical mix of ZnO/Hβ in the degradation of monocrotophos in aqueous solution, *J Mol. Catal. A: Chem, 256 (2006) 312-320*

[184] C.C. Chen, W.H. Ma, J.C. Zhao, Semiconductor-mediated photo degradation of pollutants under visible light irradiation, *Chem. Soc. Rev, 39 (2010) 4206-4219*

[185] I. Poulios, A. Avranas, E. Rekliti, A. Zouboulis, Photocatalytic degradation of Auramine O in the presence of semiconducting oxides, *J Chem. Technol. Biotechnol, 75 (2000) 205-212*

[186] M.H. Florencio, E. Pires, A.L. Castro, M.R. Nunes, C. Borges, F.M. Costa, Photodegradation of Diquat and Paraquat in aqueous solutions by Titanium dioxide: Evolution of degradation reactions and characterization of intermediates, *Chemosphere, 55 (2004) 345-355*

[187] S.G. Anju, SugunaYesodharan, E. P. Yesodharan, Zinc oxide mediated sonophotocatalytic degradation of phenol in water, *Chem. Eng. J, 189-190 (2012) 84-93*

[188] K.P. Jyothi, SugunaYesodharan, E.P. Yesodharan, Ultrasound, Ultraviolet light and combination assisted semiconductor catalyzed degradation of organic pollutants in water: Oscillation in the concentration of H_2O_2 formed insitu, *Ultrason. Sonochem, 21 (2014) 1782-1796*

[189] K.P. Jyothi, Sindhu Joseph., SugunaYesodharan, E.P. Yesodharan, Periodic Change in the concentration of Hydrogen peroxide formed during the semiconductor mediated sonocatalytic treatment of wastewater: Investigations on pH effect and other operational variables, *Res. J Recent Sci, 2 (2013) 136-14*

[190] A.A. Berlin, Kinetics of radical chain decomposition of persulphate in aqueous solution of organic compounds, *Kinetics. Catal, 27 (1986) 34-39*

[191] A.D. Nadezhdin, H.B. Dunford, The oxidation of ascorbic acid and hydroquinone by perhydroxyl radicals. A flash photolysis study, *Can J Chem, 57 (1979) 3017-3021*

[192] P.D. Phonsy, SugunaYesodharan, E.P. Yesodharan , Enhancement of semiconductor mediated photocatalytic removal of polyethylene plastic waste from the environment by oxidizers, *Res J Rec. Sci., 10 (2015) 105-112*

[193] I. Bouzaida, C. Ferronato, J.M. Chovelon, M. E. Rammah, J. M. Herrmann, Photocatalytic degradation of the anthraquinone dye, Acid Blue (AB25): A kinetic approach, J *Photochem. Photobiol. A:Chem, 168 (2004) 23-30*

[194] H.Y. Chen, O. Zahraa, M. Bouchy, Inhibition of the adsorption and photocatalytic degradation of an organic contaminant in an aqueous suspension of TiO_2 by inorganic ions, *J Photochem. Photobiol., A: Chem., 108 (1997) 37-44*

[195] A.G. Rincon, C. Pulgarin, Effect of pH, inorganic ions, organic matter and H_2O_2 on E. coli K12 photocatalytic inactivation by TiO_2. Implications in solar water disinfection, *Appl, Catal. B: Environ, 51 (2004) 283-302*

[196] C. Minero, P. Pellizari, V. Maurino, E. Pellizzetti, D. Vione, Enhancement of dye sonochemical degradation by some inorganic anions present in natural waters, *Appl. Catal. B. Environ, 77 (2008) 308-316*

[197] K.P. Vidya Lekshmi, SugunaYesodharan, E.P. Yesodharan, $MnO_2$and MnO_2 /TiO_2 mediated persulphate enhanced photocatalysis for the removal of Indigo carmine dye pollutant from water, *Eur. Chem. Bull, 6 (2017) 177-191*

[198] R.L. David, Handbook of Chemistry, 84th Ed. CRC Press, Boca Raton, Florida, USA, (2004) 779-782

[199] C. Minero, V. Maurino, E. Pelizzetti, D. Vione, Evidence for a surface dual hole-radical mechanism in the titanium dioxide photocatalytic oxidation of 2,4-D, *Environ Sci. Poll. Res, 13 (2006) 211-214*

[200] P.D. Phonsy, S.G. Anju, K.P. Jyothi, Suguna Yesodharan, E.P. Yesodharan, Semiconductor mediated photocatalytic degradation of plastics and recalcitrant organic pollutants in water: Effect of additives and fate of insitu formed H_2O_2, *J Adv. Oxid. Technol., 18 (2015) 85-97*

[201] K.P Jyothi, S. Yesodharan, E.P. Yesodharan, Contaminant salts as enhancers of sonocatalytic degradation of organic water pollutants: Effect of concentration, reaction time and adsorption on the efficiency of enhancement and the fate of concurrently formed H_2O_2, *J Env. Chem. Eng., 6 (2018) 3574-3589*

[202] C.S. Turchi D.F. Ollis, Photocatalytic degradation of organic water contaminants: mechanisms involving hydroxyl radical attack*, J Catal., 122 (1990) 178-192*

[203] K.P. Vidya Lekshmi, Suguna Yesodharan, E.P. Yesodharan, MnO_2 catalysed microwave mediated removal of trace amount of Indigo carmine dye from water, *IOSR J Appl. Chem, 1 (2014) 29-40*

[204] K.P. Vidya Lekshmi, Suguna Yesodharan, E.P. Yesodharan, Co_3O_4 mediated microwave catalysis: A new innovative Advanced Oxidation process (AOP) for the removal of dye pollutants from water, *IOSR J Appl. Chem, 3 (2016) 25-46*

[205] Y. Xu, C.H. Langford, Variation of Langmuir adsorption constant determined for TiO_2 photocatalysed degradation of acetophenone under different light intensity, *J Photochem. Photobiol A. Chem, 133 (2000) 67-71*

[206] S. Zhou, A.K. Ray, Kinetic studies for photocatalytic degradation of Eosin B on a thin film of Titanium dioxide, *Ind. Eng Chem. Res, 42 (6020-6033) 2003.*

[207] R. J. D. Miller, G.L. Mc Lendon, A.J Nozik, W. Schmickler, F. Willing, Surface Electron-transfer Processes, VCH publishing, New York, (1995)

[208] A. Andreozzi, V. Caprio, A. Insola. R. Marotta., Advanced oxidation processes for water purification and recovery, *Catal. Today, 53 (1999) 51-59*

[209] A.S. Stasinakis, Use of selected advanced oxidation processes (AOP's) for wastewater treatment – A mini review, *Global NEST J, 10 (2008) 376-385*

[210] Z. Frontistis, M. Antonopoulou, A. petala, D. venieri, I. Konstantinou, D.I. Kondarides, D. Mentzavinos, Photodegradation of ethyl paraben using simulated solar radiation and Ag_3PO_4 photocatalyst, *J Hazard. Mater., 323 (2017) 478-488*

[211] C. Papadopoulos, Z. Frontistis, M. Antonopoulou, D. venieri, I. Konstantinou, D. Mentzavinos, Sonochemical degradation of ethyl paraben in environmental samples, Statistically important parameters determining kinetics, by-products and pathways, *Ultrason. Sonochem., 31 (2016) 62-70*

[212] Y. Chen, P. Deng, P. Xie, R. Shang, Z. Wang, S. Wang, Heat activated persulfate oxidation of methyl and ethyl paraben: Effect, kinetics and mechanism, *Chemosphere, 168 (2017) 1628-1636*

[213] E. Brillas, P.L. Cabot, J Casado, in: M. Tarr (Ed), Chemical degradation methods for wastes and pollutants: Environmental and industrial applications, Marcel Dekker, New York, pp. 235-248.

[214] C.A. Marti'nez- Huitle, S. Ferro, Electrochemical oxidation of organic pollutants for the wastewater treatment: Direct and indirect processes, *Chem. Soc. Rev., 35 (2006) 1324-1340.*

[215] J. R. Steter, D.Dionisio, M.R.V. Lanza, A.J Motheo, Electrochemical and sonoelectro-chemical processes applied to the degradation of the endocrine disruptor methyl paraben, *J Appl. Electrochem., 44 (2014) 1317-1325*

[216] M. Neumann-Spallart, S.S. Shinde, M. Mahadik, C.H. Bhosale, Photoelectrochemical degradation of selected aromatic molecules, *Electrochim.Acta 111 (2013) 830-836*

[217] M. Panizza, G. Cerisola, Direct and mediated anodic oxidation of organic pollutants. *Chem. Rev. 109 (2009) 6541–6569*

[218] F.C. Moreira, S. Garcia-Segura, V.JP. Vilar, R.A.R. Boaventura, E. Brillas, Decolorization and mineralization of sunset yellow FCF azo dye by anodic oxidation, electro-Fenton, UVA photoelectro-Fenton and solar photoelectro-Fenton processes. *Appl. Catal. B Environ. 142–143 (2013) 877–890*

[219] A. Özcan, Y. Şahin, A.S. Koparal, M.A. Oturan, Degradation of picloram by the electro-Fenton process. *J Hazard Mater, 153 (2008) 718–727*

[220] K. Cho, D. Kwon, M.R. Hoffmann, Electrochemical treatment of human waste coupled with molecular hydrogen production. *RSC Adv., 4 (2014) 4596−4608*

[221] O. Weres, Electrode with surface comprising oxides of titanium and bismuth and water purification process using this electrode. *U.S. Patent, 7,494,583 B2, Feb. 24, 2009*

[222] H. Park, A. Bak, Y.Y. Ahn, J. Choi, M.R. Hoffmann, Photoelectrochemical performance of multi-layered BiOx-TiO_2/Ti electrodes for degradation of phenol and production of molecular hydrogen in water, *J Hazard. Mater., 211 (2012) 47−54*

[223] J. B. Parsa, M. Abbasi, Decolorization of synthetic and real wastewater by direct electrochemical oxidation process, *Acta Chim. Slov., 54 (2007) 792-797*

[224] C.Y. Cheng, G.H. Kelsall, Models of hypochlorite production in electrochemical reactors with plate and porous anodes, *J Appl. Electrochem., 37 (2007) 1203-1217*

[225] S. Zhou, A.K. Ray, Kinetic studies of photocatalytic degradation of Eosin B on a thin film of TiO_2, *Ind. Eng. Chem. Res., 42 (2003) 6020-6033*

[226] E. L. Cusslar, Diffusion mass transfer in fluid systems, Cambridge University Press, New York (1998)

[227] J. O.M. Bockris, B.E. Conway, E. Yeager, R. E. White (Eds), Comprehensive Treatise of Electrochemistry 2, Plenum Press, N. Y (1981).

[228] J. Saien, A.R. Soleymani, Degradation and mineralization of Direct blue71 in a circulating up-flow reactor by UV-TiO_2 process and employing a new method in kinetic study, *J Hazard. Mater., 14 (2007) 507-512*

[229] C. Minero, V.Maurino, E. Pellizzetti, D. Vione, An empirical quantitative approach to predict the reactivity of some substituted aromatic compounds towards reactive radical species ($Cl_2^{-\cdot}$, $Br_2^{-\cdot}$, $NO_2^{-\cdot}$, $SO_3^{-\cdot}$, $SO_4^{-\cdot}$) in aqueous solution, *Env. Sci. Poll. Res., 13 (2006) 212-214*

[230] P. Calza, E. Pelizzetti, Photocatalytic transformation of organic compounds in the presence of inorganic ions, *Pure Appl. Chem., 73 (2001) 1839-1848*

[231] M. Abdullah, G.K-C. Low, R.W. Matthews, Effects of common inorganic anions on rates of photocatalytic oxidation of organic carbon over illuminated titanium dioxide, *J Phys. Chem., 94 (1990) 6820-6825*

[232] M. Sayed, F. Pingfeng, H.M. Khan, P. Zhang, Effect of isopropanol on microstructure and activity of TiO_2 films with dominant: 110 facets for photocatalytic degradation of bezafibrate, *Int. J Photoenergy, (2014), doi:10.1155/2014/490264*

[233] J. Yu, W. Wang, B. Cheng, B.L. Zu, Enhancement of photocatalytic activity of mesoporous TiO_2 powders by hydrothermal surface fluorination treatment, *J Phys. Chem. C, 113 (2009) 6743-6750*

[234] D. Dionisio, A.J Motheo, C.Saez, M.A. Rodrigo, Effect of electrolyte on the electrolysis and photoelectrolysis of synthetic methyl paraben polluted wastewater, *Sep. Purif. Technol., 208 (2019) 201-207*

[235] G.M. Colonna,T. Caronna, B. Marcandalli, Oxidative degradation of dyes by ultraviolet radiation in the presence of hydrogen peroxide, *Dyes and Pigments., 41 (1999) 211–220*

[236] I. Sirés, E. Brillas, M.A. Oturan, M. A. Rodrigo, M. Panizza, Electrochemical advanced oxidation processes: Today and tomorrow. A review, *Environ Sci. Poll. Res, 21 (2014), 8336–8367*

[237] J.J. Pignatello, E.Oliveros, A.MacKay, Advanced oxidation processes for organic contaminant destruction based on the Fenton reaction and related chemistry, *Crit. Rev. Environ. Sci. Technol., 36 (2009) 1–84*

[238] S. Sarathy, M. Mohseni, Effects of UV/H_2O_2 advanced oxidation on chemical characteristics and chlorine reactivity of surface water natural organic matter, *Water Res., 44 (2010) 4087–4096*

[239] N. N Mahamuni, A. B Pandit, Effect of additives on ultrasound degradation of phenol, *Ultrason. Sonochem., 13 (2006) 165-174*

[240] Z. Eren, Ultrasound as a basic and auxiliary process for dye remediation: *A review. J Environ. Mangt., 104 (2012) 127–141*

[241] Y.G. Adewuyi, Sonochemistry: Environmental science and engineering applications, *Ind. Eng. Chem. Res., 40 (2001) 4681–4715*

[242] W. Song, A.A. De La Cruz, K. Rein, K.E. O'Shea, Ultrasonically induced degradation of microcystin-LR and -RR: Identification of products, effect of pH, formation and destruction of peroxides, *Environ. Sci. Technol., 40 (2006) 3941–3946*

[243] M. A. Behnajady, N. Modirshahla, M. Shokri, B. Vahid, Effect of operational parameters on degradation of Malachite Green by ultrasonic irradiation, *Ultrason. Sonochem., 15 (2008) 1009–1014*

[244] K. Makino, M.M. Mossoba, P. Riesz, Chemical effects of ultrasound on aqueous solutions, Evidence for hydroxyl and hydrogen free radicals ($^{\cdot}OH$ and $^{\cdot}H$) by spin trapping, *J Am. Ceram. Soc., 104 (1982), 3537–3539*

[245] K.S. Suslick, Ultrasound: The Chemical, Physical and Biological Effects, VCH publishers, New York, 1988

[246] O. Moumeni, O. Hamdaoui, Intensification of sonochemical degradation of malachite green by bromide ions, *Ultrason. Sonochem., 19 (2012) 404–409*

[247] P. V. Gayathri, SugunaYesodharan, E.P. Yesodharan, Microwave assisted ZnO mediated photocatalysis (MW/PS/UV/ZnO) as an efficient advanced oxidation process for the removal of RhB dye pollutant from water, *J Environ. Chem. Eng., 7 (2019) 103-122*

[248] C. Hachem, F. Bocquillon, O. Zahraa, M. Bouchy, Decolourization of textile industry wastewater by the photocatalytic degradation process, *Dyes Pigments., 49 (2001) 117–125*

[249] P. Kanthale, M. Ashokkumar, F. Grieser, Sonoluminescence, sonochemistry (H_2O_2 yield) and bubble dynamics: frequency and power effects, *Ultrason. Sonochem., 15 (2008) 143–150*

[250] M.A. Beckett, I. Hua, Impact of ultrasonic frequency on aqueous sonoluminescence and sonochemistry, *J Phys. Chem. A, 105 (2001) 3796–3802*

[251] B.Z. Li, L. Li, K.F. Lin, W. Zhang, S.G. Lu, Q.S. Luo, Removal of 1,1,1- trichloroethane from aqueous solution by a sono-activated persulfate process, *Ultrason. Sonochem., 20 (2013) 855–863*

[252] D. Sunartio, M. Ashokkumar, F. Grieser, Study of the coalescence of acoustic bubbles as a function of frequency, power, and water-soluble additives, *J Amer. Chem. Soc., 129 (2007) 6031–6036*

[253] W.P. Xie, Y. Qin, D.M. Liang, D. Song, D.W. He, Degradation of m-xylene solution using ultrasonic irradiation, *Ultrason. Sonochem., 18 (2011) 1077–1081*

[254] C. Minero, M. Lucchiari, D. Vione, V. Maurino,Fe(III)- enhanced Sonochemical degradation of methylene blue in aqueous solution, *Environ. Sci. Technol., 39 (2005) 8936–8942*

[255] P.N. Vijayalaxmi, P. Saritha, N. Rambabu, V. Himabindu, Y. Anjaneyulu, Sonochemical degradation of 2 chloro-5methyl phenol assisted by TiO_2 and H_2O_2, *J Hazard. Mater., 174 (2010) 151-155*

[256] B. Winter, M. Faubel, R.Vácha, P. Jungwirth, Behavior of hydroxide at the water/vapor interface, *Chem. Phys. Lett., 474 (2009) 241–247*

[257] K.P. Vidya Lekshmi, SugunaYesodharan, E.P Yesodharan, MnO_2 efficiently remove Indigo Carmine dyes from polluted water, *Heliyon, 4 (2018) 1-52*

[258] F. Guzman-Duque, C. Petrier, C. Pulgarin, G. Penuela, R.A. T. Palma, Effects of sonochemical parameters and inorganic ions during the sonochemical degradation of crystal violet in water, *Ultrason. Sonochem., 18 (2011) 440–446*

[259] H. Ghodbane, O. Hamdaoui, Degradation of Acid Blue 25 in aqueous media using 1700 kHz ultrasonic irradiation: ultrasound/Fe (II) and ultrasound/H_2O_2 combinations, *Ultrason. Sonochem., 16 (2009) 593–598*

[260] K.P. Jyothi, SugunaYesodharan, E.P. Yesodharan, Influence of commonly occurring cations on the sono, photo and sonophotocatalytic decontamination of water, *IOSR J Appl. Chem., 2 (2016) 15-24*

[261] K.P. Vidya Lekshmi, P.V. Gayathri, K.P. Jyothi, S.G Anju, SugunaYesodharan, E.P. Yesodharan, Application of ultrasound under different conditions for the purification of water contaminated with chemical and bacterial pollutants, *Gurukulam Int. J Innovations in Sci. and Tech., 1 (2016) 35-52*

[262] K.P. Jyothi, Suguna Yesodharan, E.P. Yesodharan, Sono- ,Photo- and Sonophotocatalytic decontamination of organic pollutants in water: studies on the lack of correlation between pollutant degradation and concurrently formed H_2O_2, *Current Science, 109 (2015) 189-195*

[263] P.V. Gayathri, Suguna Yesodharan, E.P. Yesodharan, Investigations on classic Fenton reaction as a simple inexpensive technique for the removal of toxic chemical pollutants from water, *Ind. J Appl. Res., 6 (2016) 28-33*

[264] V.Veena, Suguna Yesodharan, E.P. Yesodharan, Significant enhancement in the efficiency of the Fenton process by solar, electrolytic and sonolytic activation for the mineralization of Indigo Carmine dye pollutant in water, *Amer. J of Eng. Res., 8 (2019) 135-154*

[265] P.V. Gayathri, Suguna Yesodharan, E.P. Yesodharan, Purification of water contaminated with traces of rhodamine B dye by MW assisted oxidant induced and ZnO catalyzed advanced oxidation process, *Desalination and Water Treatment, 85 (2017) 161-174*

[266] J. He, X. Yang, B. Men, D.Wang, Interfacial mechanisms of heterogeneous Fenton reactions catalyzed by iron-based materials, *J Env. Sci., 39 (2016) 97-109*

[267] R.C.C. Costa, F.C.C. Moura, J.D. Ardisson, J.D. Fabris, R.M. Lago, Highly active heterogeneous Fenton-like systems based on FeO/Fe_3O_4 composites prepared by controlled reduction of iron oxides, *Appl. Catal. B: Environ, 83 (2014) 131-139*

[268] N. Clarke, G. Knowles, High purity water using H_2O_2 and UV radiation, *Effluent and Water Treatment Journal, 23 (1982) 335-341*

[269] R. Chen, J.J. Pignatello, Role of quinone intermediates as electron shuttles in Fenton and photo assisted Fenton oxidations of organic compounds, *Environ. Sci. Technol., 31 (1997) 2399–2406*

[270] N. Kang, D.S. Lee, J.Yoon, Kinetic modeling of Fenton oxidation of phenol and monochlorophenols, *Chemosphere, 47 (2002) 915–924*

[271] J.H. Sun, S.P. Sun, G.L.Wang, L.P. Qiao, Degradation of azo dye Amido black 10B in aqueous solution by Fenton oxidation process, *Dyes Pigments, 74 (2007) 647–652*

[272] M. Neamtu, A. Yediler, I. Siminiceanu, A. Kettrup, *J Photochem, Photobiol. A Chem., 157 (2003) 111–116*

[273] C. Guillard, E. Puzenat, H. Lachheb, A. Houas, J.M. Herrmann, Why inorganic salts decrease the photocatalytic efficiency?, *Int. J Photoenergy, 7 (2005) 1-9*

[274] A. Babuponnusami, K. Muthukumar, A review on Fenton and improvements to the Fenton process for wastewater treatment, *J Env. Chem. Eng., 2 (2014) 557-572*

[275] G. Ghiselli, W.F. Jardim, M.L. Litter, H.D. Mansilla, *J Photochem, Photobiol. A Chem. 167 (2004) 59–67*

[276] D.H. Bremner, R.Molina, F. Martinez, J.A. Melero, Y. Segura, Degradation of penolic aqueous solutions by high frequency sono-Fenton systems (US-Fe_2O_3/SBA-15-H_2O_2), *Appl. Catal. B: Environ. 90 (2009) 380-388*

[277] K.C. Namkung, A.E. Burgess, D.H. Bremner, H. Staines, Advanced Fenton processing of aqueous phenol solutions: a continuous system study including sonication effects, *Ultrason. Sonochem. 15 (2008) 171-176*

[278] P. Pulgarin, J. Kiwi, Overview of photocatalytic and electrocatalytic pretreatment of industrial nonbiodegradable pollutants and pesticides, *Chimia, 50 (1996) 50-55*

[279] U. Kurt, O. Apaydin, M. T. Gonuliu, Reduction of COD in wastewater from an organized tannery indudtrial region by electroFenton process, *J Hazard. Mater., 143 (2007) 23-40*

[280] W.P.Ting, M.C.Lu, Y.H. Huang, The reactor design and comparison of Fenton, electro-Fenton and photo electro-Fenton processes for mineralization of benzene sulfonic acid, *J Hazard. Mater., 156 (2008) 421-427*

[281] Y.H.Huang, C.C.Chen, G.H.Huang, S.S.Chou, Comparison of a novel electro-Fenton method with Fenton reagent in treating highly contaminated wastewater, *Water Sci. Technol., 43 (2001) 17-24*

[282] T. N. Ramesh, V.P. Sreenivasa, Removal of Indigo Carmine dye from aqueous solution using Magnesium hydroxide as an adsorbent, *Journal of Materials, Article ID 753057 (2015) 10 pages*

[283] L.G.C. Villegas, N. Mashhadi, M. Chen, D. Mukherjee, K.E. Taylor, N. Biswas, A Short review of techniques for Phenol removal from wastewater, *Curr. Pollution Rep., 2 (2016) 157-167*

[284] E.S. Rigobello, A.D.B. Dantas, L.D. Bernardo, E. M. Vieira, Removal of diclofenac by conventional drinking water treatment processes and granular activated carbon filtration, *Chemosphere, 92 (2013) 184-191*

.....ꕥ.....

ANNEXURES

Annexure I

List of Abbreviations

AC	Activated Carbon
ACP	Acetophenone
AOP	Advanced Oxidation Process
AOT	Advanced Oxidation Technology
BET	Brunauer–Emmett–Teller
BOD	Biological Oxygen Demand
CB	Conduction Band
CCR	Carbon-centered radicals
COD	Chemical Oxygen Demand
DSA	Dimensionally Stable Anode
Cz	Carbendazim
DB	Direct Blue
Dq	Diquat
Ea	Activation Energy
EAOP	Electrochemical Advanced Oxidation Process
EDAX	Energy Dispersive X-Ray Analysis
FR	Fenton reagent
FS	Ferrous Sulphate
FTIR	Fourier Transform Infra Red
IC	Indigo Carmine
LH	Langmiur-Hinshelwood
MB	Methylene blue
PL	Photoluminescence
PS	Peroxydisulfate

PZC	Point of zero charge
RhB	Rhodamine B
ROS	Reactive Oxygen Species
RY	Reactive Yellow
SEM	Scanning Electron Microscopy
SL	Sunlight
SPS	Sodium persulfate
TDS	Total Dissolved Solids
TEM	Transmission Electron Microscopy
TiO_2	Titanium Dioxide
TOC	Total Organic Carbon
TPA	Terephtalic acid
TSS	Total Suspended Solids
US	Ultra Sound
UV	Ultra Violet
VB	Valence Band
XRD	X-ray Diffraction
ZnO	Zinc Oxide

.....ꕥ.....

Annexure II

List of Publications

A. Papers published in standard refereed journals: 5

[1] O.M. Shibin, B. Rajeev, Veena Vijayan, Suguna Yesodharan, E. P. Yesodharan, ZnO Photocatalysis using solar energy for the removal of trace amounts of Alfa-Methylstyrene, Diquat and Indigo Carmine from water, *J.Adv.Oxid.Technol; 17 (2014) 297-304.*

[2] Veena Vijayan, Suguna Yesodharan, E. P. Yesodharan, Solar photocatalysis mediated by ZnO for the removal of last traces of Indigo Carmine dye pollutant from water, *Int. J of Sci. and Eng. Invention, 4 (2018) 1-23.*

[3] Veena Vijayan, Suguna Yesodharan, E.P. Yesodharan, Ultrasound induced Fenton/persulphate/H_2O_2/ZnO promoted advanced oxidation process for the mineralization of Indigo Carmine pollutant in water, *Ind. J of Appl. Res., 9 (2019) 32-38.*

[4] Veena Vijayan, Suguna Yesodharan, E. P. Yesodharan, Significant enhancement in the efficiency of the Fenton process by solar, electrolytic and sonolytic activation for the mineralization of Indigo Carmine dye pollutant in water, *Amer. J of Eng. Res. 8 (2019) 135-154.*

[5] Veena Vijayan, Suguna Yesodharan, Valsamma John Koshy, C.T. Aravinda Kumar, Usha K Aravind, E.P. Yesodharan, Role of electrodes and electrolytes on the efficiency of electrolytic contamination of water from Indigo Carmine dye pollutant, *Ind. J of Appl. Res., 9 (2019) 1-6.*

B. Papers presented in National/International Conferences: 5

[1] O.M. Shibin, B. Rajeev, Veena Vijayan, Suguna Yesodharan, E. P. Yesodharan, Zinc oxide photocatalysis using solar energy for the removal of Alpha methylstyrene, Diquat, Indigo Carmine, Paper presented in the *18th International conference on Semiconductor Photocatalysis and Solar Energy Conversion (SPASEC-18), San Diego, USA, 2013.*

[2] Veena Vijayan, Suguna Yesodharan, E.P. Yesodharan, Studies on Advanced Oxidation Processes for the irreversible transformation of dye pollutants in presence of Semiconductor oxides, Paper presented at the *International Conference on Emerging Environmental and Advanced Oxidation Technologies for Energy, Environment and Sustainability (EEAOTEES) held at Anna University Chennai, India 2014.*

[3] Veena Vijayan, Suguna Yesodharan, C.T. Aravinda Kumar, Usha K Aravind, E.P. Yesodharan, Photocatalytic degradation of Indigo Carmine in water using ZnO, Paper presented in the *International Conference on Photochemistry and its Applications (ICPA), Kottayam, India 2017.*

[4] Veena Vijayan, Suguna Yesodharan, Valsamma John Koshy, C.T. Aravinda Kumar, Usha K Aravind, E.P. Yesodharan, Degradation of Indigo Carmine using EAOP: Comparison of intermediate products in the presence of two supporting electrolytes using high resolution mass spectrometry, Paper presented in the *International Conference on Mass Spectrometry (ICM), Kottayam, India 2017*

[5] Veena Vijayan, Suguna Yesodharan, E.P. Yesodharan, Sonolysis as a potential Advanced Oxidation Process for the removal of traces of toxic Indigo Carmine dye pollutant from water, Paper presented in the *Indian Analytical Science Congress (IASC) Thiruvananthapuram, India 2019*

.....ꕥ.....

Annexure III

Reprints of Papers Published

1. O.M. Shibin, B. Rajeev, Veena Vijayan, Suguna Yesodharan, E. P. Yesodharan, ZnO Photocatalysis using solar energy for the removal of trace amounts of Alfa-Methylstyrene, Diquat and Indigo Carmine from water, *J. Adv. Oxid. Technol; 17 (2014) 297-304*

2. Veena Vijayan, Suguna Yesodharan, E. P. Yesodharan, Solar photocatalysis mediated by ZnO for the removal of last traces of Indigo Carmine dye pollutant from water, *Int. J of Sci. and Eng. Invention, 4 (2018) 1-23*

3. Veena Vijayan, Suguna Yesodharan, E.P. Yesodharan, Ultrasound induced Fenton/persulphate/H_2O_2/ZnO promoted advanced oxidation process for the mineralization of Indigo Carmine pollutant in water, *Ind. J of Appl. Res., 9 (2019) 32-38*

4. Veena Vijayan, Suguna Yesodharan, E. P. Yesodharan, Significant enhancement in the efficiency of the Fenton process by solar, electrolytic and sonolytic activation for the mineralization of Indigo Carmine dye pollutant in water, *Amer. J of Eng. Res. 8 (2019) 135-154*

5. Veena Vijayan, Suguna Yesodharan, Valsamma John Koshy, C.T. Aravinda Kumar, Usha K Aravind, E.P. Yesodharan, Role of electrodes and electrolytes on the efficiency of electrolytic contamination of water from Indigo Carmine dye pollutant, *Ind. J of Appl. Res., 9 (2019) 1-6*

Journal of
AOTs®
Advanced Oxidation Technologies

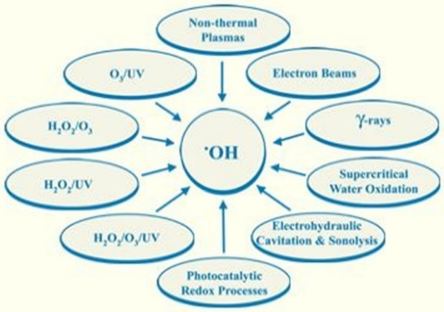

ZnO Photocatalysis Using Solar Energy for the Removal of Trace Amounts of Alfa-Methylstyrene, Diquat and Indigo Carmine from Water

Shibin O. M., Rajeev B., Veena V., Yesodharan E. P., Suguna Yesodharan*

School of Environmental studies, Cochin University of Science and Technology, Kochi 682022, India

Abstract:
Semiconductor photocatalysis using ZnO has been extensively investigated for the chemical and bacterial decontamination of water and air. In most of these cases, UV light is the source of energy and visible light induced photocatalytic degradation of trace pollutants in water has not received adequate attention. In the present study, ZnO is evaluated as a solar photocatalyst for the removal of trace amounts of three typical pollutants, i.e. alpha-Methylstyrene (AMS, a petrochemical), Diquat (herbicide) and Indigo carmine (IC, a dye) from water. Degradation by itself does not result in complete mineralisation and decontamination as seen from the significant Chemical Oxygen Demand even after the parent compound has disappeared. However, the intermediates also get mineralized eventually. The study indicates that solar photocatalysis can be used as a viable tool for the purification water contaminated with these chemicals. The degradation follows variable kinetics depending on the concentration of the substrates. H_2O_2 formed insitu in the system undergoes concurrent decomposition resulting in oscillation in its concentration. Critical parameters for optimum degradation efficiency are identified for each substrate.

Key Words: Zinc Oxide, Methyl styrene, Diquat, Indigo carmine, Photocatalysis

Introduction

Semiconductor mediated photocatalysis is fast becoming an efficient Advanced Oxidation Process (AOP) for the removal of chemical and bacterial pollutants from water (1-6). Water contaminated with organic pollutants such as pesticides, petrochemicals and dyes is a major threat to the environment. Cyano-toxins, produced and released by harmful strains of cyanobacterial algal blooms which diminish the water quality by producing undesirable color, taste and odor are another type of water pollutants (7). In addition to the toxicity, the pollutants reduce the light penetration resulting in inhibition of photosynthesis and ultimate destruction of organisms living in water bodies. Among the semiconductors tested so far, TiO_2 and ZnO have been identified as most efficient for the removal of toxic organic compounds in air or water. Following the pioneering discovery of the photosensitization effect of TiO_2 electrodes on the electrolysis of water into H_2 and O_2 by Fujishima and Honda (8), photocatalysis by semiconductors has been widely studied as a potential candidate for the efficient conversion of solar energy into chemical energy. Photocatalysis is also attracting the attention of researchers worldwide as a 'green technology' for the detoxification of harmful compounds in both water and air without utilizing or producing hazardous materials (9-12).

*Corresponding author; E-mail: sugunayesodharan@gmail.com

Generally, photocatalysis by semiconductors is the result of the interaction of photogenerated electrons and holes with the substrate. These electrons and holes can participate in reductive and oxidative reactions that lead to the decomposition of pollutants. The most widely studied catalyst in this respect is TiO_2 in view of its favorable physicochemical properties, low cost, easy availability, high stability with respect to photocorrosion and chemical corrosion and low toxicity. However, TiO_2 has a wide band gap (Anatase, E_{bg} = ca. 3.2 eV, rutile, E_{bg} = ca.3.0 eV) and can absorb light only below 400 nm, which is in the UV range that constitutes less than 5% of sunlight. Many studies have been reported on the modification of semiconductor oxides in order to extend the absorption of light to the visible range. These include dye sensitization, semiconductor coupling, impurity doping, use of coordination metal complexes and metal deposition. Deposition of noble metals such as Pt, Pd, Au, Ag etc on TiO_2 enhances the catalytic oxidation of organic pollutants. The enhancement is attributed partially to the increased light absorption (13). The metals also act as electron traps promoting the interfacial charge transfer and thus delaying the recombination of the electron-hole pair. Current status of visible light active TiO_2 photocatalysis for environmental applications has been summarized in recent reviews by Pelaez etal (14) and Wang etal (15).

Another semiconductor with potential photo-catalytic applications is ZnO with properties comparable

to those of TiO_2. Though both of them have comparable band gap energy (3.2 eV), in practice ZnO is more active in the visible region for the photocatalytic decontamination of water containing variety of organic pollutants such as pulp mill bleaching wastes, phenol, dye acid red 14 and/or heavy metals (16-19). The advantages of ZnO for visible light harvesting arise from its absorption of larger fraction of solar spectrum (20). Most widely used form of ZnO in photocatalysis is of wurtzite structure. The light scattering effect of ZnO is comparatively less due to its lower refractive index (ZnO: 2.0, TiO_2: 2.5-2.7) which is also favorable for better photocatalytic efficiency. In spite of these advantages, the number of research publications on the use of ZnO as an effective environmental photo-catalyst is less compared to TiO_2. This may be due to its instability or photocorrosion under acidic conditions resulting in the formation of $Zn(OH)_2$ which get deposited on the ZnO particle surface leading to catalytic inactivation over time.

Our earlier studies revealed that ZnO can be used as a catalyst for the degradation of certain organic pollutants in water using sunlight as the source of energy (17). In the present paper the possibility of using ZnO as a solar photocatalyst for the removal of three typical pollutants, i.e. Diquat (herbicide), Alfa methyl styrene (AMS, petrochemical) and indigo carmine (IC, a dye used in textiles, cosmetics and medical procedures) is investigated. The influence of various operational parameters such as concentration of the pollutants, pH, catalyst loading etc. on the rate of removal of the pollutants and the reaction kinetics is investigated. The chemical structure of these pollutants is as follows;

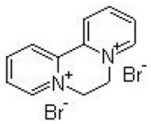

Diquat Dibromide salt

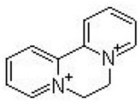

Diquat Cation (Active Form)

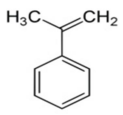

Alpha methyl styrene

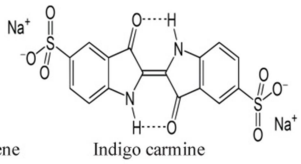

Indigo carmine

Experimental

Zinc oxide (99% pure) supplied by Merck India Ltd is used as such without further purification. The average particle size was around 15-20 x 10^{-2}µm and the BET surface area was ~15 m^2/g. The consistency of the physicochemical characteristics of ZnO used in the study with that reported in literature was confirmed by X ray diffractogram (XRD) and Scanning Electron Microscopy (SEM) measurements. The absorption spectrum of ZnO shows single broad line absorption from 460 nm to lower wavelength which is consistent with the literature data (20).

All other chemicals used were of AR grade. Doubly distilled water was used in all the experiments. The photocatalytic experiments were performed as explained earlier (17). Solar experiments were performed by placing the reactor assembly on the roof top of our laboratory at Kochi, Kerala, India (9^0 57' 51" N, 76^0 16' 59" E) during sunny days in February-May 2012 and October (2012) to (January 2013). The suspension was stirred frequently to ensure uniform mixing. Samples were drawn periodically and analyzed. AMS was determined by Gas chromatography using flame ionization detector and Elite 1301 column with hydrogen carrier gas. The instrument was earlier calibrated for quantitative estimation of the AMS at comparable concentrations. Diquat and IC concentra-tions were determined by Spectrophotometry (310 and 610 nm respectively). Suspension kept under identical conditions in the dark was used as the reference in each case to eliminate the contribution from adsorption towards the reduction in the pollutant concentration. H_2O_2 formed in the reaction system is determined quantitatively by iodometry.

Results and Discussions

Photocatalytic degradation of trace amounts of Diquat, AMS and IC in water was evaluated using ZnO suspensions of respective solutions in sunlight. No degradation of the pollutants takes place in the absence of catalyst and light indicating that these two components are essential for the degradation. The pH of the reaction system for each pollutant was maintained at respective natural value in ZnO-water suspension (AMS: 5.5, Diquat: 5.5, IC: 4.8.).

Effect of Catalyst Dosage

The effect of catalyst loading on the photo-catalytic degradation of the pollutants is tested by keeping all other reaction parameters constant. The results are plotted in Figure 1. The rate of degradation increases with increase in loading in all cases reaching an optimum and is then either stabilised or decreases. Higher degradation at higher loadings can be attributed to increase in catalyst surface area, increase of light absorption and consequently higher number of active species. However at higher loadings beyond the

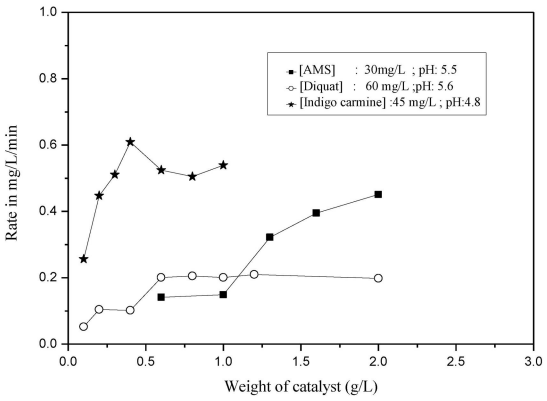

Figure 1. Effect of catalyst dosage on the degradation of various pollutants.

optimum, some of the catalyst particles are effectively in the dark and there is decrease in the light penetration. Further it is difficult to maintain the suspension homogeneous and the catalyst has a tendency to settle at the bottom of the reactor. Variation in the degree of settling influences the consistency of the sampling process, total amount of light absorption and scattering of the incident light by the catalyst. At higher loadings, the photoactivated particles may interact with the ground state particles and get deactivated. These factors together contribute to decrease in the efficiency of the catalyst at loadings above the optimum level. The optimum is different for the three pollutants, i.e. 0.4, 0.6 and 2.0 g/L for IC, Diquat and AMS respectively under otherwise identical conditions indicating that the concentration and nature of the organic substrate as well as the substrate-catalyst interaction can play a decisive role in determining the optimum catalyst loading. The optimum also depends on the geometry of the reactor and reaction conditions.

The degradation of the three pollutants in presence of ZnO at respective optimized loadings as a function of time is shown in Figure 2. The concentrations of the pollutants are kept different due to solubility constraints. The degradation increases slowly in the case of diquat while it increases sharply with time in the case of AMS and IC. The decrease in the concentration of the pollutant is not due to adsorption at least in the case of diquat and IC because their adsorption was negligible as determined by experiments. However in the case of AMS, the stabilised adsorption under standard reaction conditions can go upto 8%. As can be seen in the figure, the degradation is much more facile in the case of IC which is an anionic dye with λ_{max} of ~ 600 nm. In addition to the photocatalytic activity of ZnO induced by the UV component of sunlight, indigo carmine itself can act as a sensitizer and extend the absorption of the catalyst towards visible light. Visible light excites the dye sensitizer adsorbed on ZnO and subsequently electrons from the excited dye are injected to the conduction band of ZnO while the valence band remains unaffected. The conduction band electron forms superoxide radical anion ($O_2^{\cdot-}$) by reaction with dissolved/adsorbed O_2, resulting in the formation of Reactive Oxygen Species (ROS) such as hydroxyl radicals. These ROS are responsible for the oxidation of the organic contaminants including the dye itself or coexisting organics (21).

The degradation in all cases slows down with time mainly because the residual concentration of the substrate becomes low and the intermediates and other products may compete for same active sites at the surface. This is verified by studying the degradation at different concentrations of the pollutants.

Effect of Initial Concentration of the Pollutant

The effect of initial concentration of each of the three pollutants was examined by varying the initial concentration (depending on the solubility of the substrates) at respective optimum catalyst concentration and natural pH of the catalyst-solution suspension. The initial reaction rate vs concentration is plotted in Figure 3. In the case of AMS and IC, the rate increases with increase in concentration at lower concentration range. This is in line with many photocatalytic reactions which follow pseudo first order kinetics at lower concentration in accordance with the Langmuir-

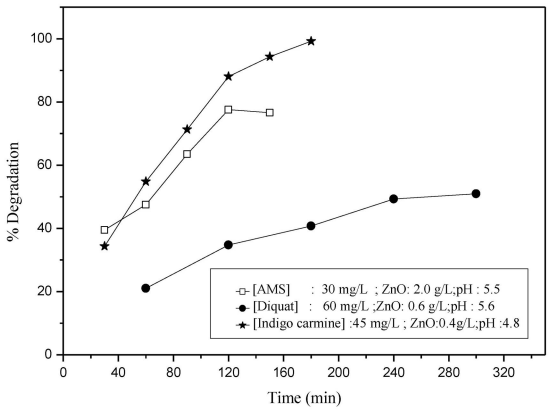

Figure 2. Photocatalytic degradation of various pollutants Vs time.

Hinshelwood model modified to accommodate reactions occurring at solid-liquid interface (22-24). The rate stabilises in the case of AMS while it decreases in the case of IC at higher concentration indicating lower order and eventual zero order kinetics. The lifetime of the reactive OH radicals is very short (only few nanoseconds) and hence they can react with molecules in the proximity of their formation. Higher substrate concentration implies more molecules per unit volume which enhances the probability of collision between the oxidizing species and the pollutant. However at much higher concentration, an inner filter effect is induced and the incident light will be largely wasted for the substrate excitation rather than the excitation of the catalyst particles and generation of reactive free radical species (25). The path length of light entering the system also decreases with increase in concentration. Similar screening effect was reported earlier also (15, 16, 26). Consequently the reaction rate is stabilised or decreases. The reaction becomes independent of the concentration of the substrate. Hence it is logical to assume that the photocatalytic degradation happens in two stages. First stage is faster and follows pseudo first order kinetics. The reaction rate is slower in the second stage. Duration of the first stage decreases with increase in concentration. Another reason for the lower rate of degradation at higher concentration may be that the major portion of the reaction occurs in the reaction zone close to the irradiated side since the irradiation intensity on this side is much higher than that on the other side (22).

At higher concentration there is competition for adsorption/degradation between the substrates and the degradation intermediates leading to decreased rate. Major intermediates formed during the photocatalytic degradation of diquat and IC have been identified and reported earlier (25, 26). In the case of AMS, acetophenone is identified as a major intermediate in the photocatalytic degradation process. However, the acetophenone also gets mineralized eventually. Comparative study of the adsorption of acetophenone and AMS on ZnO shows that it is reasonably identical. The mutual effect of AMS and acetophenone on the respective photocatalytic degradation is investigated. The results presented in Figure 4 clearly show that both AMS and acetophenone mutually inhibit the degradation by competing for the same sites on the catalyst surface. The degradation is relatively slower in the case of acetophenone which is further slowed down by the presence of AMS. The combined concentration of added and insitu formed acetophenone remains more or less the same in presence of AMS indicating that the rate of formation and degradation of the former is more or less identical. As the initial concentration of the substrate increased, the requirement of energy and catalyst surface for adsorption also increased. But the catalyst and light source are kept constant. The negative effect of increasing concentration implies that at higher concentration, the substrate is inhibiting the action of catalyst and/or light. The relative concentration of active free radicals responsible for interaction with the substrate is lower which also reduces the degradation. Thus it is clear that absorption of light, number of available adsorption sites and relative abundance of reactive free radicals vs the substrate are the major factors affecting the effect of concentration of the pollutant on the

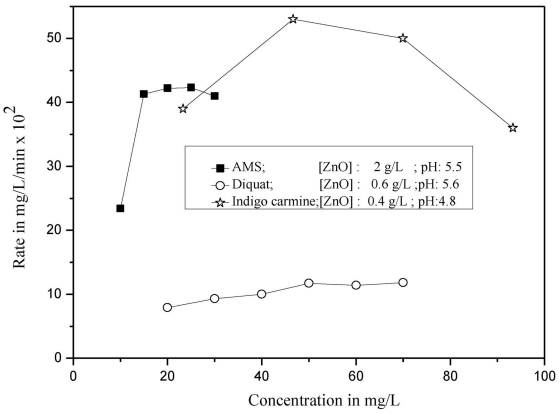

Figure 3. Effect of concentration of pollutants on their photocatalytic degradation over ZnO.

degradation. This is further confirmed from the enhanced degradation of the pollutant at higher concentration by the addition of extra amount of catalyst in between the reaction (27).

pH Effect

The role of pH on the photocatalytic behavior of semiconductor oxides is often correlated to their oxidation potential and surface charge which determines the adsorptive properties. However these are not the only factors that determine the effect of pH. In the current study, the effect of pH on the degradation of the three pollutants is investigated and the results are given in Figure 5. In the case of diquat, the substrate undergoes hydrolysis in the alkaline pH even in the absence of catalyst or light and hence only acidic range is studied. At the lower pH, degradation is quite slower and maximum degradation occurs at around pH 5. The low value at pH 3 is due to the corrosion and photo-dissolution of ZnO (22) which is enhanced by reaction with insitu generated holes as in reaction 1.

$$ZnO + 2h_{VB}^{+} \rightarrow Zn^{2+} + O^{-} \quad (1)$$

ZnO may also react with acids used for adjusting the pH to produce corresponding salt which will get deposited on the surface thereby reducing its photocatalytic activity. Adsorption of diquat on ZnO at the natural pH of the system, i.e. 5.5, is quite low and this can be attributed to its structure which consists of two aromatic rings which are not coplanar (28).

In the case of IC, the maximum degradation is seen at pH 4. The Point of zero charge of ZnO is 9 ± 0.3 below which the surface is positively charged and can adsorb large number of negatively charged IC dye. But this is not reflected in the extent of degradation. Below pH 4, due to the corrosion of the catalyst, the number of sites will be less and hence lower degradation. The lower degradation above pH 4.5 can be due to the presence of Cl^- anions (from the HCl used for pH adjustment) which can react with hydroxyl radicals leading to inorganic radical anions. These radical anions show much lower activity than $^{\cdot}OH$ (25). There will also be competition between the dye and anion for $^{\cdot}OH$ resulting in decreased degradation. In the case of IC having two sulphonic groups, single anions are formed in pure water and the tendency to aggregate is low. Presence of anions such as Cl^-, SO_4^{2-} or PO_4^{3-} used for adjusting the pH, may promote aggregation. Aggregates of two or more molecules are less accessible to OH radicals than single molecules (25). At pH above the pzc electrostatic repulsion between the negatively charged particles and the anionic dye skeleton prevents the molecules from coming into contact with the surface resulting in decreased activity. The ZnO may also form complexes in the basic pH range leading to partial insulation of the catalyst surface and its inactivation. The moderate degradation observed in the alkaline condition may be due to the increase in OH radicals formed from the hydroxyl ions OH^-.

In the case of AMS also the degradation is maximum in the pH range of 4-5. The higher degradation at the acidic pH, low degradation below PH 3 and moderate degradation in the alkaline pH can be explained as in the case of IC and Diquat. The

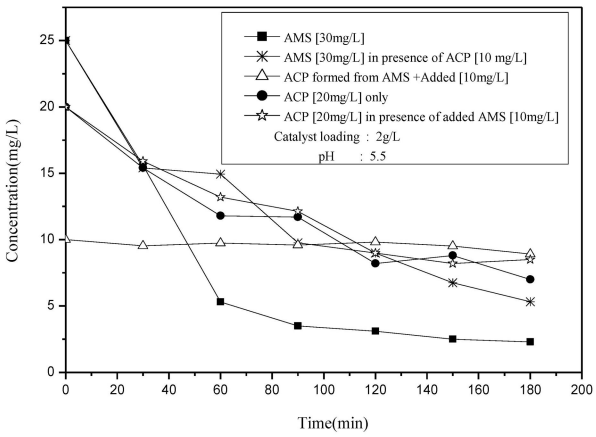

Figure 4. Mutual effect of Acetophenone and AMS on their respective degradation.

results illustrate that interpretation of the effect of pH on the photocatalytic process is very difficult because of the multiple factors such as electrostatic interaction between the semiconductor surface, solvent molecules, substrates, intermediates and charged radicals formed during the reaction process. This is consistent with the findings of other researchers as well (29).

General Mechanism

The basic mechanism of semiconductor photocatalysis consists of initial light absorption by the catalyst which produces a conduction band electron and valence band hole. Both the electron and hole must be consumed so that the material can act as a catalyst. It is generally believed that both the electrons and holes can find low energy trap sites on a sub-picosecond time scale in the semiconductor (30).

$$ZnO + h\nu\ (<380\ nm) \rightarrow h^+ + e^- \quad (2)$$

These electrons and holes can either recombine and dissipate the input energy as heat or react with electron donors and electron acceptors which are adsorbed on the semiconductor surface or trapped within the surrounding electrical double layer of the charged particles to produce strong oxidizing hydroxyl radicals which can promote the oxidation of organic compounds as follows (24):

$$O_2 + e^- \rightarrow O_2^{\cdot-} \quad (3)$$

$$h^+ + H_2O \rightarrow h^+ + {}^{\cdot}OH \quad (4)$$

$${}^{\cdot}OH + RH \rightarrow H_2O + R^{\cdot} \quad (5)$$

$$R^{\cdot} + O_2 \rightarrow ROO^{\cdot} \rightarrow \ldots \rightarrow CO_2 \quad (6)$$

H_2O_2 is detected as a byproduct in the degradation of all the pollutants tested here. However, its concentration does not increase corresponding to the degradation of the pollutant and is stabilised or even decreased even before the pollutant degradation is complete (Figure 6). Also there is no direct correlation between the concentration of the pollutant and the quantity of H_2O_2 detected. Earlier studies have attributed this to the concurrent decomposition of H_2O_2 which results in stabilization / periodic increase and decrease in its concentration, i.e. oscillation (27). Depending on the domination of formation or decomposition rate at any point of time, the net concentration of H_2O_2 varies. Various steps leading to the concurrent formation and decomposition of H_2O_2 may be summarized as follows (31-33):

$$O_2^{\cdot-} + H^+ \rightarrow HO_2^{\cdot} \quad (7)$$

$$2HO_2^{\cdot} \rightarrow H_2O_2 + O_2 \quad (8)$$

$$O_2^{\cdot-} + HO_2^{\cdot} \rightarrow O_2 + HO_2^- \quad (9)$$

$$HO_2^{\cdot-} + H^+ \rightarrow H_2O_2 \quad (10)$$

$${}^{\cdot}OH + {}^{\cdot}OH \rightarrow H_2O_2 \quad (11)$$

The decomposition of H_2O_2 and formation of more reactive OH radicals take place by any one or more of the following:

$$H_2O_2 + h\nu \rightarrow 2OH^{\cdot} \quad (12)$$

$$H_2O_2 + O_2^{\cdot-} \rightarrow OH^{\cdot} + OH^- + O_2 \quad (13)$$

$$H_2O_2 + e^- \rightarrow OH^{\cdot} + OH^- \quad (14)$$

$$2OH^- + h^+ \rightarrow OH^{\cdot} + OH^- \quad (15)$$

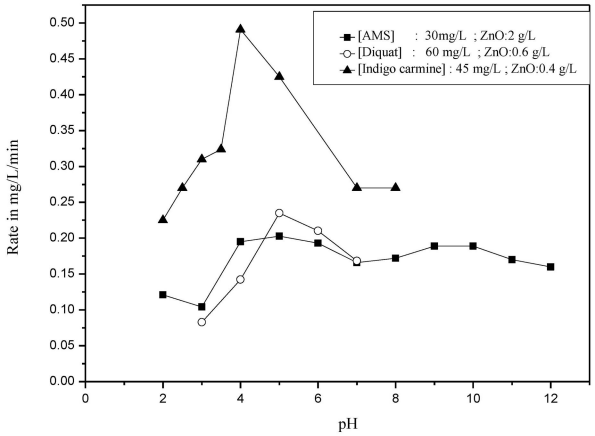

Figure 5. Effect of pH on the photocatalytic degradation of various pollutants by ZnO.

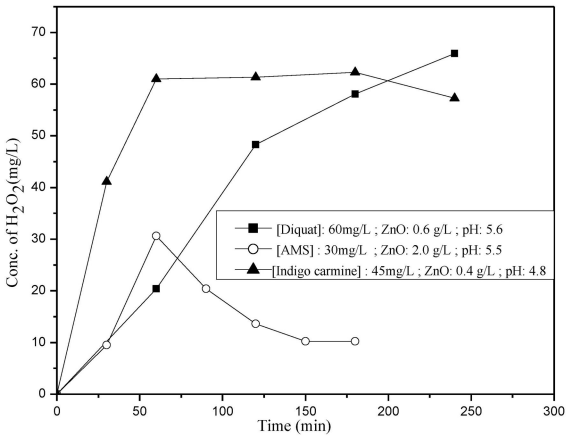

Figure 6. Concentration of H_2O_2 Vs time during the photocatalytic degradation of organic pollutants in water.

Repeated attacks by the $O_2^{\cdot-}$/$^{\cdot}OH$/$HO_2^{\cdot}$ radicals on the pollutant nuclei can lead to the mineralization producing mainly CO_2 and water.

Conclusion

Zinc oxide is found to be an efficient photocatalyst capable of mineralizing different types of chemical pollutants in water using direct sunlight as the energy source. The degradation follows pseudo first order kinetics at lower concentrations of the substrate and zero order at higher concentration. There is no uniform pattern in the effect of pH on the degradation rate which depends on a number of factors related to the characteristics of the catalyst, structure of the pollutant and substrate-surface interaction. H_2O_2 formed insitu in the process undergoes concurrent decomposition resulting in stabilization or oscillation in its concentration. The study proves that ZnO as such, without any modification, can be used as an efficient sunlight activated photocatalyst for the removal of trace amounts of at least some toxic chemical contaminants from water.

Acknowledgement

Financial support from the Cochin University of Science and Technology to one of the authors (VV) by way of Junior Research Fellowship is gratefully acknowledged.

References

(1) Matthews, R.W. *Pure and Appl. Chem.* **1992**, *64*, 1285-1290.

(2) Devipriya, S.; Yesodharan, S. *Solar Energy Materials and Solar Cells* **2005**, *86*, 309-348.

(3) Chong, M.N.; Jin, B.; Chow, C.W.K; Saint, C. *Water. Res.* **2010**, *44*, 2997-3027.

(4) Takeuchi, J.P.; Cuong, M.; Zhang, T-M.; Matsuoka, M.; Anpo, M. *Res. Chem. Intermed.* **2010**, *99*, 327-347.

(5) Ollis, D.; Pichat, P.; Serpone, N. *Appl. Catal. B: Environ.* **2010**, *99*, 377-387.

(6) Pichat, P., Ed. *Photocatalysis and Water Purification: From Fundamentals to Recent Applications*; Wiley-VCH Verlag GmbH and Co.: 2013.

(7) Antoniou, M.G.; Nicolaou, P.A.; Shoemaker, J.A; de la Cruz, A.A; Dionysiou, D.D. *Appl. Catal. B: Environ.* **2009**, *91*, 165-173.

(8) Fujishima, A.; Honda, K. *Nature* **1972**, *238*, 37-38.

(9) Frank, S.N; Bard, A.J. *J. Amer. Chem. Soc.* **1977**, *99*, 303-304.

(10) Serpone, N.; Pelizzetti, E., Eds. *Photocatalysis: Fundamentals and Applications*; John Wiley and Sons Inc.: New York, 1989.

(11) Ollis, D.F; Al-Ekabi, H. *Photocatalytic purification and treatment of water and air*; Elsevier: Amsterdam 1993.

(12) Anpo, M.; Kamath, P.V.; Eds., *Environment Benign Photocatalysts*; Springer: New York 2010.

(13) Devipriya, S.P.; Suguna Y.; Yesodharan, E.P. *Int. J Photoenergy* **2012**, Article ID 970474, 8 pages.

(14) Pelaez, M.; Nolan, N.T; Pillai, S.C; Seery, M.K; Falaras, P.; Kontos, A.G; Dunlop, P.S.M; Hamilton, J.W.J; Byrne, J.A.; O'Shea, K.; Entezari, M.H; Dionysiou, D.D. *Appl. Catal. B: Environmental* **2012**, *125*, 331-349.

(15) Wang, Z.; Chen, C.; Ma, W.; Zhao, J. In *Photocatalysis and water purification, From fundamentals to recent application*; Pichat, P., Ed.; Wiley-VCH Verlag GmbH and Co.: 2013, pp 199-240.

(16) Lam, S-M.; Sin, J.C.; Abdullah, A.Z, Mohamed A.R. *Desalination and Water Treatment* **2012**, *41*, 131-169.

(17) Hariprasad, N.; Anju, S.G.; Yesodharan, E.P.; Yesodharan, S. *Res J. Material Sci.* **2013**, *1*, 9-17.

(18) Daneshvar, N.; Salari, D.; Khataee, A.R. *J. Photochem Photobiol. A: Chem.* **2004**, *162*, 317-322.

(19) Kansal, S.K.; Singh, M.; Sud, D. *J. Hazardous Mater.* **2007**, *141*, 581-590.

(20) Sakthivel, S.; Neppolian, B.; Shankar, M.V. Arabindoo, B.; Palanichamy, M.; Murugesan, V. *Solar Energy Materials and Solar Cells* **2003**, *77*, 65-82.

(21) Chen, C.C.; Ma, W.H; Zhao, J.C. *Chem. Soc. Rev.* **2010**, *39*, 4206-4219.

(22) Evgenidou, E.; Fytianos, K.; Poulios, I. *J. Photochem Photobiol. A:Chemistry* **2005**, *175*, 29-38.

(23) Rabindranathan, S.; Devipriya, S.P; Yesodharan, S. *J. Hazard. Mater.* **2003**, *B102*, 217-229.

(24) Poulios, I.; Avranas, A.; Rekliti, E.; Zouboulis, A. *J. Chem. Technol. Biotechnol.* **2000**, *75*, 205-212.

(25) Galindo, C.; Jacques, P.; Kalt, A. *J. Photochem. Photobiol. A: Chem.* **2001**, *141*, 47-56.

(26) Florencio, M.H.; Pires, E.; Castro, A.L.; Nunes, M.R.; Borges, C.; Costa, F.M. *Chemosphere* **2004**, *55*, 345-355.

(27) Jyothi, K.P.; Sindhu J.; Yesodharan, S.; Yesodharan, E.P. *Res. J. Recent Sci.* **2013**, *2*, 136-149.

(28) Derry, J.E.; Hamor, T.E. *Nature* **1969**, *221*, 464-465.

(29) Qamar, A.; Muneer, M. *Desalination* **2009**, *249*, 535-540.

(30) Jenks, W.S. In *Photocatalysis and Water Purification: From Fundamentals to Recent Applications*; Pichat, P. Ed., Wiley-VCH Verlag GmbH and Co.: 2013, pp 25-51.

(31) Jenny, B.; Pichat, P. *Langmuir* **1991**, *7*, 947-954.

(32) Ishibashi, K.; Nosaka, Y.; Hashimoto, K.; Fujishima, A. *J. Phys. Chem. B* **1998**, *102*, 2117-2120.

(33) Yi, J.; Bahrini, C.; Schoemaecker, C.; Fittschen, C.; Choi, W. *J. Phys. Chem. C* **2012**, *116*, 10090-10097.

Received for review October 30, 2013. Revised manuscript received March 4, 2014. Accepted March 5, 2014.


www.ijsei.in
ISSN No. 2455-4286
International Scientific
Invention Journals
ISIJ
Open Access Journal
International Journal
of Science
&
Engineering Invention
(IJSEI)
ISIJ Publisher
VOLUME-04
ISSUE-03
MARCH - 2018
IJSEI Indexcopernicus ICV Value - 80.77

International Journal of Science and Engineering Invention | RESEARCH ARTICLE

Solar photocatalysis mediated by ZnO for the removal of last traces of Indigo carmine dye pollutant from water

Veena Vijayan, Suguna Yesodharan, E. P. Yesodharan*

ABSTRACT

Solar photocatalysis as a potential green technology for the removal of traces of the dye pollutant Indigo carmine (IC) from water is investigated using ZnO as the catalyst. Degradation/decolorization alone does not result in complete decontamination as seen from the significant Chemical Oxygen Demand (COD) of water even after the parent compound has disappeared completely. The degradation proceeds through many intermediates which also get mineralized eventually but slowly. Oxalic acid is identified as a stable slow mineralizing degradation product which itself is formed from other transient intermediates. Effect of various parameters such as catalyst dosage, concentration of the dye, pH, temperature, presence of contaminant salts etc. on the degradation is investigated and quantified. Oxidants such as $S_2O_8^{2-}$ and H_2O_2 have only moderate influence on the degradation. The degradation follows variable kinetics depending on the concentration of the substrate. The reaction proceeds very slowly in the absence of O_2 indicating the importance of reactive oxygen species and hydroxyl free radicals in photocatalysis. H_2O_2 formed insitu in the system undergoes concurrent decomposition resulting in stabilization in its concentration. The study demonstrates that solar photocatalysis can be used as a viable tool for the purification of water contaminated with traces of IC.

Keywords - Zinc Oxide, Solar energy, Indigo carmine, Photocatalysis, Hydrogen peroxide, Anions

I. INTRODUCTION

Dyes are used extensively in many of the modern day materials including textiles, paints, food, pharmaceuticals, printing and a host of other industries. The production, processing and application of various dyes will result in contamination of water with toxic and recalcitrant materials which are resistant to destruction by conventional physicochemical and biological treatment. In particular, the textile industry consumes large quantities of water during the dyeing and finishing operations. Even the best treatment method may not be capable of removing the last traces of coloring agents completely. In addition to the toxicity and other health hazards, the dye pollutants also reduce the light penetration through the contaminated water resulting in inhibition of photosynthesis and ultimate destruction of organisms living in those water bodies. Conventional techniques such as adsorption, ultra filtration, reverse osmosis, extraction etc. are nondestructive and simply transfer the organic pollutants from water to another medium or sludge. Thus the pollution continues unabated from a different source. Hence it is imperative that viable environment-friendly techniques are developed for the mineralization of the pollutants and decontamination of water to make it safer and reusable. Semiconductor oxide-mediated photocatalysis is fast becoming an efficient advanced oxidation process (AOP) for the removal of chemical and bacterial pollutants from water,[1-7] consequent to the pioneering discovery of the photosensitization effect of TiO_2 electrodes on the electrolysis of water into H_2 and O_2 by Fujishima and Honda.[8] Among the semiconductors tested so far, TiO_2 and ZnO are identified as most efficient for the removal of a variety of water pollutants. Semiconductor photocatalysis has also been widely investigated as a potential candidate for the efficient conversion of solar energy into chemical energy. Photocatalysis is also attracting the attention of researchers worldwide as a 'green technology' for the detoxification of harmful compounds in both water and air without utilizing or producing hazardous materials.[9-12]

School of Environmental studies
Cochin University of Science and Technology, Kochi 682022, India
Correspondence- E. P. Yesodharan (epyesodharan@gmail.com)

Volume 04, Issue 03, March 2018

Received: 13 March 2018 **Revised:** 20 March 2018 **Accepted:** 22 March 2018 **Published:** 30 March 2018

The advantages of ZnO and TiO_2 as photocatalysts include favorable physicochemical properties, low cost, easy availability and low toxicity. They have identical band gap, i.e. ZnO E_{bg} = 3.2 eV, anatase (TiO_2) E_{bg} = ~3.2 eV and rutile
(TiO_2), E_{bg} = ~3.0 eV. They can absorb light only below 400 nm, which is in the UV range that constitutes less than 5% of sunlight. Many studies have been reported on the modification of semiconductor oxides in order to extend the absorption of light to the visible range. These include dye sensitization, semiconductor coupling, impurity doping, use of coordination metal complexes and noble metal (Pt, Pd, Au, Ag etc) deposition.[13-15] The resulting enhancement in the photocatalytic degradation of organics is attributed partially to the increased light absorption (13). The metals also act as electron traps promoting the interfacial charge transfer and thus delaying the recombination of the electron-hole pair. Current status of visible light active TiO_2 photocatalysis for environmental applications has been summarized in few recent reviews by Pelaez etal[14] and Wang et al.[15]

In spite of the comparable physicochemical characteristics of ZnO and TiO_2, the former is more active in the visible region for the photocatalytic decontamination of water containing variety of organic pollutants such as pulp mill bleaching wastes, phenol, dyes and/or heavy metals.[16-20] The advantages of ZnO for visible light harvesting arise from its relatively better absorption of larger fraction of solar spectrum and light quantum.[20] Most widely used form of ZnO in photocatalysis is of wurtzite structure. The light scattering effect of ZnO is comparatively less due to its lower refractive index (ZnO: 2.0, TiO_2: 2.5-2.7) which is also favorable for better photocatalytic efficiency. In spite of these advantages, the number of research publications on the use of ZnO as an effective environmental photocatalyst is much less compared to TiO_2. This may be due to the perceived instability or photo-corrosion of ZnO under acidic conditions resulting in catalytic inactivation over time.

Indigo carmine (3,3'-dioxo-1,3,1',3'-tetrahydro-[2,2']-bi-indolylidene-5,5'-disulphonic acid disodium salt), also known as acid blue 74 (AB74), is an important industrial dye used for dying of clothes and also for medical diagnostic purposes. It can also help to target biopsies even better since the homogeneously stained or unstained areas can be correlated with intraepithelial neoplasia.[21] The chemical structure of IC is as in figure 1.

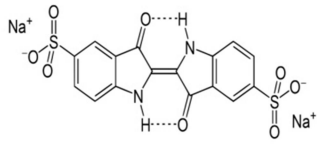

Fig 1: Structure of Indigo carmine

The dye is highly toxic, carcinogenic and has the potential to cause permanent injury to eyes. It can also lead to reproductive, developmental, neuro and acute toxicity. Other health effects include possible tumors at the site of application, cardiovascular and respiratory effects and gastrointestinal irritation.[22] Extensive application of IC will naturally lead to environmental contamination through different routes, in particular water.

Few investigations on the removal of IC from water using AOPs have been reported.[23-26] Our earlier studies revealed that ZnO can be used as an effective photocatalyst for the degradation of many organic pollutants such as phenol, α- methyl styrene, acetophenone, diquat herbicide etc. in water using sunlight as the source of energy.[27] In the current study the possibility of using ZnO as a solar photocatalyst for the removal of IC is investigated. The dye is chosen since it is one of the least investigated dye pollutants under photocatalysis The influence of various operational parameters such as concentration of the pollutants, pH, catalyst loading, temperature, presence of salt contaminants, dissolved O_2 etc. on the rate of removal of the pollutants and the reaction kinetics are investigated. Probable intermediates are also identified.

II. MATERIALS AND METHODS

Zinc oxide (~99% pure) supplied by Merck India Ltd. is used as such without further purification. The average particle size was around 15 x 10^{-2}μm and the BET surface area was ~15 m^2/g. Scanning Electron Microscopy (SEM) and X-ray diffractogram (XRD) measurements confirmed the consistency of the physicochemical characteristics of ZnO used in the current study with those reported in literature. It was also seen that the absorption spectrum of ZnO has single broad line from 460 nm to lower wavelength. This is also consistent with the literature data.[20] H_2O_2 (30.0% w/v) and Persulphate (PS) (purity~99%) were from Qualigen (India). IC (Extra Pure Grade > 99.5% purity) was from Sisco Research Laboratories Pvt. Ltd (India) and was used as such without further purification. Twice distilled water was used in all the experiments. All other

chemicals used were of AnalaR Grade or equivalent unless indicated otherwise.

The solar photocatalytic experiments were performed in a pyrex glass reactor. The reactor was placed in a tray through which water from a thermostat maintained at the required temperature was constantly circulated. The dye solution, ZnO and the additives (as and when required) were taken in the reactor. The suspension was stirred frequently to ensure uniform mixing. For solar experiments, the reactor assembly was placed on the roof top of our laboratory at Kochi, Kerala, India (9^0 57' 51" N, 76^0 16' 59" E) during sunny days in October (2016) to (January 2017) and March-May (2017). UV irradiation was done in the laboratory using a 400 W medium pressure mercury vapor lamp. Samples were drawn periodically, centrifuged for removing traces of fine suspended particles and analyzed for the IC concentration by UV-VIS Spectrophotometry at 610 nm. High Performance Liquid Chromatography coupled with Mass Spectrometry (HPLC/MS) was used to identify the reaction intermediates. Suspension kept under identical conditions in the dark was used as the reference in each case to eliminate the contribution from adsorption towards the reduction in the IC concentration. H_2O_2 was estimated by standard iodometry.

III. RESULTS AND DISCUSSIONS

Sunlight (SL) induced photocatalytic degradation of trace amounts of IC in water in presence of ZnO is investigated under various reaction conditions. No degradation of IC takes place in the absence of catalyst and light indicating that these two components are essential for the degradation. The results are shown in figure 2. The pH of the reaction system was maintained at the natural value for ZnO-water suspension, i.e. 4.8 unless indicated otherwise. The results clearly show that the decrease in the concentration of IC is not due to its adsorption on the catalyst or direct solar degradation of the dye. The maximum equilibrated dark adsorption of IC observed under the reaction conditions is less than 5%.

Evaluation of the comparative photocatalytic effect of ZnO and TiO_2 in presence of sunlight under identical conditions shows that the former is much more efficient (~90% compared to ~40% of the latter in 60 minutes) for the degradation of IC. Hence all further studies were carried out using ZnO as catalyst.

The comparative degradation of IC in presence of ZnO under UV light and sunlight under otherwise identical conditions is shown in figure 3. The IC itself undergoes moderate degradation in presence of UV (~30% in 60 min) even in the absence of the catalyst. However, the sunlight induced degradation of the dye is negligible. The photocatalytic degradation is more under sunlight than UV irradiation. This is surprising because ZnO is essentially a UV-active photocatalyst, with only modest capability to get activated under sunlight. The high solar catalytic activity may be due to the sensitization of ZnO induced by IC which is an anionic dye capable of absorbing visible light with λ_{max} of ~ 600 nm. Consequently, electrons from the sunlight-excited dye are injected to the conduction band of ZnO more easily than the promotion of an electron from the valence band

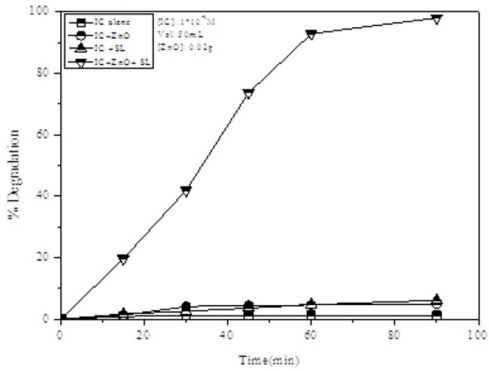

Fig 2: Degradation of IC under various conditions; SL = Sunlight

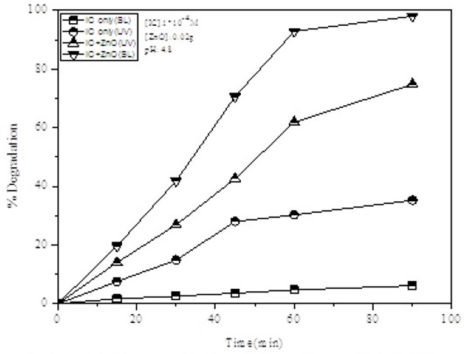

Fig. 3: Comparative photocatalytic degradation of IC under sunlight (SL) and UV light irradiation

to the conduction band under UV irradiation. The conduction band electron forms superoxide radical anion ($O_2^{\cdot-}$) by reaction with dissolved/adsorbed O_2, resulting in the formation of reactive oxygen species (ROS) such as hydroxyl radicals. These ROS are responsible for the oxidation of the organic contaminants including the dye itself or other co-existing organics.[20] The general mechanism of dye sensitization is shown in figure 4.

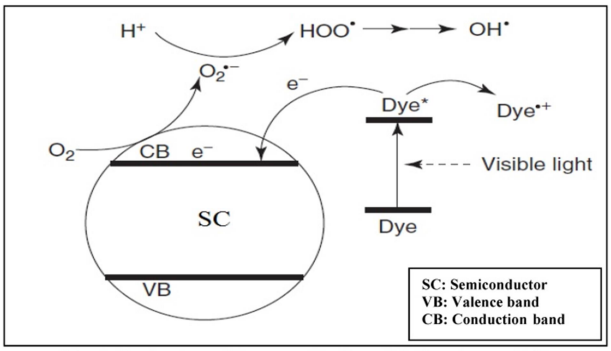

Fig. 4: Mechanism of dye sensitization of ZnO under sunlight

Thus it is observed that ZnO mediated photocatalytic degradation of IC is more efficient under sunlight compared to UV light. Hence further studies are undertaken with sunlight as the source of irradiation.

III.1 Effect of catalyst dosage

The effect of catalyst loading on the solar photocatalytic degradation of IC is investigated and the results are presented in figure 5. The % degradation increases steeply with increase in catalyst loading, reaches an optimum, decreases slightly thereafter and stabilizes. Higher degradation at higher dosages can be attributed to increase in catalyst surface area, increased adsorption of the substrate, efficient light absorption and consequent generation of higher number of active species. However beyond the optimum, in the same reactor, some of the catalyst particles will be effectively in the dark and there is decrease in the light penetration. Scattering of light at higher catalyst loading also reduces the efficiency of light absorption. Further, it is difficult to maintain the suspension homogeneous at high catalyst dosage as the catalyst particles have a tendency to settle at the bottom of the reactor. Variation in the degree of settling may also influence the uniformity of the reaction system and the consistency of the sampling

process. At higher loadings, the photo-activated particles may interact more frequently with the abundant ground state particles and get deactivated as follows.[20]:

$MO^* + MO \rightarrow MO^{\#} + MO$ (1) where

MO represents ZnO. MO^* and $MO^{\#}$ are the activated and deactivated forms respectively.

These factors together contribute to stabilization/ decrease in the efficiency of the catalyst at loadings above the optimum level. The optimum dosage of the catalyst under the reaction conditions in the current reactor is 0.02g/50 ml. However, the optimum will be different for a reactor of different size and geometry as well as other reaction parameters. Hence the catalyst dosage has to be optimized every time when the reaction and reactor parameters are different. In the current instance, all further studies were carried out at the optimized dosage of 0.02g/50 ml, unless indicated otherwise

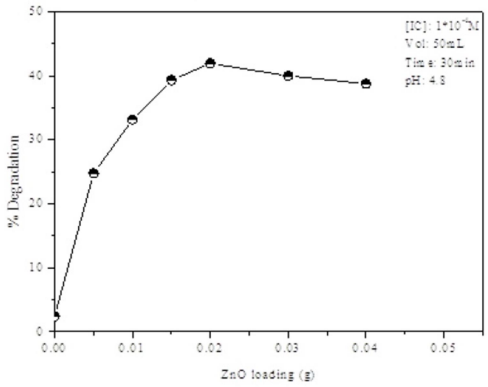

Fig. 5: Effect of ZnO loading on the Photocatalytic degradation of IC

III.2. Effect of initial concentration of IC

As can be seen from figure 2, the photocatalytic degradation of IC slows down with time. This is mainly because the residual concentration of IC becomes lower and lower with time and the insitu formed intermediates and other products may compete for the same active adsorption sites on the surface and for the reactive free radicals at the surface and in the bulk. Further, just as in the case of catalyst dosage, there will be an optimum for the substrate concentration for effective interaction with the ROS and subsequent degradation under specific experimental parameters. This is verified by studying the degradation at different concentrations of IC at the optimum catalyst dosage and natural pH of the reaction system.

The results plotted in figure 6 show the percentage degradation of IC at different concentrations. The rate of degradation at different concentrations of IC is shown in the inset figure. The percentage degradation decreases with increase in concentration. However, the initial rate of degradation increases with increase in concentration before it eventually levels off at higher concentration of $>1.5\times10^{-4}$M. This is in line with many photocatalytic reactions which follow pseudo first order kinetics at lower concentrations of the substrate in accordance with the Langmuir-Hinshelwood model modified to accommodate reactions occurring at solid-liquid interface.[28-30] The rate decreases and slowly stabilizes at higher concentration indicating lower order and eventual zero order kinetics. Once the concentration of IC is adequate to interact with the optimum available ROS and other reactive free radicals, further increase in concentration cannot result in any increase in the reaction and the removal of IC becomes independent of its concentration. At higher substrate concentration, some of the insitu formed reaction intermediates may get adsorbed onto the surface or remain in the bulk for relatively longer period resulting in less frequent interaction between fresh dye molecules and the ROS. Complete domination of the reaction system by the reactant/ intermediates/products can also result in suppression of the generation of surface initiated

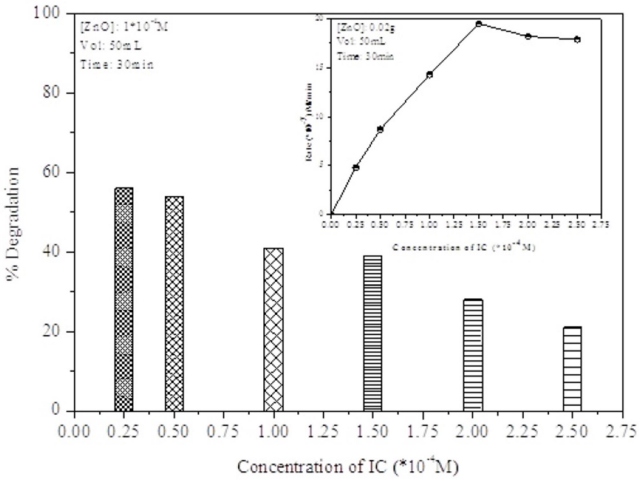

Fig. 6: Effect of concentration of IC on its % degradation. [Inset]: Rate of degradation vs Concentration

reactive free radicals. However, at any point in time, there will be an optimum for the number of substrate molecules that can interact with the reactive free radicals generated by the surface. This optimum will depend on a number of parameters such as initial concentration of the substrate, intensity of illumination, wavelength of light, mass and type of photocatalyst, type and geometry of photoreactor etc. Consequently the measurements and calculations apply only to the specific reaction conditions and cannot be generalized.

According to the Langmuir-Hinshelwood model, modified to accommodate reactions occurring at solid-liquid interface[28,29] the simplest way to represent the degradation, assuming that there is no competition with reaction by-products, is

$$R = -dC/dt = k_r K C_0 / (1+KC_0) \quad (2)$$

R is the rate of disappearance of the substrate (mg L^{-1} min^{-1}), C_0 (mg L^{-1}) is the initial concentration, K is the equilibrium adsorption coefficient and k_r is the reaction rate constant at maximum surface coverage. Equation 2 can be rewritten as

$$1/R = 1/k_r + 1/k_r K * 1/C_0 \quad (3)$$

Plot of 1/R against $1/C_0$ yields straight line in the concentration range 0.5-1.5 mg/L indicating first order kinetics and L-H mechanism (figure7, inset).

Further, integration of equation 3 yields

$$\ln (C_0/C) + K (C_0-C) = k_r K t \quad (4)$$

When C_0 is very small, above equation becomes

$$\ln (C_0/C) = k_r K t = k't \quad (5)$$

The plot of $\ln(C_0/C)$ versus irradiation time (t) for the concentration range of 0.5-1.5 $x10^{-4}$M yields straight lines (figure 7) thereby reconfirming pseudo first order kinetics. The slope of each line is the apparent rate constant of degradation *k'* at the corresponding concentration of the substrate. The results computed are given in table1.

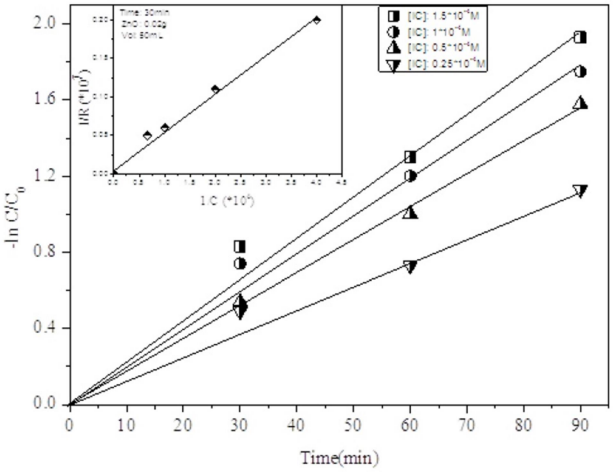

Fig. 7: Logarithmic plot of pseudo first order kinetic for the degradation of IC
[Inset]: Reciprocal plot of initial rate vs initial concentration

Table 1: Pseudo first order rate constants for the photocatalytic degradation of IC over ZnO

Sl. No.	ZnO	IC ($x10^{-5}$M))	k' x 10^{-2}(min^{-1})
1	0.02	2.5	2.00
2	0.02	5.0	1.75
3	0.02	10.0	1.47
4	0.02	15.0	1.27

The rate constant decreases with the increase in concentration of IC, which is consistent with the results reported in the case of many photocatalytic degradation studies.[30,31] For a fixed amount of catalyst and hence finite number of surface-generated ROS available for interaction, the number of substrate molecules is excessive at higher concentrations. This reduces the relative % fraction of substrate which can successfully interact with the ROS, leading to decrease in the apparent rate constant. However, it is to be noted that the above rate constant values apply only under the current specific experimental conditions and are hence not absolute.

Decrease in the rate of photocatalytic degradation and hence in the order of the reaction at higher concentrations of the substrate has been reported earlier.[32-34] Variation in the kinetics of the degradation with concentration of the substrate has been reported in the case of ZnO mediated sonophotocatalytic reactions also.[35,36]

The basic mechanism of semiconductor-mediated photocatalysis involves the formation of highly reactive oxygen species such as $^{\cdot}OH$. $HO_2^{\cdot}$, H_2O_2 etc. which interact with the substrate molecules on the surface as well as in the bulk. The most reactive among these ROS is the $^{\cdot}OH$ radicals though their lifetime is very short (only few nanoseconds). Hence they can react more efficiently with the organic pollutant molecules in the immediate proximity of their formation. At higher substrate (IC) concentration there will be more number of its molecules per unit volume and hence the probability of collision between the oxidizing species and IC also will be higher. However at very high concentration, an inner filter effect is possible and the incident light will be largely wasted for the excitation of the substrate rather than the excitation of the catalyst particles and the generation of reactive free radical species.[32] The path length of light entering the system also decreases with increase in concentration of the substrate. Similar screening effect was reported earlier also.[35] Another reason for the lower rate of degradation at higher concentration (which

is dependent on the reactor geometry also) is that the major portion of the reaction occurs in the reaction zone close to the irradiated side where the irradiation intensity is much higher.[36] Consequently a substantial fraction of the substrate (which is on the other side) will not get adequately activated to effect the degradation. As a result of all or some of these factors, the reaction rate is stabilised or even decreases at higher concentration of IC. The stability beyond the optimum concentration suggests that the reaction rate becomes independent of the concentration of the substrate. Hence it is logical to assume that the photocatalytic degradation happens in two stages. In the first stage the reaction is faster and follows pseudo first order kinetics. The reaction rate is slow in the second stage reaching zero order eventually. Duration of the first stage decreases with increasing concentration of the substrate.

As the initial concentration of the substrate is increased, the requirement of energy, catalyst surface for adsorption and number of ROS for effective interaction also increase correspondingly. But when the catalyst and the light source are kept the same, the ROS generated will be constant. The stabilization effect at higher concentration beyond the optimum implies that the substrate cannot interact with correspondingly more ROS. In other words, the relative concentration of ROS for interaction with the substrate becomes lower and this leads to stable/reduced degradation. Thus it may be confirmed that absorption of light by the catalyst, intensity of illumination, wavelength of light, number of available catalyst surface sites and relative abundance of reactive free radicals vs the substrate are the major factors which may influence the effect of concentration of the pollutant on the degradation. Enhancement of the stabilized degradation of the pollutant at higher concentration of the substrate, by the addition of extra amount of catalyst in between the reaction, also supports this conclusion.

III.3. Insitu formation and effect of H_2O_2

H_2O_2 is formed as a by-product/intermediate in many photocatalytic reactions. Recent studies on the sono, photo and sonophotocatalytic degradation of organic pollutants revealed that the H_2O_2 formed undergoes concurrent decomposition resulting in oscillation in its concentration.[37] In the current study also H_2O_2 formation is observed (figure 8).

Since the precise estimation of H_2O_2 in the system in presence of the colored dye is difficult the same is not done while the degradation/decolorization of the dye is in progress. The concentration of H_2O_2 is determined immediately after the decolorization is complete. At this stage, the H_2O_2 concentration in the system is 20 mg/L. Since IC is known to produce a number of relatively stable intermediates which also degrade very slowly, the irradiation is continued and the H_2O_2 is also measured periodically. The H_2O_2 continues to increase for some more time and stabilizes after about 4 hr. However, the mineralization is still in progress which takes about 6 hr (see Section.III.9) to be completed. During this period, the concentration H_2O_2 does not increase corresponding to the mineralization and gets stabilized indicating simultaneous formation and decomposition as reported earlier. When the rates balance each other, the concentration of H_2O_2 is stabilized.

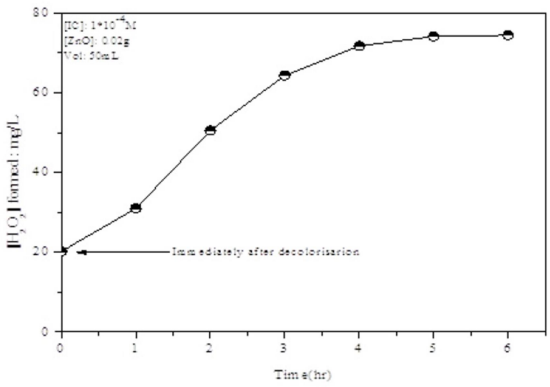

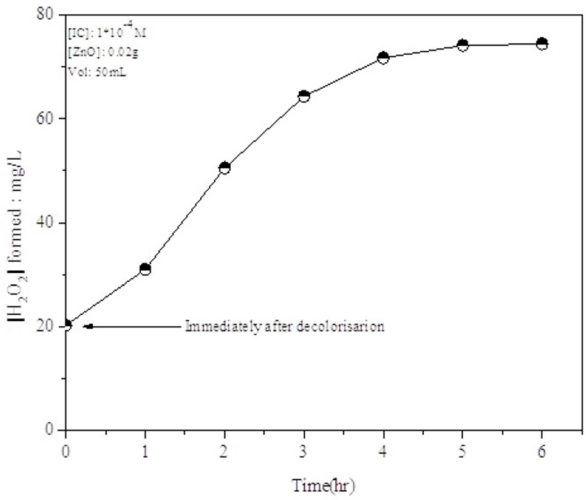

Fig. 8: Formation of H_2O_2 during the degradation of IC

Being a good oxidant of photocatalytic reactions, the insitu formed H_2O_2 (oxidation potential is 1.77 eV)) can influence the degradation of IC. This is verified by externally adding H_2O_2 at different concentrations to the reaction system and evaluating the effect on the degradation of IC. The results are shown in figure 9. The slow photodegradation in the absence of any catalyst is enhanced moderately by added H_2O_2. H_2O_2 also enhances the ZnO catalyzed photodegradation significantly. With increase in concentration of H_2O_2 (>10 mg/L), the degradation increases slowly upto 40 mg/L. Thereafter, the degradation is stabilized and addition of more H_2O_2 has no effect on the already stabilized degradation rate.

In the case of ZnO, the adsorption of H_2O_2 is negligible and hence most of the latter will be in solution.[37] H_2O_2 is known to serve as a reservoir of reactive free radicals such as $^{\cdot}OH$ and $HO_2^{\cdot}$, in addition to being a good oxidant by itself. Further, more ROS are formed on irradiation of ZnO in presence of O_2. They interact with the pollutant IC leading to its degradation. The H_2O_2 decomposes in parallel through multiple interactions as in reactions 6-10 thereby resulting in stabilization in its concentration.[36-38] Thus, above a critical concentration of H_2O_2, instead of generating more ROS such as $^{\cdot}OH$, it becomes a major competitor to the substrate to consume the ROS in the system (reactions 9 and 11). This leads to decreased or stabilized degradation of IC.

$$H_2O_2 + e_{CB}^- \rightarrow {}^{\cdot}OH + OH^- \quad (6)$$

$$O_2^{\cdot-} + H_2O_2 \rightarrow {}^{\cdot}OH + OH^- + O_2 \quad (7)$$

$$H_2O_2 + 2\,e_{cb}^- + 2H^+ \rightarrow 2\,H_2O \quad (8)$$

$$H_2O_2 + 2\,h_{vb}^+ \rightarrow O_2 + 2H^+ \quad (9)$$

$$H_2O_2 + hv \rightarrow 2\,{}^{\cdot}OH \quad (10)$$

$$H_2O_2 + {}^{\cdot}OH \rightarrow HO_2^{\cdot} + H_2O \quad (11)$$

At higher concentration, H_2O_2 absorbs more light, its decomposition is enhanced and more reactive $^{\cdot}OH$ radicals are produced. These radicals can competitively interact with the H_2O_2 itself, the substrate IC or the reaction intermediates. Scavenging of the radicals by H_2O_2 reduces the efficiency of pollutant degradation.

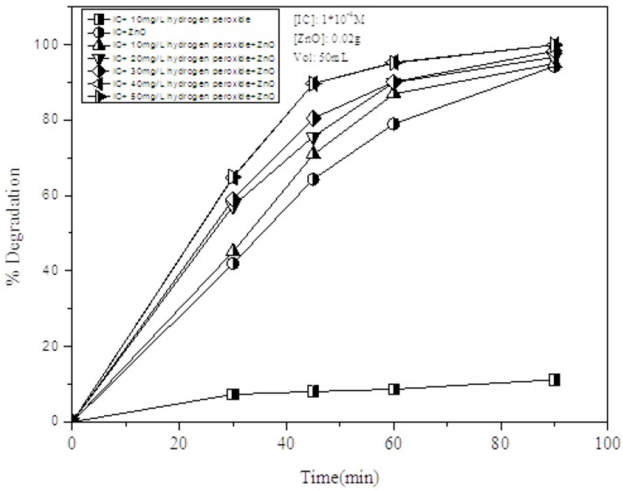

Fig.9. Effect of H_2O_2 on the solar photocatalytic degradation of IC

HO_2 radicals (oxidation potential = ~1.70 eV) are less reactive than $^{\cdot}OH$ (oxidation potential = ~2.80 eV) towards the organic pollutants.[39] Hence the contribution of H_2O_2 at higher concentration (when more of the $HO_2^{\cdot}$ radicals are in the system) towards the degradation of the dye is relatively less and eventually the degradation is stabilized.

III.4. Effect of persulphate (PS)

Persulphate ($S_2O_8^{2-}$) is a more powerful oxidant (E_0 = ~2.01eV) than even H_2O_2 (E_0 = ~1.77eV). It is a solid at room temperature and offers advantages of stability, ease of handling and transportation, high aqueous solubility and relatively lower cost. PS has been proven to be good enhancer of UV photocatalytic degradation of many pollutants while the enhancement is 'moderate' to 'negligible' under sunlight irradiation.[27] In the current instance of ZnO mediated solar photocatalysis, the enhancement in the degradation of IC by PS is only moderate as seen in figure 10. The effect of concentration of PS on the degradation is given in the inset which also confirms that the enhancement is only moderate.

At smaller concentration of PS (upto 20 mg/L) the effect is negligible. However, as the concentration increases further, the degradation increases slowly, reaches an optimum at 30 mg/L and stabilizes thereafter. At the respective optimum concentrations of PS (30 mg/L) and H_2O_2 (40 mg/L) the enhancement effected is more or less the same. Combination of H_2O_2 and PS at the respective optimum concentrations does not produce any extra enhancement which remains same as in the case of H_2O_2 only.

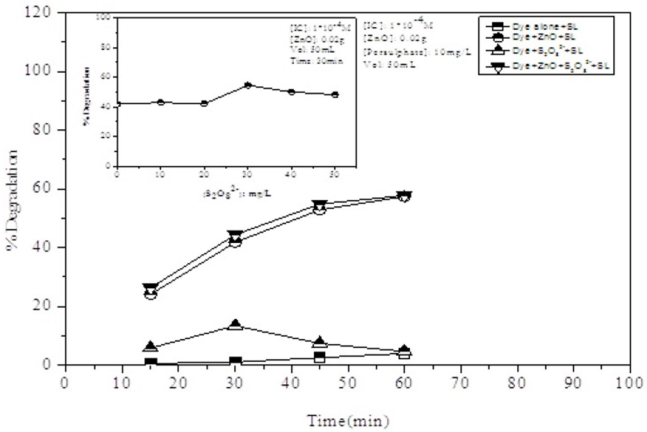

Fig.10: Effect of PS on the degradation of IC. [Inset]: Effect of concentration of PS on the degradation

The reactions leading to the enhancement in the photocatalytic degradation of IC by PS can be generally explained as follows:

PS generates highly reactive $SO_4^{\cdot-}$ radical anions under photocatalytic conditions insitu These radicals interact with the substrate IC and initiate/enhance their degradation. Higher concentration of PS will generate more $SO_4^{\cdot-}$ radicals under UV irradiation leading to a series of chain reactions as follows (equations 12-22)[40]:

$S_2O_8^{2-} \rightarrow 2SO_4^{\cdot-}$ (12)

$S_2O_8^{2-} + RH \rightarrow SO_4^{\cdot-} + HSO_4^- + R^\cdot$ (13)

RH: organic pollutant

$SO_4^{\cdot-} + H_2O \rightarrow SO_4^{2-} + H^+ + {}^\cdot OH$ (14)

$SO_4^{\cdot-} + RH \rightarrow R^\cdot + HSO_4^-$ (15)

${}^\cdot OH + RH \rightarrow R^\cdot + H_2O$ (16)

$R^\cdot + {}^\cdot OH \rightarrow$ Intermediates→products (17)

$SO_4^{\cdot-} + R^\cdot \rightarrow$ Chain termination (18)

$SO_4^{\cdot-} + {}^\cdot OH \rightarrow$ Chain termination (19)

$2SO_4^{\cdot-} \rightarrow S_2O_8^{2-}$ Chain termination (20)

$2\,{}^\cdot OH \rightarrow H_2O_2$ Chain termination (21)

$2R^\cdot \rightarrow$ RR Chain termination/ (22)

Further degradation

Various ROS such as H_2O_2, $HO_2^\cdot$, ${}^\cdot OH$ etc. and $SO_4^{\cdot-}$ formed during the irradiation interact with IC on the surface of the catalyst as well as in the bulk, leading to its degradation into various intermediates and eventual mineralization. However, the enhancement in the degradation in the present case under solar irradiation is not as significant as under UV light irradiation. Visible light activation of PS and the formation of reactive species as above are relatively weak under solar radiation compared to UV light.[27,30,31] The reactive $SO_4^{\cdot-}$ radicals may also get deactivated as in reactions 18-20 thereby making the enhancement in the degradation of IC only marginal. The $SO_4^{\cdot-}$ radicals can also interact with PS and form less reactive $S_2O_8^{\cdot-}$ radicals as follows:

$SO_4^{\cdot-} + S_2O_8^{2-} \rightarrow SO_4^{2-} + S_2O_8^{\cdot-}$ (23)

Consequent to the above reactions combined with the lower rate of generation under sunlight, the net concentration of $SO_4^{\cdot-}$ in the system is diminished. Hence, the enhancement in the solar photocatalytic degradation of IC in presence of PS also is relatively less.

It has been reported earlier[41] that PS can be even three times more effective than H_2O_2 for the UV-photocatalytic degradation of polyethylene plastics (PEP) pollutant. This is attributed to the trapping of photoproduced electrons by PS (reaction 24) thus inhibiting the electron-hole recombination. The resulting reactive sulphate radical anions which are even more powerful oxidants can further enhance the degradation.

$S_2O_8^{2-} + e \rightarrow SO_4^{2-} + SO_4^{\cdot-}$ (24)

The SO_4^{2-} can get adsorbed on the surface and interact with the photoproduced holes producing even more $SO_4^{\cdot-}$ radicals.

$h^+ + SO_4^{2-} \rightarrow SO_4^{\cdot-}$ (25)

Since S is a strong oxidizing agent, the $SO_4^{\cdot-}$ (Reduction potential is 2.6 eV) can accelerate the degradation process by itself as well as by producing more $^{\cdot}OH$ radicals.

$SO_4^{\cdot-} + H_2O \rightarrow SO_4^{2-} + {}^{\cdot}OH + H^+$ (26)

$SO_4^{\cdot-}$ + Pollutant → SO_4^{2-} + degradation/mineralization products (27)

The absence of any additive or synergic effect on the degradation of IC in presence of the combination of PS and H_2O_2 under ZnO/sunlight shows that the formation of $SO_4^{\cdot-}$ and other ROS is weak under visible light. Further, the interactions leading to the deactivation of insitu generated reactive $^{\cdot}OH$ and other free radicals may be still active even in the combined presence of the oxidants. Together they make the enhancing effect of PS or PS/H_2O_2 on the degradation only moderate or even negligible

III.5. pH effect

The effect of pH on the photocatalytic behavior of semiconductor oxides is often correlated with their oxidation potential and surface charge which determine the adsorptive properties. However other factors such as characteristics of the substrate and reaction intermediates, presence of pH-sensitive contaminants etc. also influence the effect of pH. In the current study, the effect of pH on the degradation of IC is investigated and the results are given in figure 11. Optimum degradation is observed at pH 4 which decreases thereafter with increase in pH. Hence all further studies are made at the natural pH of 4.8 of the suspension. The low degradation at pH < 3 is due to the corrosion and photo-dissolution of ZnO which are enhanced by reaction with insitu generated valence band holes as in reaction 28.

$ZnO + 2h_{VB}^+ \rightarrow Zn^{2+} + O^-$ (28)

The effect of pH on the degradation/disappearance of IC is not due to adsorption as seen from the results of adsorption studies at different pH (dye + ZnO). The effect of pH on the dye as such also is not much.

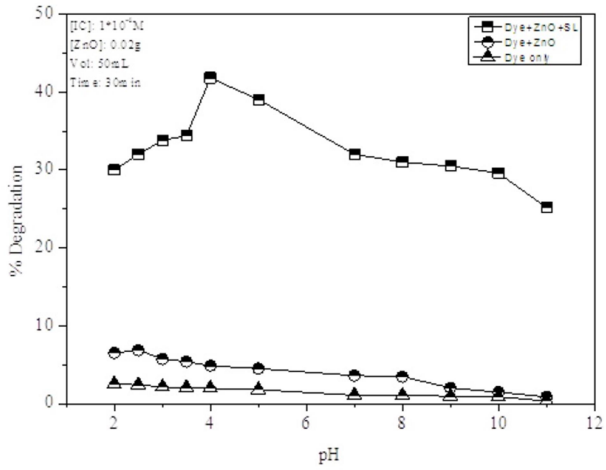

Fig. 11: Effect of pH on the degradation of IC

As expected, the adsorption remains fairly steady at ~ 5% in the acidic to neutral range of 3-7 (after adjusting for the mild decolorization of ~ 2 % in this pH range). IC is a weak acid which dissociates less towards acidic pH and will be in neutral electric form φ-SO_3H.[42] Hence adsorption is moderate in the acidic range with no electrostatic repulsion between the surface and the dye. The adsorption is negligible under alkaline condition. This may be attributed to the surface characteristics of ZnO. The PZC of ZnO is 9±0.3. The surface of ZnO will

be negatively charged above this pH and hence the anionic dye IC (φ-SO_3^-) will get repelled. The degradation of IC also is less in this range.

The ZnO may also form complexes in the basic pH range (reaction 29) leading to partial insulation of the catalyst surface and consequent inactivation.

$$ZnO + H_2O + 2OH^- \rightarrow [Zn(OH)_4]^{2-} \quad (29)$$

In many instances adsorption is considered to be an important prerequisite for heterogeneous catalytic processes. However, in the current case, the adsorption of IC is much smaller compared to the high percentage degradation of the dye. This shows that a sizable part of the photocatalytic degradation of IC is taking place in the bulk. Similar observations are reported in the case of photocatalytic degradation of other substrates as well.[30,31,43]

It is well recognized that the effect of pH on the photocatalytic process is complicated and cannot be explained based on individual parameters in isolation because it depends on multiple factors such as electrostatic interaction between the semiconductor surface, solvent molecules, substrates, intermediates and charged radicals formed during the reaction process.[29]

III.6. Temperature effect

The effect of temperature on the photocatalytic degradation of IC in presence of ZnO is tested in the range of 15-50^{0}C. The degradation increases with increase in temperature upto 30^{0}C and stabilizes thereafter (figure 12). The rate constant k_{app} is determined at various temperatures and the apparent activation energy (E_a) is calculated from the Arrhenius equation

$$\ln k_{app} = (-Ea/kT) + \ln A \quad (30)$$

by plotting ln k_{app} vs (1/T). k_{app} is the rate constant, T is the temperature of reaction in kelvin and A is the Arrhenius factor.

The E_a as computed is 16.0 kJ mol^{-1}. This is the total activation energy of both adsorption and photocatalytic degradation.[42] However, in the case of ZnO the adsorption of IC is relatively small (<5%) and hence the value can be considered as true activation energy. This value is close to the Ea value of 14.4 kJ mol^{-1} reported by Barka etal[42] for the photocatalytric degradation of IC on TiO_2 coated nonwoven fibres. The activation energy for the photocatalytic degradation of acid blue dye on Degussa P-25 also is comparable as reported by Bouzaida et al.[44]

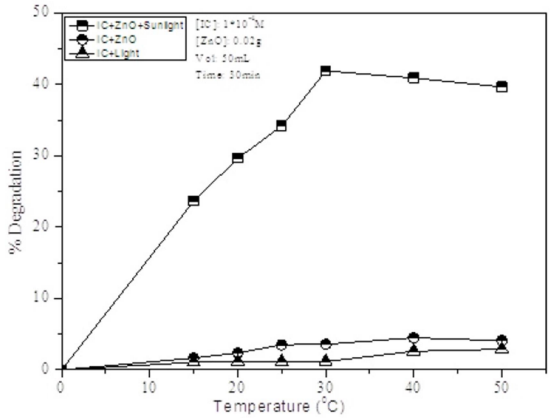

Fig 12: Effect of temperature on the degradation of IC

As the temperature increases, adsorption of the dye which is already very low, decreases further. At low temperature, the degradation is lower in spite of better adsorption because the energy is not enough. At 40^{0}C when the adsorption is less, the degradation is more. This again confirms that adsorption is important though it is not the sole parameter that determines the degradation. Once the catalyst is activated by thermal

and/or photo energy, the reactive free radicals are generated and the reaction can take place in the bulk as well.

III.7. Effect of anions

Many of the anionic contaminants which are naturally present in water inhibit the efficiency of AOPs for the degradation of organic pollutants.[45,46] Instances of anions functioning as enhancers of the degradation of pollutants also have been reported.[47,48] In this context, the effect of some of the commonly occurring anions in water, i.e. SO_4^{2-}, Cl^-, PO_4^{3-}, CO_3^{2-} and HCO_3^- on the efficiency of solar photocatalytic degradation of IC is tested and the results are presented in figure 13.

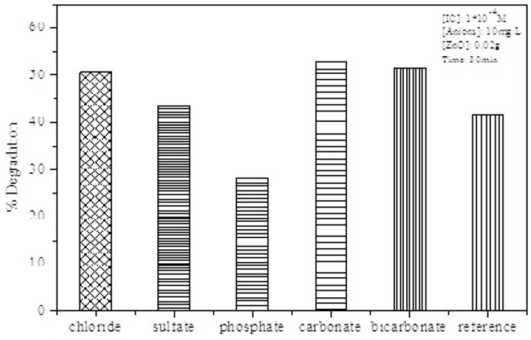

Fig. 13: Effect of various salts/anions on the degradation of IC

The results showed that the anion SO_4^{2-} has no effect while Cl^-, CO_3^{2-} and HCO_3^- enhance the degradation moderately. As expected based on previous results,[30,31,48-50] PO_4^{3-} is a strong inhibitor of the degradation of IC.

The effect of concentration of the anions on the degradation is also tested. In the case of the enhancing anions Cl^-, CO_3^{2-} and HCO_3^-, with increase in their concentration, the degradation of IC increases. In the case of SO_4^{2-}, the concentration effect is less. In the case of PO_4^{3-}, the inhibition is more with increase in its concentration. The inhibiting anions become better inhibitors and the enhancing anions become better enhancers with increase in their concentration. In all cases, the effect is stabilized eventually resulting in no further enhancement or inhibition as the case may be, beyond a critical concentration. However, the concentration of anions in all these cases was varied within a narrow range only (0-15 mg/L) and any conclusion based on the limited data may not be appropriate. More in-depth investigation is needed in view of the complexity and inconsistency of the effect of anions on AOPs, as reported in previous studies.

The inhibition of the photocatalytic degradation of organics by anions/salts is often explained based on blocking of the active surface sites on the catalyst by preferential adsorption (of the anions), surface layer formation and/or scavenging of reactive $^{\cdot}OH$ radicals. Since the Point of Zero Charge (PZC) of ZnO is ~9±0.3 the surface is positively charged when the pH is lower than this value and negatively charged when the pH is higher. Hence, at the natural pH of ~ 5 of the system all the anions tested here can get strongly adsorbed on ZnO. The adsorption of IC on ZnO in presence of the anions is measured experimentally and it is seen that the adsorption is inhibited in presence of PO_4^{3-} and HCO_3^- while other anions do not influence the adsorption much. The cation was kept the same in all cases, i.e., Na^+. Had the competitive adsorption of the anions been the main cause of the inhibition, it should have been in the order:

$$PO_4^{3-} > HCO_3^{2-} > SO_4^{2-} \sim Cl^- \sim CO_3^{2-} \quad (31)$$

This sequence is not strictly followed except in the case of PO_4^{3-} which is the only strong inhibitor of the degradation of IC. Other anions are enhancers or have 'no effect'. Hence, the preferential adsorption by the anion is not the major cause of inhibition, though it may be one of the many factors. This is even more true in the case of poorly adsorbing substrates such as IC on ZnO. The degradation proceeds primarily in the bulk of the medium and it is not a surface initiated process.

Presence of anions can also reduce the diffusion coefficient of the organic pollutant in the reaction medium. Consequently, the pollutant molecules will be less accessible to the reactive $^{\cdot}OH$ and this also can contribute to the inhibition. Another possible reason for the inhibition by anions is the formation of an inorganic layer on the catalyst surface. The efficiency of layer formation depends on the solubility of the salts.[51] The higher the solubility of the salt the lower will be the layer formation. The solubility of the salts (in mg/g of water at 20^0C) tested here is in the order;

Na_2SO_4 (40.8) ≥ Na_2CO_3 (39.7) > NaCl (36.1) > Na_3PO_4 (16.3) > $NaHCO_3$ (11.1) (32)

Correspondingly the layer formation, if any, will be in the order:

$HCO_3^- > PO_4^{3-} > Cl^- \geq CO_3^{2-} \geq SO_4^{2-}$ (33)

If layer formation is the major cause, the inhibition must be in the same order as above. The experimentally observed anion effect in the current instance is not fully consistent with equation (33) except in the case of PO_4^{3-} .The anions Cl^-, CO_3^{2-}, HCO_3^- and SO_4^{2-} are mild enhancers or have 'no effect'. In many other AOPs, these anions function as inhibitors. In the present case, they are mild enhancers and hence it may be presumed that their inhibiting efficiency (part of which is attributed to layer formation) is compensated for or even overpowered by other factors.

Many anions are known to scavenge the reactive $^{\cdot}OH$ radicals. The scavenging rate constants in the case of some of the anions are summarized in Table 2.[51]

Table 2: Scavenging rate constants of $^{\cdot}OH$ by various anions

Anion	Scavenging Rate constants ($mol^{-1}s^{-1}$)
Cl^-	4.3×10^9
CO_3^{2-}	3.9×10^8
SO_4^{2-}	1×10^{10}
$H_2PO_4^{3-}$	2×10^4
HCO_3^-	8.5×10^6

However, scavenging of the reactive $^{\cdot}OH$ radicals by the anions can explain only inhibition (of PO_4^{3-} in this case) and not the 'no effect' (of SO_4^{2-}) or enhancement (by the anions Cl^-, CO_3^{2-} and HCO_3^-). Hence there must be more efficient alternative processes taking place to effect the enhancement even after compensating for the potential inhibition caused by adsorption of the anions on the surface, surface layer formation and the trapping of reactive $^{\cdot}OH$ radicals.

Scavenging of the $^{\cdot}OH$ by anions would yield respective radical anion species which are also reactive towards organic compounds, although less efficiently than $^{\cdot}OH$.[49] In the case of the anions with 'enhancing effect' or 'no effect' in the present case, the radical anions are formed as follows:

$^{\cdot}OH + HCO_3^- \rightarrow H_2O + CO_3^{\cdot-}$ (34)

$^{\cdot}OH + CO_3^{2-} \rightarrow OH^- + CO_3^{\cdot-}$ (35)

$^{\cdot}OH + Cl^- \rightarrow OH^- + Cl^{\cdot}$ (36)

$Cl^{\cdot} + Cl^- \rightarrow Cl_2^{\cdot-}$ (37)

$^{\cdot}OH + SO_4^{2-} \rightarrow OH^- + SO_4^{\cdot-}$ (38)

These radical anions $CO_3^{\cdot-}$, $Cl_2^{\cdot-}$, etc. undergo slower recombination or deactivation compared to $^{\cdot}OH$. Hence they are more readily available for longer time than $^{\cdot}OH$ to react with the substrate and effect degradation. Thus the relatively lower reactivity is compensated by the better availability for reaction with the substrate. Many of the $^{\cdot}OH$ radicals would undergo recombination and get deactivated if they are not reacting with the anions. Enhancement in the degradation of the substrate occurs when the reaction rate between added anions and $^{\cdot}OH$, forming radical anion, is higher than that between substrate and $^{\cdot}OH$. However, both the rates would be much lower than radical-radical recombination. Even those radical anions which are formed at or near the surface of the catalyst can diffuse into the solution bulk and react with the substrate. The $^{\cdot}OH$ radical concentration is relatively less in the bulk compared to the surface and/or its immediate neighborhood and hence their recombination also is slow. Consequently, the $^{\cdot}OH$ will interact with the more abundant substrate molecules and anions, both of which can lead to enhanced degradation as explained above. Hence, it may even be said that the anions are protecting the $^{\cdot}OH$ radicals from unproductive recombination by transforming them into radical anions. However, this process is dependent on the concentration of the anions and other reaction parameters.[49] Above a particular concentration of the anion, the relative concentration of $^{\cdot}OH$ radicals available to interact with them is less. Similarly, once the degradation of the substrate has progressed substantially and its concentration in the system is less (towards the later stages of reaction), the radical anion $X^{\cdot-}$ which has only substrate as the sink, cannot sustain the enhanced degradation rate. From that point onwards, the anion-caused enhancement slows down gradually and eventually the effect is stabilized as in the present case or even reversed to inhibition as reported in literature.[49]

It is well known that pH of the reaction medium has strong influence on the AOP degradation of many water pollutants. Anions, especially carbonate and bicarbonate, are expected to increase the pH of the medium. Hence the possibility of anion effect arising at least partially from the variation in pH is examined. In the presence of HCO_3^- and CO_3^{2-} (10 mg/L each), the pH of the reaction medium increases to 6.3 and 7.1 respectively from 4.8. The variation in pH in the presence of other anions tested here is not significant. Comparison of the degradation of IC at these pH values shows decrease from ~42% (pH = 4.8) to ~35% (pH = 6.3) and ~33% (pH = 7.1). Thus, based on sole pH variation, the effect of HCO_3^- and CO_3^{2-} should have been decrease in degradation of IC. However, in presence of these anions, the photocatalytic degradation of IC is enhanced moderately. Hence it may be inferred that the effect of anions, at least under the experimental conditions tested here, is not primarily due to any change in the pH of the system.

The above results clearly show that a universally applicable explanation to account for the effect of anions in different kinds of photocatalytic systems with different catalysts, substrates and reaction conditions is not possible and it will be more appropriate to consider individual systems to explain specific effects in specific cases.

III.8. Effect of oxygen

All mechanisms proposed for the photocatalytic degradation of organics involve the participation of O_2 through the formation of reactive oxygen species (ROS) such as $O_2^{\cdot-}$, $HO_2^{\cdot}$, $^{\cdot}OH$, H_2O_2 etc. In order to confirm the effect of O_2 on the photocatalytic degradation of IC, the reaction system is degassed with N_2 and the experiments were carried out under otherwise identical conditions. The degradation is almost fully inhibited in the degassed system thereby illustrating that O_2 (and ROS resulting from it) is essential for the photocatalytic degradation of IC. The formation of H_2O_2 also is negligible in the degassed system.

Thus it can be seen that the photocatalytic degradation of IC on ZnO is facile, even though adsorption of the dye on the catalyst is only moderate as long as there is O_2 present in the reaction system. Hence the main role of the catalyst and its activated surface is the generation of ROS. These reactive species interact with the substrate as well as the insitu formed reaction intermediates mainly in the bulk resulting in eventual mineralization. Turchi and Ollis[52] have also demonstrated that adsorption of the substrate is not an essential requirement for photocatalytic reactions, even though the adsorption characteristics of the components can influence the rate of degradation of the organic compounds on the surface.

III.9. Chemical oxygen demand and effect of intermediates

The decolorization of dyes need not necessarily lead to mineralization and the possibility of formation of even more toxic intermediates cannot be ruled out. In order to verify the mineralization of IC under the current experimental conditions, the chemical oxygen demand (COD) of the optimized reaction system ZnO /IC under sunlight irradiation at various intervals is determined. The results presented in figure 14 show that decolorization does not result in corresponding mineralization. However, when the decolorization is complete (in 90 minutes), the COD decreases significantly. Thereafter it remains steady for long (over 200 minutes) even when the irradiation is continued. The stable COD for long duration shows that after the initial decolorization and partial mineralization of relatively unstable intermediates formed insitu, the more stable intermediates take longer time for mineralization. Eventually they also get mineralized and the COD becomes almost zero.

III.10. Reaction intermediates

It has been reported that the degradation of IC under AOP yields stable intermediates such as acetic acid, tartaric acid, malic acid, oxalic acid, anthranilic acid etc.[23,53,54] In the current study, only two of these could be detected consistently; oxalic acid and acetic acid, even though the possibility of formation of other intermediates cannot be ruled out. In any case, the effect of the likely intermediates on the degradation of IC is evaluated and the results are shown in figure 15.

The results show that the degradation is inhibited by all intermediates at least at the concentration studied here. Maximum inhibition is observed in the case of oxalic acid. The inhibition is in the decreasing order:

Oxalic acid > Tartaric acid > Pyruvic acid > Malic acid ≈ Malonic acid > Acrylic acid ≈ Acetic acid (39)

The effect of concentration of the strongest inhibitor among the intermediates, i.e., oxalic acid, at different reaction time intervals is verified and the results are shown in Table 3.

The concentration of the oxalic acid is kept lower so that it will be comparable to the insitu formed quantity. The

results show that the inhibition by oxalic acid increases with increase in its concentration. The inhibition may be due to the competition between IC and oxalic acid for the adsorption as well as interaction with the ROS formed during the irradiation.

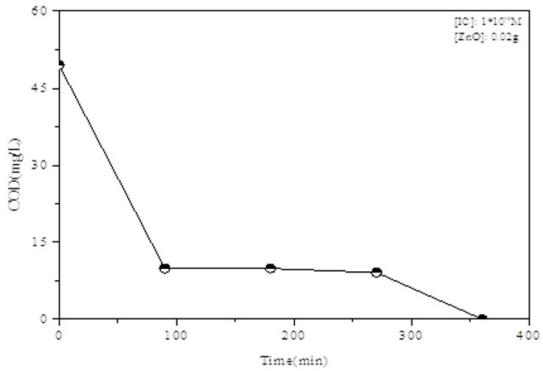

Fig. 14: Chemical oxygen demand (COD) of the IC/ZnO system during solar irradiation

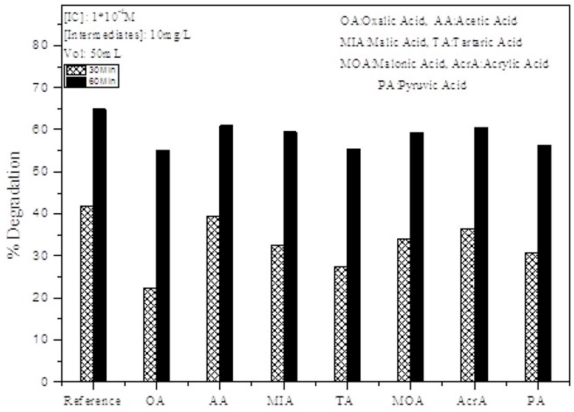

Fig. 15: Effect of likely intermediates on the degradation of IC

Table 3: Effect of oxalic acid at different concentrations on the degradation of IC at different reaction times

Intermediate added	Concentration (mg/L)	% Degradation of IC after (in min)			
		30	60	90	120
Nil (Reference)	0	42.0	62.5	74.0	89.5
Oxalic acid	2	37.7	55.0	67.2	84.2
	4	32.8	49.4	64.2	80.5
	10	28.2	45.5	61.0	76.0
	20	24.8	42.7	54.5	67.9

The eventual mineralization of IC is confirmed from the LC/MS spectral analysis of the reaction system after continuous irradiation for 8 hours when the COD was observed to be nil. The mass chromatogram shown in figure 16 reconfirms the absence of any organic contaminant after 8hr of irradiation.

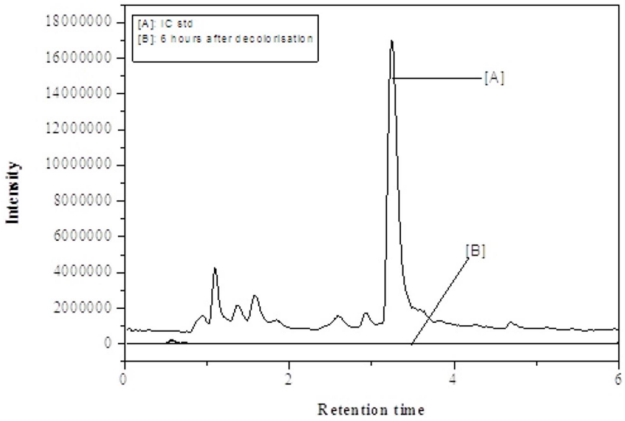

Fig.16: Mass chromatogram of the reaction mixture [A] initially and [B] after 8 hr irradiation

Major transient intermediates present in the system immediately after decolorization as identified by LC/MS are listed in Table 4. However, eventually they also get degraded and mineralized as seen from the 'Nil' COD value and the LC/MS data.

III.11. General Mechanism

The basic mechanism of UV activated semiconductor oxide photocatalysis consists of initial light absorption by the catalyst which promotes the electron from the valence band to the conduction band resulting in the generation of hole in the valence band (reaction 40).

Table 4: Major transient intermediates formed during the mineralization of IC

Sl No.	m/z	Proposed structure
1	188	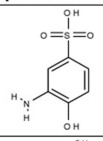
2	200	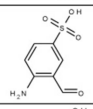
3	216	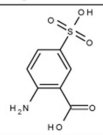

4	226	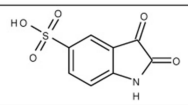
5	258	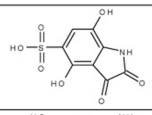
6	260	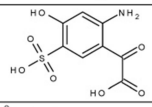
7	357	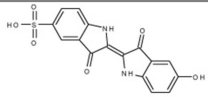
8	423	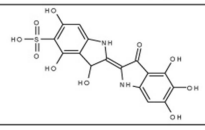

Semiconductor (ZnO) + hv → $h^+ + e^-$ (40)

Both the electron and hole must be consumed so that the material can act as an efficient catalyst. It is generally believed that both the electrons and holes can find low energy trap sites on a sub-picosecond time scale in the semiconductor.[55] These electrons and holes can either recombine and dissipate the input energy as heat (reaction 41) or react with electron donors and electron acceptors which are adsorbed on the semiconductor surface or trapped within the surrounding electrical double layer of the charged particles to produce strong oxidizing hydroxyl radicals which can promote the oxidation of organic compounds.[56] Dissolved oxygen and surface oxygen play important role by scavenging the electrons generated on photoactivated ZnO and forming superoxide radical anion and other reactive species. Various reaction steps can be presented as follows:

$h^+ + e^-$ → Heat (41)
$O_2 + e^-$ → $O_2^{\cdot-}$ (42)
$O_2^{\cdot-} + 2H^+ + e-$ → H_2O_2 (43)
$h^+_{VB} + H_2O$ → $H^+ + {}^{\cdot}OH$ (44)
$O_2^{\cdot-} + H^+$ → $HO_2^{\cdot}$ (45)
$2\,HO_2^{\cdot}$ → $H_2O_2 + O_2$ (46)
$HO_2^{\cdot} + O_2^{\cdot-} + H_2O$ → H_2O_2+O2 +.OH (47)
$H_2O_2 + e^-$ → ${}^{\cdot}OH + OH^-$ (48)
${}^{\cdot}OH + {}^{\cdot}OH$ → H_2O_2 (49)
$h^+_{VB} + OH^-$ → ${}^{\cdot}OH$ (50)

Various ROS formed as above interact with the organic molecules, such as IC in this case, resulting in the formation of various intermediates and eventual mineralization.

${}^{\cdot}OH + RH$ → $H_2O + R^{\cdot}$ (51)
RH is the dye or the intermediates formed insitu
$R^{\cdot} + O_2$ → $ROO^{\cdot}$ →….→ mineralized products (52)

In presence of low energy visible light irradiation, the formation of electron hole pair as above is not easy since the band gap energy of ZnO is higher at 3.2 eV. Hence, the high solar catalytic activity of ZnO for the degradation of IC may be due to the sensitization induced by IC as explained in the beginning of Section 3.

Surface sensitization of a wide band gap semiconductor photocatalyst such as ZnO by physisorbed or chemisorbed dyes can expand the wavelength range of excitation for the photocatalyst and/or increase the efficiency of the excitation process. The first step is the excitation of the sensitizer followed by charge transfer to the semiconductor. The excited state can inject either a hole, or more commonly, an electron to the particle. When a monolayer of a dye is dispersed on the

photocatalyst with high surface area, the charge injection will be more efficient. Extension of the the photoactive wavelength range of the catalyst to the visible range is important for the harnessing of sunlight. Photosensitization of semiconductors by various dyes has been monitored by nanosecond and picosecond flash photolysis as well as femtosecond spectroscopy. The rates of injection of electron as well as the back electron-transfer from the dye to the photocatalyst depend upon the nature of the dye molecules, properties of the catalyst particles and the interactions between the dye and particles.[57]

IV. CONCLUSION

Solar photocatalysis using ZnO as the catalyst is found to be an efficient method for the removal of trace amounts of Indigocarmine dye pollutant from water. The degradation follows pseudo first order kinetics at lower concentrations of the substrate. H_2O_2 formed insitu in the process undergoes concurrent decomposition resulting in stabilization in its concentration. Oxidants H_2O_2 and persulphate influence the degradation moderately. The salt/anion contaminants present in water influence the degradation differently with the effect varying from inhibition to 'no effect' or even enhancement depending on the nature of the anion and the multitude of interactions involving the substrate, reaction intermediates and the catalyst. The degradation proceeds through many transient intermediates which degrade further on continued irradiation to give organic acids such as oxalic acid and acetic acid. They inhibit the degradation of IC though eventually they also get mineralized. The inhibition is attributed to the competition between the substrate and the insitu formed intermediates for surface sites as well as reactive oxygen species. The degradation is practically negligible in nitrogen flushed systems thereby confirming the role of O_2 (and the reactive oxygen species formed insitu) in the degradation. The results are discussed in detail and suitable mechanisms for the observed effects are proposed.

V. ACKNOWLEDGEMENT

Financial support from the University Grants Commission (India) to one of the authors (VV) by way of BSR Fellowship is gratefully acknowledged.

REFERENCES

[1] R.W. Matthews, Photocatalytic oxidation of organic contaminants in water: an aid to environmental preservation", *Pure and Appl.Chem*, 64, 1992, 1285-1290

[2] S. Devipriya and SugunaYesodharan., Photocatalytic degradation of pesticide contaminants in water, *Solar Energy Materials and Solar Cells*, 86, 2005, 309-348

[3] M.N. Chong, B. Jin, C.W.K. Chow and C. Saint, New developments in Photocatalytic water treatment technology; a review, *Water. Res,* 44, 2010, 2997-3027

[4] J.P. Takeuchi, M. Cuong, T.M. Zhang, M. Matsuoka and M. Anpo, Recent advances in visible light –responsive titanium oxide based photocatalysis, *Res. Chem. Intermed,* 99, 2010, 327-347

[5] D. Ollis, P. Pichat and N. Serpone, TiO2 photocatalysis – 25 years, Appl. *Catal. B: Environ,* 99, 2010, 377-387

[6] P. Pichat, Ed., Photocatalysis and Water Purification: From Fundamentals to Recent Applications, *Wiley-VCH Verlag GmbH and Co*, 2013

[7] M.G. Antoniou, P.A. Nicolaou., J.A. Shoemaker, A.A. de la Cruz, and D.D. Dionysiou, Detoxification of water contaminated with cyanotoxin microsystin-LR by utilizing thin TiO2 photocatalyst films, *Appl. Catal. B: Environ ,* 91, 2009, 165-173

[8] A. Fujishima and K. Honda, Electrochemical photolysis of water at a semiconductor electrode, *Nature*, 238, 1972, 37-38

[9] S.N. Frank and A.J. Bard, Heterogeneous photocatalytic oxidation of cyanide ion in aqueous solution at titanium dioxide powder, *J Amer. Chem. Soc.* 99, 1977, 303-304

[10] N. Serpone and E. Pelizzetti, Eds. "Photocatalysis: Fundamentals and Applications", *John Wiley and Sons Inc. New York*, 1989.

[11] D. F. Ollis and H. Al-Ekabi, Photocatalytic purification and treatment of water and air, *Elsevier*, Amsterdam, 1993.

[12] M. Anpo and P.V. Kamath, Eds., "Environment Benign Photocatalysts", *Springer*, New York, 2010.

[13] S. P. Devipriya, SugunaYesodharan. And E.P. Yesodharan, Removal of Chemical and Bacterial Pollutants from Water Using Pt/TiO2-Coated Ceramic Tiles", *Int. J Photoenergy*, Article ID 970474,2012.

[14] M. Pelaez. N.T. Nolan, S.C. Pillai, M.K. Seery, P. Falaras, A.G. Kontos, P.S.M. Dunlop, J.W.J. Hamilton, J.A. Byrne, K. O'Shea, M.H. Entezari and D.D. Dionysiou, A review on the visible light

active titanium dioxide photocatalysts for environmental applications, *Appl. Catal. B: Environmental*, 125, 2012, 331-349,

[15] Z. Wang, C. Chen, W. Ma and J. Zhao, in Photocatalysis and water purification, From fundamentals to recent application", *Ed.; Wiley-VCH Verlag GmbH and Co,* 2013, 199-240

[16] S. M. Lam, J.C. Sin, A.Z. Abdullah and A.R. Mohamed, Degradation of wastewaters containing organic dyes photocatalysed by ZnO: A review, *Desalination and Water Treatment* 41, 2012, 131- 169

[17] N. Hariprasad S.G. Anju, E.P. Yesodharan and SugunaYesodharan., "Sunlight induced removal of Rhodmine B from water through semiconductor photocatalysis", *Res J Material Sci.*, 1, 2013, 9-17

[18] N. Daneshvar, D. Salari and A.R. Khataee, Photocatalytic degradation of azo dye acid red 14 in water on ZnO as an alternative catalyst to TiO2", *J Photochem Photobiol. A: Chem.* 162, 2004, 317-322

[19] S.K. Kansal, M. Singh and D. Sud, Studies on the photodegradation of two commercial dyes in aqueous phase using different photocatalysts, *J Hazardous Mater*, 141, 2007, 581-590

[20] S. Sakthivel, B. Neppolian, M.V. Shankar, B. Arabindoo, M. Palanichamy and V, Murugesan, Solar photocatalytic degradation of azo dye: comparison of photocatalytic efficiency of ZnO and TiO_2", Solar *Energy Materials and Solar Cells*, 77, 2003, 65-82

[21] C.F.I. Jabs, H.P. Drutz, and R.I. Summit, The role of intra operative cystoscopy in prolapsed and incontinence surgery, *Am J Obst.Gynecol*, 185, 2001, 1368-1373

[22] D. L. Jeffords, P.H. Lange and W. C. DeWolf, Severe hypertensive reaction to indigocarmine", *Urology*, 9, 1977, 180-181

[23] M. Vautier, C. Guillard and J. M. Hermann, Photocatalytic degradation of dyes in water: Case study of Indigo and Indigo carmine, *J Catal.*, 201, 2001, 46-51

[24] C. Galindo, P. Jacques, and A. Kalt, Photochemical and photocatalytic degradation of an Indigo dye: A case study of acid blue 74 (AB 74)", *J Photochem. Photobiol A: Chem,* 141, 2001, 47-53

[25] S. Flox, C. Ammar, E. Arias, A.V. Brillas. Vargas-Zavala. and R. Abdelhadi, Electrofenton and photoelectrofenton degradation of indigo carmine in acidic aqueous medium", *Appl. Catal.B: Environ,*67, 2006, 93-99

[26] R.M.M. Othman, F.M. Ibrahem, Study of photocatalytic oxidation of indigo carmine dye on Mn-supported TiO2, *J Photochem. Photobiol A: Chem*,189, 2007, 80-85

[27] O. M. Shibin, B. Rajeev, V. Veena, E.P. Yesodharan and SugunaYesodharan, ZnO photocatalysis using solar energy for the removal of trace amounts of Alfa-Methylstyrene, Diquat and Indigo carmine from water, *J Adv. Oxid. Technol,* 17, 2014, 297-304

[28] S. Anandan, A. Vinu, N. Venkatachalam, B. Arabindoo and V. Murugesan, Photocatalytic activity of ZnO impregnated Hβ and mechanical mix of ZnO/Hβ in the degradation of monocrotophos in aqueous solution", *J Mol. Catal. A: Chem*, 256, 2006, 312-320

[29] S. Rabindranathan, S. Devipriya and SugunaYesodharan, Photocatalytic degradation of phosphamidon on semiconductor oxides", *J Hazard.Mater*, 102, 2003, 217-229

[30] B. Rajeev, SugunaYesodharan. and E.P. Yesodharan, Photocatalytic degradation of alpha-methyl styrene in presence of ZnO, *J Water. Process Eng*, 8 , 2015, 108-118

[31] O.M. Shibin, SugunaYesodharan. and E.P. Yesodharan, Sunlight induced photocatalytic degradation of herbicide diquat in water in presence of ZnO", *J Env. Chem. Eng,* 3, 1101-1116, 2015.

[32] B. Rajeev, Suguna Yesodharan and E.P. Yesodharan, Sunlight induced ZnO mediated photocatalytic degradation of acetophenone in water, *IOSR J Appl Chem. 2016, 55-70*

[33] C.C. Chen, W.H. Ma, and J.C. Zhao, Semiconductor-mediated photodegradation of pollutants under visible light irradiation, *Chem. Soc. Rev*, 39, 2010, 4206-4219

[34] Poulios, A. Avranas, E. Rekliti, and A. Zouboulis, Photocatalytic degradation of Auramine O in the presence of semiconducting oxides, *J Chem. Technol. Biotechnol*, 75, 2000, 205-212

[35] M.H. Florencio, E. Pires, A.L. Castro, M.R. Nunes, C. Borges and F.M. Costa, Photodegradation of Diquat and Paraquat in Aqueous Solutions by Titanium Dioxide: Evolution of Degradation Reactions and Characterization of Intermediates, *Chemosphere*, 55, 2004, 345-355

[36] S.G. Anju, SugunaYesodharan and E. P. Yesodharan, Zinc oxide mediated

sonophotocatalytic degradation of phenol in water, *Chem. Eng. J*, 189-190, 2012, 84-93

[37] K.P. Jyothi, SugunaYesodharan. and E.P. Yesodharan, Ultrasound, Ultraviolet light and combination assisted semiconductor catalyzed degradation of organic pollutants in water: Oscillation in the concentration of H2O2 formed insitu", *Ultrason. Sonochem*, 21, 2014, 1782-1796

[38] K.P. Jyothi, Sindhu Joseph., Suguna Yesodharan and E.P. Yesodharan, Periodic Change in the Concentration of Hydrogen peroxide formed during the Semiconductor Mediated Sonocatalytic treatment of Wastewater: Investigations on pH Effect and Other Operational Variables, *Res. J Recent Sci*, 2, 2013, 136-14

[39] A.D. Nadezhdin and H.B. Dunford, The oxidation of ascorbic acid and hydroquinone by perhydroxyl radicals. A flash photolysis study, *Can J Chem*, 57, 1979, 3017-3021

[40] A.A. Berlin, Kineticsa of radical chain decomposition of persulphate in aqueous solution of organic compounds, *Kinetics. Catal*, 27,1986, 34-39

[41] P.D. Phonsy, SugunaYesodharan and E.P. Yesodharan , Enhancement of semiconductor mediated Photocatalytic removal of polyethylene plastic waste from the environment by oxidizers, *Res J Rec. Sci*, 10, 2015, 105-112

[42] N. Barka, A. Assabane, A. Nounah, and I.A. Ichou, I. A. , "Photocatalytic degradation of Indigo Carmine in aqueous solution bymTiO2 – coated non-woven fibres", *J Hazardous Mater*, 152, 2008,1054-1059

[43] C. Minero, G. Mariella, V. Maurino, D. Vione, D and E. Pelizzetti, Photocatalytic Transformation of Organic Compounds in the Presence of Inorganic Ions. 2. Competitive Reactions of Phenol and Alcohols on a Titanium Dioxide−Fluoride System", *Langmuir* 16, 2000, 8964-8972

[44] I. Bouzaida, C. Ferronato, J.M. Chovelon, M. E. Rammah, and J.M. Herrmann, Photocatalytic degradation of the anthraquinone dye, Acid Blue (AB25): a kinetic approach", *J Photochem. Photobiol. A: Chem*, 168, 2004, 23-30

[45] C. Guillard, E. Puzenat, H. Lachheb, A. Houas, J.M. Herrman, Why inorganic salts decrease the TiO_2 photocatalytic efficiency?, *Int. J. Photoenergy*, 7 , 1-9, 2005.

[46] A.G. Rincon and C. Pulgarin, Effect of pH, inorganic ions, organic matter and H_2O_2 on E. cli K12 photocatalytic inactivation by TiO_2. Implications in solar water disinfection", *Appl,Catal. B: Environ*, 51, 2004, 283-302

[47] C. Minero, P. Pellizari, V. Maurino, E. Pellizzetti. and D. Vione, Enhancement of dye sonochemical degradation by some inorganic anions present in natural waters", *Appl. Catal. B. Environ*, 77, 2008, 308-316

[48] K.P. VidyaLekshmi, SugunaYesodharan. and E.P. Yesodharan, MnO_2 and MnO_2 /TiO_2 mediated persulphate enhanced photocatalysis for the removal of Indigo carmine dye pollutant from water, *Eur. Chem. Bull*, 6, 2017,177-191

[49] R.L. David, *Handbook of Chemistry*, 84th Ed. CRC Press, Boca Raton, Florida, USA , 2004, 779-782

[50] C. Minero, V. Maurino, E. Pelizzetti and D. Vione, Evidence for a surface dual hole-radical mechanism in the titanium dioxide photocatalytic oxidation of 2,4-*D", Environ Sci. Poll. Res*, 13, 2006, 211-214

[51] K.P. Jyothi SugunaYesodharan. And E.P. Yesodharan, Contaminant salts as enhancers of sonocatalytic degradation of organic water pollutants: Effect of concentration, reaction time and adsorption on the efficiency of enhancement and the fate of concurrently formed H_2O_2, *J Env. Chem Eng.* Doi.org/doi:10.1016/j.Jece.2016.12.05

[52] C.S. Turchi and D.F. Ollis, Photocatalytic degradation of organic water contaminants: mechanisms involving hydroxyl radical attack, *J Catal.*, 122 , 1990, 178-192

[53] K.P. VidyaLekshmi, SugunaYesodharan and E.P. Yesodharan, MnO_2 catalysed microwave mediated removal of trace amount of Indigo carmine dye from water", *IOSR J Appl Chem* , 2014, 29-40

[54] K.P. VidyaLekshmi, SugunaYesodharan. and E.P. Yesodharan, Co_3O_4 mediated microwave catalysis: A new innovative Advanced Oxidation process (AOP) for the removal of dye pollutants from water", *IOSR J Appl Chem*, 1, 2016, 25-46

[55] Y. Xu and C.H. Langford, Variation of Langmuir adsorption constant determined for TiO_2 photocatalysed degradation of acetophenone under different light intensity", *J Photochem Photobiol A. Chem*, 133, 2000, 67-71

[56] S. Zhou and A.K. Ray, Kinetic studies for Photocatalytic degradation of Eosin B on a thin

- -

film of Titanium dioxide, *Ind. Eng Chem. Res*, 42, 6020-6033, 2003.

[57] R J D. Miller, G.L. Mc Lendon, A.J. Nozik, W. Schmickler and F. Willing, Surface Electron-transfer Processes", VCH *publishing*, New York, 1995.


ISSN - 2249-555X
IMPACT FACTOR:3.919
A Peer Reviewed, Referred, Refereed
& Indexed International Journal
Journal DOI :10.36106/ijar
INDEX COPERNICUS IC VALUE : 74.50
Indian Journal Of Applied Research
INDIAN
JOURNAL
OF APPLIED
RESEARCH
Journal for All Subjects
www.ijar.in
VOLUME : 9 | ISSUE :10| October 2019

Original Research Paper

Volume-9 | Issue-10 | October - 2019 | PRINT ISSN No. 2249 - 555X | DOI : 10.36106/ijar

Environmental Science

ULTRASOUND INDUCED FENTON/PERSULPHATE/H_2O_2/ZNO PROMOTED ADVANCED OXIDATION PROCESS FOR THE MINERALIZATION OF INDIGO CARMINE POLLUTANT IN WATER

Veena Vijayan	School of Environmental Studies Cochin University of Science and Technology Kochi 682022
Suguna Yesodharan	School of Environmental Studies Cochin University of Science and Technology Kochi 682022
E. P. Yesodharan*	School of Environmental Studies Cochin University of Science and Technology Kochi 682022 *Corresponding Author

ABSTRACT Indigo carmine (IC), widely used in textile industry, food colorings, medical diagnostics etc. is a major dye pollutant of water. Ultrasonic (US) degradation of IC in water under different conditions is investigated. The effect of US frequency (200, 350 , 620 and 1000 kHz) and power (20, 40, 60 and 80W) on the degradation profile is evaluated. Optimum degradation is obtained at 350 kHz and 80W in the acidic medium. Combination with Fe^{2+}, H_2O_2, peroxydisulphate and ZnO enhances the sonodegradation efficiency significantly. The influence of salts/ anions likely to be present in water on the sonolytic degradation varies from inhibition to 'no effect'. Major intermediates formed during the degradation of the dye are identified using LC/MS technique. Eventually the degradation leads to complete mineralization as confirmed by the absence of chemical oxygen demand (COD). Optimum parameters for the mineralization are identified experimentally and appropriate reaction mechanisms are proposed.

KEYWORDS : Sonolysis; Indigo Carmine, Mineralization; Water purification

1.INTRODUCTION

Development of efficient, economical and environment-friendly technologies for water purification is a high priority area today. Of the many types of industries, textile industry is one of the leading polluters of water/water bodies in terms of toxicity, color and organic load. The absolute removal of dyes and related harmful byproducts from the aquatic environment is a great technological challenge even though the removal of color is not that difficult. Some of the common methods for the treatment of dye-bearing wastewater include coagulation/ flocculation, activated carbon adsorption and membrane treatment. However, they fail to degrade the organic chemicals and simply transfer them from one medium to another. Removal of the last traces of toxic pollutant dye by converting them into harmless products is essential to make the water reusable [1]. Advanced Oxidation Processes (AOPs) have high potential in this respect. This methodology is based on the insitu production of highly oxidizing hydroxyl radicals (OH), which can react nonselectively with most of the organic compounds. The commonly used AOPs include photolysis/photocatalysis, UV/H_2O_2, Fenton treatment, photo Fenton, sonolysis, sonocatalysis etc. [2-7]. Among these, sonolysis is one of the most versatile techniques which is widely investigated for wastewater treatment due to the major advantages of safety, cleanliness and energy efficiency. Several reports are available on the sonolytic degradation of chlorinated organic compounds, phenolic compounds, organic dyes, pesticides, endocrine disrupting compounds, perfluorinated chemicals, pharmaceuticals and microcystins [7-12].

Three types of reactions involved in sonolysis are pyrolysis, reaction of $^{\cdot}OH$ and $^{\cdot}H$ and supercritical water oxidation [13,14]. Ultrasound can produce $^{\cdot}OH$ and $H^{\cdot}$ by acoustic cavitation (reaction 1). Generally hydrophobic and volatile compounds undergo degradation via pyrolysis in the interface region. Supercritical water oxidation process provides an additional route for the degradation. The radical generation in sonolysis and subsequent reactions are shown in reactions (2) - (5) [13-15].

$$H_2O +)))\ \rightarrow\ H^{\cdot} + {}^{\cdot}OH \quad (1)$$
$$^{\cdot}H + O_2\ \rightarrow\ HO_2^{\cdot}\ \rightarrow\ OH + \tfrac{1}{2}O_2 \quad (2)$$
$$2\,^{\cdot}OH\ \rightarrow\ H_2O_2 \quad (3)$$
$$2HO_2^{\cdot}\ \rightarrow\ H_2O + O_2 \quad (4)$$
$$^{\cdot}H + H_2O_2 \rightarrow OH + H_2O \quad (5)$$

Indigo Carmine (IC), (5.5'–indigo disulfonic acid disodium salt) is a dark blue dye mainly used in the textile industry for the dyeing of polyester fibers and denim (blue jeans) [16]. In the field of medical diagnostics it is administered intravascularly in a variety of applications such as; to locate urethral orifices, to endoscopically examine gastric cancer and to adjust the position of a catheter in the chemotherapy of hepatic and oral maxillofacial tumours [17,18]. It can also help to target biopsies even better since the homogeneously stained or unstained areas can be correlated with intraepithelial neoplasia. It is also a pH indicator. IC is also used as dye in food and cosmetics industry.

The dye is highly toxic, carcinogenic and has the potential to cause permanent injury to eyes. It can also lead to reproductive and developmental disorders as well as neuron and acute toxicity. Other health effects include possible tumors at the site of application, cardiovascular and respiratory effects and gastrointestinal irritation [18].

Several processes have been suggested for removal of IC and other dyes from wastewater including adsorption, microwave, photochemical and electrochemical methods [19-24]. In the present study, investigation of the sonochemical degradation of the pollutant dye IC is carried out. The effect of various operational parameters such as frequency of US, power density, pH, presence of various additives such as Fe^{2+}, H_2O_2, $S_2O_8^{2-}$ and anions/salts on the efficiency of degradation is investigated. The chemical structure of IC is shown in figure 1.

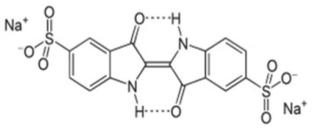

Fig. 1. Chemical structure of Indigo Carmine

2. MATERIALS AND METHODS

2.1. Materials

IC (>99.6%) and ZnO (>99.5%) used in the study are from Sigma Aldrich India. H_2O_2 (30.0% w/v) and $K_2S_2O_8$ (PDS, AnalaR-99%) from Qualigen (India) were used as such without further purification. Various other chemicals used were also of AnalaR grade or equivalent, unless indicated otherwise.

2.2. Sonolysis

Sonication of the reaction system was carried out in a jacketed glass reactor of 500 ml capacity. Ultrasound (US) of different frequencies was generated using an L3 ELAC Nautic ultrasound generator powered by an allied signal R/F generator (T& C power conversion, model AG1006). The variable frequencies used were 200, 350, 620, and 1000 kHz. The power applied varied from 20 to 80W. The temperature was maintained at 25±1°C by circulating cooling water from a thermostat. Typical reactor assembly is shown in figure 2. The

Volume-9 | Issue-10 | October - 2019 | PRINT ISSN No. 2249 - 555X | DOI : 10.36106/ijar

disappearance of the dye is followed by using UV/Vis spectrophotometry at a wavelength of 609 nm. The intermediates were detected using LC/MS (Waters Xevo G2 Q-TOF).

2.3. Analysis of chemical oxygen demand (COD)

Open reflux method is used to determine COD of the samples [25]. The sample (50 ml) was pipetted out into a refluxing flask. $HgSO_4$ (1g) was added along with several glass beads. Sulphuric acid reagent (5.5g Ag_2SO_4 in 543mL Conc.H_2SO_4) was added (5 ml) slowly with mixing to dissolve $HgSO_4$. The sample was cooled while mixing to avoid the possible loss of volatile materials. $K_2Cr_2O_7$ solution (0.05 N, 25 ml) was also added and mixed well. Remaining (70mL) sulfuric acid reagent was added through the open end of the condenser. The whole mixture was refluxed for two hours and cooled thereafter to room temperature. The mixture was

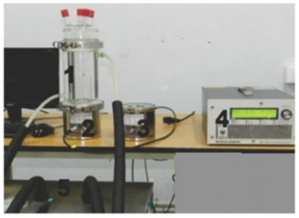

Fig.2. Sonoreaction assembly, 1: Glass reactor, 2, 3: Variable frequency generators, 4: Power supply unit, 5: Thermostat

diluted to 150mL and the excess $K_2Cr_2O_7$ was titrated against 0.05N Ferrous Ammonium Sulfate (FAS) solution using Ferroin as the indicator. The end point was sharp change in color from blue green to reddish brown. A blank was also carried out under identical conditions using the reagents and distilled water in place of the sample.

COD is calculated using the following equation:

COD (as mg O_2/L) = (A-B) × M × 8000 / mL sample (6) where;

A = mL FAS used for blank

B = mL FAS used for sample

M = Molarity of FAS

8000 = milliequivalent weight of oxygen × 1000mL/L

3.RESULTS AND DISCUSSION

Preliminary experiments have shown that irradiation by US (sonolysis) is a viable method for the degradation of traces of Indigo Carmine dye pollutant in water. Hence the process and the influence of various reaction parameters on its efficiency are investigated in detail.

3.1. Effect of frequency of US

The effect of frequency of US on the degradation of IC is measured by performing experiments at four different frequencies, i.e. 200, 350, 620 and 1000 kHz keeping the power constant (80W). The degradation pattern is given in figure 3.

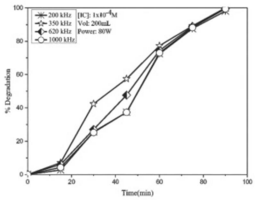

Fig. 3: Effect of US frequency on the sonochemical degradation of IC

The rate of degradation does not have any direct correlation with the frequency and is the highest at 350 kHz. The degradation is less at both the lower frequency (200 kHz) and the higher frequency (1000 kHz). Hence simple increase in the frequency does not guarantee increased sonodegradation of the pollutant. A distinct difference in the degradation with frequency was observed only during the early stage of sonolysis (upto 60 minutes). Later on, the degradation efficiency was comparable (>80%) The optimum frequency for the degradation of IC is therefore taken as 350 kHz.

The size of the bubble (resonance size), number of bubbles formed, life time of the acoustic bubble in the multibubble field and the intensity of collapse are the important factors in sonolytic degradation which in turn depend on the ultrasonic frequency and power [26]. The resonant size of the bubbles decreases with increase in the frequency [27], i.e., the size of the bubble will be in the order 200 kHz > 350 kHz > 620 kHz > 1 MHz. At lower frequency, the bubble pulsation occurs slowly and the life time of the cavitating bubble will be more. Thus, chances of recombination of the reactive ˙OH in the interface get enhanced. At higher frequency, the size of the cavity is reduced. However the availability of reaction site and the number of cavitational events become higher and consequently more ˙OH radicals are generated resulting in faster reaction. The cavitation bubbles become more dispersed and more accessible for the reacting species which also result in enhanced degradation of the substrate [28]. The life time of an acoustic bubble in a multibubble field, which may vary with the applied frequency, is another important factor in sonolytic degradation of organics. Sunartio et al. [29] reported that the life time of a cavitating bubble increases with decreasing frequency, i.e. in the present case, maximum lifetime is at 200 kHz and the least at 1 MHz. Chowdhuri and Vijayaraghavan [15] compared the sonolytic effects at two different frequencies of 200 and 350 kHz and concluded that the life time of the bubble in the acoustic field is comparable at the two frequencies though the relative life time of the cavitating bubble is more at 200 kHz. However the number of cavitations is higher at 350 kHz thereby generating more hydroxyl radical. Consequently degradation of IC is enhanced when frequency is increased from 200 to 350 kHz. But with further increase in the frequency, the relative life time of the bubble becomes lower and therefore the collapse of the bubble will be less violent. This results in decreased formation of ˙OH. This is the likely reason for the lower efficiency of degradation at higher frequencies of 620 and 1000 kHz

3.2. Effect of power

The effect of power of US on the degradation of IC is monitored by varying the power (20W, 40W, 60W and 80W) at a fixed frequency of 350 kHz. The results are shown in figure 4. After the initial induction period, efficiency of degradation increases with increase in power, with maximum degradation at 80W. Acoustic intensity dissipated into the solution is directly related to the applied power [30]. At the appropriate power, the bubble growth starts and reaches the resonant size. This is followed by collapse of the bubbles and subsequent formation of ˙OH.

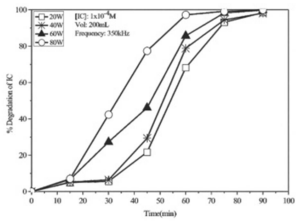

Fig.4: Effect of US power on the sonolytic degradation of IC

The hike in power can also enhance the negative pressure exerted by ultrasound. As a result, the bubble expands more in the rarefaction stage and the cavity reaches the resonance size instantly. Consequently pyrolysis and ˙OH formation reaction takes place at accelerated rate [31]. In any case, in the current study, the degradation of IC is completed even at the lower power of US and the net time taken for complete degradation is only marginally less at higher power even though the degradation is more dependent on sono power in the early stages of the reaction.

3.3. Effect of Concentration of IC

The effect of concentration of IC on its sonodegradation is investigated at the optimized frequency (350 kHz) and power (80W) of US. The percentage degradation decreases with increase in concentration (figure 5). However more appropriate measure of the efficiency is the rate of degradation. The rate of degradation of IC at different concentrations is plotted in the inset of figure 5. The rate increases with increase in concentration of IC, reaches an optimum at $1x10^{-4}$M and decreases thereafter. Accordingly, $1x10^{-4}$M of IC is chosen as the optimum concentration for further studies.

Volume-9 | Issue-10 | October - 2019 | PRINT ISSN No. 2249 - 555X | DOI : 10.36106/ijar

The degradation of pollutants in water under sonolysis involves their interaction with ˙OH radicals formed insitu as shown in reactions (1) – (5). However most of the ˙OH will recombine and produce H_2O_2 inside the cavitation bubble and at the gas-liquid interface as shown in reaction (3). H_2O_2 is detected in the present system also. It is also possible that the pollutant molecule inside or in the neighborhood of a disintegrating bubble can get thermally degraded due to the supercritical conditions of high local temperature and pressure [13,32].

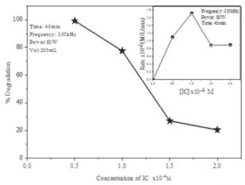

Fig.5: Effect of concentration of IC on its sonochemical degradation

The initial degradation of the dye will be dependent on the relative concentration of dye molecules at the interface of the cavitation bubble and the ˙OH radicals. IC is a low volatile compound and its relative concentration at the cavitation-bubble interface will be less. Consequently, the sonochemical degradation also will be slower. The rate determining step is the generation of ˙OH either from water or the deprotonation of insitu formed H_2O_2 or both under sonolysis. At lower dye concentration, the ˙OH radicals have lesser number of dye molecules to interact with and the rate of degradation is slower. The degradation takes place primarily in the bulk of the solution where the ˙OH radical concentration is low because only a small part of the radicals generated at the bubble surface can diffuse into the bulk. With increase in concentration of IC, the frequency of interaction between the substrate and the ˙OH is more and the rate of degradation increases steadily until the optimum is reached. Beyond the optimum concentration, the rate of ˙OH radical generation and/or its diffusion into the bulk may not be adequate to interact with correspondingly more of the pollutant molecules and the rate slows down and even decreases. At higher concentration of the dye, the penetration of US into the system and consequently the generation of ˙OH are inhibited. This also leads to decrease in the degradation. Moreover, as the reaction proceeds, more and more intermediates are formed which will compete with IC for the ˙OH radicals resulting in further decrease in the rate. Similarly, the concentration of the dye molecules inside the bubble and the bubble-solution interface also will be relatively less in comparison to its overall concentration. This also results in apparent decrease in the rate of degradation at higher concentration. Hence optimization of the concentration of the dye in water is important for achieving efficient and economical decontamination of the polluted water.

3.4. Effect of pH

The pH of the reaction medium is known to have strong influence on all AOPs including US-induced degradation of organic pollutants. Therefore the effect of pH on the sonochemical degradation of IC was studied. The results are shown in figure 6. It is observed that the degradation is more efficient in the acidic region than in the alkaline region. At lower pH, the formation of hydrogen peroxide by the recombination of hydroxyl radicals will be less [33]. Therefore, the number of hydroxyl radical available for the reaction with IC in the liquid region is more. Similarly, the number of reaction sites will increase at this pH due to the increased bubble repulsion caused by the accumulation of hydronium ion in the interface region [34]. This also enhances the degradation at lower pH.

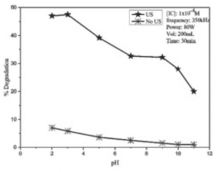

Fig.6: Effect of pH on the sonochemical degradation of IC

3.5. Effect of power density

The effect of power density (power/volume) of US on the sonodegradation of IC was studied by taking different volumes of the reaction solution keeping the power applied constant at 80W. By increasing the US power density from 0.16 to 0.8 W/mL (volume decreasing from 500 to 100 mL), the degradation increases steeply initially and slowly thereafter, to level off eventually (figure 7). This implies that the relative volume of the reactants and the applied US power have to be optimized in order to achieve efficient sonodegradation.

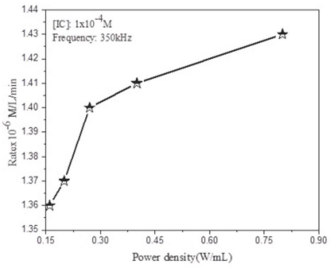

Fig 7: Effect of US power density on the sonodegradation of IC

3.6. Formation of H_2O_2

The formation of H_2O_2 during the sonochemical degradation of organics by recombination of insitu formed ˙OH has been reported earlier [34]. In the present study also, H_2O_2 is formed in the system and its concentration at different times of sonication is measured after the decolorisation. The concentration could not be measured precisely when the system is colored. The results are plotted in figure 8. It is seen that even after the decolourisation, the concentration of H_2O_2 is increasing showing that formation as well as the recombination of ˙OH radicals is continuing. These free radicals interact further with the intermediates formed on decolorization. Eventually, the intermediates also get fully degraded and the system is mineralized completely.

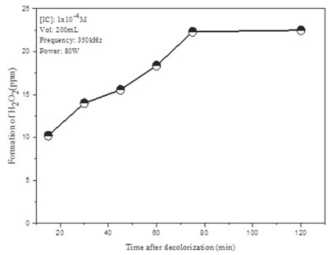

Fig.8: Formation of H_2O_2 during the sonochemical degradation of IC

Under US irradiation, the O_2 present in the solution would be split into reactive ˙O radicals (reaction 7) which interact with H_2O molecules and form reactive ˙OH and H_2O_2 (reaction 8,9) The 'hot spot effect' of US irradiation in water will also enhance the formation of ˙OH due to the pyrolysis of water molecules as in reaction (10). This as well as reaction (11) and (12) will also result in the formation of more reactive oxygen species (ROS) such as ˙OH, $HO_2^{\cdot}$ and H_2O_2 which will facilitate the degradation and mineralization of the substrate IC (reaction 13).

$O_2 \rightarrow 2\,{}^{\cdot}O$ (7)

$O + H_2O \rightarrow 2\,{}^{\cdot}OH$ (8)

${}^{\cdot}OH + {}^{\cdot}OH \rightarrow H_2O_2$ (9)

$H_2O \quad +>>> \rightarrow \quad H^{\cdot} + {}^{\cdot}OH$ (10)

$H^{\cdot} + O_2 \rightarrow O + {}^{\cdot}OH$ (11)

$H^{\cdot} + O_2 \rightarrow HO_2^{\cdot}$ (12)

IC + ROS (˙OH, $HO_2^{\cdot}$, H_2O_2 etc.) →→ Intermediates →→ Mineralization (CO_2, H_2O) (13)

3.7. Effect of hydrogen peroxide

Since H_2O_2, a powerful oxidant, is formed insitu during the sonolytic process, it is quite possible that the rate of degradation of IC is enhanced by its increasing presence in the system. The effect of H_2O_2

Volume-9 | Issue-10 | October - 2019 | PRINT ISSN No. 2249 - 555X | DOI : 10.36106/ijar

on the degradation of IC is investigated by initially adding different concentrations of H_2O_2 (10-50 mg/L) under standardized sonoconditions The results are shown in figure 9.

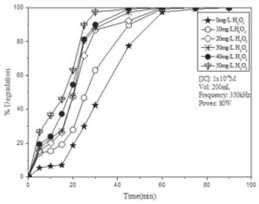

Fig.9: Effect of H_2O_2 on the sonochemical degradation of IC

The degradation is enhanced in the presence of H_2O_2. Control experiments in the presence of H_2O_2 without sonication showed no significant degradation within the time frame of experiments. The degradation increases with increase in the concentration of H_2O_2. At lower concentration, there is an induction period, which is probably due to the slower generation of OH radicals. However, eventually the rate is enhanced at all concentrations. Complete (100%) degradation is achieved in about 25 min. with 50mg/L of added H_2O_2, while it takes approximately 60 minutes at lower concentrations. The enhancement can be attributed to the additional OH formed during the sonication by the pyrolysis of hydrogen peroxide as in reaction (14) [35, 36].

$$H_2O_2 \rightarrow 2\,OH \qquad (14)$$

However the OH can also act as a scavenger of H_2O_2 thereby reducing the net concentration of H_2O_2 as follows:

$$H_2O_2 + {}^{\cdot}OH \rightarrow H_2O + HO_2^{\cdot} \qquad (15)$$

The detrimental effect of H_2O_2 at higher concentration [37-39] on the AOP degradation of organics is not quite evident here. However the enhancement in degradation with increase in H_2O_2 concentration slows down at higher concentration indicating that the scavenging of OH by H_2O_2 is also taking place in parallel. The enhancement by added H_2O_2 can be explained in two possible ways: i) H_2O_2 molecules that enter the cavitation bubbles during sonication are broken into OH radicals, which enter the solution, interact with and degrade the IC. ii) The H_2O_2 oxidizes IC directly. However the higher rate of enhancement is not sustained later on. This can be explained as follows: In the beginning, added H_2O_2 decomposes faster in presence of US producing maximum OH radicals which can degrade IC. However, the decomposition of H_2O_2 to water and oxygen ($H_2O_2 \rightarrow H_2O + O_2$) also occurs in parallel which restricts the continued availability of the oxidizing species for IC degradation. Further, even in those experiments without externally added H_2O_2, the H_2O_2 formed in-situ will be accelerating the reaction rate. Hence the effect of initially added H_2O_2 is not that prominent in the later stages of the reaction.

3.8 Effect of Fe^{2+}

The insitu formation of H_2O_2 in the reaction system opens up the possibility of enhancing the degradation significantly, by introducing Fe^{2+} to the system and promoting a Fenton like reaction. This will initiate a combination AOP, i.e. SonoFenton and its associated additive or even synergistic effect. In order to verify this possibility, the effect of added Fe^{2+} on the degradation of IC is investigated. $FeSO_4$ is added to the dye solution prior to sonication by keeping the frequency and power constant at 350 kHz and 80W respectively. All reaction parameters are kept the same as those in the case of regular sonolysis. In order to maintain the ideal Fenton condition [40,41], the initial pH of the solution was maintained at 4-5. The results are compared with those under simple sonolysis as well as comparable Fenton conditions and are shown in figure 10. The sonodegradation increases in the presence of Fe^{2+}. The percentage degradation of IC after 15 min of sonication in presence of 50 mg/L Fe^{2+} is 99%. During this period, the degradation under simple Fenton is 40% while it is only 5% under simple sonolysis.

The synergy index of sonoFenton process in comparison to the additive effect of sono and Fenton process is calculated for this time period, using the relation,

Synergy index (US + Fenton) = $R_{(US+F)} / (R_{US} + R_F)$ (16) where

$R_{(US+F)}$, R_{US} and R_F are the rates of degradation under sonoFenton, sono and Fenton conditions respectively. In this case, the synergy index (SI) is 2.2, suggesting very strong synergy by

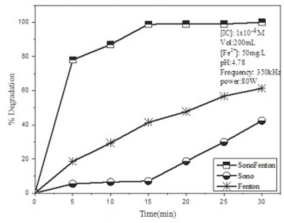

Fig.10: Effect of added Fe^{2+} on the sonochemical degradation of IC

combining the two processes, especially in the early stages of reaction. This reconfirms the formation of H_2O_2 insitu under sonication which makes the Fenton process possible in presence of added $FeSO_4$. The Fenton process results in the formation of more reactive free radicals such as OH, $HO_2^{\cdot}$ etc. as in reactions (17) – (21). However, with time of reaction, the synergy/additive effect becomes less and less significant (SI decreases to ~1.25 and ~ 1.0 after 25 and 30 min. respectively) probably because the concentration of the dye has become too low to show any significant enhancement in the rate of degradation by the combination process (over the sum of the degradation by respective individual processes).

Various reactions taking place in presence of Fe^{2+} and H_2O_2 (Fenton reaction) under US irradiation can be summarized as follows:

$$Fe^{2+} + H_2O_2 \rightarrow Fe^{3+} + OH + {}^{\cdot}OH \qquad (17)$$

$$H_2O_2 +))) \rightarrow 2\,OH \qquad (18)$$

$$H_2O_2 + OH \rightarrow H_2O + HO_2^{\cdot} \qquad (19)$$

$$Fe^{3+} + H_2O_2 \rightarrow Fe(OH)^{2+} + H^+ \qquad (20)$$

$$Fe(OH)^{2+} +))) \rightarrow Fe^{2+} + HO_2^{\cdot} \qquad (21)$$

$$2Fe^{3+} \rightarrow 3Fe^{2+} \qquad (22)$$

$$Fe^{3+} + HO_2^{\cdot} \rightarrow Fe^{2+} + H^+ + O_2 \qquad (23)$$

Thus it is seen that the US induced formation of OH radicals in aqueous solutions is enhanced in the simultaneous presence of Fe^{2+} and H_2O_2. Complex redox reactions also take place leading to the formation of hydroperoxide radicals and reduced Fe^{2+} ions [40] which also results in enhanced degradation of the pollutant.

3.9 Effect of persulfate

The enhancement in the sonochemical degradation of IC in presence of H_2O_2 opens up the possibility of using another powerful oxidant persulfate. Accordingly, sonolysis of IC was done in the presence of peroxydisulfate (PDS) as an additive. It is observed that the degradation is faster in the presence of PDS. The sonodegradation of IC is ~ 30% in the absence of PDS while it is ~ 62% in presence of PDS (15 mg/L) in 20 minutes. The results are shown in figure 11. Sonolysis of PDS results in the formation of sulfate radical anion which is a selective oxidant (2.6 V). Oxidative degradation of organic compounds by sulfate radical is well documented [42]. The degradation is increasing with increase in concentration of PDS, in the range 10-25mg/L. The degradation is complete in less than 1 hr. even at the lowest concentration of PDS, i.e., 10mgL. PDS can diffuse to the interfacial region where pyrolysis also produces sulfate radical.

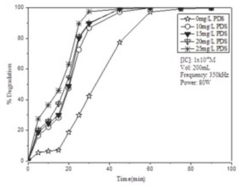

Fig.11: Effect of PDS on the sonochemical degradation of IC

Various ROS such as H_2O_2, $Ho_2^{\cdot}$, OH etc. and $SO_4^{\cdot-}$ formed during the irradiation by radical inter conversion reactions interact with IC in the bulk, leading to its degradation into various intermediates and eventual mineralization (reactions 24 – 32) . The results also show that both H_2O_2 and PDS have comparable enhancing efficiency. The OH radicals

Volume-9 | Issue-10 | October - 2019 | PRINT ISSN No. 2249 - 555X | DOI : 10.36106/ijar

interact more with the $SO_4^{\cdot-}$ resulting in the destruction of both by chain termination (reaction 29). Hence addition of more PDS is necessary to sustain the generation of $SO_4^{\cdot-}$ and consequently the degradation of IC to drive the reaction to completion, especially so at later stages of reaction when the rate becomes slower. However, too much excess of PDS can lead to deactivation of $SO_4^{\cdot-}$ as in reaction (33).

Various reactions leading to the formation and interactions of $SO_4^{\cdot-}$ are as follows:

$S_2O_8^{2-} +))) \rightarrow 2SO_4^{\cdot-}$ (24)

$SO_4^{\cdot-} + RH \rightarrow R^{\cdot} + HSO_4^-$ (25) Where RH=IC

$So_4^{\cdot-} + H_2O \rightarrow SO_4^{2-} + H^+ + {}^{\cdot}OH$ (26)

$S_2O_8^{2-} + RH \rightarrow SO_4^{\cdot-} + HSO_4^- + R^{\cdot}$ (27)

${}^{\cdot}OH + (RH, R^{\cdot}) \rightarrow$ Intermediates $\rightarrow$ products (28)

$SO_4^{\cdot-} + (R^{\cdot}, {}^{\cdot}OH) \rightarrow$ Chain termination (29)

$2SO_4^{\cdot-} \rightarrow S_2O_8^{2-}$ Chain termination (30)

$2\,{}^{\cdot}OH \rightarrow H_2O_2$ Chain termination (31)

$2R^{\cdot} \rightarrow RR$ Chain termination/Further degradation (32)

$SO_4^{\cdot-} + S_2O_8^{2-} \rightarrow SO_4^{2-} + S_2O_8^{\cdot-}$ (33)

3.10. Effect of addition of ZnO

ZnO has been proven to be a good catalyst for the sono and photo degradation of many organic pollutants in water. Hence the effect of ZnO on the sono degradation of IC is tested under standardized condition for sonolysis. The degradation increases moderately in presence of the catalyst (figure 12). With increase in catalyst dosage, the degradation increases slowly reaches an optimum at 0.06g and stabilizes thereafter. The sonodegradation is more in the presence of ZnO compared to that with ultrasound alone. This may be because in presence of ZnO under US irradiation, more hydroxyl radicals are produced which will react with more of the IC molecules and degrade them. ZnO is an efficient catalyst offering surface sites for the adsorption of the substrate leading to enhanced interaction with the surface generated ${}^{\cdot}OH$ radicals. It is known that presence of suspended particles of appropriate size and amounts in water lead to increase in the acoustic noise and rise in the temperature in the irradiated liquid [43,44]. Presence of suspended solids in the liquid can provide more nucleation sites for cavitation bubbles at their surface. This will result in decrease in the cavitation thresholds which is responsible for the

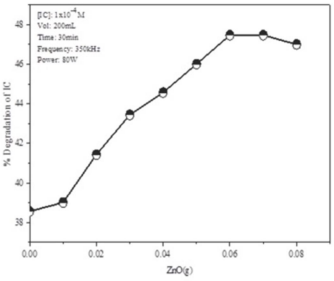

Fig.12: Effect of ZnO at different dosages on the sonochemical degradation of IC

increase in the number of bubbles when the liquid is irradiated by US. Increase in the number of cavitation bubbles increases the pyrolysis of water which also leads to increase in the generation of reactive free radicals and degradation of IC under sonication. However, any increase in the catalyst dosage beyond the optimum will only result in the aggregation of particles which will limit the number of catalytically active accessible sites at the surface. Higher dosage of suspended particles will also disturb the transmission of ultrasound in the aqueous medium. Hence there is no further increase in degradation of the pollutant beyond a particular dosage. The sonoluminescence resulting in UV irradiation may also accelerate the reaction through photocatalysis since ZnO is an efficient photocatalyst [27,37,43].

3.11. Comparative degradation efficiency of IC in presence of additives

Further to the experiments conducted in presence of various additives individually as above, preliminary studies were made on the efficiency of various combinations for the degradation of IC (in terms of the time taken for complete decolorization). The results are shown in figure 13.

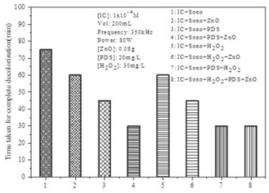

Fig.13: Comparison of the time taken for complete decolorization of IC in presence of different additives

Accordingly the most efficient systems for the degradation of IC are: i) sonolysis in presence of ZnO and PDS (US/PDS/ZnO), ii) sonolysis in presence of H_2O_2 and PDS (US/PDS/ H_2O_2) and iii) sonolysis in presence of PDS,H_2O_2 and ZnO (US/PDS/H_2O_2/ZnO). Sonolysis in presence of H_2O_2 and ZnO (US/H_2O_2/ZnO) as well as in presence of PDS (US/PDS) are also efficient, though slightly less than the earlier three systems. The relative efficiency of various systems for the deciolorization is in the order:

(US/PDS/ZnO) ≈ (US+PDS+H_2O_2+ZnO) ≈ (US/PDS/H_2O_2) > US/H_2O_2/ZnO ≈ US/PDS > US/H_2O_2 ≈ US/ZnO (34)

The relative efficiency of the additives for enhancing the efficiency of degradation of the pollutant may vary with the concentration of the additive which may be attributed to the multiple interactions of various reactive free radicals at different stages of reaction leading to different intermediates [43,44]. However, such variation is not significant in the present case for the decolorization of IC.

3.11 Effect of anions

Anions/salts likely to be present in most of natural waters are known to influence the efficiency of many AOPs for water purification. In this context, the effect of few such anions i.e., SO_4^{2-}, Cl^-, CO_3^{2-}, HCO_3^-, and PO_4^{3-} on the rate of sonolytic degradation of IC is investigated and the results are presented in figure 14. The anions have no effect on the degradation of IC at the concentration studied here except in the case of PO_4^{3-} which is known to be a strong inhibitor of most AOPs. Studies at different concentration ranges of various anions (5-15 mg/L) on the degradation of IC confirm that the concentration effect is negligible at least in this range. This suggests that sonolysis is an efficient source of AOP activation for the removal of IC even from natural water containing dissolved salts. However, at much higher concentration of the anions (which is not natural in most water sources), the possibility of inhibition cannot be ruled out as has been reported in few earlier studies [44].

Since the efficiency of sonolysis for the degradation of IC in water is higher in the presence of additives such as PDS, H_2O_2, ZnO and/or their combination, the effect of anions is tested under

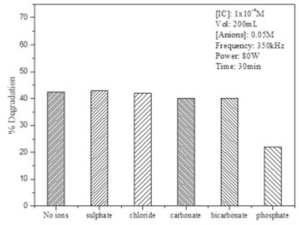

Fig. 14. Effect of common anions in water on the sonolytic degradation of IC

these conditions as well. In these cases also anions have practically no effect except the inhibition by PO_4^{3-}. This implies that the most efficient systems identified earlier, i.e. US/PDS/ZnO, US/PDS/H_2O_2/ZnO or US/PDS/H_2O_2 can be used for the decontamination of water from IC even in the presence of moderate amount of natural anions.

3.12. Mineralization studies

The efficiency of any AOP for the decontamination of water depends on its ability to completely mineralize the pollutants into harmless

Volume-9 | Issue-10 | October - 2019 | PRINT ISSN No. 2249 - 555X | DOI : 10.36106/ijar

products. The mineralization in this case is tested by measuring the chemical oxygen demand (COD) of the system at different times of sonication. The COD disappears completely in 10 hr. time by simple sonication in the absence of any oxidant or catalyst (figure 15). The time taken for complete mineralization of IC is much less in presence of specific additives, as shown in figure 16.

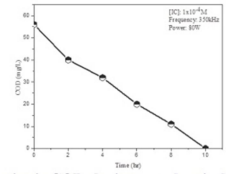

Fig. 15.: Reduction in COD during sonochemical degradation of IC

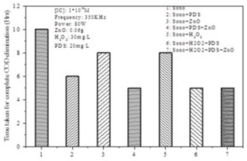

Fig.16: Comparison of the time taken for complete mineralization of IC under sonolysis in presence of different additives

The efficiency of mineralization of various systems is in the order: (US/PDS/ZnO) ≈ (US/PDS/H_2O_2) ≈ (US+PDS+H_2O_2+ZnO) > US/PDS > US/H_2O_2 ≈ US/ZnO (35)

The mineralization as well as the decolorization follows the same pattern thereby suggesting that the degradation of the intermediates formed during the decolorization is also facilitated by the oxidants.

The longer time taken for mineralization compared to decolorization shows that the former proceeds through the formation of recalcitrant intermediates which take longer time to be irreversibly transformed into harmless CO_2, H_2O_2 and salts. Various intermediates formed during degradation of IC are analyzed by LC/MS and are shown in Table 1.

Table 1: Major intermediates identified during the sonodeg radation of IC

m/z	Molecular structure
188	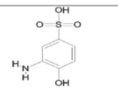
216	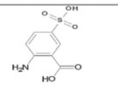
225	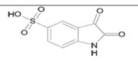
257	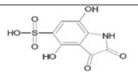
357	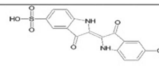
423	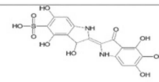

4.CONCLUSION

Ultrasound irradiation at appropriate power and frequency is an efficient mode of activation in advanced oxidation process (AOP) for the decolorization as well as mineralization of Indigo Carmine dye pollutant in water. The mineralization, which is confirmed by measuring the chemical oxygen demand, proceeds through a number of intermediates. These intermediates are identified and characterized by LCMS. Combination of sonolysis with additives such as Fe^{2+}, H_2O_2, peroxydisulphate and ZnO enhances the efficiency of the process for decolorization as well as mineralization. The presence of salts/anions commonly found in water does not inhibit the degradation or mineralization, except in the case of PO_4^{3-} ions. Hence the sonolytic AOP, under suitably standardized conditions, is a potential technique for the decontamination of water from Indigo Carmine (IC) pollutants even in the case of natural effluents containing moderate amounts of salt contaminants.

Acknowledgement

Financial support from the Cochin University of Science and Technology, Cochin, India to one of the authors (VV) by way of BSR Senior Research Fellowship is gratefully acknowledged.

REFERENCES

1. G.M. Colonna, T. Caronna, B. Marcandalli, Oxidative degradation of dyes by ultraviolet radiation in the presence of hydrogen peroxide, Dyes and Pigments. 41 (1999) 211–220
2. U.I.Gaya, A.H. Abdullah, Heterogeneous photocatalytic degradation of organic contaminants over titanium dioxide: A review of fundamental, progress and problems, J. Photochem. Photobiol. C: Photochem. Rev., 9 (2008) 1-12
3. I. Sirés , E Brillas, M.A. Oturan, M. A. Rodrigo , M Panizza, Electrochemical advanced oxidation processes: today and tomorrow. A review, Environ Sci Poll. Res, 21 (2014), 8336–8367
4. J.J. Pignatello, E. Oliveros, A. MacKay, Advanced oxidation processes for organic contaminant destruction based on the Fenton reaction and related chemistry. Crit. Rev. Environ. Sci. Technol. 36 (2009) 1–84
5. E. Brillas, I Sires, M.A. Oturan, Electro-Fenton process and related electrochemical technologies based on Fenton's reaction chemistry. Chem Rev. 109 (2009) 6570–6631
6. S. Sarathy, M. Mohseni, Effects of UV/H2O2 advanced oxidation on chemical characteristics and chlorine reactivity of surface water natural organic matter. Water Res. 44 (2010) 4087–4096.
7. P. Chowdhury, T. Viraraghavan, Sonochemical degradation of chlorinated organic compounds, phenolic compounds and organic dyes – a review. Sci. Total Environ. 407 (2009) 2474–2492.
8. F. Guzman-Duque, C. Petrier, C. Pulgarin, G. Penuela, R.A. Torres-Palma, Effects of sonochemical parameters and inorganic ions during the sonochemical degradation of crystal violet in water. Ultrason. Sonochem. 18 (2011) 440–446
9. Z. Eren, Ultrasound as a basic and auxiliary process for dye remediation: a review. J. Environ. Manage 104 (2012) 127–141.
10. Adewuyi, Y.G., 2001. Sonochemistry: environmental science and engineering applications. Ind. Eng. Chem. Res. 40, 4681–4715.; Song, W., De La Cruz, A.A., Rein, K., O'Shea, K.E., 2006.
11. Ultrasonically induced degradation of microcystin-LR and -RR: Identification of products, effect of pH, formation and destruction of peroxides. Environ. Sci. Technol. 40, 3941–3946.
12. Behnajady, M.A., Modirshahla, N., Shokri, M., Vahid, B., 2008. Effect of operational parameters on degradation of Malachite Green by ultrasonic irradiation. Ultrason. Sonochem. 15, 1009–1014.
13. Makino, K., Mossoba, M.M., Riesz, P., 1982. Chemical effects of ultrasound on aqueous solutions. Evidence for hydroxyl and hydrogen free radicals (_OH and _H) by spin trapping. J. Am. Ceram. Soc. 104 (12), 3537–3539.
14. Suslick, K.S., 1988. Ultrasound: The Chemical, Physical and Biological Effects. VCH publishers, New York
15. Chowdhury, P., Viraraghavan, T., 2009. Sonochemical degradation of chlorinated organic compounds, phenolic compounds and organic dyes – a review. Sci. Total Environ. 407, 2474–2492.
16. Eren, Z., 2012. Ultrasound as a basic and auxiliary process for dye remediation: a review. J. Environ. Manage 104, 127–141
17. E. Gutiérrez-Segura, M. Solache-Ríos, A. Colín-Cruz, Sorption of indigo carmine by a Fe-zeolitic tuff and carbonaceous material from pyrolyzed sewage sludge, J. Hazard. Mater. 170 (2009) 1227–1235.
18. C F I Jabs, H P Drutz, R I Summit Jr, The role of intra operative cystoscopy in prolapsed and incontinence surgery, Am J Obst.Gynecol, 185 (2001) 1368-1373
19. U.R. Lakshmi, V.C. Srivastava, I.D. Mall, D.H. Lataye, Rice husk ash as an effective adsorbent: evaluation of adsorptive characteristics for Indigo Carmine dye, J.Environ. Manage. 90 (2009) 710–720.
20. N. Barka, A. Assabbane, A. Nounah, Y. Aît Ichou, Photocatalytic degradation of indigo carmine in aqueous solution by TiO2-coated non-woven fibres, J. Hazard.Mater. 152 (2008) 1054–1059.
21. A.G.S. Prado, J.D. Torres, E.A. Faria, S.C.L. Dias, Comparative adsorption studies of indigo carmine dye on chitin and chitosan, J. Colloid Interface Sci. 277 (1) (2004) 43–47
22. P.V Gayathri, Suguna Yesodharan, E.P. Yesodharan, Microwave assisted ZnO mediated photocatalysis (MW/PS/UV/ZnO) as an efficient advanced oxidation process for the removal of RhB dye pollutant from water, J Environ. Chem. Eng. 7 (2019) 103-122.
23. C. Hachem, F. Bocquillon, O. Zahraa, M. Bouchy, Decolourization of textile industry wastewater by the photocatalytic degradation process, Dyes Pigm. 49 (2) (2001) 117–125.
24. C. Fernandez-Sanchez, A. Costa-Garcia, Voltammetric studies of indigo adsorbed on pre-treated carbon paste electrodes, Electrochem. Comm. 2 (11) (2000) 776–781.
25. A.D. Eaton, L.S. Clesceri, E.W. Rice, A.E. Greenberg, Standard methods for the examination of water and wastewater, American public health association, Washington 515-516 (2005).
26. P. Kanthale, M. Ashokkumar, F. Grieser, Sonoluminescence, sonochemistry (H2O2 yield) and bubble dynamics: frequency and power effects. Ultrason. Sonochem. 15 (2008) 143–150.
27. M.A. Beckett, I. Hua, Impact of ultrasonic frequency on aqueous sonoluminescence and sonochemistry. J. Phys. Chem. A 105 (2001) 3796–3802.
28. B.Z. Li, L. Li, K.F. Lin, W. Zhang, S.G. Lu, Q.S. Luo, Removal of 1,1,1- trichloroethane from aqueous solution by a sono-activated persulfate process. Ultrason. Sonochem. 20

Volume-9 | Issue-10 | October - 2019 | PRINT ISSN No. 2249 - 555X | DOI : 10.36106/ijar

(2013) 855–863.
29. D. Sunartio, M. Ashokkumar, F. Grieser, Study of the coalescence of acoustic bubbles as a function of frequency, power, and water-soluble additives. J. Am. Chem. Soc. 129 (2007) 6031–6036.
30. W.P. Xie, Y. Qin, D.M. Liang, D. Song, D.W. He, Degradation of m-xylene solution using ultrasonic irradiation. Ultrason. Sonochem. 18 (2011) 1077–1081.
31. C. Minero, M.Lucchiari, D. Vione, V. Maurino, Fe(III)- enhanced Sonochemical degradation of methylene blue in aqueous solution, Environ. Sci. Technol. 39 (2005) 8936–8942.
32. S. Merouani, O. Hamdaoui, F. Saoudi, M. Chiha, Influence of experimental parameters on sonochemistry dosimetries: KI oxidation, Fricke reaction and H2O2 production. J. Hazard. Mater. 178 (2010) 1007–1014.
33. B. Winter, M. Faubel, R. Vácha, P. Jungwirth, Behavior of hydroxide at the water/vapor interface. Chem. Phys. Lett. 474 (2009) 241–247.
34. K.P. Vidya Lekshmi, Suguna Yesodharan, E.P Yesodharan, MnO2 efficiently remove Indigo Carmine dyes from polluted water, Heliyon 4 (2018) 1-52.
35. F. Guzman-Duque, C. Petrier, C. Pulgarin, G. Penuela, R.A. Torres-Palma, Effects of sonochemical parameters and inorganic ions during the sonochemical degradation of crystal violet in water. Ultrason. Sonochem. 18 (2011) 440–446.
36. H. Ghodbane, O. Hamdaoui, Degradation of Acid Blue 25 in aqueous media using 1700 kHz ultrasonic irradiation: ultrasound/Fe (II) and ultrasound/H2O2 combinations. Ultrason. Sonochem. 16 (2009) 593–598.
37. K.P. Jyothi, Suguna Yesodharan, E.P. Yesodharan, Ultrasound (US), Ultraviolet light (UV) and combination (US + UV) assisted semiconductor catalysed degradation of organic pollutants in water: Oscillation in the concentration of hydrogen peroxide formed in situ, Ultrason. Sonochem. 21(2014)1787-1796
38. K.P. Vidya Lekshmi, P.V. Gayathri, K.P. Jyothi, S.G Anju, Suguna Yesodharan, E.P. Yesodharan, Application of ultrasound under different conditions for the purification of water contaminated with chemical and bacterial pollutants, Gurukulam Int. J Innovations in Sci. and Tech. 1 (2016) 35-52
39. O.M. Shibin, B. Rajeev, V. Veena, E.P. Yesodharan, Suguna Yesodharan, ZnO photocatalysis using solar energy for the removal of trace anounts of ∝-methyl styrene, diquat and indigo carmine from water, J Adv. Oxid. Technol. 17(2014) 297-304
40. P.V. Gayathri, Suguna Yesodharan, E.P. Yesodharan, Investigations on classic Fenton reaction as a simple inexpensive technique for the removal of toxic chemical pollutants from water, Ind. J Appl. Res. 6 (2016)28-33
41. Veena Vijayan, Suguna Yesodharan, E.P. Yesodharan, "Significant Enhancement in the efficiency of the Fenton process by Solar, Electrolytic and Sonolytic Activation for the Mineralization of Indigo Carmine dye pollutant in water", Amer. J of Eng. Res., 08 (2019) 135-154.
42. P.V. Gayathri, Suguna Yesodharan, E.P. Yesodharan, Purification of water contaminated with traces of rhodamine B dye by MW assisted oxidant induced and ZnO catalyzed advanced oxidation process, Desalination and Water Treatment 85 (2017) 161-174
43. S.G. Anju, Suguna Yesodharan, E.P. Yesodharan, ZnO mediated sonophotocatalytic degradation of phenol in water, Chem. Eng. J. 189-190 (2012) 84-93
44. K.P. Jyothi, Suguna Yesodharan, E.P. Yesodharan, Contaminant salts as enhancers of sonocatalytic degradation of organic pollutants: Effect of concentration, reaction time and adsorption on the efficiency of enhancement and the fate of concurrently formed H2O2 , J Env. Chem. Eng. 6 (2018) 3574-3589

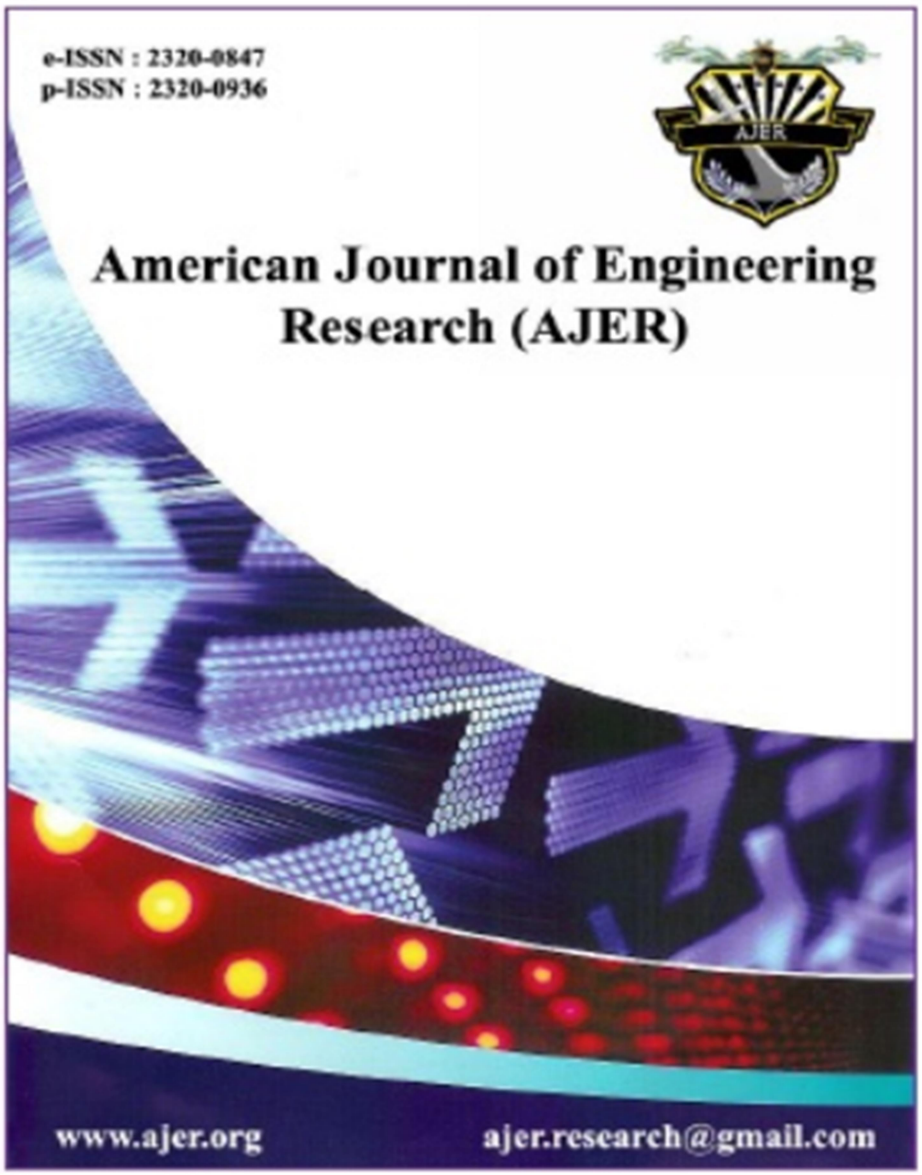
e-ISSN : 2320-0847
p-ISSN : 2320-0936
AJER
American Journal of Engineering Research (AJER)
www.ajer.org
ajer.research@gmail.com

American Journal of Engineering Research (AJER) **2019**

American Journal of Engineering Research (AJER)
e-ISSN: 2320-0847 p-ISSN : 2320-0936
Volume-8, Issue-6, pp-135-154
www.ajer.org
Research Paper Open Access

Significant Enhancement in the Efficiency of the Fenton Process by Solar, Electrolytic and Sonolytic Activation for the Mineralization of Indigo Carmine Dye Pollutant in Water

VeenaVijayan, SugunaYesodharan, E.P. Yesodharan
School of Environmental StudiesCochin University of Science and Technology, Cochin 682022, India
Corresponding Author: E.P. Yesodharan

ABSTRACT :*Advanced Oxidation Processes (AOPs) are projected as relatively cleaner technologies for environmental remediation, in particular for water pollution abatement. One of the major sources of industrial water pollution is the textile industry due to the use of large quantity of water and various toxic and hazardous chemicals at different stages of the operation. Fenton process is a simple, cheaper and convenient method for the degradation and mineralization of many recalcitrant chemical pollutants in water. In this paper, the Fenton process is investigated as a potential tool for the degradation and eventual mineralization of a textile dye, Indigo carmine(IC) in water. The efficiency of the process is accelerated by activation sources such as light, ultrasound and electrochemical energy. Relevant reaction parameters such as ratio of the components Fe^{2+} and H_2O_2 of the Fenton reagent, concentration of the reagent, pH, concentration of the dye, natural contaminants in water, kinetics, volume of the reaction system, oxidants etc. are identified and optimized. The optimized ratio of Fenton reagent is 1:3 (Fe^{2+}:H_2O_2) at the optimum pH~4.5. Periodic replenishment of the components, especially H_2O_2, is essential to achieve mineralization. Complete mineralization of the dye was observed after nine hours of treatment and was confirmed by the COD elimination. Various reaction intermediates formed during the degradation process are identified by LC/MS method. Probable mechanism of the degradation process is also proposed.*

KEYWORDS: *Advanced Oxidation Process; Fenton Reaction; Solar Fenton; ElectroFenton, Sono Fenton; Indigo Carmine*

Date of submission: 28-05-2019 Date of acceptance: 10-06-2019

I. INTRODUCTION

The textile industry consumes enormous amounts of water during dyeing and finishing operations. Typical medium-scale textile factories produce approximately 1000 m^3 of wastewater per day. It is estimated that around 30% of the applied dyes remain unfixed and are discharged in the effluent. Dye-bearing wastewaters are toxic for the environment since dyes are stable compounds and may be carcinogenic. The presence of dyes in water is also undesirable; because even a small amount of these coloring agents is highly visible, and may be toxic to the aquatic environment [1-4]. Conventional biological treatment processes are often less successful because most dyes are practically not biodegradable.

Advanced Oxidation Processes (AOPs) have been widely investigated in recent years as viable, environment-friendly and economical techniques for the removal of toxic and hazardous pollutants such as dyes, pesticides, phenols etc. and the reduction of several heavy metals from water. The techniques include photocatalysis, sonocatalysis, electrocatalysis, wet air oxidation, Fenton process, photofenton process and their combinations which are primarily based on the formation of highly reactive $^{\cdot}OH$ radicals [6 -12]. According to the reactive phase, AOPs are classified into homogeneous and heterogeneous types. Examples of homogeneous type AOPs include Fenton based processes such as classic Fenton (H_2O_2 + Fe^{2+}), Fenton like processes (Fe^{2+} + H_2O_2 + $metal^{n+}$), sono-, photo- and electro-Fenton processes based on O_3, H_2O_2, O_3-UV, H_2O_2-UV and O_3-H_2O_2-UV etc. All processes involving suspended catalysts belong to the category of heterogeneous AOPs. However these processes have gained only limited acceptance so far, as viable and effective methods for the large-scale decontamination of wastewater due to complexity of the process, cost, operational constraints etc.

.

American Journal of Engineering Research (AJER) 2019

In this contest, the simple inexpensive classic Fenton process and its variations become important [13]. The hydroxyl radicals produced insitu in the Fenton process are nonselective in degrading organic pollutants [14]. Fenton's reagent is particularly promising due to its low cost, low toxicity of the reagents (Fe(II) and H_2O_2), and the simplicity of the technology. Several studies have shown that the Fenton's process is effective for the degradation of a number of organic compounds [15-17.].In the present study, the possibility of application of Fenton process under various conditions for the removal of the toxic recalcitrant dye Indigo carmine(IC) from water is examined.

IC (5.5'–indigo disulfonic acid disodium salt) is a dark blue dye mainly used in the textile industry for the dyeing of polyester fibers and denim (blue jeans). Indigo Carmine is also used as dye in food and cosmetics industry. Several processes have been suggested for the removal of IC and other dyes from wastewater. These include adsorption, photochemical and electrochemical methods. However no systematic studies have been reported on the application of Fenton process for the removal of last traces of IC from water and make it reusable. The gap is addressed in this study. The structure of Indigo carmine is shown in figure 1.

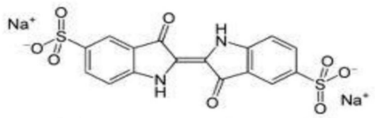

Fig.1. structure of Indigo Carmine

II. MATERIALS AND METHODS

II.1. Materials

IC (>99.6%) and ZnO (>99.5%) used in the study are from Sigma Aldrich India. H_2O_2 (30.0% w/v) and $FeSO_4.7H_2O$ (FS) from Qualigen (India) were used as such without further purification. Various other chemicals used were also of AnalaR grade or equivalent, unless indicated otherwise.

II.2. Degradation/Mineralization Experiments

In a typical experiment, the dye solution of required concentration is mixed with appropriate combinations of $FeSO_4$ (FS) and H_2O_2 in a 250 ml closed beaker. The reaction mixture is continuously stirred by using a magnetic stirrer. The reaction volume is maintained at 50 ml, unless indicated otherwise. The degradation is monitored by analyzing the IC remaining in the system by using UV-VIS spectrophotometry at 609 nm. H_2O_2 is analysed by standard iodometry. The reaction intermediates and products were identified by using Agilant 6460 Triple quad LC-MS.

In the case of solar degradation, the experiments in presence of sunlight were performed in a jacketed pyrex reactor. The dye solution (50 ml) together with the Fenton reagent and/or other additives was taken in the inner compartment and cooling water from a thermostat (29 ± 1^0C) was circulated through the outer jacket. The experiments were performed by placing the system at the roof top of our laboratory at Kochi, Kerala, India (9^0 57' 51" N, 76^0 16' 59" E) during sunny days in February-May, September-December 2017and 2018. The suspension/solution was stirred frequently to ensure uniform mixing. Samples were drawn periodically, filtered through 0.45μmfilter in the case of suspensions and analyzed for the remaining dye concentration. Solutions/suspension kept under identical conditions in the dark was used as the reference in each case to eliminate the contribution from adsorption and dark reaction, if any, towards the reduction in the dye concentration.

Sonolytic degradation of IC under different experimental conditions is investigated using ultrasound (US) of frequency in the range 200 kHz - 1 MHz and power in the range of 20-80W, as the source of energy. The degradation profile was evaluated as in the case of photolysis. Electrochemical experiments were done using bismuth oxide doped titanium dioxide (BiO_2/TiO_2) coated on titanium plate as the anode and carbonfelt cathode in presence of sodium sulfate supporting electrolyte The experiments were conducted under static anodic potential of 3.4V.

II.3. Analysis of Chemical Oxygen Demand (COD)

Open reflux method was used to determine the COD of the samples [18]. 50mL of the sample was pipetted out into a refluxing flask. $HgSO_4$ (1g) was added to this along with several glass beads. Five (5) mL of sulfuric acid reagent (5.5g Ag_2SO_4in 543mL Conc.H_2SO_4) was added slowly with mixing to dissolve $HgSO_4$. The sample was cooled while mixing to avoid the possible loss of volatile materials. $K_2Cr_2O_7$ solution (25 mL, 0.05N) was also added and mixed well. Remaining (70mL) sulfuric acid reagent was added through the open end of the condenser. The whole mixture was refluxed for two hours and cooled thereafter to room temperature. It was then diluted to 150mL and the excess $K_2Cr_2O_7$ was titrated against 0.05N Ferrous Ammonium Sulphate

(FAS) solution using ferroin as the indicator. The end point was sharp change in color from blue green to reddish brown. A blank experiment was also carried out under identical conditions using the reagents and distilled water in place of the sample.

COD is calculated using the following equation:

COD as mg O_2/L = (A-B) × M × 8000/Volume of the sample, where

A = mL FAS used for blank

B = mL FASused for sample

M = Molarity of FAS

8000 = Milliequivalent weight of oxygen × 1000mL/L

III. RESULTS AND DISCUSSIONS

III.1. Optimization of Fe^{2+}/H_2O_2 ratio

Preliminary experiments have shown that IC can be decolorized by Fenton reagent at room temperature. The degradation/decolorization is practically negligible in presence of the individual components (Fe^{2+} or H_2O_2). The efficiency of the Fenton process for the degradation of any organics depends on the relative concentration of the reagent components $FeSO_4$ (FS) and H_2O_2. Hence detailed investigations were made for optimizing the ratio of these critical components for the degradation of IC in water. The concentration of IC is kept constant at $1x10^{-4}$M. The%degradation of IC at varying ratios of FS and H_2O_2 at different times of reaction is evaluated. The results are plotted in figure 2.

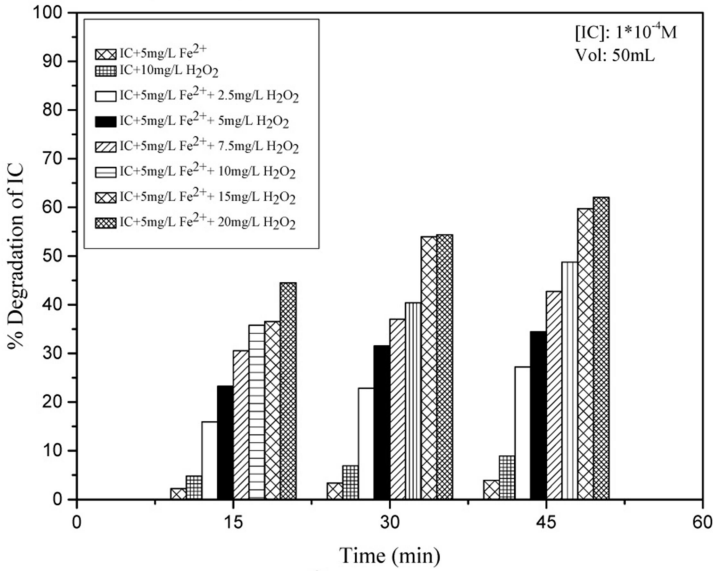

Fig.2: Optimization of Fe^{2+}/H_2O_2 ratio for the degradation of IC

As seen from the figure the optimum ratio of Fe^{2+}/H_2O_2 under the reaction condition is 5:15. Further increase in H_2O_2 dosage leads to stabilization of the degradation. The actual quantity of Fenton reagent in the ratio of Fe^{2+}/ H_2O_2= 5:15 (1:3)is further optimized as follows:

III.2. Effect of concentration of Fenton reagent on the degradation of IC

The effect of quantity of the Fenton reagent at the optimized ratio of 1:3 on the decolorization of IC is evaluated and the results are presented in figure 3. The degradation of IC increases with increase in the concentration of Fenton reagent. Eventually the degradation is stabilized (at Fe^{2+}:H_2O_2 = 10:30) probably because the concentration of the dye has become relatively less forthe effective utilization of the higher availability of FR. However, this optimized quantity depends on other reaction and reactor parameters and may vary under another set of conditions. Hence every time when the reaction conditions are changed, the optimum also needs to be reworked.

American Journal of Engineering Research (AJER) 2019

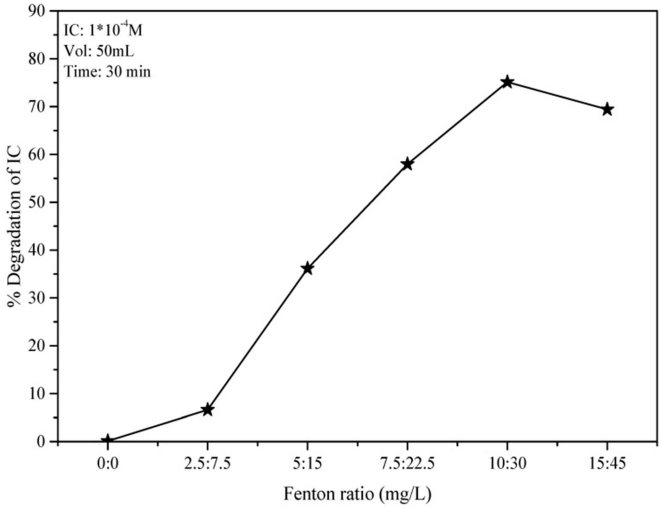

Fig.3: Effect of concentration of Fenton reagent on the rate of degradation of IC

The degradation of IC at different times, using the optimized ratio of the Fenton reagent (1:3) and the quantity [10:30mg/L (Fe^{2+}:H_2O_2)] is studied keeping the concentration of IC constant. The results are shown in figure 4. It is observed that the degradation of IC progresses steadily with time. However, the rate of increase in percentage degradation and consequently the rate of reaction decrease with time, probably because of decrease in the concentration of available IC. Eventually the degradation/decolorization reaches 100%, indicating that the intermediates formed during the degradation does not significantly retard the interaction between the Fenton reagent and IC. This shows that the Fenton process is efficient for the complete decolorization of IC in water.
The decreasing rate of decolorization with time indicates that the relative concentration of IC and FR at any point in time of reaction influences the rate of degradation. This is further verified from the effect of initial concentration of IC on its degradation, keeping other parameters constant.

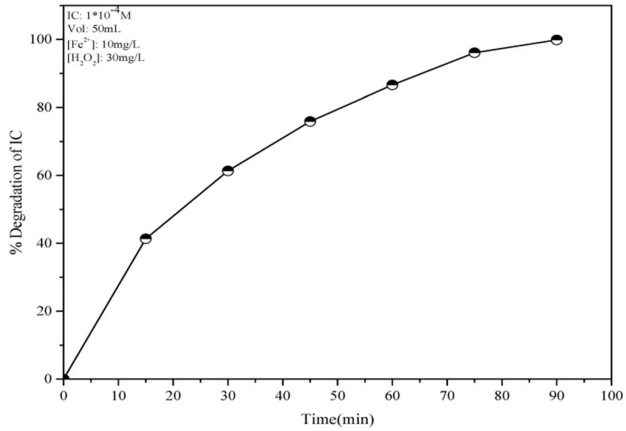

Fig.4: Effect of time on the efficiency of Fenton degradation of IC

American Journal of Engineering Research (AJER) **2019**

III.3. Effect of initial concentration of IC on the Fenton degradation

The effect of concentration of IC on the % degradation is presented in figure 5. The % degradation decreases slowly with increase in concentration of IC. .However, the rate of degradation increases steadily with increase in the concentration (Inset of Fig. 5).Beyond a particular optimum concentration ($1*10^{-4}$M), the rate of degradation slows down. This may be because the concentration of the Fenton reagent is not adequate enough to interact with the higher number of IC molecules available in the system and increase the rate of reaction. Based on these data, $1*10^{-4}$M solution of IC is chosen as the optimum for further investigations.

III.4. Effect of pH on the Fenton degradation of IC

The pH is a very important and critical parameter in the efficiency of the Fenton's process. Change in pH of the solution, results in variation in the concentration of Fe^{2+} and consequently the rate of production of $^{\bullet}OH$ radicals which are responsible for oxidation of IC [19].The influence of pH on the decolorization of IC was investigated by keeping all other parameters constant and the result is presented in figure 6.The results show that Fenton process is favored only in the acidic pH range especially upto pH~ 5. Above pH 5, the generation of $^{\bullet}OH$decreases sharply due to the formation of Fe^{3+} ions which tend to precipitate in the form $Fe(OH)_3$ as in reaction (1).

$$Fe^{3+} + 3^{-}OH \rightarrow Fe(OH)_3 \quad (1)$$

This reaction is favored at higher pH [20]. Therefore, the initial pH value has to be in the acidic range (<5) to generate the maximum amount of $^{\bullet}OH$ radicals and thus to oxidize the organic compounds.

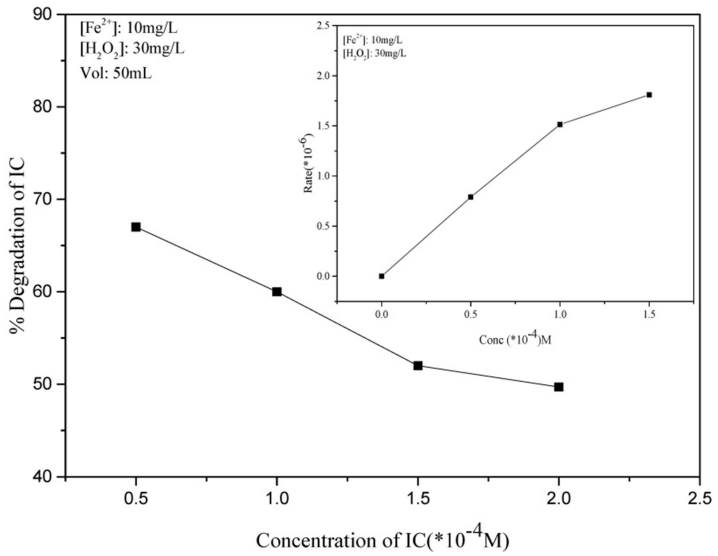

Fig.5: Effect of initial concentration of IC on its Fenton degradation [Inset: Concentration Vs Rate plot]

American Journal of Engineering Research (AJER) 2019

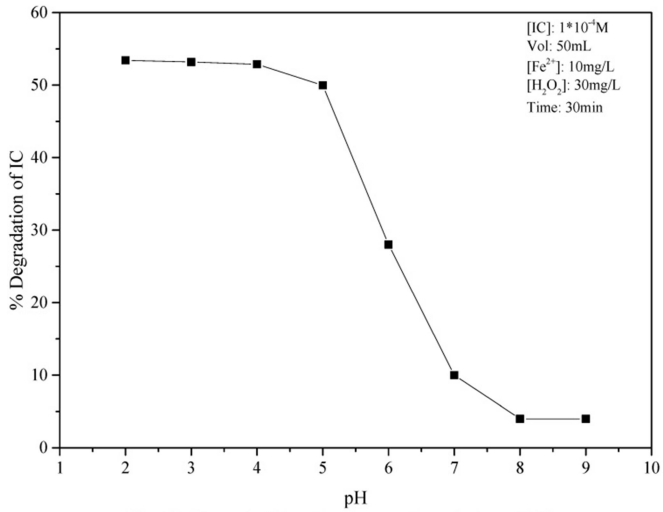

Fig.6: Effect of pH on the Fenton degradation of IC

III.5. Effect of Persulfate on the Fenton degradation of IC

Persulfates ($S_2O_8^{2-}$) are proven to be strong oxidants in AOPs due to the insitu formation of highly reactive $SO_4^{\cdot-}$radical anions. Hence the probability of enhancing the efficiency of the Fenton process by the addition of persulfate (PS) is tested at various concentrations and the results are presented in figure 7.

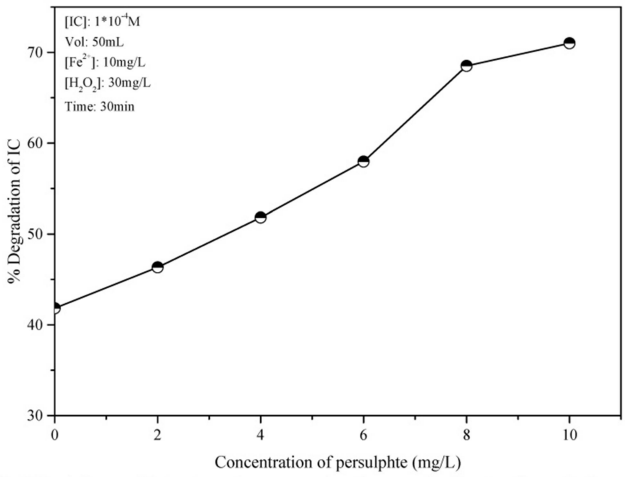

Fig.7: Effect of persulfate at various concentrations on the Fenton degradation of IC

The results show that persulfates enhance the Fenton reaction (FR)- induced degradation of IC moderately. Persulfate anion is the most powerful oxidant of the peroxygen family of compounds and one of the strongest oxidants used in environmental remediation. In addition to its direct oxidation capability, persulfates

can be induced to form highly reactive sulfate radicals, which are also powerful oxidants as the hydroxyl radicals.

$S_2O_8^{2-} + 2H^+ + 2e^- \rightarrow 2HSO_4^-$ (2)

$S_2O_8^{2-}$ + Initiator $\rightarrow 2SO_4^{\cdot-}$ (3)

Both $SO_4^{\cdot-}$ and $^{\cdot}OH$ have similar oxidation potential ($^{\cdot}OH$= 2.80, $SO_4^{\cdot-}$ = 2.60)andhence presence of persulfate is expected to enhance the Fenton degradation at least additively. However, the effect of PS on the Fenton process is not quite significant. This may be because the $SO_4^{\cdot-}$generatedinsitumay be getting deactivated by interactions as follows:

$SO_4^{\cdot-} + {}^{\cdot}OH \rightarrow$ Chain termination (4)

$SO_4^{\cdot-} + S_2O_8^{2-} \rightarrow SO_4^{2-} + S_2O_8^{\cdot-}$ (5)

$SO_4^{\cdot-} + SO_4^{\cdot-} \rightarrow S_2O_8^{2-}$ (6)

Hence it may not be economically viable to use PS in the Fenton process for the decolorization of IC, since it provides no additional advantage.

III.6. Effect of salts/anions on the Fenton degradation of IC

The presence of chemical contaminants such as salts/anions/cations is known to influence the efficiency of AOPs for the mineralization of pollutants in water. Anions are used at different stages of the dyeing process and are hence likely to be present in the effluent water from dye related operations. In this context, the effect of few common anions (Cl^-, CO_3^{2-}, HCO_3^-, PO_4^{3-}) which are likely to be present in many natural water sources on the efficiency of the decolorization of IC by the Fenton process is examined. The results are presented in figure8.

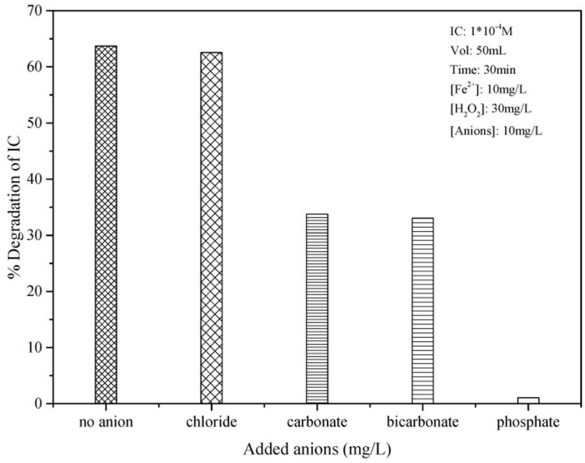

Fig 8: Effect of anions on the Fenton degradation of IC

Anions of the specified concentration are added to the reaction system individually and the Fenton degradation of IC in their presence was compared with the normal system. Results show that chloride has no effect on the degradation while carbonate and bicarbonate are good inhibitors. Phosphate is a strong inhibitor which retards the degradation of IC almost completely.

The main reason for the inhibition by anions may be the scavenging of the reactive $^{\cdot}OH$ radicals formed insitu during the Fenton reaction resulting in the formation of radical anions as follows [20-22]:

$^{\cdot}OH + HCO_3^- \rightarrow H_2O + CO_3^{\cdot-}$ (7)

$^{\cdot}OH + CO_3^{2-} \rightarrow OH^- + CO_3^{\cdot-}$ (8)

$^{\cdot}OH + SO_4^{2-} \rightarrow OH^- + SO_4^{\cdot-}$ (9)

$^{\cdot}OH + NO_3^- \rightarrow OH^- + NO_3^{\cdot-}$ (10)

$^{\cdot}OH + Cl^- \rightarrow OH^- + Cl^{\cdot}$ (11)

$Cl^{\cdot} + Cl^- \rightarrow Cl_2^{\cdot-}$ (12)

American Journal of Engineering Research (AJER) 2019

The radical anions formed in the process are also moderately active for the degradation of organics. Their concentration will be increasing steadily in the system, unlike the ˙OH radicals which decrease progressively by recombination and deactivation as in reactions (13) and (14).

$^{\cdot}OH + {}^{\cdot}OH \rightarrow H_2O_2$ (13)

$^{\cdot}OH + H_2O_2 \rightarrow H_2O + HO_2^{\cdot}$ (14)

Hence, reasonable rate of degradation will continue even in presence of the ˙OH radical-scavenging anions. The scavenging rate constants for the anions are given in table 1.

Table 1: Scavenging rate constants for the anions

Anions	Scavenging rate constants ($mol^{-1}s^{-1}$)
NO_3^-	1.4×10^8
Cl^-	4.3×10^9
CO_3^{2-}	3.9×10^8
SO_4^{2-}	1×10^{10}
$H_2PO_4^-$	2×10^4
CH_3COO^-	7.0×10^7
HCO_3^-	8.5×10^6

If the inhibition was exclusively due to scavenging of the ˙OH radicals, it should have been in the order:
$SO_4^{2-} > Cl^- > CO_3^{2-} > NO_3^- > CH_3COO^- > HCO_3^- > H_2PO_4^-$

Since this sequence is not followed, scavenging of the anions cannot be considered as the main reason for the inhibition.The very strong inhibition in presence of PO_4^{3-}in this homogeneous system is surprising even though anions are known to inhibit many heterogeneous AOPs due to the blocking of the catalytically active surface sites. In this homogeneous system with no suspended catalyst particles this possibility for inhibition is ruled out. In the case of PO_4^{3-} it is possible that the radical anion formed from phosphate is practically not active like other radical anion. It is also possible that the $Fe^{2+}$of the Fenton reagent will interact with PO_4^{3-} thereby decreasing the amount of the cationsneeded for the formation of ˙OH by the Fenton reaction.

Another reason for the anion effect in the case of Fenton reaction is the variation in pH in presence of the anions. Even mild variation in the pH, especially from the optimum of ~ 4 can affect the Fenton process strongly. The pH of the system with various anions is shown in figure9.

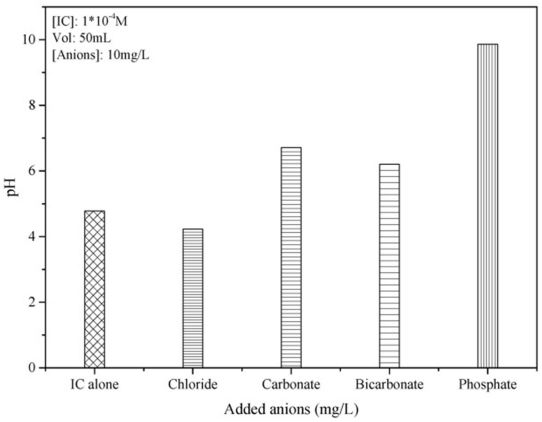

Fig.9: pH of the dye solution in presence of anions

The pH decreases moderately in presence of Cl^- which is a favorable condition for Fenton reaction. As expected in this case the anion has no effect. CO_3^{2-} and HCO_3^- increase the pH of the medium which is unfavorable for the Fenton degradation. Hence the inhibition can be attributed to this. By the same yardstick, the inhibition by PO_4^{3-} also can be explained because the pH~9 in presence of PO_4^{3-} is totally unfavorable for the degradation as seen in figure6.

American Journal of Engineering Research (AJER) 2019

III.7. Effect of ZnO on the Fenton degradation of IC

Earlier studies have shown that ZnO and TiO_2 mediated photo, sono and microwave (MW) activated AOPis efficient for the degradation and mineralization of a variety of pollutants[23-25]. Of these two widely investigated semiconductor oxides, ZnO has been proven to be more active for solar energy harvesting due to its better absorption characteristics in the visible range of solar spectrum. In this context, experiments were done to verify whether ZnO can be used beneficially in the Fenton process, either under ambient condition or in presence of powerful activation sources such as sunlight, UV-Vis light or ultrasound. The results are presented in figure 10.

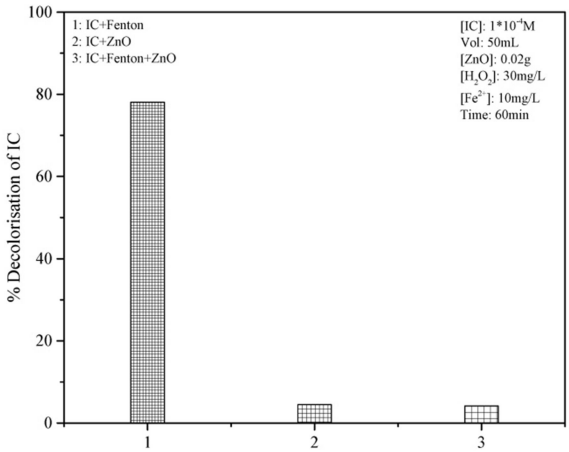

Fig.10: Effect of ZnO on the Fenton degradation of IC

In this heterogeneous system, in the absence of any light irradiation, ZnO inhibits the Fenton degradation of IC almost completely.

The adsorption of H_2O_2 on ZnO and consequent decrease in the concentration of the former as the cause of the inhibition is ruled out since the adsorption has been experimentally observed to be negligible. Hence, the suspended ZnO particles may be inhibiting effective interaction between Fe^{2+} and H_2O_2 thereby reducing the rate of formation of reactive $^{\cdot}OH$ radicals. The substrate also may get shielded from interaction with the reactive free radicals by the ZnO particles which also may lead to the inhibition. Presence of ZnO also increases the pH of the medium which is another unfavorable factor for the Fenton reaction as stated earlier. The pH of the standard IC-FR system increases from 4.5 to 7.5 in presence of ZnO (figure 11). The effect of pH (Fig. 6) clearly illustrates that the degradation is severely inhibited at pH 7. However, when the pH of the suspension with ZnO is modified to acidic condition of normal Fenton system, i.e. 4.5, the degradation of IC proceeds faster, though the rate is less compared to that of normal Fenton (without ZnO). The result is shown in figure 11 inset. Hence at least one of the main causes for the inhibition by ZnO is its effect on the pH.

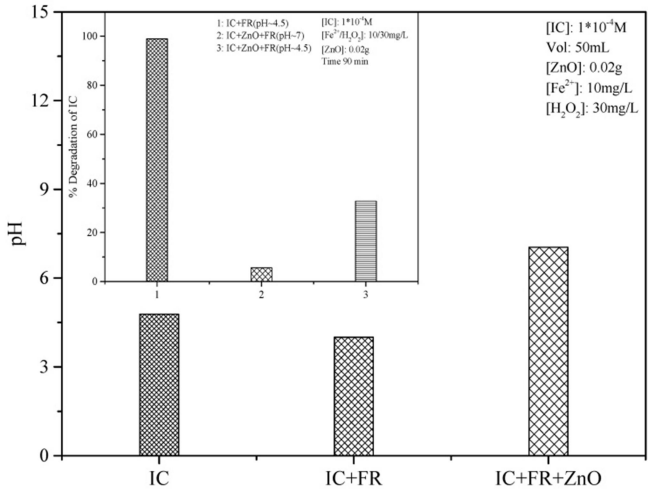

Fig.11: pH of the solution with and without ZnO
[Inset: Effect of ZnO on the Fenton degradation of IC with and without adjusting the pH]

The effect of variation in ZnO dosage on the efficiency of the normal Fenton system is experimentally verified and the results are plotted in figure 12. The degradation of IC decreases with increase in the amount of ZnO and is almost completely inhibited above 0.010g. The effect of varying amounts of ZnO on the pH of the system is shown in the inset of the figure. The data clearly shows that increase in the pH of the system is one of the major causes of the inhibition in presence of ZnO.

The inhibiting effect of ZnO is further verified by adding ZnO in between to the Fenton degradation in progress and observing the effect. It is observed that the degradation which was proceeding smoothly, stopped instantly and stabilized. No further degradation was observed even after long time. The result is shown in figure 13.

III.8. Effect of volume of the reactor

Since Fenton reaction is a relatively simple facile process which proceeds smoothly as long as there is sufficient concentration of the reagents and the substrate, the effect of volume of the reaction system on the rate of degradation of IC is tested under optimized reaction parameters in the same reactor. The results which are shown in figure 14 confirm the expected outcome, i.e. the rate of degradation is maintained as long as the ingredients are available in required quantities. The initial increase in degradation with increase in volume from 25 to 50mL shows that there is an optimum volume at which the Fenton process is more efficient compared to very low volume.This also indicates that the volume of the reaction system is not a constraint for the scaling up of the process at industrial level.

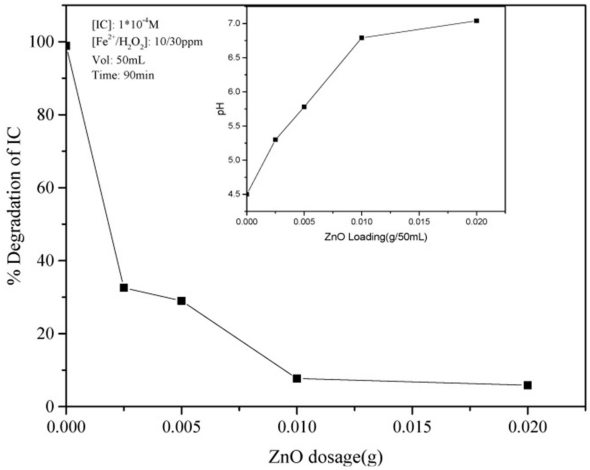

Fig.12: Effect of increasing dosage of ZnO on the Fenton degradation of IC

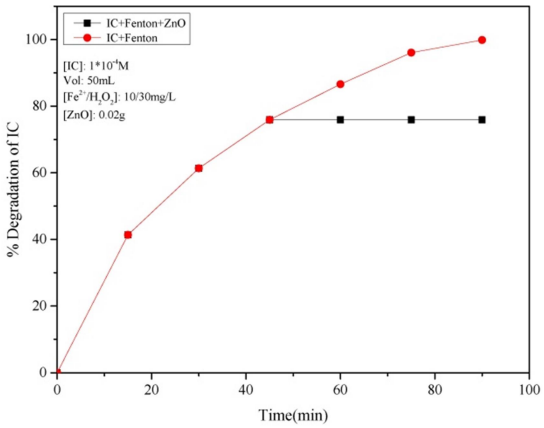

Fig 13: Effect of in between addition of ZnO on the Fenton degradation of IC

American Journal of Engineering Research (AJER) 2019

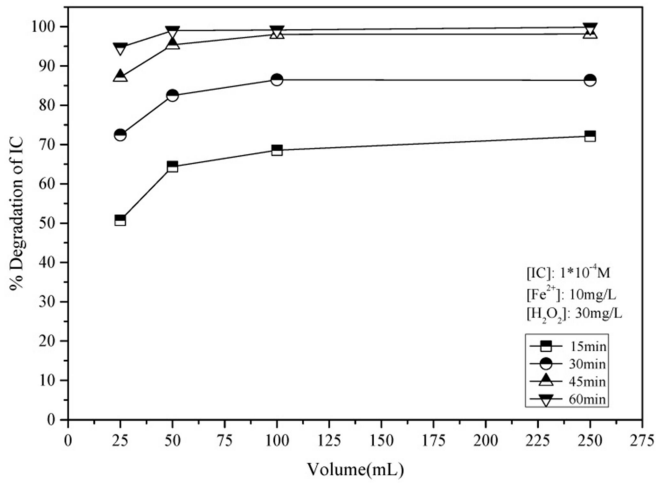

Fig.14: Effect of volume on the Fenton degradation of IC

III.9. Mineralization of IC during Fenton degradation

The efficiency of any water purification technique depends ultimately on its ability for mineralizing the chemical pollutant and bringing down the Chemical Oxygen Demand (COD)/total organic carbon (TOC) to 'nil' or acceptable level. In this context, the COD of the IC/Fenton reaction system is measured at different times of reaction and the results are plotted in figure 15.

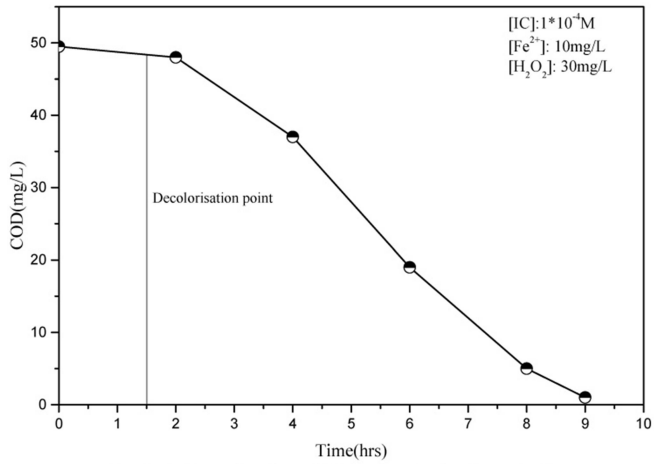

Fig 15: Mineralization of IC during Fenton degradation

As seen in the figure, the COD remains fairly steady till decolorization of IC and decreases steeply thereafter indicating that at least some of the intermediates formed during the decolorization are not stable and get mineralized fast. Continuation of the Fenton reaction results in complete mineralization. Hence it may be confirmed that Fenton process is an efficient inexpensive method for the complete removal of IC pollutant from water. Various intermediates present in the system at 50% degradation are analyzed by LC/MS and the results

American Journal of Engineering Research (AJER) 2019

are shown in table 2. Eventually these intermediates also get degraded as seen from the complete elimination of COD in 9 hr. of Fenton reaction.

III.10. Activation of Fenton process by external energy sources

The efficiency of Fenton process has been reported to be enhanced by activation using external energy sources[26]. In this context, the application of three sources of energy, i.e., light (photofenton), ultrasound (sonofenton), and electrolysis (electrofenton) on the efficiency of the Fenton process for the degradation of IC is tested and the results are as follows:

III.10.1.Solar Photofenton process

The time taken for complete decolorization of IC in presence of Fenton reagent is reduced from 90 min. to 15min. under solar irradiation. Presence of ZnO in classic Fenton has been proven to decrease the efficiency of the process, primarily due to change in pH (see Section III.7). However, being a good solar photocatalyst, ZnO is likely to enhance the efficiency of Fenton process under sunlight. This possibility is tested under solar Fenton and the results of decolorization of IC are compared with and without ZnO under different conditions (figure 16).The efficiency of decolorization is in the order:

Solar Fenton > Solar photocatalytic Fenton in presence of ZnO (pH adjusted to the regular Fenton pH) > Fenton >ZnO Photocatalysis>photocatalytic Fenton in presence of ZnO (no pH adjustment).

The results clearly demonstrate the superiority of the solar Fenton process for the degradation of IC. The presence of ZnO is unable to accelerate the degradation and overtake the efficiency of the simple photofenton process. This is probably because the extra OH radicals generated by the photocatalytic action of ZnO is not enough to compensate for the ZnO-inhibition in the generation of OH radicals by the interaction of $Fe^{2+}$and H_2O_2. Hence it may be presumed that Solar Fenton process is highly efficient for the decontamination of water from traces of IC pollutants.

III.10.2. Sonofenton Process

The effect of ultrasound (US) with frequency 350 KHz and power 80W as a source of activation on the Fenton degradation of IC is investigated.Experiments were carried out under the conditions optimized for normal Fenton. The results are shown in figure 17.

The time taken for complete decolorization of IC under sonofenton(30 min.) is much less compared to sono only (75 min.) or Fenton only (90 min.). The results also show that the combined process (sonofenton) is synergistic and is worth investigating in depth.

Table 2: Intermediates formed during the Fenton degradation of IC

m/z	Molecular structure
422	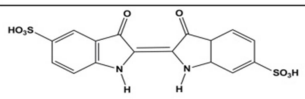
216	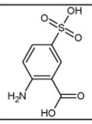
202	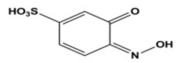
226	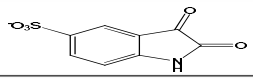
243	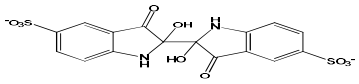

American Journal of Engineering Research (AJER) 2019

423	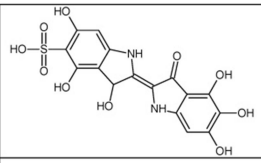
225	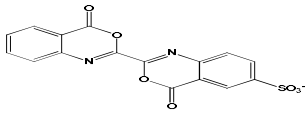
357	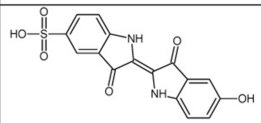
258	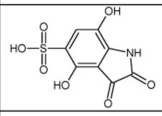
116	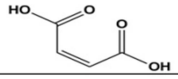

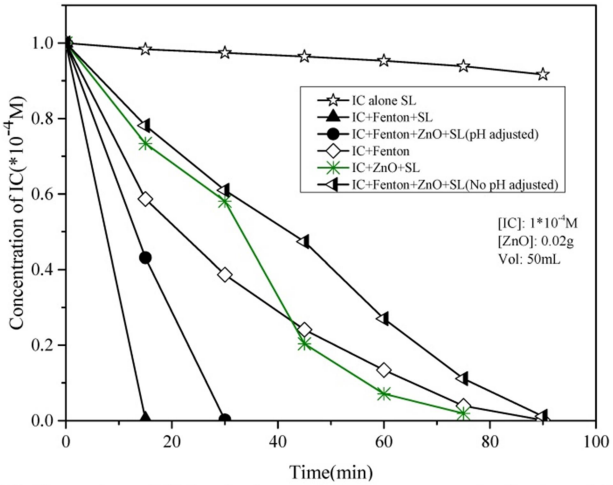

Fig 16: Comparison of different solar photoFenton processes for the degradation of IC

American Journal of Engineering Research (AJER) 2019

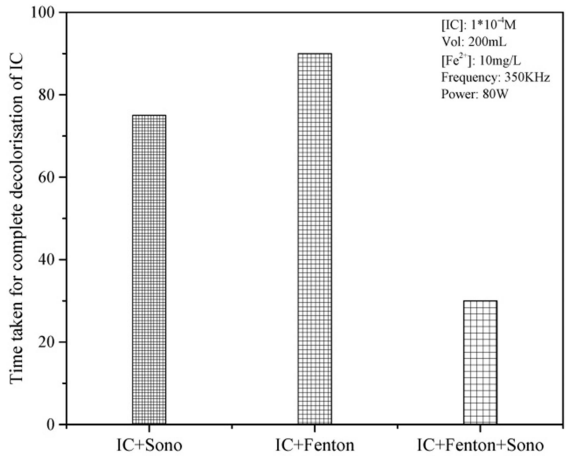

Fig.17: Comparison of Fenton and SonoFentonprocesses for the degradation of IC

Ultrasound coupled with Fenton's reagent utilizes the advantages of the two methods to generate more ·OHradicalswhich can effectively enhance the degradation of IC. Also cavitation under US gives additional activation through pyrolysis, which will enhance the degradation. In heterogeneous sono- Fenton process, acoustic cavitation can enhance mass transfer, dispersion, and deaggregation of particles. [27].The increased formation of reactive ·OH radicals under Fenton, Ultrasound irradiation and the combination process can be summarized as follows[28,29]:

$Fe^{2+} + H_2O_2 \rightarrow Fe^{3+} + HO^- + HO^{\cdot}$ (Fenton) (15)

$H_2O_2 +))) \rightarrow 2HO^{\cdot}$ (US) (16)

$H_2O_2 + HO^{\cdot} \rightarrow H_2O + HO_2^{\cdot}$ (Fenton, US) (17)

$Fe^{3+} + H_2O_2 \rightarrow Fe(OOH)^{2+} + H^+$ (Fenton) (18)

$Fe(OOH)^{2+} +))) \rightarrow Fe^{2+} + HO_2^{\cdot}$ (US) (19)

$Fe^{3+} + HO_2^{\cdot} \rightarrow Fe^{2+} + H^+ + O_2$(Fenton, US) (20)

In Fenton process, the propagation of US waves into the media results in two effects, i.e., enhanced interaction of Fe^{2+} with H_2O_2 and enhanced regeneration of Fe^{2+} in the system. This leads to more efficient generation of ·OH radicals and consequently enhanced degradation of the pollutant. This is in addition to the US-induced generation of free radicals in the gas bubble and/or in the bulk of the system as follows:

$H_2O +))) \rightarrow {}^{\cdot}H + {}^{\cdot}OH$ (21)

${}^{\cdot}H + O_2 \rightarrow HO_2^{\cdot} \rightarrow {}^{\cdot}OH + 1/2O_2$ (22)

$2\,{}^{\cdot}OH \rightarrow H_2O_2$ (23)

$2HO_2^{\cdot} \rightarrow H_2O + O_2$ (24)

Various parameters relevant for US-Fenton process such as power and frequency of the US, relative concentration of H_2O_2 and Fe^{2+}, presence of sono active catalyst, effect of cross-contaminants on the efficiency of the process etc. can be further evaluated and optimized for improving the efficiency of the process which is beyond the scope of the current study.

III.10.3. ElectroFenton (EF) Process

Earlier studies have shown that electrochemical process can be a viable AOP for the mineralization of pollutants from water [30-32]. Combination of electrochemical and Fenton process (EF) is another hybrid like photo-Fenton process worth investigating for enhanced efficiency of the Fenton process. Appropriately designed EF process has the advantage of insitu generation of H_2O_2 and Fe^{2+} and can thus avoid the drawbacks of the chemical Fenton process. In the electrochemically assisted Fenton process also, the •OH is produced via the usual Fenton's reaction. However in this case, Fenton's reagent is electrochemically generated in situ, thus avoiding the use of high quantities of H_2O_2 and iron (II) salt. It was developed and extensively applied over the last two decades [33,34].

American Journal of Engineering Research (AJER) 2019

In the present study, the electrolytic degradation of IC is combined with the classic Fenton process. Bismuth doped titanium dioxide on titanium anode and carbonfelt cathode in presence of sodium sulfate supporting electrolyte which has been proven to be an efficient electrochemical system for the degradationof IC is chosen for the study. Fe^{2+} is added to the system and together with the insitu formed H_2O_2 a Fenton like system is evolved. The degradation of the dye is faster in the case of electroFenton compared with that of the normal electrolytic or Fenton reaction. The results are shown in figure 18. As in the case of sono-Fenton and photo-Fenton, electro-Fenton process also is synergistic.

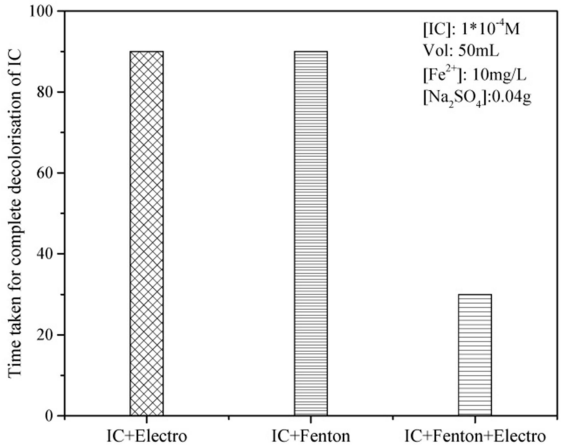

Fig.18: Comparison of Fenton and electro-Fenton process for the degradation of IC

In the electro-Fenton process, pollutants are destroyed by the action of Fenton reagent in the bulk as well as the anodic oxidation at the anode surface. Hence the insitu H_2O_2 production is slower because O_2 solubility in water is low and the current efficiency also is low at lower pH of the Fenton reagent. One way to sustain the efficiency of electro-Fenton process is to continuously add H_2O_2 and Fe^{2+}. However the efficiency of Fe^{2+} regeneration from Fe^{3+} is slow even at optimal current density. Consequently, the rate of degradation will slow down with time. The efficiency of the electro-Fenton process depends on the nature of the electrodes, pH, catalyst concentration, electrolyte, dissolved O_2 level, temperature, current density etc. Detailed investigation on these factors will be important in identifying the optimum conditions. However this is beyond the scope of the current study and is not undertaken here.

III.10.4. Comparison of different hybrid Fenton processes for the decolorization of IC

Comparison of various types of Fenton processes for the decolorization of IC is shown in figure 19.The combination process is more efficient and synergic compared to simple Fenton process with the efficiency being in the order;

Photofenton>Electrofenton ≈ Sonofenton ≈Photocatalytic (ZnO) fenton (pH adjusted) >Photocatalytic (ZnO) fenton (no pH adjustment) > Fenton

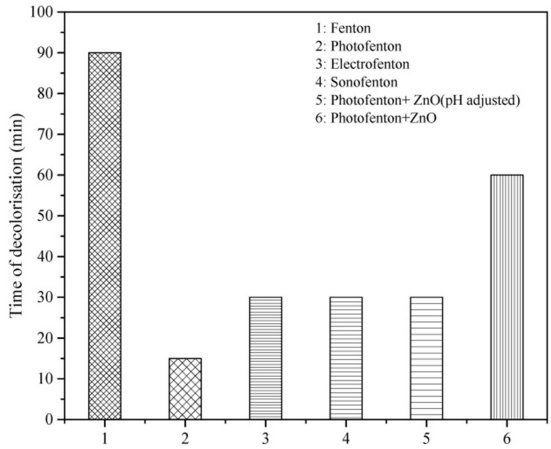

Fig.19: Comparison of different combinations of Fenton process for the decolorisation of IC

Comparative rate and synergy of the combination process over respective individual processes are computed and tabulated in Table 3.

Table 3: Comparative rate of degradation of IC under Fenton and combination Fenton process

Process	Initial rate of degradation (x10-7 mg/L/min)	Synergy
Fenton	13.7	-
Photolysis	8.7	-
Solar PhotoFenton	33.0	1.47
Sono	2.3	-
SonoFenton	19.0	1.19
Electro	8.3	-
ElectroFenton	23.0	1.06

However, the synergy decreases with time of reaction, possibly because of the formation of intermediates which also compete with the substrate for the reactive free radicals.The results in Fig.19 reveal that solar photo-Fenton is the most efficient process (among those tested here) for the decolorization of IC. Photocatalytic Fenton with ZnO as the catalyst (after adjusting the pH to that of classic Fenton) is only as efficient as electro and sono-Fenton. Presence of ZnO increases the pH of the system which is detrimental to the efficiency of Fenton process as has been discussed earlier. Hence adjustment of the pH to the optimum pH of normal Fenton is important in any combination Fenton process. In any case, presence of a solar photocatalyst such as ZnO may be beneficial for the efficiency of the solar process, which is verified by testing the role of solar photocatalysis in the mineralization of IC (which is verified by COD reduction).

III.10.5. Comparison of the COD reduction using different combinations of Fenton reaction

The efficiency of various Fenton processes for the total mineralization of IC is verified experimentally by reduction in chemical oxygen demand (COD) of the system under respective processes and the results are presented in figure 20.

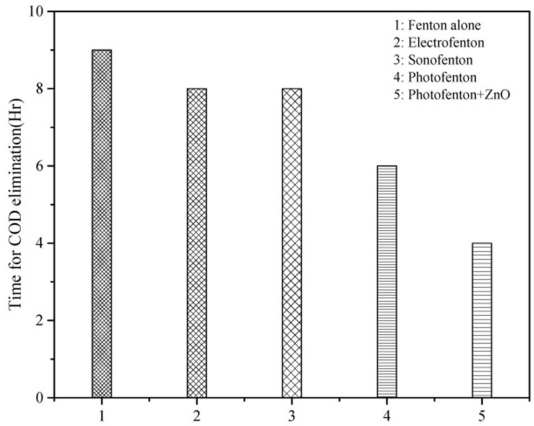

Fig.20: Comparison of the COD reduction using different combinations of Fenton process

Solar photocatalyticfenton with ZnO catalyst is identified as the most efficient process for COD reduction. The comparative efficiency is in the order;
ZnO-solar photocatalyticfenton>Photofenton>Sonofenton ≈ Electrofenton> Fenton.

III.11. General Mechanism

The first step in the Fenton reaction is the oxidation of ferrous to ferric ions and decomposition of H_2O_2 into $^{\cdot}OH$ radicals as follows:

$Fe^{2+} + H_2O_2 \rightarrow Fe^{3+} + OH^- + {}^{\cdot}OH$ (25)

The Fe^{3+} is reduced by excess H_2O_2 to regenerate Fe^{2+} and more free radicals as in reaction (26)

$Fe^{3+} + H_2O_2 \rightarrow Fe^{2+} + HO_2^{\cdot} + H^+$ (26)

Other possible reactions are:

$Fe^{2+} + {}^{\cdot}OH \rightarrow Fe^{3+} + OH^-$ (27)

$Fe^{2+} + HO_2^{\cdot} \rightarrow Fe^{3+} + HO_2^-$ (28)

$Fe^{3+} + HO_2^{\cdot} \rightarrow Fe^{2+} + O_2 + H^+$ (29)

The highly reactive free radicals may get deactivated by self-scavenging, interaction with other radicals and/or H_2O_2

${}^{\cdot}OH + {}^{\cdot}OH \rightarrow H_2O_2$ (30)

${}^{\cdot}OH + H_2O_2 \rightarrow HO_2^{\cdot} + H_2O$ (31)

$HO_2^{\cdot} + HO_2^{\cdot} \rightarrow H_2O_2 + O_2$ (32)

${}^{\cdot}OH + HO_2^{\cdot} \rightarrow H_2O + O_2$ (33)

In the absence of any organic substrate to be oxidized, H_2O_2 self-decomposes as in reaction (34).

$2H_2O_2 \rightarrow 2H_2O + O_2$ (34)

In presence of organic molecules (R), such as IC in the current instance, the degradation can take place as in reactions (36) – (37) or dimerization occurs as in (38). Eventually mineralization takes place as in (39).

${}^{\cdot}OH + R \rightarrow H_2O + R^{\cdot} \rightarrow$ (Partial mineralization + Colorless intermediates) (35)

$R^{\cdot} + Fe^{2+} \rightarrow R^- + Fe^{3+}$ (36)

$R^{\cdot} + Fe^{3+} \rightarrow R^+ + Fe^{2+}$ (37)

$R^{\cdot} + R^{\cdot} \rightarrow RR$ (38)

$R^{\cdot}$ or R^- or R^+ or RR + ${}^{\cdot}OH$, $HO_2^{\cdot}$, H_2O_2 etc.

→ intermediates→ → →CO_2 +H_2O + salts (mineralization) (39)

Thus at room temperature and pressure itself, a series of reactive free radicals are generated and these can interact with the dye in a variety of ways to produce intermediates and eventually mineralize the pollutant. The decolorization/mineralization is accelerated by external energy sources such as UV light, sunlight, ultrasound, microwave, electrolysis etc. Relevant mechanisms are discussed in respective sections in this paper.

IV. CONCLUSION

Classic Fenton reaction involving use of simple Fe^{2+} salt and H_2O_2 at the optimized ratio under ambient conditions is revisited and used as an effective advanced oxidation technique for the removal of traces of the toxic dye pollutant Indigo Carmine from water. pH is a critical parameter in the process. Many naturally occurring contaminant salts in water adversely affect the mineralization of the dye. The volume of the reactants is not a constraint as long as the necessary ingredients are available in the required ratio. These factors together with the relative simplicity of the process make Fenton reaction a promising candidate for economic and efficient waste water treatment. ZnO which is an efficient photocatalyst in many AOPs inhibit the Fenton degradation in the presence as well as absence of light, probably due to change in pH and the presence of suspended particles which inhibit the interaction between Fe^{2+} and H_2O_2 and thereby the formation of $^{\cdot}OH$. The degradation is enhanced synergistically by external sources of activation such as sunlight, ultrasound and electrochemical energy.Photocatalytic-Fenton process withZnO as the catalyst is more efficient than other processes including photo-Fenton for the mineralization of the dye pollutant. Various intermediates formed during the degradation are identified by LC/MS.

ACKNOWLEDGEMENT

Financial support from the Cochin University of Science and Technology, Cochin, India to one of the authors (VV) by way of BSR Senior Research Fellowship is gratefully acknowledged.

REFERENCES

[1]. Crini, G., Non-Conventional Low-Cost Adsorbents for Dye Removal A Review. Bioresources Technology, 97, 1061–1085 (2006)
[2]. Orfao, J.J.M., Silva, A.I.M., Pereira, J.C.V., Barata, S.A., Fonseca, I.M., FariaP.C.C.,Pereira, M.F.R. (2006). Adsorption of a Reactive Dye on Chemically Modified Activated Carbons—Influence of pH,.J Coll. and Interface Sci., 296, 480–489 (2006).
[3]. Hartono, S.B., Ismadji, S., Sudaryanto, Y., Irawaty W.,Utilization of teak sawdust from timber industry as precursor of activated carbon preparation for removal of dyes from synthetic effluent. J. Ind. Eng. Chem. 11, 864–869 (2005).
[4]. Jumasiah, A., Chuah, T.G., Gimbon, J., Choong, T.S.Y., Azni, I. Adsorption of Basic Dye onto Palm Kernel Shell Activated Carbon: Sorption Equilibrium and Kinetics Studies.,Desalination 186, 57–64 (2005).
[5]. Urses, A. G., Do˘gar, C., Karaca, S., Ac¸ikyildiz, M. Bayrak R. J. (2006). J. Hazard.Mater. 131, 254–259 (2006).
[6]. Hoffmann, M. R., Martin, S. T., Choi, W. Bahnemann, D.W., Environmental applications of semiconductor photocatalysis, Chem. Rev. 95, 69-96 (1995).
[7]. Andreozzi, A., Caprio, V., Insola, A. Marotta, R., Advanced oxidation processes for water purification and recovery, Catal. Today, 53, 51-59 (1999)
[8]. Gaya, U.I., Abdullah, A.H., Heterogeneous photocatalytic degradation of organic contaminants over titanium dioxide: A review of fundamental, progress and problems, J. Photochem. Photobiol. C: Photochem. Rev., 9, 1-12 (2008).
[9]. Devipriya, S, Yesodharan.S.,Photocatalytic degradation of pesticide contaminants in water, Solar Energy Materials and Solar Cells, 86, 309-348 (2005).
[10]. Ollis, D., Pichat, P., Serpone N., TiO_2 photocatalysis – 25 years, Applied Catalysis B: Environmental, 99, 377-387 (2010).
[11]. Rauf, M.A., Ashraf S.S. (2009). Fundamental principles and application of heterogeneous photocatalytic degradation of dyes in solution, Chem. Eng. J. 151, 10-18 (2009).
[12]. He, J., Yang, X., Men, B., Wang D., Interfacial mechanisms of heterogeneous Fenton reactions catalyzed by iron-based materials, J Env. Sci. 39, 97-109. (2016)
[13]. Costa, R.C.C., Moura, F.C.C., Ardisson, J.D., Fabris, J.D., Lago, R.M.. Highly active heterogeneous Fenton-like systems based on FeO/Fe_3O_4 composites prepared by controlled reduction of iron oxides, Appl. Catal. B: Environ, 83, 131-139 (2014).
[14]. Clarke, N., Knowles, G. (1982). High purity water using H_2O_2 and UV radiation.Effluent and Water Treatment Journal, 23, 335-341 (1982).
[15]. Chen, R., Pignatello, J.J., Role of quinone intermediates as electron shuttles in Fenton and photo assisted Fenton oxidations of organic compounds. Environ. Sci. Technol. 31, 2399–2406 (1997).
[16]. Kang, N., Lee, D.S., Yoon, J.,Kinetic modeling of Fenton oxidation of phenol and monochlorophenols. Chemosphere 47, 915–924 (2002).
[17]. Sun, J.H., Sun, S.P., Wang, G.L., L.P. Qiao., Degradation of azo dye Amido black 10B in aqueous solution by Fenton oxidation process. Dyes and Pigments 74, 647–652 (2007).
[18]. Eaton, A.D., Clesceri, L.S., Rice, E.W., Greenberg, A.E., Standard methods for the examination of water and waste water, American public health association, Washington 515-516 (2005).
[19]. Neamtu, M., Yediler, A., Siminiceanu, I., Kettrup, A., J. Photochem, Photobiol. A Chem. 157, 111–116 (2003)
[20]. Gayathri P. V.,SugunaYesodharan, Yesodharan, E. P., Purification of water contaminated with traces of Rhodamine B dye by nicrowave-assisted, oxidant induced and ZnO catalyzed advanced oxidation process, Desalination and Water Treatment 85, 161-174 (2017)
[21]. Jyothi K P.,SugunaYesodharan, Yesodharan, E P., Contaminant salts as enhancers of sonocatalytic degradation of organic water pollutants: Effect of concentration, reaction time and adsorption on the efficiency enhancement and the fate of concurrently formed H2O2, J Env. Chem. Eng. 6, 3574-3589 (2018)
[22]. Guillard, C., Puzenat, E., Lachheb, H., Houas, A., Herrmann, J.M., Why inorganic salts decrease the photocatalytic efficiency?, Int. J Photoenergy, 7 1-9 (2005)
[23]. Shibin, O.M., Rajeev, B., Veena, V., Yesodharan, E.P., SugunaYesodharan, Zinc oxide photocatalysis using solar energy for the removal of trace amounts of Alfa-methyl styrene Diquat and Indigo Carmine from water, J Adv. Oxid. Technol. 17, 297-304 (2014)
[24]. VidyaLekshmi, K.P., SugunaYesodharan, Yesodharan, E.P., MnO_2 and MnO_2/TiO_2 mediated persulfate enhanced photocatalysis for the removal of Indigo Carmine dye pollutant from water, Eur. Chem. Bull. 6, 177-191 (2017)
[25]. Gayathri, P.V., Yesodharan, E P., SugunaYesodharan., Investigations on classic Fenton reaction as a simple inexpensive technique for the removal of toxic chemical pollutants from water, Ind. J Applied Res. 6, 28-33 (2016)

[26]. Babuponnusami, A., Muthukumar, K., A review on Fenton and improvements to the Fenton process for wastewater treatment, J Env. Chem. Eng. 2, 557-572 (2014)

[27]. Ghiselli, G., Jardim, W.F., Litter, M.L., Mansilla, H.D., J. Photochem, Photobiol. A Chem. 167, 59–67 (2004).

[28]. Bremner, D.H., Molina, R., Martinez, F., Melero, J.A., Segura, Y., Degradation of penolic aqueous solutions by high frequency sono-fenton systems (US-Fe_2O_3/SBA-15-H_2O_2), Appl. Catal. B: Environ. 90, 380-388 (2009).

[29]. Namkung, K.C., Burgess, A.E., Bremner, D.H., Staines, H., Advanced fenton processing of aqueous phenol solutions: a continuous system study including sonication effects, Ultrason. Sonochem.15, 171-176 (2008).

[30]. Pulgarin, P.,Kiwi, J., Overview of photocatalytic and electrocatalytic pretreatment of industrial nonbiodegradable pollutants and pesticides, Chimia 50 (50-55) (1996)

[31]. Kurt, U., Apaydin, O., Gonuliu, M. T., Reduction of COD in wastewater from an organized tannery indudtrial region by electrofenton process, J Hazard. Mater. 143 (23-40) (2007)

[32]. Ting, W.P.,Lu, M.C.,Huang, Y.H., The reactor design and comparison of Fenton, electro-fenton and photo electro-fenton processes for mineralization of benzene sulfonic acid, J Hazard. Mater. 156, 421-427 (2008)

[33]. Brillas, E., Sirés, I., Oturan, M.A., Electro-Fenton process and related electrochemical technologies based on Fenton's reaction chemistry, Chem Rev. 109, 6570–6631 (2009).

[34]. Huang, Y.H., Chen, C.C.,Huang, G.H.,Chou, S.S., Comparison of a novel electro-Fenton method with fenton reagent in treating highly contaminated wastewater, Water Sci. Technol. 43, 17-24 (2001)

E.P. Yesodharan" Significant Enhancement in the Efficiency of the Fenton Process by Solar, Electrolytic and Sonolytic Activation for the Mineralization of Indigo Carmine Dye Pollutant in Water"American Journal of Engineering Research (AJER), vol.8, no.06, 2019, pp.135-154


ISSN - 2249-555X
IMPACT FACTOR:3.919
A Peer Reviewed, Referred, Refereed
& Indexed International Journal
Journal DOI :10.36106/ijar
INDEX COPERNICUS IC VALUE : 74.50
Indian Journal Of Applied Research
INDIAN
JOURNAL
OF APPLIED
RESEARCH
Journal for All Subjects
www.ijar.in
VOLUME : 9 | ISSUE :11 | November 2019

Original Research Paper

Volume-9 | Issue-11 | November - 2019 | PRINT ISSN No. 2249 - 555X | DOI : 10.36106/ijar

Environmental Science

ROLE OF ELECTRODES AND ELECTROLYTES ON THE EFFICIENCY OF ELECTROLYTIC DECONTAMINATION OF WATER FROM INDIGO CARMINE DYE POLLUTANT

Veena Vijayan	School of Environmental Studies, Cochin University of Science and Technology, Kochi 682022, India.
Suguna Yesodharan	School of Environmental Studies, Cochin University of Science and Technology, Kochi 682022, India.
C. T. Aravinda Kumar	School of Environmental Sciences, Mahatma Gandhi University, Kottayam 686560, India Inter University Instrumentation Centre, Mahatma Gandhi University, Kottayam 686560, India
Usha K Aravind	School of Environmental Sciences, Mahatma Gandhi University, Kottayam 686560, India Inter University Instrumentation Centre, Mahatma Gandhi University, Kottayam 686560, India
Valsamma John Koshy	Inter University Instrumentation Centre, Mahatma Gandhi University, Kottayam 686560, India
E. P. Yesodharan*	School of Environmental Studies, Cochin University of Science and Technology, Kochi 682022, India. *Corresponding Author

ABSTRACT Electrochemical Advanced Oxidation Processes (EAOP) using 'bismuth oxide doped titanium dioxide coated on titanium plate' ($BiO_x/TiO_2/Ti$) as the anode, stainless steel plate (SS) as cathode and NaCl solution as the electrolyte ($BiO_x/TiO_2/Ti$,NaCl,SS) is found to be an efficient method for the decolorization of Indigo Carmine (IC) dye pollutant in water. However, this process does not lead to mineralization even after continued electrolysis for 10 hr. This is due to the formation of a number of stable organochlorine intermediates, as identified by LC/MS. Another system ($BiO_x/TiO_2/Ti$, Na_2SO_4, graphite) can lead to complete electrolytic mineralization and elimination of COD, even though the rate of decolorization is slower compared to ($BiO_x/TiO_2/Ti$,NaCl,SS). The effect of various reaction parameters on the efficiency of decolorization/mineralization of IC is investigated and optimized. Presence of salts/anions such as carbonate, bicarbonate, nitrate, etc. enhances the decolorization. The study illustrates that an electrolytic system which is highly efficient for the degradation of a pollutant need not necessarily be good for the mineralization. This observation is important in the design of appropriate electrolytic system for the efficient purification of wastewater so that it can be repeatedly recycled.

KEYWORDS : Electrocatalysis; Advanced oxidation process; Indigo Carmine, Water treatment

1.INTRODUCTION

Manufacture and use of synthetic dyes, especially in textiles, is a massive industry today. Around 30% of the dyes used in the textile industry does not get fixed on the target and are discharged in the respective factory effluent. Dyes are highly visible and even minor release into the water bodies may be unacceptable aesthetically as well as environmentally. Dyes can also obstruct light penetration into the water bodies, thus inhibiting the biological processes based on photosynthesis. Many of these dyes are also toxic, carcinogenic, mutagenic or teratogenic to various microbiological or animal species. Due to low biodegradability of dyes, the conventional treatment process is not very efficient for their removal from wastewater. Such techniques simply transfer the pollutants from one medium to another (water to water, water to soil and water to air) causing secondary pollution. In this context, advanced oxidation processes (AOP) are gaining importance as tertiary treatment techniques for the removal of even small concentration of chemical pollutants [1-6].

In recent years, electrochemical techniques have been gaining acceptance as powerful tools for wastewater remediation [7-9]. The advantage of this technology is its environmental compatibility because the main reactant is the electron which is not a pollutant [7]. Other advantages are related to its versatility, high energy efficiency, availability of automation, safety and mild reaction conditions. It can also be operated in combination with other techniques such as sonoelectrochemical [10], photoelectrochemical [11] processes etc.

Among the electrochemical methods, anodic oxidation is perhaps the most popular one for the treatment of wastewaters containing persistent organic pollutants (POPs). The pollutants are removed using high oxygen evolution potential anode which generates highly reactive hydroxyl radicals (·OH) insitu [12,13]. These radicals instantly interact with the pollutant leading to the degradation and eventual mineralization. The reaction involved in the formation of ·OH is:

$$M + H_2O \rightarrow M(OH) + H^+ + e^- \quad (1)$$

In presence of chloride, AOP oxidation of organic compounds proceeds through chlorinated intermediates. The organochlorine compounds (RCl) formed during the degradation of the pollutant have different genotoxic, carcinogenic and/or mutagenic effects depending on the chemical structure. Hence it is important that the chemistry of the pollutant and its possible interactions in chloride medium are verified before the electrolytic method is proposed for wastewater treatment.

Graphite, platinum, dimensional stable electrode (DSA), stainless steel (SS) and air diffusion electrode (ADE) are frequently used as cathodic materials. When graphite or ADE is used as cathode, it is often fed with air or pure oxygen to generate H_2O_2 through the electrochemical reduction of O_2. This process which can be considered as anodic oxidation is normally termed as AO-H_2O_2. Use of Na_2SO_4 as the supporting electrolyte is usually preferred because: (i) it is relatively cheap, (ii) it could be oxidized into $S_2O_8^{2-}$ which also participates in the degradation of organics and (iii) it does not produce hazardous compounds during the process in most cases. Further, the presence of Na_2SO_4 is also reported to promote degradation of organics in many AOPs. [14, 15].

Indigo Carmine (IC, 5.5'–indigo disulfonic acid disodium salt, molecular weight: 466.36) which is used as the test pollutant in this study is a dark blue dye mainly used in the textile industry for the dyeing of polyester fibers and denim (blue jeans) [16]. IC is also used in food and cosmetics industry. Several processes have been suggested for removal of IC and other dyes from wastewater including

Volume-9 | Issue-11 | November - 2019 | PRINT ISSN No. 2249 - 555X | DOI : 10.36106/ijar

adsorption, photochemical, sonochemical and microwave processes [17-19]. In the present study, another AOP, i.e., electrolytic oxidation, is investigated as a potential method for the removal of small quantities of IC from water with special reference to the characteristics of the electrodes and electrolytes. The structure of Indigo Carmine is shown in figure 1.

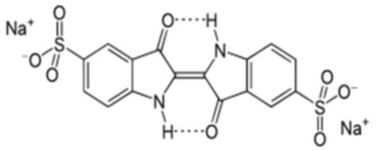

Fig. 1. Chemical structure of Indigo Carmine

2. MATERIALS AND METHODS

2.1. Materials

The Indigo Carmine dye used in the study was (99%) of AnalaR grade, from Sigma- Aldrich (India). Synthetic wastewater containing IC of desired concentrations was prepared by dissolving the dye in double distilled water. The Zinc oxide (99.9%) used was from Merck India. (BET surface area: ~12m^2/g) All other materials/chemicals used were of AnalaR grade or equivalent, unless indicated otherwise.

2.2. Electrodes used

The following electrodes used in the study were purchased from Titanium Tantalum Products limited Chennai, India:

- Ti Cathode – 50 x 25 x1 (mm)
- Nb Cathode - 50 x 25 x 1 (mm)
- MMO/Ti-50 x25x1(mm) , MMO coating of 6µ thickness, MMO: Mixed metal oxide
- Pt/Ti-50 x 25 x 1 (mm), Pt plating of 3µ thickness
- Pt/Nb-50 x 25x1 (mm), Nb plating of 3µ thickness

Further, the following electrodes were from in-house:

- Graphite rod (made by separating the electrode from a used dry cell)
- Bismuth oxide doped titanium dioxide, coated on titanium plate ($BiO_x/TiO_2/Ti$) as the anode and Stainless steel plate (SS) as cathode are the same as described in previous studies [20-22]

2.3. Electrolysis Experiments

The experimental setup is shown in figure 2. Two single compartment electrolytic cells are used in parallel. The anode and the cathode were immersed vertically in an aqueous solution of the target IC pollutant mixed with 0.05M NaCl or Na_2SO_4 as the case may be. The height of the electrodes dipped in the solution was 3.5cm with an inter-electrode distance of 4.0 cm, unless indicated otherwise. A constant cell current (3.4V) was applied to the electrodes with a DC power supply. The samples were drawn periodically during the electrolytic process, filtered if needed and were analyzed for IC remaining in the system using UV/Vis spectrophotometry at a wavelength of 609 nm. The reaction intermediates were identified by using LC-MS (Q-TOF) instrument (Waters Xevo G2 Q-TOF). Open reflux method is used to determine the COD of the samples [23].

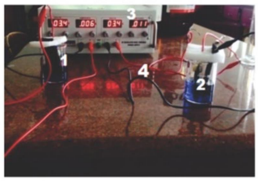

Fig 2: Electrolytic experimental set up

1, 2: Electrolytic cells, 3: Power supply unit, 4: Anode (red) and Cathode (black)

3.RESULTS AND DISCUSSION

Preliminary studies were made on the electrolytic oxidation of IC in water using different anode/cathode/electrolyte system. These include $BiO_x/TiO_2/Ti$, MMO/Ti, Pt/Ti or Pt/Nb as anode and SS, graphite, Ti or Nb as cathode. The electrolyte was NaCl or Na_2SO_4. The anodes, cathodes and electrolytes were used in different permutations and combinations. Most of the systems, except those listed in Table1 were not efficient for the decolorization/degradation of IC and were hence not investigated further.

Table1: Preliminary results on potential electrolytic systems for the degradation of IC

[IC]: 1x10^{-4}M, [Electrolyte]: 5x10^{-2}M

Anode	Cathode	Electrolyte	Preliminary electrolysis data
$BiO_x/TiO_2/Ti$	SS	NaCl	Decolorization in 10min
$BiO_x/TiO_2/Ti$	Graphite	NaCl	Decolorization in 10 min
$BiO_x/TiO_2/Ti$	Graphite	Na_2SO_4	Decolorization in 90 min
MMO/Ti	Graphite	Na_2SO_4	Decolorization in 120 min
Pt/Ti	Graphite	NaCl	Decolorization in 10 min
Pt/Ti	Graphite	Na_2SO_4	Decolorization in 90 min

Based on the data presented in Table 1, three electrode-electrolyte systems, i.e., ($BiO_x/TiO_2/Ti$, NaCl, SS), ($BiO_x/TiO_2/Ti$, NaCl, graphite) and ($BiO_x/TiO_2/Ti$, Na_2SO_4, graphite) were selected for further investigation on the electrochemical degradation of IC. The efficiency of the system is determined from the time taken for the decolorization and total mineralization of the dye. The system with Pt/Ti anode, though efficient, is not investigated further, since it is relatively more expensive.

3.1. Electrolytic degradation of Indigo Carmine using $BiO_x/TiO_2/Ti$ anode and stainless steel (SS) cathode with NaCl as supporting electrolyte ($BiO_x/TiO_2/Ti$, NaCl, SS)

The degradation/decolorization of IC is tested using 50 mL of 1x10^{-4}M solution of the dye. The supporting electrolyte (NaCl) concentration was 0.05 M. Potential applied was 3.4V. The length of the electrode dipped in the solution was 3.5 cm. Complete decolorization is obtained in 10 minutes as confirmed by UV/Vis spectrophotometry. Figure 3 shows the complete disappearance of the absorbance at 609 nm (which corresponds to IC), after 10 minutes of electrolysis.

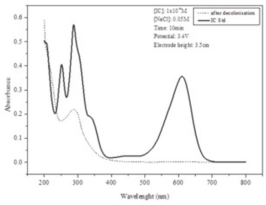

Fig 3: UV/Vis spectrum of IC: before and after decolorization [$BiO_x/TiO_2/Ti$, NaCl, SS)

The effect of various reaction parameters on the efficiency of the system is evaluated as follows:

3.1.1. Effect of pH on the degradation of IC

The effect of variation of initial pH on the time taken for decolorization of IC during electrolytic oxidation is shown in figure 4. The decolorization is faster in extreme acidic medium (pH~2-3), probably because at low pH, the chlorine resulting from the Cl$^-$ ions present in the solution forms hypochlorous acid, which has higher oxidation potential (1.63V) than hypochlorite (0.89V) [24]. Under comparable pH conditions and reaction times, the decolorization is very small and even negligible in the absence of electrolysis, as shown in the inset of the figure.

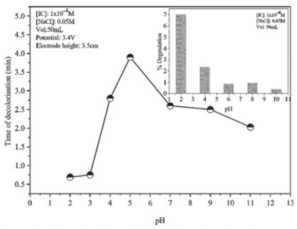

Fig 4: Effect of pH on the electrochemical degradation of IC [$BiO_x/TiO_2/Ti$, NaCl,SS]

[Inset]: % Degradation of IC at different pH without electrolysis

Volume-9 | Issue-11 | November - 2019 | PRINT ISSN No. 2249 - 555X | DOI : 10.36106/ijar

The reactions leading to the formation of HClO are;

Anode: $2Cl^- \rightarrow Cl_2 + 2e^-$ (2)

Cathode: $2H_2O + 2e^- \rightarrow H_2 + 2OH^-$ (3)

In the bulk solution, Cl_2 hydrolysis takes place as follows:-

$Cl_2 + H_2O \rightarrow HClO + H^+ + Cl^-$ (4)

Under alkaline medium, deprotonation of the HClO as well as the interaction with the OH^- ions provides hypochlorite (ClO^-) as follows:

$HClO \leftrightarrow H^+ + ClO^-$ (5)

$HClO + {}^-OH \rightarrow ClO^- + H_2O$ (6)

At the anode, O_2 evolution competes with Cl_2 evolution according to the equation,

$H_2O \rightarrow 2H^+ + ½O_2 + 2e^-$ (7)

Acidity increases the efficiency of Cl_2 discharge and the rate of dye oxidation. The type and concentration of the active chlorine species present in solution is dependent on its pH [25]. The predominant species at various pH are: Cl_2 (pH<3), HClO (pH: 3-7.5) and ClO^- (pH>7.5). If the Cl^- concentration in solution is decreased, the pH interval for the predominance of the HClO species will extend further towards lower pH. For e.g., at very low [Cl^-] of 0.005 mol L^{-1} at 25°C, the predominance of HClO occurs at pH ~1-7.5. However, extreme acidic pH may not be advisable for large scale applications and hence the natural pH of the system (~7.4) at which the degradation rate is still good is chosen for further studies. Moreover faster decolorization reactions do not guarantee the mineralization of the dye or reduction in toxicity, which is the yardstick for measuring the efficiency of the purification process.

3.1.2.Effect of Initial Concentration of IC

The influence of the initial concentration of IC on its decolorization was studied in the range of 2-60 mg/L. The time for decolorization increases with increase in concentration (figure 5). The rate of decolorization increases with increase in the concentration and is eventually stabilized or decreases thereafter (inset of figure 5). This is consistent with the variable kinetics with concentration, reported for many AOP degradation of organics [26,27]. With increase in concentration of the dye, there will be more number of interactions with the reactive free radicals and hence increase in the degradation. However at a particular concentration of the dye, the optimum number of molecules which can effectively utilize the reactive oxygen species (ROS) is

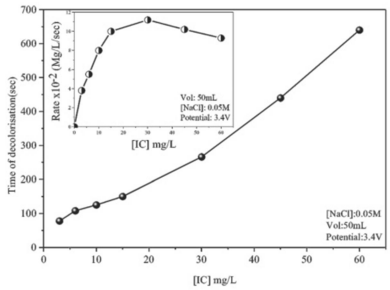

Fig 5: Effect of concentration of IC on its electrolytic degradation
[BiO_x/TiO_2/Ti, NaCl, SS] {Inset: Conc. Vs Rate plot}

reached and the rate becomes constant. Above this optimum, increase in concentration will not lead to increased interaction. It is also possible that more and more intermediates are formed in the system especially at higher concentrations of IC and they will be competing with the substrate for the ROS. This will result in gradual decrease in rate of degradation of the parent compound. Also at higher concentration, the dye molecules tend to associate into larger molecules. This lowers the rate of diffusion of the dye to the anode surface with consequent decrease in the removal rate [28].

3.1.3.Effect of electrolyte (NaCl) concentration

Figure 6 shows the effect of concentration of NaCl electrolyte on the rate of the dye removal.

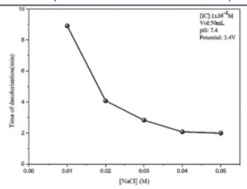

Fig 6: Effect of electrolyte (NaCl) concentration on the decolor ization of IC
[BiO_x/TiO_2/Ti, NaCl,SS]

Increased chloride concentration increases the rate of removal of the dye thereby reducing the time needed for decolorization. This enhancement can be attributed to the increased efficiency of Cl_2 discharge with increase in the concentration of NaCl. At the anode, O_2 evolution competes with Cl_2 evolution as in equation 7. As the concentration of NaCl increases, the discharge potential of Cl_2 will be less than that of O_2 and consequently the formation of the oxidant will be more and the decolorization of IC will be faster [29]. However, beyond an optimum concentration of NaCl, the potential applied being constant, the evolution of Cl_2 and O_2 as well as the formation of reactive species will be stabilized and the decolorization also levels off. At this stage, the decolorization can be enhanced probably by increasing the applied potential which is verified in the subsequent sections.

3.1.4.Effect of potential on the degradation of IC

The effect of applied potentials (1.0 – 3.4V) on the electrochemical degradation of IC is verified and the results presented in figure 7.

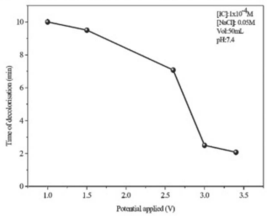

Fig 7: Effect of applied potential on the electrolytic degradation of IC
[BiO_x/TiO_2/Ti, NaCl,SS]

The efficiency increases with increase in potential, as is reflected in decrease in the time taken for complete decolorization, and reaches an optimum at potential of 3.0 V. This can be attributed to increase in the evolution of Cl_2 and consequently of HClO generation resulting in increased degradation of IC. This also implies that with increase in the area of the electrodes immersed in the electrolyte, the generation of reactive species will also be increasing leading to increasing interaction with the dye and decrease in the time taken for decolorization. This is illustrated in the following section.

3.1.5.Effect of area/length of electrode immersed in the electrolyte

As the area of electrode immersed in the electrolyte is increased (by increasing the height of the electrode dipped in the solution), the time required for decolorization of IC decreases (figure 8).

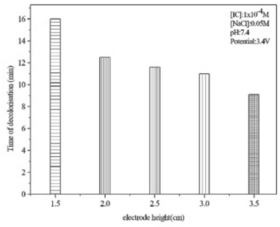

Fig 8: Effect of electrode height immersed in the electrolyte on the electrolytic degradation of IC [BiO_x/TiO_2/Ti, NaCl,SS]

Volume-9 | Issue-11 | November - 2019 | PRINT ISSN No. 2249 - 555X | DOI : 10.36106/ijar

With increase in the exposed area of the electrode more number of reactive Cl_2, HOCl, Cl^- ions are generated in the solution leading to faster decolorization of IC.

3.1.6.Effect of inter-electrode distance

Another parameter which determines the efficiency of electrolytic process is the distance between the electrodes, i.e., inter-electrode distance. In this context, the effect of inter electrode distance on the efficiency of degradation of IC is verified. The results are shown in figure 9. Color removal efficiency is enhanced by reducing the distance between cathode and anode.

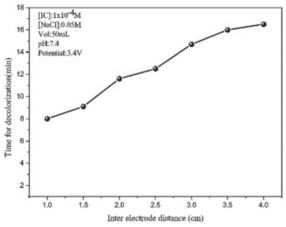

Fig 9: Effect of inter-electrode distance on the electrolytic degradation of IC
[BiO_x/TiO_2/Ti, NaCl,SS]

This can be explained based on the increase of electrical current with decreasing the inter-electrode distance and consequent increase in the frequency of collisions of the ions. Decrease of the space between anode and cathode leads to low resistance of the electrolyte which also in turn results in increased generation of reactive species and consequently increase in the reaction rate. In this study, the inter-electrode distance is optimized at 1.0 cm.

3.1.7.Effect of anions/salts

The wastewater from the dyeing process in textile industry will contain considerable amount of salts/anions naturally as well as from the chemicals used in various stages. They may also affect the efficiency of the electrolytic degradation of the dye in water. Hence, the effect of few individually added salts on the electrochemical degradation of IC is evaluated under the conditions standardized earlier. The results are plotted in figure 10.

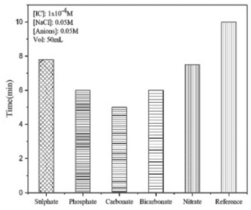

Fig. 10: Effect of anions on the electrolytic degradation of IC [BiO_2/TiO_2/Ti/SS/NaCl]

Sulfate, phosphate, carbonate, bicarbonate and nitrate anions are found to enhance the degradation. The enhancement is in the order:
Carbonate > Phosphate ≈ Bicarbonate > Nitrate ≥ Sulphate

The enhancement of AOP degradation of organic pollutants in water by anions is explained based on the efficient and sustained formation of respective radical anions which do not get deactivated by recombination as in the case of OH radicals [15, 30-33].

The anions are known to get oxidized at the anode surface followed by formation of radical anion species. Such species can continue to produce stable oxidants. Various possible reactions taking place in the case of typical anions are:

$SO_4^{2-} \rightarrow SO_4^{\cdot-} + e$ (8)
$PO_4^{3-} \rightarrow PO_4^{\cdot 2-} + e$ (9)
$CO_3^{2-} \rightarrow CO_3^{\cdot-} + e$ (10)
$NO_3^- \rightarrow NO_3^{\cdot} + e$ (11)

These radicals can combine forming stable peroxide salt oxidants as follows:

$SO_4^{\cdot-} + SO_4^{\cdot-} \rightarrow S_2O_8^{2-}$ (12)
$PO_4^{\cdot 2-} + PO_4^{\cdot 2-} \rightarrow P_2O_8^{4-}$ (13)
$CO_3^{\cdot-} + CO_3^{\cdot-} \rightarrow C_2O_6^{2-}$ (14)
$NO_3^{\cdot} + NO_3^{\cdot} \rightarrow N_2O_6$ (15)

The oxidants can also interact with the $^{\cdot}OH$ radicals present in the system forming other radicals and anions as follows:

$SO_4^{\cdot-} + {}^{\cdot}OH \rightarrow HSO_5^-$ (16)
$PO_4^{\cdot 2-} + {}^{\cdot}OH \rightarrow HPO_5^{2-}$ (17)
$CO_3^{\cdot-} + {}^{\cdot}OH \rightarrow HCO_4^-$ (18)
$Cl^- + {}^{\cdot}OH \rightarrow Cl^{\cdot} + OH^-$ (19)
$Cl^{\cdot} + Cl^- \rightarrow Cl_2^{\cdot-}$ (20)

Thus many new types of oxidants/radicals are formed which can influence the degradation of IC.
The $^{\cdot}OH$ is also formed from water electrolytically as:
$H_2O \rightarrow {}^{\cdot}OH + H^+ + e$ (21)

However, photoluminescence study [34,35] does not reveal consistent increase in the concentration of $^{\cdot}OH$, probably due to the recombination/interaction of $^{\cdot}OH$ to generate H_2O_2 or $HO_2^{\cdot}$.
${}^{\cdot}OH + {}^{\cdot}OH \rightarrow H_2O_2$ (22)
${}^{\cdot}OH + H_2O_2 \rightarrow HO_2^{\cdot} + H_2O$ (23)

It is also possible that the effect of anions may be due to the change in the pH of the solution in their presence. Hence the pH of the reaction medium in presence of the anions is measured. It is observed that the pH remains practically unaffected by the anions except in the presence of PO_4^{3-}, CO_3^{2-} and HCO_3^- where the pH varies in the range 5.5-8.5. The pH effect on the decolorization of IC in this range is the same as at the natural pH of IC solution in the absence of anions (7.4) (see inset of figure 4). Hence change in pH is not the cause of the anion effect at lease at the concentration studied here.

3.1.8.Chemical Oxygen Demand/Mineralization

The efficiency of any AOP as a decontamination tool depends on its ability to mineralize the pollutants to harmless products such as CO_2, H_2O, and salts, which is verified by the elimination of chemical oxygen demand (COD). In the current study also, the COD of the electrochemical system [BiO_x/TiO_2/Ti, NaCl,SS] is measured immediately after decolorization (10 min.) and after extended time (300 min.) of electrolysis. The COD remains unchanged even after 300 min. This suggests that electrolysis of the system leads to degradation/decolorization of IC to stable colorless compounds which cannot be degraded further. In this context, the reaction intermediates in the system after decolorization are analyzed by LC-MS. The identified intermediates are listed in table 2.

Table 2: Major intermediates formed during electrochemical degradation of IC under

Mol.weight	Molecular formula	Molecular structure
163	$C_8H_5NO_3$	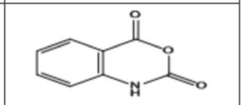
371	$C_{16}H_7N_2O_7S$	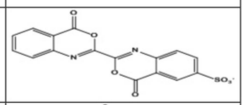
454	$C_{16}H_{10}N_2S_2O_{10}$	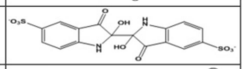
198	$C_7H_4NSO_4$	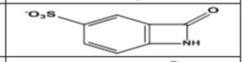
226	$C_8H_4NSO_5$	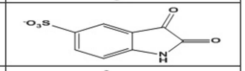
454	$C_{16}H_{10}N_2S_2O_{10}$	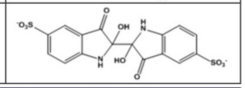

Volume-9 | Issue-11 | November - 2019 | PRINT ISSN No. 2249 - 555X | DOI : 10.36106/ijar

523	$C_{16}H_8Cl_2N_2S_2O_{10}$	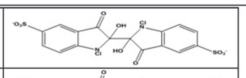
472	$C_{16}H_9N_2ClS_2O_9$	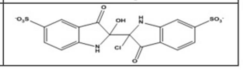

Some of the intermediates are chloro compounds which are relatively more stable and mineralize only slowly. The faster decolorization can be attributed to the transformation of IC into various chloro-compounds. However, same chloro compounds make mineralization slower. The source of chlorine is the electrolyte NaCl. Thus it is clear that the electrolysis system [BiO_x/TiO_2/Ti, NaCl,SS], which is highly efficient for the decolorization of IC, is not appropriate for its mineralization and hence for the purification of water.

The data in Table 1 shows that replacement of SS by graphite as the cathode gives same efficiency for decolorization of IC. Hence [BiO_x/TiO_2/Ti, NaCl, graphite] system is tested for mineralization efficiency. In this case also, the COD remains unchanged even after 300 min. of electrolysis thereby indicating that the system with NaCl as the electrolyte is not suitable for the mineralization of IC. In this context, another electrolyte Na_2SO_4 is used in place of NaCl and the experiments are repeated using the electrode system BiO_x/TiO_2/Ti and SS. The color of the dye remains unchanged even after 480 min. of electrolysis indicating that this system is not suitable for the degradation/decolorization of IC. When the cathode SS is replaced by graphite rod [BiO_x/TiO_2/Ti, Na_2SO_4, graphite] the decolorisation does take place and is complete in 90 minutes. Few more electrolytes other than NaCl, i.e. CO_3^{2-}, HCO_3^-, and PO_4^{3-} were also tested with the same electrode combination (BiO_x/TiO_2/Ti/ graphite). Of these, CO_3^{2-} has almost same efficiency for decolorisation (90 min.) as SO_4^{2-} while the other two electrolytes do not favor decolorization. Based on these observations, Na_2SO_4 is chosen as the convenient and safer electrolyte with BiO_x/TiO_2/Ti/graphite electrode system for further studies.

3.1.9.Studies with Na_2SO_4 as electrolyte

The efficiency of electrolytic decolorization of IC in the [BiO_x/TiO_2/Ti, Na_2SO_4, graphite] system is not affected by varying the concentration of SO_4^{2-} in the range of 0.25 to 0.60g/L, as is observed experimentally. In this case also, the degradation is more in the acidic pH with maximum in the range 2-4. Similarly, the decolorization is enhanced with increase in the area of the electrode exposed to the electrolyte and with decrease in the inter-electrode distance. Thus the optimized parameters for the decolorization of IC in the [BiO_x/TiO_2/Ti, Na_2SO_4, graphite] system are: [Na_2SO_4] = 0.05M, pH = 2-4, area of the graphite electrode dipped in the electrolyte: 7.2 cm^2, inter electrode distance: 1.0 cm.

Various intermediates formed during the electrolysis in this case (immediately after decolorization) as analyzed by LC-MS are listed in Table 3. There are no chloro-compounds and hence the mineralization is expected to be faster. The COD measurements show ~77% decrease in 5 hr. and complete mineralization in 10 hr. of electrolysis. In the case of NaCl electrolyte under identical conditions, the COD decreases by ~23% only in 10 hr. (figure 11).

The possibility of exploiting the superior decolorization efficiency of NaCl and mineralization efficiency of Na_2SO_4 by using their combination (1:1) as electrolyte is examined experimentally. The COD values at two different time periods of electrolysis, i.e. 5 and 10 hr. are determined and compared with those in electrolytic systems with different electrolyte-electrode combinations. The results are presented in Table 4. The mineralization efficiency in SO_4^{2-} electrolyte (cathode: graphite) is reduced in the presence of Cl^- and the efficiency of the combination is in between that in presence of SO_4^{2-} and Cl^- as electrolyte individually (~23% COD decrease in the case of NaCl, ~ 100% COD removal in the case of Na_2SO_4 and ~76% COD decrease in the case of NaCl+Na_2SO_4 combination in 10 hr. electrolysis). The degradation of IC and its mineralization are facilitated by insitu formed (during the electrolysis in Na_2SO_4 electrolyte) SO_4^- radical anions which are very strong oxidants (oxidation potential: 2.5-3.1V) and can facilitate the breakdown

Table 3: Intermediates formed during electrolytic degradation of IC in SO_4^{2-} electrolyte

Mol. weight	Molecular formula	Molecular structure
90	$C_2H_2O_4$	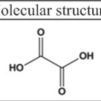
172	$C_6H_6SO_3N$	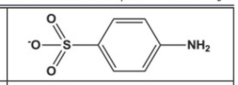
202	$C_6O_5H_4SN$	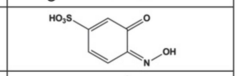
153	$C_7H_7O_3N$	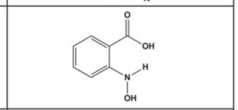
428	$C_{13}H_{12}N_2S_2O_9$	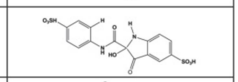
420	$C_{16}H_8N_2S_2O_8$	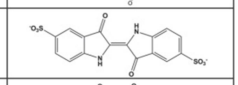
422	$C_{16}H_{10}N_2S_2O_8$	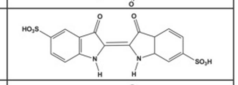
188	$C_6H_6SNO_4$	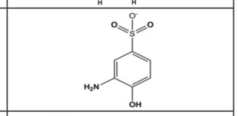
116	$C_4H_4O_4$	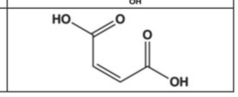

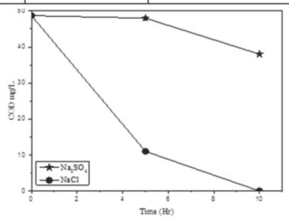

Fig.11: Comparison of NaCl and Na_2SO_4 as electrolytes for the mineralization of IC

[IC] = $1x10^{-4}$M, [Electrolyte] = $5x10^{-2}$M, Anode: BiO_x/TiO_2/Ti, Cathode: Graphite

Table 4. Mineralization efficiency of various systems in Cl^- and SO_4^{2-} electrolytes

[IC] = $1x10^{-4}$M, [NaCl] = 0.05M. [Na_2SO_4] = 0.05M, Anode: BiO_x/TiO_2/Ti

Cathode	Electrolyte	Initial COD before electrolysis (mg/L)	COD after 5 hr. electrolysis (mg/L)	COD after 10 hr. electrolysis (mg/L)
SS	NaCl	48.7	48.3	37.1
Graphite	NaCl	48.7	48.0	37.3
Graphite	Na_2SO_4	48.7	11.5	0.5 (~ 0)
Graphite	NaCl/Na_2SO_4 (1:1)	48.7	32.5	11.8

of organics by attacking the C-C bond [36]. Unlike in the case of Cl^-, the SO_4^- does not gives rise to any recalcitrant 'difficult to mineralize' intermediates such as chloro-compounds and this is favorable for the mineralization. The study clearly shows that [BiO_x/TiO_2/Ti, Na_2SO_4, graphite] is a promising electrochemical system for the decontamination of water from IC pollutant.

4.CONCLUSION

Electrochemical Advanced Oxidation Processes (EAOP) with suitably

Volume-9 | Issue-11 | November - 2019 | PRINT ISSN No. 2249 - 555X | DOI : 10.36106/ijar

designed and optimized electrode/electrolyte systems is successfully used for the decontamination of water from the dye pollutant Indigo Carmine. The method is based on the electrochemical generation of highly reactive ˙OH and other radicals in solution which interact with the pollutants and oxidize them irreversibly. Of the different combinations of electrodes and electrolytes tested, the most efficient system consists of $BiO_x/TiO_2/Ti$ anode, Graphite cathode and Na_2SO_4 electrolyte. NaCl as the electrolyte makes the system extremely efficient for the decolorization of the dye, due to the faster formation of various Cl- based oxidants. However, these oxidants transform the pollutants into more recalcitrant chloro-compounds thereby making the mineralization difficult and slower. Various intermediates formed during the process are identified by LC-MS. The effect of various reaction parameters on the efficiency of the decolorization/ mineralization process is evaluated experimentally and relevant parameters are optimized.

REFERENCES

[1]. A. Andreozzi, V. Caprio, A. Insola. R. Marotta., Advanced oxidation processes for water purification and recovery, Catal. Today, 53 (1999) 51-59

[2]. U.I. Gaya, A.H. Abdullah., Heterogeneous photocatalytic degradation of organic contaminants over titanium dioxide: A review of fundamental, progress and problems, J. Photochem. Photobiol. C: Photochem. Rev., 9 (2008) 1-12

[3] D. Ollis, P. Pichat, N. Serpone, TiO2 photocatalysis – 25 years, Applied Catalysis B: Environ, 99 (2010) 377-387

[4] Z. Frontistis, M. Antonopoulou, A. petala, D. venieri, I Konstantinou, D.I. Kondarides,D. Mentzavinos, Photodegradation of ethyl paraben using simulated solar radiation and Ag3PO4 photocatalyst, J Hazard. Mater., 323 (2017) 478-488

[5] C. Papadopoulos, Z. Frontistis, M. Antonopoulou, D. venieri, I Konstantinou, D. Mentzavinos, Sonochemical degradation of ethyl paraben in environmental samples, Statistically important parameters determining kinetics, by-products and pathways, Ultrason. Sonochem. 31 (2016) 62-70

[6] Y. Chen, P. Deng, P. Xie, R. Shang, Z. Wang, S. Wang, Heat activated persulfate oxidation of methyl and ethyl paraben: Effect, kinetics and mechanism, Chemosphere 168 (2017) 1628-1636

[7] K. Rajeshwar, J. G Ibanez, Fundamentals and Application in Pollution Abatement, Academic Press San Diego, CA (1997)

[8] E. Brillas, P.L. Cabot, J. Casado, in: M. Tarr (Ed), Chemical Degradation Methods for Wastes and pollutants, Environmental and Industrial Applications, Marcel Dekker, New York, pp. 235-248.

[9] C.A. Marti'nez- Huitle, S. Ferro, Electrochemical oxidation of organic pollutants for the wastewater treatment: Direct and indirect processes Chem. Soc. Rev. 35 (2006) 1324-1340.

[10] J.R. Steter, D.Dionisio, M.R.V. Lanza, A.J. Motheo, Electrochemical and sonoelectro-chemical processes applied to the degradation of the endocrine disruptor methyl paraben, J Appl. Electrochem. 44 (2014)1317-1325

[11] M. Neumann-Spallart, S.S. Shinde, M. Mahadik, C.H. Bhosale, Photoelectrochemical degradation of selected aromatic molecules, Electrochim. Acta 111 (2013) 830-836

[12] M. Panizza, G. Cerisola, Direct and mediated anodic oxidation of organic pollutants. Chem. Rev. 109 (2009):6541–6569

[13] F.C. Moreira, S. Garcia-Segura, V.J.P. Vilar, R.A.R. Boaventura, E. Brillas, Decolorization and mineralization of sunset yellow FCF azo dye by anodic oxidation, electro-Fenton, UVA photoelectro-Fenton and solar photoelectro-Fenton processes. Appl. Catal. B Environ. 142–143 (2013) 877–890

[14] A. Özcan, Y. Şahin, A.S. Koparal, M.A. Oturan, Degradation of picloram by the electro-Fenton process. J Hazard Mater 153 (2008)718–727

[15] K.P. Jyothi, Suguna Yesodharan, E.P. Yesodharan, Contaminant salts as enhancers of sonocatalytic degradation of organic water pollutants: Effect of concentration, reaction time and adsorption on the efficiency of enhancement and the fate of concurrently formed H2O2, J Env. Chem. Eng. 6 (2018) 3574-3589

[16] E. Gutiérrez-Segura, M. Solache-Ríos, A. Colín-Cruz, Sorption of indigo carmine by a Fe- zeolitic tuff and carbonaceous material from pyrolyzed sewage sludge, J. Hazard. Mater. 170 (2009) 1227–1235

[17] U.R. Lakshmi, V.C. Srivastava, I.D. Mall, D.H. Lataye, Rice husk ash as an effective adsorbent: Evaluation of adsorptive characteristics for Indigo Carmine dye, J. Environ. Management. 90 (2009) 710–720

[18] N. Barka, A. Assabbane, A. Nounah, Y. Aït Ichou, Photocatalytic degradation of indigo carmine in aqueous solution by TiO2-coated non-woven fibers, J. Hazard.Mater. 152 (2008) 1054–1059

[19] K.P. Vidya Lekshmi, SugunaYesodharan, E.P Yesodharan, MnO2 efficiently remove Indigo Carmine dyes from polluted water, Heliyon 4 (2018) 1-52

[20] K. Cho, D. Kwon, M.R. Hoffmann, Electrochemical treatment of human waste coupled with molecular hydrogen production. RSC Adv. 4 (2014) 4596–4608

[21] O.Weres, Electrode with surface comprising oxides of titanium and bismuth and water purification process using this electrode. U.S. Patent 7,494,583 B2, Feb. 24, 2009

[22] H. Park, A. Bak, Y.Y. Ahn, J. Choi, M.R. Hoffmann, Photoelectrochemical performance of multi-layered BiOx-TiO2/Ti electrodes for degradation of phenol and production of molecular hydrogen in water. J. Hazard. Mater. 211 (2012) 47–54.

[23] A.D. Eaton, L.S. Cleseeri, E.W. Rice, A.E. Greenberg, Standard methods for the examination of water and wastewater, American public health association, Washington (2005) 515-516

[24] J. B. Parsa, M. Abbasi, Decolorization of synthetic and real wastewater by direct electrochemical oxidation process, Acta Chim. Slov. 54 (2007) 792-797

[25] C.Y. Cheng, G.H. Kelsall, Models of hypochlorite production in electrochemical reactors with plate and porous anodes, J Appl. Electrochem. 37 (2007) 1203-1217

[26] S.G. Anju, Suguna Yesodharan, E.P. Yesodharan, Zinc oxide mediated sonophotocatalytic degradation of phenol in water, Chem. Eng. J. 189-190 (2012) 84-93

[27] S. Zhou, A.K. Ray, Kinetic studies of photocatalytic degradation of Eosin B on a thin film of TiO2, Ind. Eng. Chem. Res. 42 (2003) 6020-6033

[28] E. L. Cusslar, Diffusion mass transfer in fluid systems, Cambridge University Press, New York (1998)

[29]. J. O'M. Bockris, B.E. Conway, E. Yeager, R. E. White (Eds), Comprehensive Treatise of Electrochemistry 2, Plenum Press, N. Y (1981).

[30] J Saien, A.R. Soleymani, Degradation and mineralization of Direct blue71 in a circulating up-flow reactor by UV-TiO2 process and employing a new method in kinetic study, J Hazard. Mater. 14 (2007) 507-512

[31] C. Guillard, E. Puzenat, H. Lachheb, A. Houas, J-M. Herrmann, Why inorganic salts decrease the TiO2 photocatalytic efficiency?, Int. J. Photoenergy 7 (2005) 1-9

[32] P. Calza, E. Pelizzetti, Photocatalytic transformation of organic compounds in the presence of inorganic ions, Pure Appl. Chem. 73 (2001) 1839-1848

[33] M. Abdullah, G.K-C. Low, R.W. Matthews, Effects of common inorganic anions on rates of photocatalytic oxidation of organic carbon over illuminated titanium dioxide, J. Phys. Chem. 94 (1990) 6820-6825

[34] M Sayed, F. Pingfeng, H.M. Khan, P. Zhang, Effect of isopropanol on microstructure and activity of TiO2 films with dominant {110 facets for photocatalytic degradation of bezafibrate, Int. J. Photoenergy (2014), doi:10.1155/2014/490264

[35] J. Yu, W. Wang, B. Cheng, B.L. Zu, Enhancement of photocatalytic activity of mesoporous TiO2 powders by hydrothermal surface fluorination treatment, J. Phys. Chem. C 113 (2009) 6743-6750

[36] D. Dionisio, A.J. Motheo, C. Saez, M.A. Rodrigo, Effect of electrolyte on the electrolysis and photoelectrolysis of synthetic methyl paraben polluted wastewater, Sep. Purif. Technol. 208 (2019) 201-207

Annexure IV

Copy of the certificate awarded for "Best Poster Presentation" at the ISAC National Conference 2019

iasc 2019

INDIAN ANALYTICAL SCIENCE CONGRESS 2019

Recent Advances in Analytical, Bioanalytical and Separation Techniques
September 19-21, 2019, Thiruvananthapuram, India

Certificate

Award for the best ~~Oral~~ / Poster Presentation

Presented to :

Prof. / Dr. / Mr. / Ms. VEENA VIJAYAN, CUSAT

For the paper entitled: Sonolysis as a potential advanced oxidation process for the removal of traces of toxic indigo carmine dye pollutant from water

Chairman, Organising Committee

Indian Analytical Science Congress 2019

Convener, Organising Committee

Organised by Indian Society of Analytical Scientists

.....ꕥ.....